

Electrostatic and Non-Electrostatic Interactions of Positively Charged Polypeptides with Negatively Charged Lipid Membranes

Dissertation

zur Erlangung des akademischen Grades
Doctor rerum naturalium (Dr. rer. nat.)

vorgelegt der

Naturwissenschaftlichen Fakultät II (Chemie und Physik)
der Martin-Luther-Universität Halle-Wittenberg

von Herrn Diplomchemiker Christian Schwieger
geb. am 09. April 1976 in Halle (Saale)

Gutachter:

1. Prof. Dr. rer. nat. Alfred Blume
2. Prof. Dr. rer. nat. Andreas Janshoff

Tag der Verteidigung: 02. Feb. 2008

urn:nbn:de:gbv:3-000013374

[<http://nbn-resolving.de/urn/resolver.pl?urn=nbn%3Ade%3Agbv%3A3-000013374>]

to my parents

Contents

1	INTRODUCTION	1
1.1	Biological and model membranes.....	1
1.2	Lipid polymorphism.....	2
1.3	Motivation and aim of this work.....	3
2	THE MODEL SYSTEM	5
2.1	The lipids.....	5
2.2	The peptides.....	7
2.3	Membrane electrostatics.....	10
3	INTERACTION OF POLYLYSINE WITH PG CONTAINING MEMBRANES	13
3.1	Introduction.....	13
3.2	Differential scanning calorimetry.....	14
3.2.1	Influence of PLL on the phase behaviour of pure DPPG membranes.....	14
3.2.2	Influence of PLL on the phase behaviour and the miscibility of mixed DPPG/DPPC and DPPG/DMPC membranes.....	16
3.3	Infrared spectroscopy.....	20
3.3.1	Pure DPPG membranes.....	21
3.3.2	PLL complexes with mixed DPPG/DPPC membranes.....	27
3.4	Isothermal titration calorimetry.....	29
3.4.1	Phase dependent binding.....	30
3.4.2	Chain length dependent binding.....	33
3.4.3	Temperature dependent binding.....	35
3.5	Monolayer experiments.....	38
3.6	X-ray diffraction.....	40
3.6.1	Polymorphism and structure of DPPG in pure water.....	40
3.6.2	Polymorphism and structure of DPPG in NaCl solution.....	43
3.6.3	Influence of poly(L-lysine) on the bilayer structure.....	44
3.7	Summary.....	48

4	INTERACTION OF POLYARGININE WITH PG CONTAINING MEMBRANES	51
4.1	Introduction.....	51
4.2	Differential scanning calorimetry.....	52
4.2.1	Influence of PLA on the phase behaviour of DPPG membranes.....	52
4.2.2	Influence of PLA binding on the miscibility of DMPC/DPPG membranes.....	57
4.3	Isothermal titration calorimetry.....	61
4.4	Monolayer experiments.....	66
4.5	Infrared spectroscopy.....	70
4.5.1	Complexes with pure DPPG.....	70
4.5.2	Complexes with mixed DMPC/DPPG membranes.....	83
4.6	Fluorescence experiments.....	86
4.7	Summary.....	89
4.8	Comparison of PLL and PLA binding to PG membranes.....	92
5	INTERACTION OF POLYLYSINES AND POLYARGININES WITH PA CONTAINING MEMBRANES	97
5.1	Thermotropic phase behaviour.....	97
5.1.1	Polylysine / PA complexes.....	97
5.1.2	Polyarginine / PA complexes.....	99
5.2	Domain formation in mixed DMPC/DMPA membranes.....	102
5.2.1	Influence of PLL binding.....	102
5.2.2	Influence of PLA binding.....	103
5.3	Binding enthalpies.....	106
5.3.1	PLL binding to PA membranes.....	106
5.3.2	PLA binding to PA membranes.....	108
5.4	The methylene stretching vibrations.....	109
5.4.1	Polylysine / PA complexes.....	109
5.4.2	Polyarginine / PA complexes.....	110
5.5	Influence of polypeptide binding on the interfacial hydration.....	111
5.5.1	PLL binding.....	111
5.5.2	PLA binding.....	113
5.6	Secondary structure of the polypeptides.....	114
5.6.1	PLL.....	114
5.6.2	PLA.....	116

5.7	Polypeptide adsorption to DMPA monolayers	117
5.7.1	PLL adsorption	117
5.7.2	PLA adsorption	119
5.8	Summary and comparison of polypeptide binding to PG and PA membranes	121
6	SUMMARY	123
7	CONCLUSIONS	127
8	ZUSAMMENFASSUNG	128
9	APPENDIX	131
9.1	Materials	131
9.1.1	Polylysines	131
9.1.2	Polyarginines	131
9.1.3	Lipids	131
9.1.4	Others.....	131
9.2	Experimental	132
9.2.1	Vesicle preparation	132
9.2.2	Differential scanning calorimetry	132
9.2.3	Infrared spectroscopy.....	132
9.2.4	Isothermal titration calorimetry	133
9.2.5	Monolayer adsorption experiments.....	133
9.2.6	Monolayer pressure/area isotherms	133
9.2.7	X-ray diffraction	134
9.2.8	Fluorescence experiments.....	134
9.3	Summarizing Tables	136
10	REFERENCES	139
11	ACKNOWLEDGMENTS	151
12	PUBLICATIONS	153
13	CURRICULUM VITAE	155

Abbreviations

DPPG	1,2-dipalmitoyl- <i>sn</i> -glycero-3-phosphoglycerol
DMPG	1,2-myristoyl- <i>sn</i> -glycero-3-phosphoglycerol
POPG	1-palmitoyl-2-myristoyl- <i>sn</i> -glycero-3-phosphoglycerol
DPPC	1,2-dipalmitoyl- <i>sn</i> -glycero-3-phosphocholine
DMPC	1,2-dimyristoyl- <i>sn</i> -glycero-3-phosphocholine
DMPA	1,2-dimyristoyl- <i>sn</i> -glycero-3-phosphitic acid
DLPA	1,2-dilauroyl- <i>sn</i> -glycero-3-phosphitic acid
DPPG-d ₆₂	DPPG with perdeuterated acyl chains
DPPC-d ₆₂	DPPC with perdeuterated acyl chains
DMPC-d ₅₄	DMPC with perdeuterated acyl chains
PS	phosphatidylserine
DHP	di-hexadecyl-phosphate
PLL	poly(L-lysine)
PDLL	poly(D,L-lysine)
PLA	poly(L-arginine)
K, Lys	lysine
R, Arg	arginine
DSC	differential scanning calorimetry
ITC	isothermal titration calorimetry
FT-IR	Fourier transform infrared spectroscopy
SAXS	small angle X-ray scattering
WAXS	wide angle X-ray scattering
CD	circular dichroism
NMR	nuclear magnetic resonance
ESR	electron spin resonance
FRET	fluorescent resonance energy transfer
FCS	fluorescence correlation spectroscopy
BAM	Brewster angle microscopy
cryo-TEM	cryo-transmission electron microscopy
L _α	lamellar liquid crystalline phase
P _β	ripple phase
L _β , L _{β'}	lamellar gel phase, tilted lamellar gel phase
L _c	lamellar crystalline phase

Lc_m	metastable lamellar crystalline phase
Cr	recrystallized phase
LE	liquid expanded
LC	liquid condensed
S	solid analogues phase
SUV	small unilamellar vesicle
LUV	large unilamellar vesicle
GUV	giant unilamellar vesicle
MLV	multilamellar vesicle
DTGS	Deuterated Triglycine Sulfate
v_{as}	anti-symmetric stretching vibration
v_s	symmetric stretching vibration
δ	deformation vibration
R_c	Ratio of lipid to peptide charges
n	number of monomer units
T_m	main transition temperature
T_{pre}	pre transition temperature
T_{sub}	sub transition temperature
ΔH	Enthalpy change
ΔS	Entropy change
ΔG	free energy change
ΔP	difference Power
ΔC_p	heat capacity difference
$\Delta_R C_p$	heat capacity change upon reaction
Q	heat
$\tilde{\nu}$	wavenumber
π	surface pressure
$\Delta\pi$	surface pressure difference
π_0	initial surface pressure
π_{tr}	surface pressure at the LE \rightarrow LC phase transition
A_m	molecular area
σ	surface charge density
ψ^0	surface potential
z	charge number

1 Introduction

1.1 Biological and model membranes

Biological membranes surround cells and cell compartments. On the one hand their purpose is to demarcate closed reaction volumes, on the other hand they have to assure and modulate a selective exchange of material and information. Furthermore, charge and concentration gradients across the membrane drive many biochemical reactions. These challenging tasks are accomplished by establishing a complex composition while having high dynamics of the membrane compounds. The constituents of a membrane are a vast variety of proteins and lipids. Very often, specific functions, as ion transport or catalysis of reactions, are accomplished by membrane proteins, whereas the lipids provide the environment for binding, folding and diffusion of the proteins and reactants. To assure fast lateral reorganisation of the lipids high mobility is important. This is the reason why a lipid membrane can be regarded as “two dimensional fluid”.

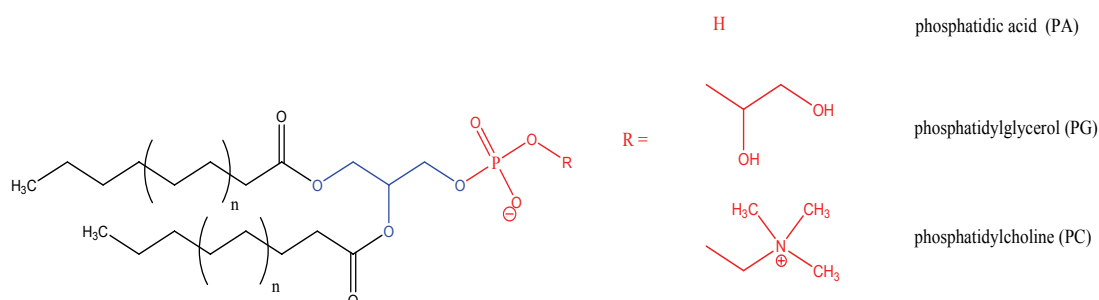


Figure 1.1: General structure of phospholipids. Black: fatty acids, blue: glycerol backbone, red: headgroup. The acyl chain length ranges between 10 and 20 carbon atoms and can be different at both positions. Acyl chains can have different degrees of unsaturation. R can be hydrogen in PA or a short hydrophilic alcohol like glycerol (in PG), serine (in PS), choline (in PC), ethanolamine (in PE), inositol (in PI).

The lipids found in biological membranes are chemically very different, but all have a hydrophobic and a hydrophilic molecule part. One major class of compounds are phospholipids. They consist of a glycerophosphoric acid backbone, which is esterified at the *sn*-1 and *sn*-2 position with long chain fatty acids and mostly with a short hydrophilic alcohol at the phosphoric acid moiety (Figure 1.1). The fatty acids vary in length and degree of unsaturation, the headgroup alcohols vary in chemical structure and charge. These variations cause a wide range of different properties and allow the membrane to adjust to specific needs.

Model membranes are used to study specific interactions. They consist of only one or a few compounds and can be easily prepared by dispersing lipids in aqueous solution. Dependent on

the technique used and the lipid composition different aggregates are formed by self-aggregation of the lipids. The most common model systems are vesicles (also called liposomes) of different size and lamellarity (SUV, LUV, MLV, GUV).

1.2 Lipid polymorphism

The amphiphilicity of lipids is the reason for spontaneous self aggregation in aqueous solution. The driving force for this process is the exclusion of water from the hydrophobic parts of the molecules, which is commonly known as the hydrophobic effect (Lee 1991; Tanford 1980). Different structures might be formed, depending on the molecular geometry (Israelachvili 1985) and the chemical composition of the aqueous solution (pH, ionic strength, water content). This is known as lyotropic mesomorphism. The type of aggregate typically formed by membrane lipids is the bilayer lamella. It consists of a micro-segregated hydrocarbon core that is shielded on both sides by a hydrated headgroup layer. This structure is commonly called lipid membrane. Other possible aggregation structures are micelles and hexagonal or cubic phases. Transitions between these structures are possible.

Dependent on temperature lamellar structures exist in different degrees of organisation. Transitions between these states are first order phase transitions. The transition temperatures depend sensitively on the lipid composition. This so called thermotropic mesomorphism plays a major role in this work. Therefore, it shall be briefly introduced:

Biological membranes normally exist in the *liquid crystalline* L_{α} phase. This phase is characterized by a high translational and rotational mobility of the lipids in the plane of the membrane. The headgroups are well hydrated and occupy a molecular area of approximately $60 - 70 \text{ \AA}^2$. Neither the headgroup nor the hydrocarbon chains are restricted in their reorientational motions. Conformational freedom of the hydrocarbon chains is assured by a high proportion of gauche conformers.

When the temperature decreases below the main transition temperature (T_m) a so called *ripple phase* (P_{β}) forms, in the case of phosphatidylcholine (PC) and phosphatidylglycerol (PG) membranes. This name has been coined because lamella in this phase show periodic undulations which can be observed in TEM images. The origin of the undulations is not quite clear at present. Probably, the molecules assemble in different configurations (chain tilt, curvature, interdigitation), which causes the rippling (de Vries et al. 2005; Heimburg 2000; Lenz and Schmid 2007). Another explanation is that an unequal ordering of hydrocarbon chains and headgroup region is compensated by a shift of the lipid molecules along their long axis (Cevc 1991). The P_{β} phase is a stable intermediate between the fluid crystalline phase L_{α} and the tilted gel phase L_{β} .

On further reducing the temperature the *gel phase* (L_β or L_β')¹ is formed at the pre-transition temperature (T_{pre}). If no ripple phase exists, the gel phase is directly formed at T_m . In the gel phase, the dynamics of all motional modes is reduced. The headgroups are less hydrated than in the fluid-crystalline phase. The molecular area is reduced to ca. 40 \AA^2 . The hydrocarbon chains are all-trans and might be tilted with respect to the bilayer normal. The acyl chains still have some rotational freedom along their long axis but are organised in a regular hexagonal lattice.

At even lower temperatures ($T < T_{sub}$) *crystalline L_c phases* might exist. In these phases the headgroup is even less hydrated and the hydrocarbon chains are oriented almost perpendicular to the bilayer surface. The rotational motions of the hydrocarbon chains are restricted and chain and headgroup lattices are formed.

1.3 Motivation and aim of this work

Proteins are bound to the membranes either as “intrinsic” or “peripheral” proteins. Intrinsic proteins are located within the hydrocarbon core of the membrane, whereas peripheral proteins are bound only to the membrane surface. A major driving force for the binding of peripheral proteins is electrostatic attraction between the negatively charged membrane and protein segments that accumulate positively charged amino acids (lysine, arginine, histidine) (Heimburg et al. 1999; Heimburg and Marsh 1995; Kim et al. 1991; Langner and Kubica 1999 and references therein; Montal 1999; Wang et al. 2004). Very often intrinsic membrane proteins are attracted by the membrane via electrostatic interaction, too, before being inserted (Langner and Kubica 1999) and electrostatic anchors bind to the membrane surface and stabilize the protein in its inserted conformation. The strength of electrostatic interactions is modulated by adjustment of the lateral distribution of negatively charged lipids within the membrane as well as by protein and lipid headgroup phosphorylation or hydrolysis (McLaughlin and Aderem 1995).

It was found, that many cell penetrating peptides (CPP's) or protein transduction domains (PTD's) contain sequences rich in arginine and lysine (Futaki 2005; Magzoub and Graeslund 2004). This indicates that electrostatic interactions also play a role in mechanisms that allow macromolecules to translocate the membrane barrier. These interactions can be strong enough to destroy the membrane structure (venoms, antibiotics).

Electrostatic interactions between positively charged peptides and negatively charged lipid membranes are the topic of this work. It will be examined how these interactions are influenced by the lipid phase state, the membrane composition, and the peptide architecture. Another goal of this work is to study how binding of model peptides influences the membrane

¹ The “prime” indicates that acyl chains are tilted.

properties, i.e. how the thermotropic phase behaviour and the structure of the membrane in different phase states are affected. Furthermore, the influence of the peptide-membrane interaction on the miscibility of negatively charged and zwitterionic lipids within one membrane layer will be determined. Attention is also directed to the secondary structure of the peptide that possibly forms upon binding to the membrane and the question of how this structure influences the binding process. The study is performed with different model membranes and homopolypeptides of varying chain length, composed of lysine and arginine, respectively.

A main objective of this work is to reveal the specificity of these two amino acids in their interaction with negatively charged membranes. This implies the examination of non-electrostatic contributions (e.g. hydrophobic interactions or hydrogen bonding) to the overall free energy change of binding.

2 The model system

2.1 The lipids

The negatively charged lipids that were chosen as model compounds for this study are phosphatidylglycerol (PG) and phosphatidic acid (PA). Both lipids bear one negative charge at the phosphate group. However, their different headgroup architecture leads to different properties. The charge of PG molecules is shielded by the bulky headgroup glycerol, whereas the charge of PA molecules is exposed directly at the membrane surface. It has been shown that this causes different electrostatic interaction strength with monovalent anions (Cevc 1990; Eisenberg et al. 1979). The lipids are used pure or in mixtures with zwitterionic phosphatidylcholine (PC), which reduces the charge density of the membranes and gives rise to the possibility of lateral phase separation. The study is mainly focused on interactions with PG containing membranes. However, also experiments with PA containing membranes will be presented to reveal the specificity of these two lipids in peptide binding. In the following two paragraphs individual properties of PG and PA membranes will be highlighted.

Phosphatidylglycerol

Phosphatidylglycerol bilayers show a very peculiar phase transition behaviour which is dependent on pH and ionic strength of the solution (Alakoskela and Kinnunen 2007; Heimburg and Biltonen 1994; Lamy-Freund and Riske 2003; Schneider et al. 1999; Zhang et al. 1997). At low ionic strength DMPG bilayers undergo a gel to fluid phase transition over a wide temperature range and several still not very well defined transitional structures lead to high viscosity of the suspensions. In DSC this transition is reflected by a heat capacity profile with several peaks and no straight forward interpretation.

To avoid these complications we used for this study DPPG bilayers instead of the more common DMPG bilayers. Due to its longer acyl chains DPPG shows even at low ionic strength a sharp cooperative main phase transition ($P_{\beta} \rightarrow L_{\alpha}$) (Schneider et al. 1999). The midpoint of this transition is still salt concentration and buffer dependent (Wilkinson et al. 1987), but was found to be constant in a range of 100 – 500 mM NaCl solution (Blume and Garidel 1999). Therefore, we performed all experiments presented in this study in a 100 mM NaCl solution. Under these conditions a pre-transition is found at 34.6 °C and the main transition at about 41 °C, connected with transition enthalpies of 1.4 kcal/mol and 8.9 kcal/mol, respectively (Durvasula and Huang 1999; Huang and Li 1999; Zhang et al. 1997). After low temperature incubation several stable and metastable subgel phases are formed (Erand et al. 1992; Zhang et

al. 1997). In the gel phase L_{β} , the acyl chains are tilted by 29° with respect to the bilayer normal and the headgroups are oriented parallel to the surface (Pascher et al. 1987).

The gel phases of PG membranes are structurally and thermodynamically very similar to gel phases formed by zwitterionic PC. This is due to the fact that the repulsive electrostatic interaction between PG headgroups is compensated by attractive intermolecular hydrogen bonds between glycerol hydroxyl and phosphate groups of adjacent molecules (Boggs 1987; Pascher et al. 1987; Zhang et al. 1997).

The apparent pK_{app} value of the phosphodiester groups in a PG membrane is 2.9. In solutions of lower pH it is protonated and T_m shifts to about 20°C higher values. The phosphate groups are completely charged when the pH is higher than 5 (Watts et al. 1978). However, if electrostatic interactions are examined, one has to be aware of the fact, that the apparent pK_{app} is shifted by altering the membrane surface potential, according to:

$$pK_{app} = pK_{int} - \frac{e\psi^0}{kT \ln 10} \quad (1)$$

In the case of polycation binding, which is examined in this work, the additionally applied positive potential shifts the pK_{app} to lower values. Thus, the presence of the completely deprotonated, i.e. singly negatively charged, form of DPPG is assured.

Phosphatidic acid

In dependence of the pH value phosphatidic acid (PA) can exist as a neutral, singly negatively or doubly negatively charged molecule. The two pK_{app} values of a PA membrane are 3.5 and 10.5 for the first and the second dissociation step, respectively (Blume and Eibl 1979; Eibl and Blume 1979). Thus, PA is singly negatively charged at neutral pH. However, it is known that binding of divalent cations shifts the second pK_{app} according to equation (1) into the neutral pH regime, inducing the dissociation of the second proton (Faraudo and Travesset 2007; Garidel 1997; Laroche et al. 1991). This effect could also be induced by polycation binding. Main transition temperature (T_m) and membrane structure strongly depend on the degree of dissociation (α). T_m is maximal $\alpha = 0.5$. It decreases slightly in the region of $0.5 < \alpha < 1.5$, i.e. in between the two pK_{app} values. An average dissociation of 1.5 protons per PA molecule results in a 4–5 $^\circ\text{C}$ lower transition temperature than an average dissociation of 0.5. The absolute values of T_m are unexpectedly high compared to other negatively charged lipids ($T_m(\text{DMPA}^-) = 52^\circ\text{C}$, $T_m(\text{DPPA}^-) = 71^\circ\text{C}$; at $\alpha = 1$). This is explained by a very tight hydrogen bond network within the headgroup layer.

When the membrane is completely deprotonated ($\alpha = 2$) T_m is decreased by ca. 25°C . This is due to increased electrostatic repulsion between adjacent two fold negatively charged headgroups, the loss of intermolecular hydrogen bonding, increased hydration of the headgroups, and the fact that the acyl chains tilt to compensate for the higher hydrodynamic

radii of the headgroups. The chain tilt consequently reduces the van der Waals interaction energy.

The transition temperature of membranes in the completely protonated state ($\alpha = 0$) is ca 7–9 °C lower than T_m of a singly negatively charged membrane ($\alpha = 1$). This reduction of T_m with the decrease of headgroup charges is unexpected and different to the situation described above for PG membranes. Nonetheless, it can be explained with the inability of completely protonated PA to form intermolecular hydrogen bonds.

2.2 The peptides

The model peptides that were used for this study are poly(L-lysine) (PLL) and poly(L-arginine) (PLA) in different degrees of polymerisation. Lysine and arginine are the two most common positively charged amino acids.

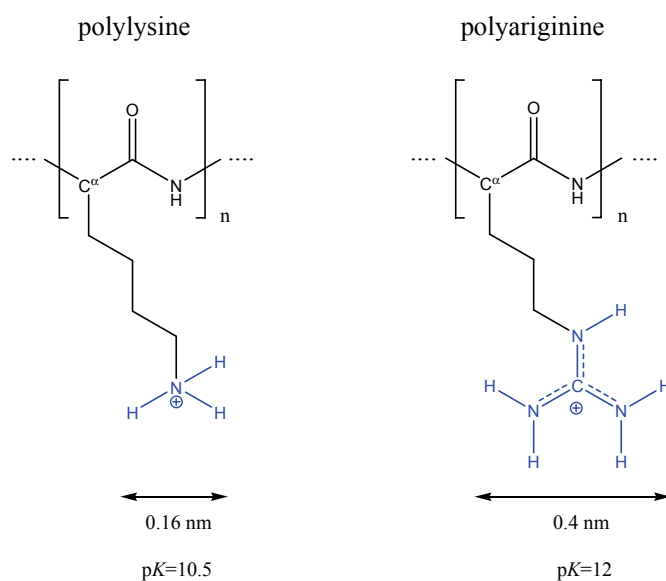


Figure 2.1: Chemical structures and some properties of lysine (left) and arginine (right) integrated in a peptide backbone. The charged end groups are coloured in blue.

They are very similar in their chemical structure (Figure 2.1). Besides the amino acid functionalities they both possess a side chain which is constructed of a hydrophobic spacer and, at neutral pH, a singly positively charged end group. This end group is an ammonium group for lysine and a guanidinium group for arginine. All specificities must be caused by different properties of these groups. Differences are found in size, charge distribution, and hydrogen bonding abilities. The ammonium group of lysine is smaller and the charge is located at the nitrogen atom. Contrary, the guanidinium group is bulky and the charge is delocalized in

orbitals of the carbon and the three nitrogen atoms. Therefore, guanidinium is a softer ion than ammonium and arginine less hydrophilic than lysine (Monera et al. 1995; White and Wimley 1998)². A further characteristic of arginine is its propensity to donate up to five strong hydrogen bonds and to form strong bidentate hydrogen bonds (Calnan et al. 1991; Fuchs and Raines 2006; Tang et al. 2007). This makes arginine and other guanidylated molecules (e.g. creatine) to a biologically relevant recognition unit for phosphoryl, sulfonyl and carboxyl moieties.

PLL and PLA are simple highly charged homopolypeptides that are biologically less relevant, but allow us to study some principles of electrostatic peptide-membrane interactions.

In the following paragraphs specific properties of these two peptides are described and available research results are summarized.

Polylysine

It was found that poly(L-lysine) is a good model for cytolytic and antimicrobial peptides. It is used to study the electrostatic interactions (Blondelle et al. 1999; Shai 1999), because it is a highly positively charged polypeptide that is able to adopt all three common secondary structures, i.e. random coil, α -helix and β -sheet. That has been proven for bulk solution (Greenfield et al. 1967; Jackson et al. 1989) as well as for membrane surfaces containing negatively charged lipids (Carrier and Pezolet 1984; Fukushima et al. 1988; Hammes and Schullery 1970).

Vice versa, it was found that poly(L-lysine) influences many membrane properties. It was reported that long PLL increases the main transition temperature of PG membranes (Carrier et al. 1985; Papahadjopoulos et al. 1975; Takahashi et al. 1992) as well as of PA membranes (Galla and Sackmann 1975a; Hartmann and Galla 1978; Takahashi et al. 1996). On the other hand it was found that the transition temperature of lipopolysaccharide (LPS) containing membranes was not affected by the addition of PLL (Lasch et al. 1998) and that short PLLs (ca 20 monomer units) even decreased the transition temperature of membranes containing PG (Carrier and Pezolet 1986) or PA (Laroche et al. 1988). This shows that the interaction of PLL with negatively charged lipids is strongly dependent on the nature of the lipid headgroup and on the chain length of the PLL itself.

Furthermore, it was reported that PLL has an influence on the lamellar-hexagonal phase transition (De Kruijff and Cullis 1980), the membrane curvature (Dolowy 1979), fusion rates (Gad et al. 1985), vesicle adhesion (Menger et al. 2003), membrane rupture (Diederich et al.

² Many different hydrophobicity scales are published. The results are not unambiguous and depend on the method used to define the scale. There are also scales, where Arg is assessed to be more hydrophilic than Lys (Alakoskela and Kinnunen 2007; Ben-Tal et al. 1996a; Engelman et al. 1986; Radzicka and Wolfenden 1988). Often Arg and Lys are described by similar values. However, the papers cited in the text seem to be the most relevant in the here discussed context, because the hydrophobicity values originate from membrane partitioning experiments.

1998), and the permeability (Yaroslavov et al. 2003). It has even been described that PLL of a certain chain length might be translocated through the membrane, probably using defects produced upon binding (Menger et al. 2003; Shibata et al. 2003).

Of outstanding importance is also the notion of domain formation in mixed lipid membranes induced by the binding of PLL. Domain formation has been shown by ^2H -NMR (Franzin and Macdonald 2001), fluorescence (Carrier et al. 1985), FT-IR spectroscopy (Lasch et al. 1998), Raman spectroscopy (Carrier and Pezolet 1984), ESR (Galla and Sackmann 1975a), and electron microscopy (Hartmann et al. 1977) for different membrane mixtures. However, in most of the studies statements can only be made about gel phase domains, because different transition temperatures are used as an indicator for different domains. Although some methods, namely NMR, ESR or fluorescence techniques (FRET, FCS), are capable of detecting domains in the fluid membrane state, measurements have rarely been done above T_m . A lipid demixing in the fluid membrane state that would be of biological relevance has not been shown up to now.

Besides publications on the influence of PLLs many studies have been performed on the interaction of oligolysines with negatively charged membranes (Kim et al. 1991; Loura et al. 2006; Mosior and McLaughlin 1992a; Roux et al. 1988), including theoretical studies on the thermodynamic of binding (Ben-Tal et al. 2000; Ben-Tal et al. 1996b; Denisov et al. 1998; Murray et al. 1999). These authors show that the binding of oligolysines is of pure electrostatic nature and occurs only peripherally with a membrane peptide equilibrium distance of approximately 2.5 Å, indicating that at least one layer of water separates it from the membrane. However, for PLL binding it is still unclear whether hydrophobic interactions are involved in the binding and whether the PLL might penetrate the headgroup region (Carrier et al. 1985; Hartmann and Galla 1978). The experimental results obtained for oligolysines differ from those of PLL, in that no domain formation induced by the oligolysines could be observed. This finding might be connected to the inability of oligolysines to form defined secondary structures.

Polyarginine

During the last years it became clear, that the accumulation of arginines plays a key role in membrane translocation of peptides. Thus, many studies were made to determine the parameters that ensure and enhance cellular uptake of natural and synthetic arginine rich peptides. These works were initialized by the finding, that HIV-TAT (the 13 amino acid transduction domain of the HI virus), which comprises 6 Arg and two Lys residues, enters cells with ease (Vives et al. 1997). Substituting the lysines with arginines enhanced the cellular uptake (Futaki et al. 2001). Also simple oligoarginines were shown to cross the cell membrane more readily than HIV-TAT (Mitchell et al. 2000; Wender et al. 2000; Wender et al. 2002). In contrast, homopolymers of lysine, ornithin, and histidine were not internalized (Mitchell et al.

2000). This shows that not only the charge but some specific properties of the guanidyl group are responsible for this behaviour. Moreover it was shown that the only necessity for cellular uptake is the guanidyl function. This was deduced from the fact that the variation of side chain length (Wender et al. 2000; Wender et al. 2002), backbone spacings (Rothbard 2002), backbone chemistry (Umezawa et al. 2002; Wender et al. 2002) and stereochemistry (Mitchell et al. 2000) did not inhibit (sometimes even enhanced) the cellular uptake.

Despite the clear evidence for cellular uptake the mechanism is not fully understood. Therefore, this behaviour was often described as “arginine magic”. Particularly it is not clear, whether the translocation pathway involves endocytosis or the peptides are directly transported through the hydrophobic membrane barrier. Although the former pathway seems to be more probable for a highly charged peptide, there is some indication that also the latter is used (Rothbard et al. 2004; Sakai et al. 2005; Tang et al. 2007).

A key factor is probably the pronounced ability of the guanidyl group to form strong bidentate hydrogen bonds with H-bond accepting counter-anions (Onda et al. 1996; Rothbard et al. 2004; Rothbard et al. 2005). It was shown that such conjugates of poly- and oligoarginines with amphiphilic anions, such as aliphatic acids, sulfates or phosphates can be transferred into and across hydrophobic solvents as octanol (Rothbard et al. 2004) or chloroform (Sakai and Matile 2003; Sakai et al. 2005). Furthermore, the partitioning of polyarginine (PLA) into (Thoren et al. 2004) and the translocation through (Sakai et al. 2005) negatively charged lipid model membranes was shown. Due to its ability to adapt to different environments by counter anion binding, polyarginine was titled “molecular chameleon” (Sakai et al. 2006).

Despite these interesting and biological relevant features polyarginines have been rarely studied up to now and little is known about the PLA membrane interaction.

2.3 Membrane electrostatics

There are different theories that describe the electrostatic interaction in vicinity of a charged membrane with more or less accuracy. More sophisticated models calculate the electrostatic potential as summation of the potentials of every individual charge (discreteness of charges) and take into account the finite sizes of interacting ions. However, more simple theories, that regard a membrane as homogeneously charged plane and interacting ions as point charges, describe many experimental findings surprisingly well (Cevc 1990; McLaughlin 1989; Tatulian 1999). Most common is the use of the Gouy-Chapman model in combination with the mass action law and the Boltzmann distribution. This approach shall be shortly introduced.

The negatively charged lipids furnish the membrane with a homogenous electrostatic surface potential ψ^p that decays gradually with increasing distance from the membrane. The surface potential influences the distribution of co- and counterions in vicinity of the

membrane. Co-ions will be depleted and counterions accumulated at the membrane surface. The distribution of the ions in the electrostatic field can be described by the well known Boltzmann relation, which yields:

$$c_s = c_b \cdot e^{\left(\frac{-ze\psi^0}{kT}\right)} \quad (2)$$

with c_s being the concentration at the membrane surface, c_b being the bulk concentration, z the charge of the ion including its sign and ψ^0 the surface potential of the membrane. The accumulation of protons in the vicinity of negatively charged membranes increases the interfacial pH and is responsible for the apparent pK_{app} value being higher than the intrinsic one (equation (1), page 6). The surface potential ψ^0 can be calculated from the surface charge density using the Gouy-Chapman theory:

$$\sigma = \sqrt{2000 \cdot \varepsilon_r \varepsilon_0 RT \sum c_i \left[\exp\left(\frac{-z_i e \psi^0}{kT}\right) - 1 \right]} \quad (3)$$

with σ being the surface charge density, ε_r the dielectric constant of water, ε_0 the permittivity of free space and c_i the bulk concentrations of the respective ion species³. If the aqueous medium contains only symmetric electrolytes this equation simplifies⁴ to:

$$\sigma = \sqrt{8000 \cdot \varepsilon_r \varepsilon_0 RT c_b} \sinh\left(\frac{ze\psi^0}{kT}\right) \quad (4)$$

The surface charge density σ can finally be directly determined from the molecular area (A_m) of the lipids in the membrane or the monolayer, according to:

$$\sigma = \frac{e \cdot z_{lip}}{A_m} \quad (5)$$

with z_{lip} being the charge of the lipid headgroup. Equations (3) and (4) show that the surface potential depends on the concentration of the ions in the bulk solution. High salt concentrations screen the electrostatic potential and diminish the electrostatic interaction of charged solutes with the membrane. Also the phase state of the membrane modulates the electrostatic interaction, because according to equation (5) σ decreases as the bilayer expands at the gel to fluid phase transition. This effect is even more pronounced if lipid monolayers are compressed. Moreover, the value of ε_r influences the surface potential. Unfortunately, the exact value of ε_r is not easy to determine in vicinity of the lipid headgroup layer. It ranges between 80 for aqueous bulk solution and 2.5 for the hydrophobic core of a membrane. The value of ε_r in the interfacial layer depends on the degree of hydration and the orientation of bound water

³ In the above given equation the concentration can be inserted in common units of mol/l. That is the reason for the appearance of the factor 2000 instead of 2.

⁴ For this simplification the identity $\sinh x = \frac{1}{2}(e^x - e^{-x})$ is used.

molecules. Therefore it also changes with the phase state of the membrane. It is assumed to take values between 30 and 50 (Cevc 1990).

A further correction has to be made, when ions not only accumulate at the membrane surface due to electrostatic attraction, but also bind specifically to the lipid headgroups. This aspect was included in the Gouy-Chapman theory by Stern (1924). He introduced the ‘‘Stern layer’’, a layer of chemically adsorbed counter- and/or co-ions that form an inner sphere complex with the lipid headgroups. The charge density of this layer is dependent on the fraction of adsorbed ions, which can be calculated on basis of the mass action law, if the binding constants are known:

$$K = \frac{n_{ad}}{n_s(L - n_{ad})} \quad (6)$$

with n_{ad} being the number of adsorbed ions, n_s the number of free ions at the interface and L the number of lipid binding sites. n_s can be calculated according to equation (2) from the bulk concentration. If the number of bound ions and their charge is known, the surface charge density of the stern layer can be determined as:

$$\sigma_{stern} = \frac{z \cdot e \cdot n_{ad}}{L \cdot A_m} \quad (7)$$

The addition of equation (5) and (7) gives the total charge density of the surface, which can be inserted in equation (4) to calculate the surface potential under consideration of ion adsorption (Tatulian 1999). The influence of ion adsorption on the surface potential is small if only monovalent ions are present. However, in the case of di- or multivalent ion binding, the surface potential can be significantly reduced or even reversed (Tatulian 1999).

3 Interaction of polylysine with PG containing membranes

3.1 Introduction

Although the influence of PLL binding on different lipid systems was already studied by several groups and principle findings have been reported in literature (see chapter 2.2), a systematic study of the thermotropic behaviour of PGs and its dependence on PLL-chain length is still missing. No extensive DSC studies were presented up to now. The work presented in this chapter was focused on DPPG as a negatively charged membrane component. We varied the PLL chain length in six steps from 14 – 906 monomer units as well as the lipid to peptide mixing ratio (R_c)⁵ and the membrane composition. Furthermore, we correlated the thermotropic behaviour of the DPPG/PLL complexes with the secondary structure of the membrane bound PLL, which we recorded for the first time over the whole temperature range from gel- to liquid crystalline phase. It turned out that not only the secondary structure influences the phase behaviour of the membrane, but that the phase state of the membrane also determines the secondary structure of the bound peptide.

We will show based on FT-IR spectroscopic results that long chain PLLs are bound as α -helices to gel phase DPPG but gradually convert to a random coil structure when the sample is heated into the liquid-crystalline phase of the lipid. This transition from an α -helix to a random coil becomes highly cooperative when DPPG is mixed with the neutral DPPC. In this case the membrane phase transition triggers the cooperative secondary structure transition of the membrane bound polypeptide. It will be also shown that in the mixed PG/PC system phase separation of neutral and charged lipid components can be induced by long chain PLLs. Furthermore we will show that the secondary structure of the polypeptide determines also the structure of the DPPG/PLL complex, which was revealed by X-ray diffraction. ITC studies give information about the thermodynamics of binding. Finally we will present evidence for non electrostatic contribution to the binding process. For this purpose monolayer experiments proved to be very instructive.

The combination of all these methods and the systematic variation of binding parameters yield information about thermodynamics of binding as well as the phase behaviour and the structure of the formed complexes and allow us to draw a comprehensive picture on DPPG/PLL interaction.

⁵ R_c is the charge ratio of lipid charges over peptide charges. Thus it refers to the amount of negatively charged lipids and the lysine or arginine side chains.

3.2 Differential scanning calorimetry

3.2.1 Influence of PLL on the phase behaviour of pure DPPG membranes

In the course of this study we performed several series of DSC-experiments on the system of negatively charged PG containing membranes with PLL under variation of i) the PLL-chain length, ii) the lipid-to-peptide-mixing-ratio (R_c) and iii) the membrane charge density. The latter was adjusted by using mixtures of zwitterionic DPPC or DMPC with zero net charge and negatively charged DPPG.

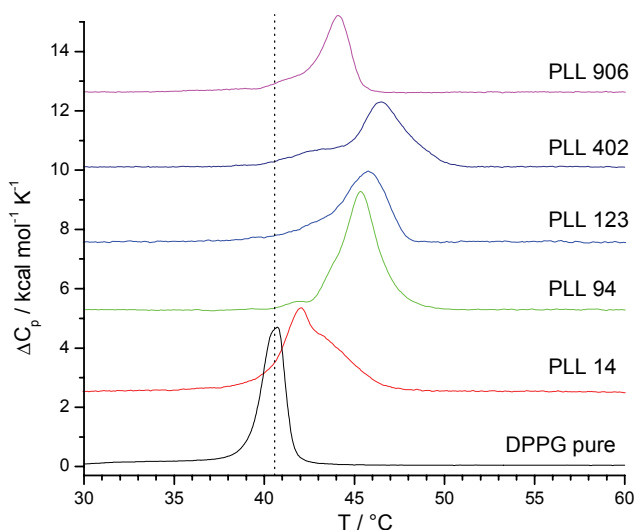


Figure 3.1: DSC-plots of the gel-to-liquid-crystalline phase transition of DPPG/PLL complexes with an equimolar charge ratio ($R_c = 1$) and different PLL chain length. Measurements are performed in 100 mM NaCl solution at pH = 6.

DSC curves in the range of the $L_{\beta'} \rightarrow L_{\alpha}$ phase transition of DPPG-membranes complexed with equimolar amounts (with respect to charges) of PLL are shown in Figure 3.1. The endothermic transition seen in the DSC scans is the so-called main transition and the associated temperature is the main transition temperature, T_m . In DPPG multilamellar systems also a $P_{\beta'}$ -phase exists and the so-called pre-transition is seen below the main transition (Schneider et al., 1999). However, in small unilamellar vesicles this transition is usually not resolved or even absent (Heimburg 2000). The black curve represents the phase transition of the uncomplexed DPPG-vesicles. The other curves show the phase transitions of DPPG/PLL complexes formed with PLL of different chain length. It is obvious that T_m of the complexes is increased with respect to the free DPPG membrane. The value of increase is dependent on the chain length of the PLL. While the shorter peptides, PLL 14 and PLL 72 cause a shift in T_m of

a little more than 1 °C, the longer peptides (PLL 123-906) produce a shift of 4-6 °C. In a general way, T_m seems to increase with the chain length of the absorbed PLL. However, we find a lower T_m for the complex DPPG/PLL 906 than for the complex DPPG/PLL 402. This is in contrast to the general trend.

The general rise in main transition temperature indicates a stabilisation of the gel phase ($L_{\beta'}$) upon binding of PLL. Since the negative charges of the membrane are screened by oppositely charged PLL and consequently the electrostatic repulsion between neighbouring DPPG molecules is reduced, this may result in better packing and higher van der Waals attractions between the lipid molecules thus leading to a higher T_m (Cevc et al. 1980). The chain length dependence is obviously caused by different binding constants of the PLL-chains to the lipid vesicles. In general, the binding constant increases with the chain length of the peptide, which is not an enthalpic but essentially an entropic effect (Montich et al. 1993). Although the mobility of the bound peptide is confined (Ben-Tal et al. 2000), the system gains a much higher entropy by counter ion release (Wagner et al. 2000). This occurs during the complexation of two polyelectrolytes, as which both, membrane and PLL, can be understood. Before binding, counter ions (chloride and sodium) are bound to the polyelectrolyte and therefore restricted in their translational degrees of freedom. After binding those ions are released and may now move free in the solution. This leads to a gain in translational entropy, which is the main driving force of binding (May et al. 2000). The effect is the larger the higher the number of associated and thus during the binding released counter ions is. This explains why the stabilisation of the gel phase and consequently the rise in T_m is more pronounced for PLL 402 than for PLL 14. An additional gain in entropy comes from the release of water molecules from the binding sites (Garidel and Blume 1999; Lehmann and Seelig 1994). The sharing of water of hydration between PLL and vesicle membrane is another effect which is responsible for the increase in T_m . Indication for H₂O release upon PLL binding arises from ITC experiments (see below).

The lower transition temperature of the complex DPPG/PLL 906 compared to DPPG/PLL 402 can be explained by steric effects. For very long peptide chains it is more difficult to bind to the membrane surface in such a way to get maximal coverage. This is consistent with a model of two dimensional packing of stiff cylinders (Novellani et al. 2000), which claims that the porosity of a package rises with the cylinder length. Overall we see two competitive effects with increasing peptide chain length: the increase of the binding constant and the larger steric hindrance. These two competitive effects lead to a maximal T_m for a PLL with intermediate chain length, namely PLL 402.

The same experiments were repeated with lipid and with peptide excess concentrations ($R_c = 2$ and 0.5, respectively). The results are shown in Figure 3.2. The general finding of an increase in T_m after PLL binding remains valid for these conditions. But in contrast to the case of $R_c = 1$, the half width of the transition peaks gets considerably wider and the peaks get

structured into different components, which are apparent as shoulders and side peaks. This indicates that several consecutive transitions occur in the system.

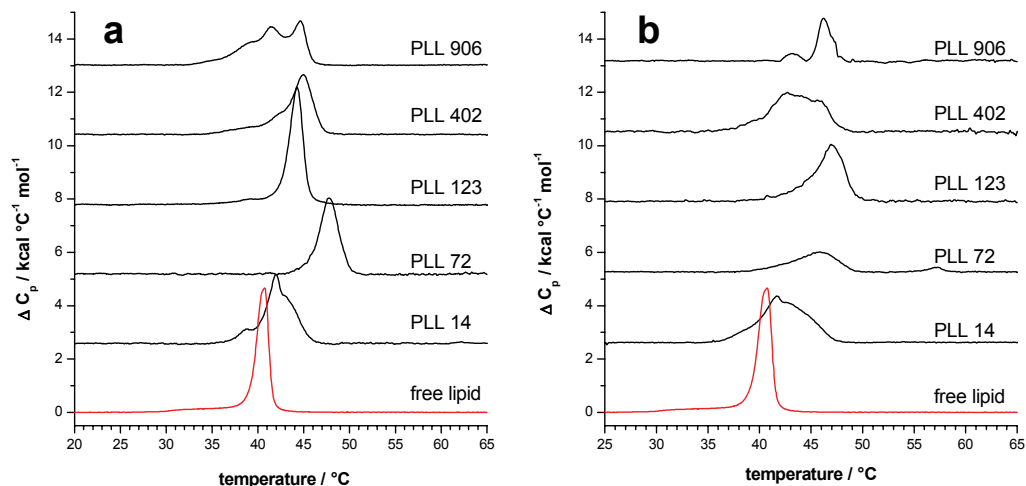


Figure 3.2: DSC-plots of the gel-to-liquid-crystalline phase transition of DPPG/PLL complexes with a mixing ratio of **a:** $R_c = 0.5$ (PLL excess) and **b:** $R_c = 2$ (DPPG excess). Measurements are performed in 100 mM NaCl solution at pH = 6.

Triphasic transitions were already observed by Papahadjopoulos et al. (1975) and Carrier et al. (1985; 1986). These findings were interpreted as being caused by domain formation in the membrane or by a heterogeneity of the complexes. The tendency to form domains is more pronounced in the complexes with longer peptides. Consequently PLL 906 induces the largest splitting of the transition peak. The chain length dependence in the domain forming capacity is also reported by other authors (Franzin and Macdonald 2001; Macdonald et al. 1998). Furthermore it was found that the transition peaks do not shift in a continuous fashion. This means that domains form in more or less well defined structures. That could be completely uncovered membrane regions (T_m about 41 °C), completely covered membrane in a 1:1 stoichiometry or intermediate structures. Also the secondary structure of the peptide (which is discussed below) should have an influence on the structure of the domain. In the case of an equimolar mixing ratio (Figure 3.1) domain formation is less probable, because every lipid molecule is screened by the same electrostatic field and there are no charge differences throughout the membrane.

3.2.2 Influence of PLL on the phase behaviour and the miscibility of mixed DPPG/DPPC and DPPG/DMPC membranes

The pure negatively charged DPPG membrane is a simple model system, but biologically less relevant. We therefore performed additional experiments with mixed membranes by adding zwitterionic DPPC or DMPC to negatively charged DPPG. Thus the surface charge

density of the membrane is reduced, which will have effects on binding constants, saturation concentrations and steric effects during binding. In addition, negatively charged and neutral lipids can demix and domain formation gets even more probable compared to pure DPPG membranes (Russ et al. 2003). Demixing of membrane lipids might play an important role in physiological processes and was already described for different lipid mixtures (Denisov et al. 1998; Franzin and Macdonald 2001; Heimburg et al. 1999; May et al. 2000).

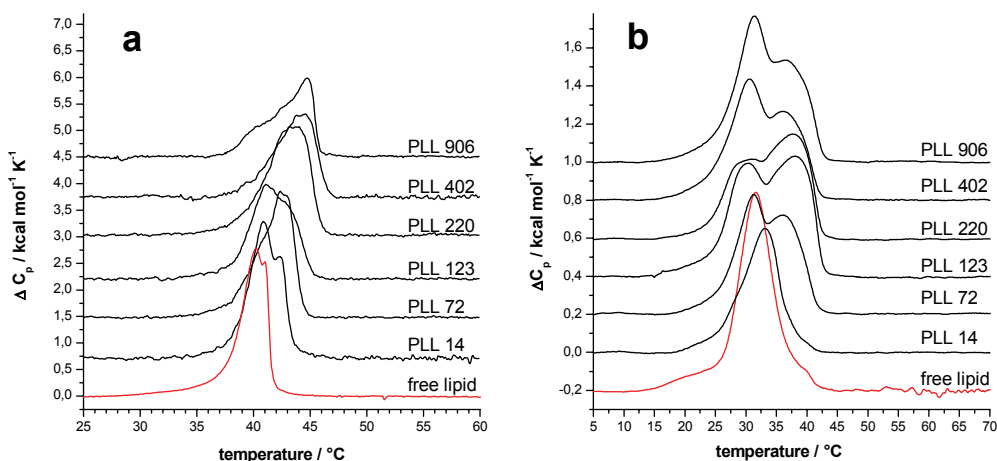


Figure 3.3: DSC-plots of the complexes of PLL of different chain length with **a:** DPPG/DPPC (1/1, mol/mol) and **b:** DPPG/DMPC (1/1, mol/mol). The charge ratio $R_c = 1$ and 0.5 respectively. Measurements are performed in 100 mM NaCl solution at pH = 6.

Figure 3.3a shows DSC plots of mixed DPPG/DPPC membranes (1:1) complexed with PLL of different chain length in a mixing ratio $R_c = 1$ (R_c refers only to the DPPG component in the lipid mixture!). Again, a general rise in main transition temperature after PLL binding is observed. The maximal transition temperatures (ca. 44.7 °C) are lower than for the binary DPPG/PLL mixtures (ca. 47 °C). This is expected, because the DPPC component is uncharged and does not bind PLL (data not shown). Only the DPPG binds PLL and its transition is shifted. The chain length dependence is more pronounced than in the case of pure DPPG membranes. Since we observe a continuous increase in T_m with increasing chain length, we conclude that an increasing binding constant dominates over unfavourable steric interactions. This effect is to be expected, because in the mixed membrane we have less binding sites per area, which gives the PLL more space to pack at the surface. Furthermore, we observe an increasing half width of the transition peaks with increasing polypeptide chain length. This is an indication that domain formation occurs, which is more pronounced in the complexes with longer PLL. The domain formation leads now to the separation of free DPPC, the remaining DPPG molecules with bound PLL having a higher transition temperature. However, the separated domains will not be pure DPPC or DPPG, respectively, but only enriched in one of the components. The domains seem to become larger with longer PLL chain length, as indicated by the change of the DSC peaks. Macdonald et al. (1998) suggested that the area of

the domains increases proportional to the square root of the polyelectrolyte molar mass. However, the domains get also less defined in their composition, because the PLL packing gets less ideal and more porous, which leads to wider transition peaks. Similar results were described by Franzin et al. (2001) for membranes containing PS. They measured a smaller PS accumulation in domains induced by longer PLL.

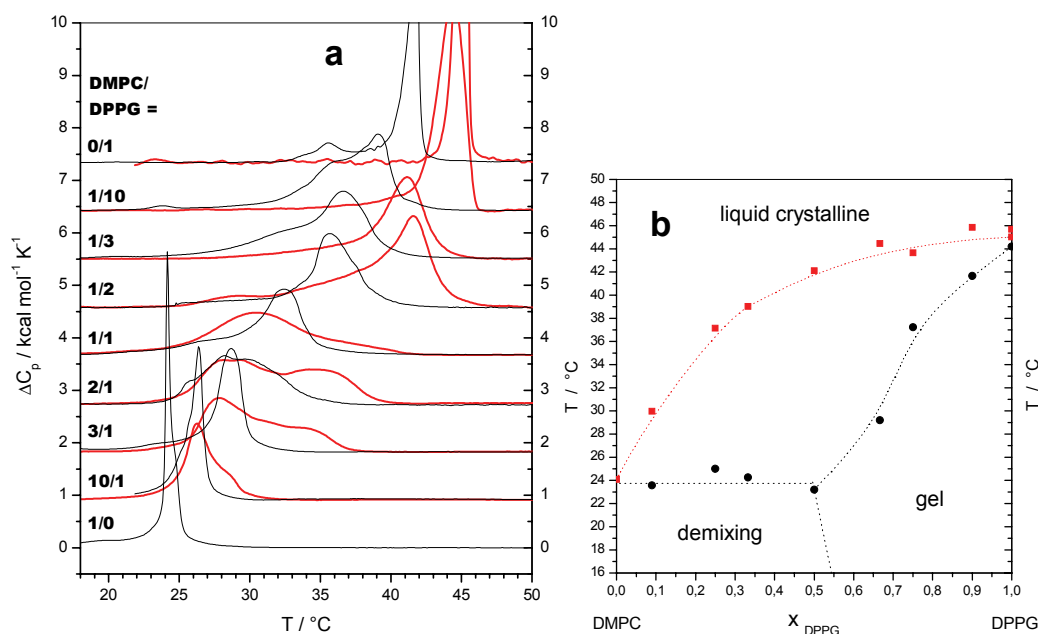


Figure 3.4: **a:** DSC plots of the phase transition range of different binary lipid mixtures DMPC/DPPG (—) and of the respective mixtures complexed with adequate amounts of PLL 220 to yield a lipid-to-peptide charge ratio of one ($R_c = 1$) (—). **b:** possible phase diagram for the mixture DMPC/DPPG being complexed with PLA 184 constructed from T_{on} (●) and T_{off} (■) of the red graphs shown in **a**. Measurements are performed in 100 mM NaCl solution at pH = 6.

For DPPC/DPPG mixtures the domain formation is not easy to observe, because the pure components have the same transition temperature. Therefore, we also investigated mixtures of DPPG with DMPC. These two components mix nearly ideally (Garidel et al. 1997b) and a 1:1 mixture has a transition into the liquid-crystalline phase that occurs at a temperature of 31°C, in between those of the pure components (DMPC: 24 °C, DPPG 41 °C). This DMPC/DPPG mixture has therefore the advantage that the transition peaks of DPPG- and DMPC-enriched domains will be much better separated. The results of the experiment of addition of different PLL to this lipid mixture in a mixing ratio of $R_c = 0.5$ are shown in Figure 3.3b. After addition of PLL the peaks split into two components at about 30 – 31 °C and 35 – 38 °C. The unequal distance from the original transition peak shows that the peptide binding domains are much more enriched in DPPG, than the free ones in DMPC. Again PLL 14 does not induce domain formation. The separation of the two transition components is the best pronounced for a PLL of intermediate chain length (PLL 123).

To achieve a more comprehensive view about the influence of PLL binding on the mixing behaviour of DMPC and DPPG we made a series of experiments with different DMPC/DPPG mixtures (Figure 3.4). It can be seen that the domain formation is especially pronounced in membranes with lower PG content. In these membranes PC molecules are excluded from the binding domain to increase its charge density. PLL binding does not lead to a splitting of the transition peak if the DPPG content of the membrane is higher than 50%. However, the transition peaks are shifted to higher temperatures and broadened. This indicates a wide gel/fluid co-existence range. The determination of the on- and offset temperatures allows a construction of a very rough phase diagram, which is presented in Figure 3.4. The nearly constant onset temperatures in the region of high PC content indicate a macroscopic gel phase demixing in this region. Equally, the appearance of constant offset temperatures over a certain range of compositions should indicate a demixing in the liquid crystalline phase. This might be the case for membranes with PG mole fractions greater than 0.6 (Figure 3.4b). At lower DPPG mole fractions T_{off} decreases continuously, indicating that no fluid-fluid demixing is encountered in membranes of these compositions. Nevertheless domains of different composition might form in the wide and asymmetric phase transition range.

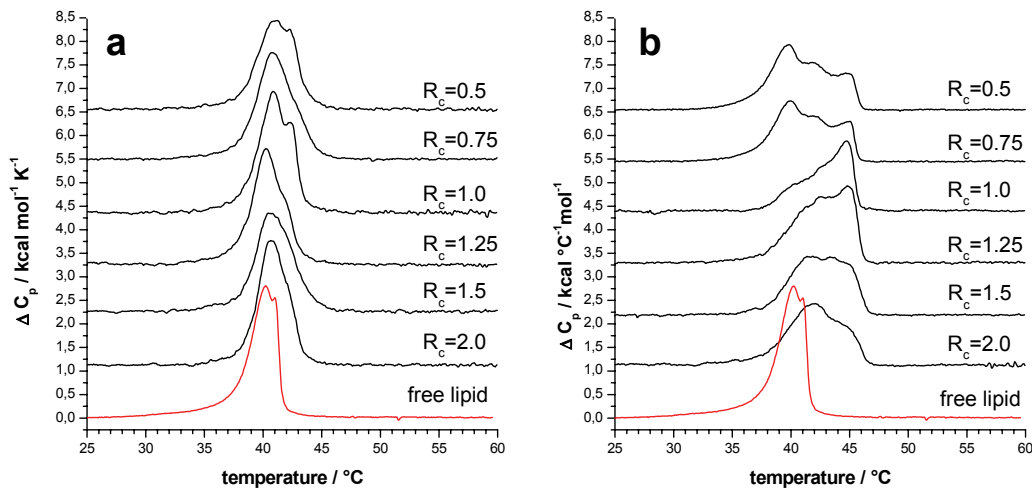


Figure 3.5: DSC plots of the complexes of DPPG/DPPC (1/1, mol/mol) and PLL 14 (a) or PLL 906 (b) in different mixing ratios R_c . Measurements are performed in 100 mM NaCl solution at pH = 6.

To study the influence of peptide content in the complexes (R_c) on T_m and on the domain formation, we made a series of experiments with various amounts of PLL bound to mixed DPPC/DPPG membranes (1:1 mol/mol). The properties should change with R_c up to the isoelectric point and beyond that we would expect a stable saturated complex. However, also charge overloading with charge reversal are possible (May et al. 2000). According to Franzin et al. (2001) domain formation should be most favourable for high lipid contents ($R_c > 1$) and long PLL chains. The results for complexes with the shortest and longest PLL ($n = 14$ and 906,

respectively) are shown in Figure 3.5. In Figure 3.5a the transition peaks for complexes with PLL 14 are rather narrow. Domain formation is probably not very pronounced or the domains are too small to produce a cooperative phase transition at increased in T_m which can be observed by the DSC experiment. The influence of R_c on the domain formation is small. Under similar experimental conditions also other authors (Carrier et al. 1985; Franzin and Macdonald 2001; Laroche et al. 1988) could not detect domain formation for short PLLs neither with PG- nor with PA or PS containing membranes. Nevertheless, also small molecules, as pentyllysine (net charge 5) or spermine (net charge 4) are able to induce lipid segregation at lower ionic strength of the solvent (Denisov et al. 1998) Also small synthetic polyelectrolytes may induce domain separation in mixed membranes (Macdonald et al. 2000). In contrast to the short PLLs for the sample with PLL 906 domain formation is much more obvious (Figure 3.5b), as the peaks are much broader and resolved into different components. This is consistent with the chain length dependence of domain formation mentioned above. In addition, we observed a clear influence of the peak shapes on R_c . The transition peak consists of three components, which was also observed in the binary DPPG/PLL complexes. For the charge neutralized complex ($R_c = 1$) the three components are less separated than in the case of lipid or peptide excess concentrations. The reason is probably the uniform coverage of the membrane surface. In the case of peptide excess ($R_c = 0.5$), the low temperature component has the highest intensity, whereas for $R_c = 1$ it is the high temperature component, and for lipid excess ($R_c > 1$) the intermediate one. The complex with $R_c = 1$ is the most favourable one and thus its transition temperature is the highest. For the complexes of $R_c > 1$ not all lipids are bound and consequently T_m is lower. Complexes formed with peptide excess are unfavourable because of steric reasons and electrostatic repulsion between the excess positive charges. The long polypeptide chains are probably only partially bound, the positively charged ends and loops extend into the solution and prevent further binding of other polypeptide molecules. Thus, optimal charge compensation cannot occur and the transition temperature is not as much increased as in the case of optimal binding and charge compensation.

3.3 Infrared spectroscopy

To obtain detailed information on which structures of the membrane are altered by PLL absorption and whether the secondary structure of the PLL changes upon binding we studied the complexes of PLL with the liposomes by FT-IR as a function of temperature, membrane composition and peptide chain length. These temperature dependent studies by FT-IR will be compared to the results of the DSC experiments. Figure 3.6 shows an example of an FT-IR spectrum of a DPPG/PLL complex with the characteristic vibrational bands at two different temperatures, below and above the phase transition temperature.

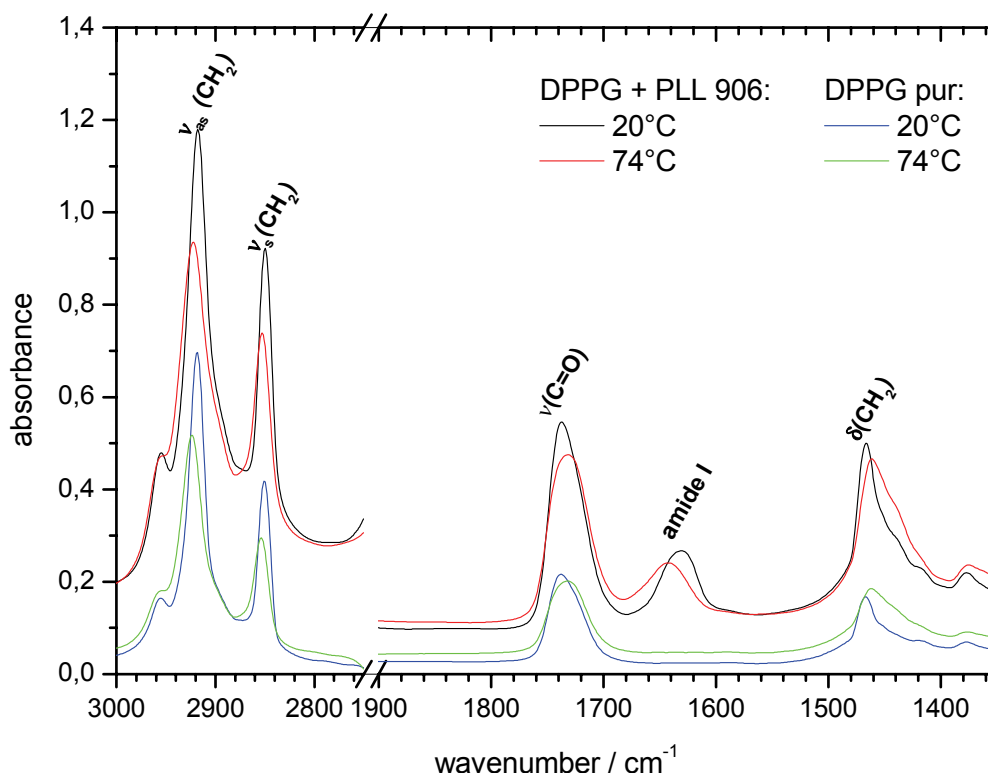


Figure 3.6: FT- IR spectra with all characteristic bands that are discussed in the text of the complexes of DPPG with PLL 906 at 20 °C (—) and 74 °C (—) as well as of an uncomplexed DPPG membrane at 20 °C (—) and 74 °C (—). Measurements are performed in 100 mM NaCl solution at pH = 6.

3.3.1 Pure DPPG membranes

The CH₂ stretching bands

The frequencies of CH₂-stretching vibrations ($\nu_{as}(\text{CH}_2)$, $\nu_s(\text{CH}_2)$) reflect the order of the acyl chains in the hydrophobic region of the membrane. Highly ordered acyl chains with all trans conformation as observed in the gel phase lead to lower vibrational frequency. With increasing fractions of gauche isomers and decreasing van der Waals attractions in the liquid-crystalline phase the absorption maxima of the stretching bands will be shifted to higher frequency (Tamm and Tatulian 1997)⁶. In Figure 3.7 the frequency of the symmetric CH₂ stretching vibration ($\nu_s(\text{CH}_2)$) of pure and complexed DPPG is plotted against temperature.

⁶ A more detailed discussion of the frequency shift of the methylene stretching vibrations is given in chapter 4.5.1.

The transition from gel to liquid crystalline phase is clearly visible by the increase in frequency. The transition temperature determined by FT-IR compares well with the DSC results. Again we find an increase of T_m upon PLL binding, which is more pronounced for the longer polypeptide chains. As observed before in the DSC we see indications for domain formation in the samples prepared with the longer PLL (402 and 906), where the traces show a two step transition. We conclude that even though concentrations in the DSC and the IR experiments are different, similar results are obtained meaning that a change of total concentration has no measurable effect on the system behaviour.

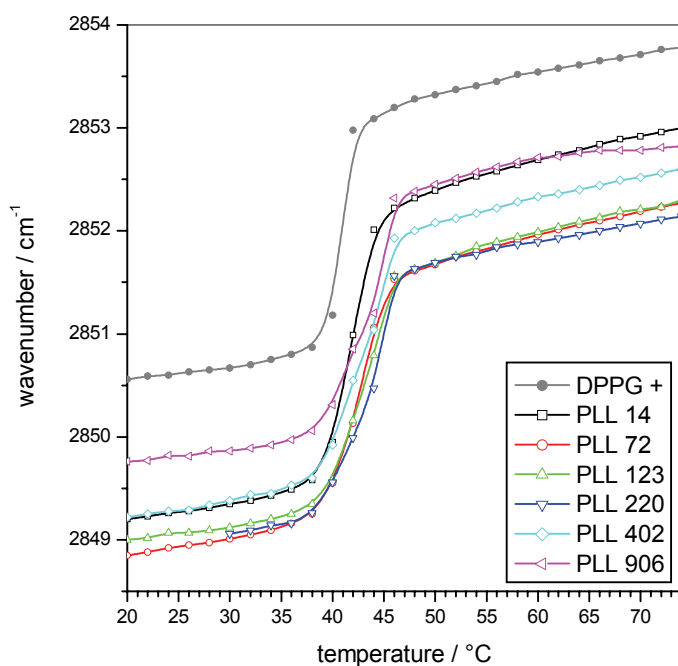


Figure 3.7: Wavenumber of the maximum of the $\nu_s(\text{CH}_2)$ vibrational band in complexes of DPPG with PLL of different chain length. The lipid-to-peptide mixing ratio $R_c = 1$. The presented data are recorded in the cooling scan.

The CH_2 stretching vibrations of the DPPG/PLL complexes are shifted to lower wavenumber in both, the gel and the liquid crystalline phase. This indicates, that the binding of PLL probably induces a higher order in the hydrophobic part of the membrane. The screening of the negative membrane charges by the bound peptide allows a better packing of the lipid molecules. The increase in conformational order of the acyl chains and the increase intermolecular vibrational coupling of the methylene stretching vibrations is also discussed by (Carrier and Pezolet 1984) who compared Raman intensities. These effects might be due to a decreased tilt angle as it was stated by (Takahashi et al. 1992), which would enhance the van der Waals contact area.

The extent of the wavenumber shift depends again on the PLL chain length. Intermediate length PLL (PLL 72 – 220) causes the largest downshift in vibrational frequencies, whereas shorter and longer PLL cause a smaller shift. Interestingly, the smallest shift is caused by the longest PLL 906. T_m and the wavelength of the absorption maxima do not show the same the same chain length dependence (Figure 3.11b). Neither the absolute wavenumber, nor the wavenumber shift between the gel and liquid-crystalline phase are directly correlated with T_m . Obviously, the increased order in the hydrophobic region is not the only factor that influences T_m . Otherwise it might also be that other factors than order influence the wavenumber of the methylene stretching vibrations. This will be more extensively discussed in chapter 4.5.1.

The low wavenumbers for the CH_2 stretching bands are only reached after one heating and cooling cycle of the whole system. After addition of PLL to a DPPG membrane at room temperature only a slight change in the spectrum will be observed. Only when the membrane has passed into the liquid-crystalline phase the system is able to organize to an energetically favourable structure. Therefore, only data recorded in the cooling scan are presented. The presence of a meta-stable phase before the first heating was also observed in the DSC experiments.

The lipid C=O band

Characteristic vibrational bands of the headgroup region are the carbonyl stretching vibration (ν_{CO}) and the phosphodiester band. The wavenumber of these bands is influenced by hydrogen bonding to water or to other hydrogen bond donor groups. For stronger hydrogen bonds and/or more hydrogen bond donors the vibrational frequency of the lipid ester C=O group will be shifted to lower wavenumber (Blume et al. 1988). Therefore the C=O stretching band is a good indicator for the hydration of a membrane in the headgroup region. Actually, the observed band profile is due to at least two underlying bands separated by ca. 15 cm^{-1} originating from non-hydrated and hydrated C=O groups (Blume et al. 1988). In Figure 3.8 the position of the absorption maximum is plotted against the temperature. At the phase transition the wavenumber of the band is downshifted, because the intensity of the lower frequency C=O band increases, i.e. the membrane is better hydrated in the liquid-crystalline phase than in the gel phase. Comparing the lipid/PLL complexes with the free DPPG membrane, we observe a small downshift in C=O band frequency upon PLL addition. The chain length dependence is less pronounced than for the CH_2 vibrations, but follows the same tendency. By PLL adsorption, the available space for hydration water will be reduced, because complexes with stacked bilayers are formed that are bridged by PLL. The water of hydration will be shared by bound PLL and the lipid headgroups. The lower frequency of the C=O band for the complexes indicate that the water molecules form slightly stronger and better directed hydrogen bonds to the lipid carbonyl groups. This effect is more pronounced in the gel phase than in the liquid-crystalline phase. A shift of the carbonyl band to lower wavenumbers was also explained with

the formation of intermolecular hydrogen bonds between the carbonyls and the headgroup phosphates in quasi-crystalline subgel phases (Epand et al. 1992; Zhang et al. 1997). However, in these cases a band developed at 1732 cm^{-1} . In the present cases no such component could be shown, neither by Fourier self deconvolution nor in the second derivative spectra. In any case the lower wavenumbers of the carbonyl stretching band is an indication for better ordering in the headgroup region of the membranes.

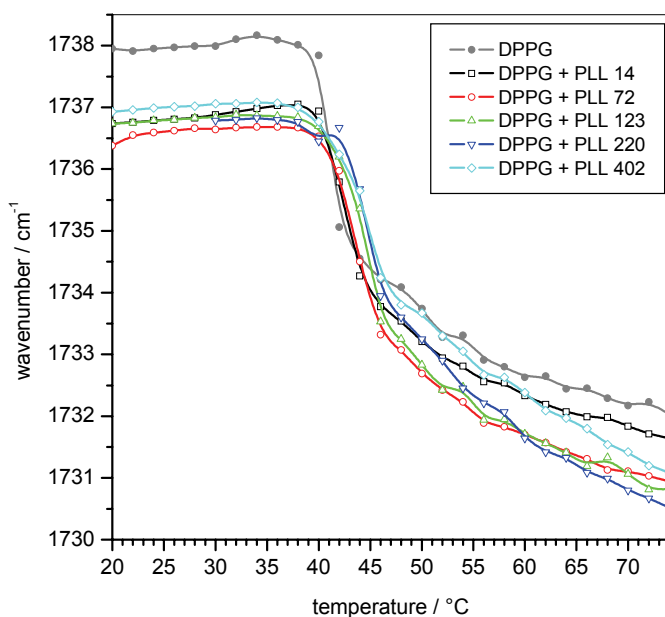


Figure 3.8: Wavenumber of the maximum of the $\nu(\text{CO})$ vibrational band in complexes of DPPG with PLL of different chain length. The lipid-to-peptide charge ratio $R_c = 1$.

The peptide amide I band

Analysis of the amide-I absorption band gives information about the secondary structure of the peptide. PLL has the ability to adopt the three most common secondary structures, the α -helix, β -sheet, and random coil (Greenfield et al. 1967). In neutral solution PLL forms a random coil. Increasing the pH value over 10.5, which is the pK value of the lysine side chain, it adopts an α -helix at low temperatures and a β -sheet after heating above $50\text{ }^\circ\text{C}$ (Carrier et al. 1990). The corresponding amide-I reference bands are given in Jackson et al. (1989) and could be reproduced here (Figure 3.9). The β -sheet gives a sharp band with a maximum at 1611 cm^{-1} and a less intense one at 1680 cm^{-1} . The amide I vibration of the α -helix is found at 1637 cm^{-1} with a shoulder at about 1623 cm^{-1} and that of the random coil structures at 1644 cm^{-1} . Compared to proteins, these bands are found at unusually low wavenumbers. Jackson et al. (1989) assigned this peculiarity of PLL to a better vibrational coupling of the transitional dipole moments in a homopolypeptide and extremely high polar interactions with the solvent.

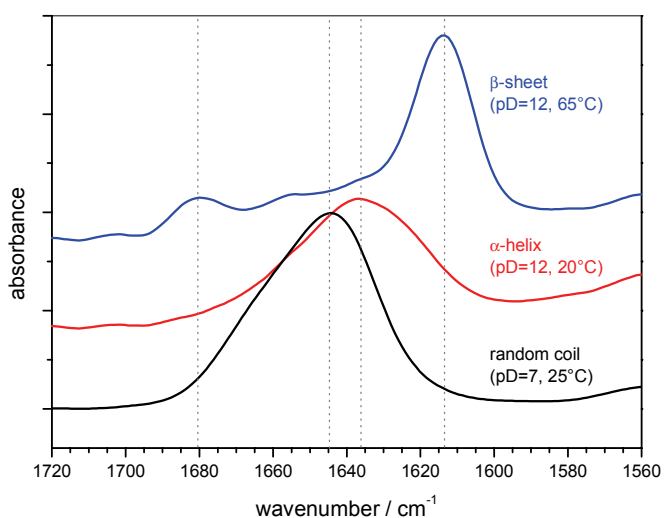


Figure 3.9: Amide I bands of PLL 123 at three different conditions resulting in random coil (—) (pD = 7, 25 °C), α -helix (—) (pD = 12, 20 °C) and β -sheet (—) (pD = 12, 65 °C) secondary structure.

The amide I bands observed for the DPPG/PLL complex are a superposition of the helix and the random coil component, which can be identified by calculating the 2nd derivative spectrum. An example of an experimental amide I band of a DPPG/PLL complex at two different temperatures is shown in Figure 3.10. It is evident that the global band position of the amide I band shifts to higher frequency at higher temperature. In the 2nd derivative spectrum it can be seen that a band corresponding to an α -helix is evident at lower temperature and that at higher temperature only a band characteristic for a random coil is present. For the interpretation of the experiments at different temperature we used for simplification the global maximum of the amide I band. Its position is plotted in Figure 3.11a as a function of temperature for different DPPG/PLL complexes. The band frequency is in the range typical for an α -helix or a random coil conformation. The shortest peptide PLL 14 always stays in a random coil structure. All longer peptides can form α -helices when bound to gel phase lipids with a remaining fraction being in random coil conformation. We observe a clear chain length dependence: the longer the polypeptide, the lower the wavelength of the amide I band, i.e. the higher the proportion of α -helix. This can be explained by the higher binding constant of longer polypeptides. The analysis of the 2nd derivative spectra reveals similar trends, namely that the low frequency band at 1623 cm⁻¹ characteristic for a bent α -helix (Jackson et al. 1989) becomes more intense at the expense of the component at 1638 cm the longer the PLL chain length is.

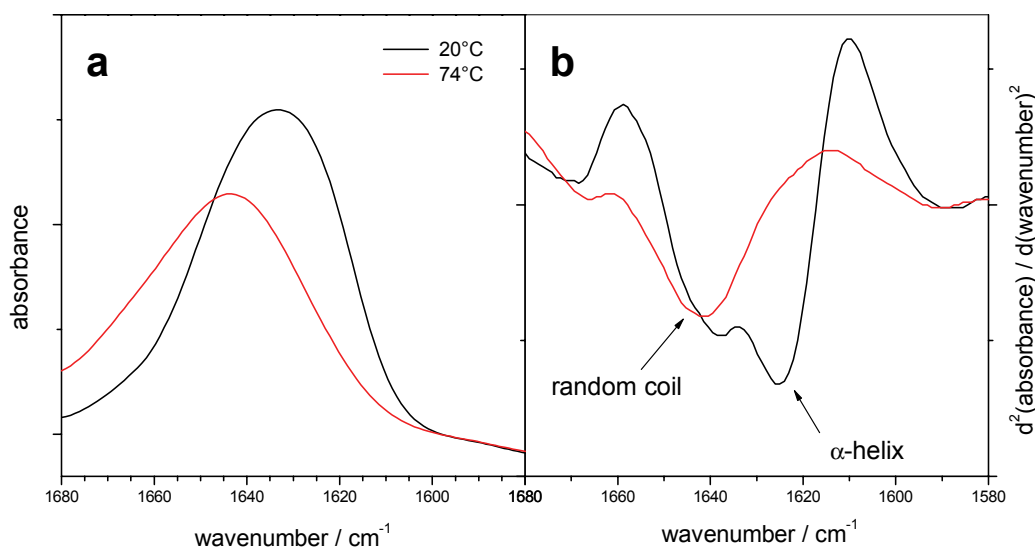


Figure 3.10: Amide I band of the complex DPPG/PLL 220 at 20 °C (—) and 74 °C (—) (a) and its second derivative spectra (b).

With increasing temperature the maximum of the amide I band is shifted to higher wavenumbers in all complexes, i.e. the fraction of random coil structure increases. This is apparently caused by a lowering of the charge density of the membrane at the phase transition and/or a concomitant desorption of PLL from the membrane surface. However, the peptide cannot be completely desorbed, because we still observe a remarkable influence on the CH₂ and C=O stretching vibrations in the fluid crystalline phase. Moreover isothermal titration calorimetric (ITC) experiments show that PLL binds to liquid crystalline vesicles in a 1:1 stoichiometry (see below). Therefore we assume that PLL in a random coil conformation remains bound to the membrane surface. Only for the complex DPPG/PLL 72 and DPPG/PLL 123 is the α-helix to random coil transition partially coupled to the lipid phase transition as indicated by the larger wavenumber shift at T_m . For the longer peptides we just see a continuous increase in wavenumber with increasing slope over the whole temperature range. In no case a β-sheet is observed, as can be concluded from the lack of a low and high frequency components at about 1611 and 1680 cm⁻¹, respectively, in the 2nd derivative spectra. Whereas in the bulk phase at increased pH α-helices transform to β-sheets with rising temperature, the membrane seems to stabilize the helical conformation. Obviously the charge neutralization that is achieved by binding to an oppositely charged membrane surface is not completely comparable with the charge removal that is achieved by deprotonation.

Similar results were also reported by Carrier and P  zolet (1984), who observed α-helices bound to DPPG in the gel phase by Raman spectroscopy. They also stated that short PLLs do not form α-helices on membrane surfaces (Carrier and P  zolet 1986). However, they studied only two different chain lengths of PLL and determined the structure only at 20 °C. We now

present for the first time information about the complete thermotropic behaviour of PLL bound to DPPG membrane. In contrast to the results published by Carrier and Pézolet (1984) and our own results shown here, Fukushima et al. (1989) claimed that PLL binds in 50% α -helical and in 50% β -sheet structure to pure DMPG membranes as deduced from CD data. The drawback of this work is that the authors measured in the transition range of a complexed DMPG membrane at 25 °C and at very low ionic strength. The lack of additional salt leads on one hand to an increased electrostatic interaction, but on the other hand it complicates the phase transition of DMPG even more (Schneider et al. 1999). Thus, the membrane state was not well defined in their measurements and different peptide conformations might well arise from peptide being bound to different membrane structures.

Interestingly, we find that the phase transition temperature T_m of DPPG is much better correlated with the secondary structure of the peptide than with the hydrophobic order or the headgroup hydration. PLL 14 that adopts only a random coil structure increases T_m only slightly, whereas all peptides that are bound as α -helices increase T_m much more and with the same chain length dependence, as found for the tendency for α -helix formation.

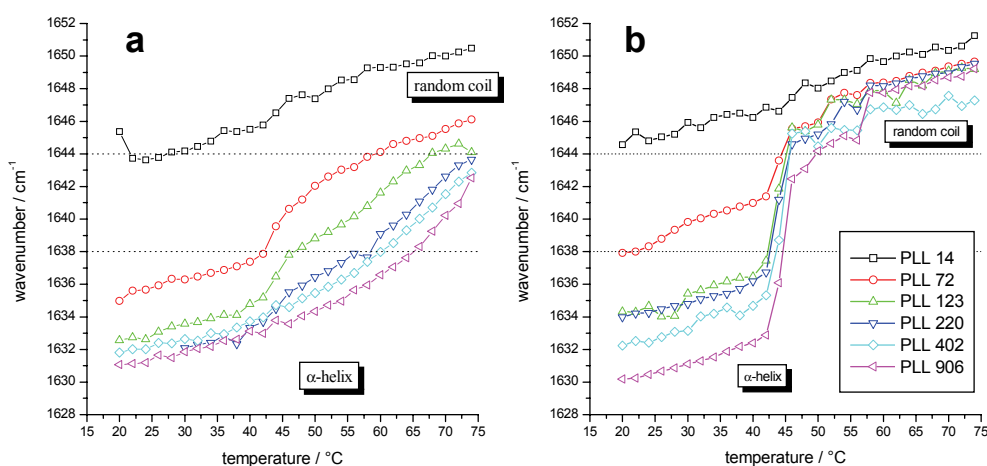


Figure 3.11: Wavenumber of amide-I vibrational band maxima of PLL bound to pure DPPG membranes (a) and DPPC/DPPG mixed membranes (1/1 mol/mol) (b). The lipid-to-peptide charge ratio $R_c = 1$. The dotted lines indicate the typical frequencies for α -helical (1638 cm⁻¹) and random coil (1644 cm⁻¹) structures.

3.3.2 PLL complexes with mixed DPPG/DPPC membranes

We performed IR experiments also with mixed DPPG/DPPC membranes (1/1, mol/mol). In the spectral range of the CH₂ and the C=O vibrations all the tendencies for shifts in frequency are very similar to the pure DPPG system. However, the frequency shift of the amide I band is remarkably different (Figure 3.11b). In the gel state of the DPPG/DPPC membrane the secondary structure of the bound peptide is similar to that one we observed for pure DPPG,

namely α -helical for all longer PLL. But at T_m the wavenumber of the amide I band suddenly increases strongly and shifts to values larger than 1644 cm^{-1} . In the liquid-crystalline phase of the DPPG/DPPC membrane all peptides form almost exclusively random coils.

This behaviour could be explained by the reduced surface charge density in liquid-crystalline mixed DPPG/DPPC membranes. To form α -helices the positive charges of the lysine side chains need to be neutralized. In bulk solution this can be accomplished by a change in pH to values higher than the pK value of the side chain, i.e. a deprotonation of the terminal ammonium group of the side chain. When the peptide adsorbs to a pure DPPG membrane, the positive charges are neutralised by the negative membrane potential. After co-addition of neutral lipids, i.e. DPPC, the negative surface potential of the membrane might be too low to neutralise the lysine side chain charges, preventing the formation of a defined α -helical secondary structure. Therefore all PLL will bind as random coil to an ideally mixed DPPG/DPPC membrane in the fluid state.

However, the peptide is bound as α -helix to gel state DPPG/DPPC membranes. This indicates that PLL binding definitely must induce domain formation in the gel phase membrane. The DPPG molecules will move to the PLL binding sites, thus forming negatively charged domains that offer a high enough surface charge density for the PLL to form an α -helical structure. These domains will coexist with DPPC rich domains with lower surface charge density. Due to their higher lateral mobility in the fluid membrane state, the lipids will remix after passing the phase transition temperature. Consequently the regions of high negative surface charge disappear and a sudden change of the peptide secondary structure from α -helix to random coil is induced at the main transition temperature. This leads to a system, where a secondary structure change of a membrane bound peptide is triggered by the phase transition of the membrane itself. The only results that point in the same direction were published by Laroche et al.(1988), who found that short PLL (ca 20 monomers) being bound to DPPA membranes undergoes β -sheet to random coil transition upon heating above the membrane phase transition.

The notion of domain formation in the gel phase of mixed membranes induced by bound peptides is supported by an additional FT-IR spectroscopic experiment. To be able to detect the phase transitions of hypothetical domains separately, we used binary lipid mixtures, in which one component had perdeuterated acyl chains. This allows us to simultaneously observe the CH_2 and the CD_2 stretching vibration that are due to the isotopic shift of the CD_2 vibrations to lower wavenumbers well separated in the spectra. These two bands reflect the behaviour of the DPPG and the perdeuterated DPPC component, respectively. If the lipids demix in the gel phase and organize in different domains of which one is bound to PLL, we should observe slightly different transition temperatures for the perdeuterated DPPC and the non deuterated DPPG component. Similar experiments were performed to prove domain formation on mixed LPS/DMPE and DMPA/DMPC membranes upon interaction with PLL by Lasch et al. (1998)

and Laroche et al. (1988). Our results are shown in Figure 3.12. We see that the two lipids undergo their main transition at two slightly different temperatures, indicating that they are organized in separate domains. The second derivatives of the wavenumber plots presented in Figure 3.12b reveal that a minor fraction of either lipid still contributes to the transition of the other component. That signifies that the lipids are not completely separated, but that a small quantity of DPPC is present in the DPPG domains and vice versa. The relative intensity changes observed in the plots in Figure 3.12 indicate that the DPPG-rich domains contain less DPPC than the DPPC-rich domains contain DPPG, i.e. the miscibility gap induced by the PLL is not symmetric.

The well separated transition temperatures indicate that PLL is only bound to one domain, namely the DPPG rich domain. The DPPC rich domain undergoes its transition at the same temperature as in the absence of PLL. Due to the lack of charges PLL will not interact with DPPC molecules. This was proven by DSC and FT-IR experiments with pure DPPC membranes (results not shown). However, the DPPG rich domains undergo its transition at a temperature that was also found for pure DPPG membranes complexed with PLL.

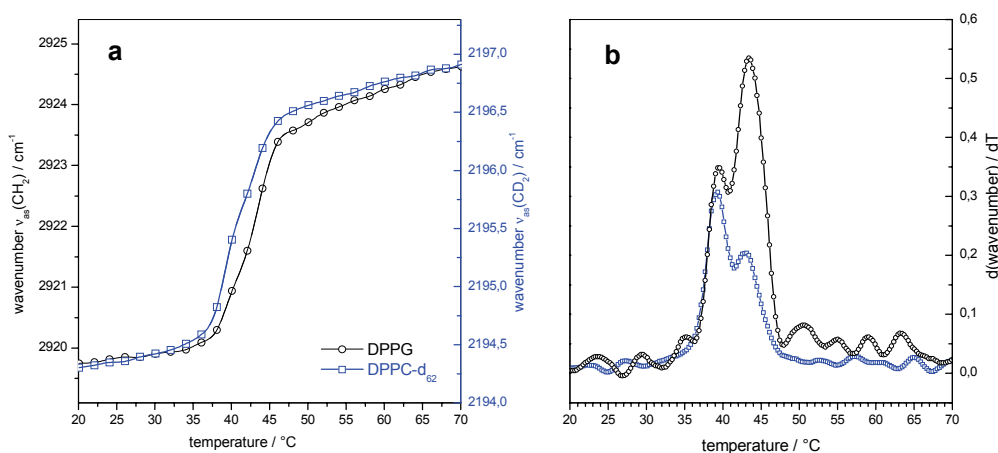


Figure 3.12: Temperature dependence of the antisymmetric methylene stretching vibrations of DPPG (circles) and deuterated DPPC (squares) in a equimolar mixed membrane, which is complexed with PLL 906, $R_c = 1$ (a) and its first derivatives (b). The derivative was taken after interpolating the data with a spline function. The peak maxima in (b) indicate the transition temperatures of either lipid species.

3.4 Isothermal titration calorimetry

To get deeper insight in the binding mechanism of PLL to PG membranes we performed a series of ITC experiments. ITC experiments suffer from the aggregation of the vesicles upon PLL binding, which makes the experiments difficult to interpret. Thus we were not able to determine all the binding parameters that can normally be deduced from ITC experiments. Nevertheless, some general trends can be elucidated. All experiments presented in this chapter

are done by titrating vesicle suspensions into the ITC cell, which was filled with PLL solutions. Titrations that were performed in the other direction (PLL into vesicle suspension) did not give reproducible results. We performed binding studies in dependence on the membranes phase state, the PLL chain length and the temperature within one membrane phase. To study the temperature dependent binding of PLL to fluid state PG membranes we used besides the saturated DPPG also unsaturated POPG, which, due to its lower T_m , allowed us to measure at moderate temperatures.

3.4.1 Phase dependent binding

After FT-IR experiments showed that PLL binds in different manner to gel and to fluid state membranes, we performed ITC measurements below ($30\text{ }^\circ\text{C}$) and above ($60\text{ }^\circ\text{C}$) T_m of DPPG vesicles. Figure 3.13 shows the heat profile of the titration of DPPG vesicles in either phase state to a PLL 402 solution. In both phases the binding is exothermic.

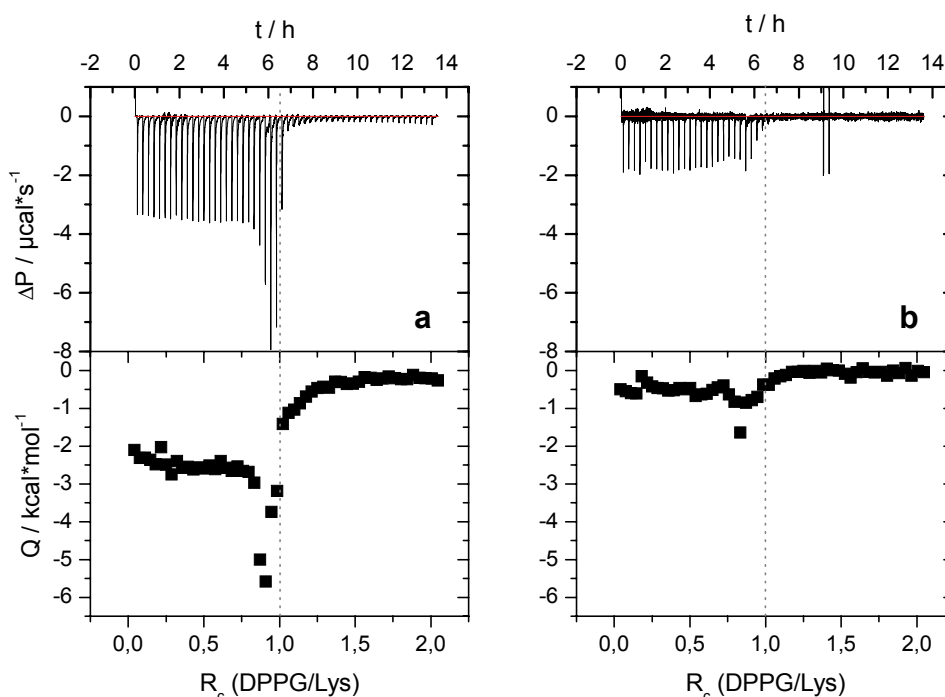


Figure 3.13: Titration of DPPG vesicles (20 mM) in into PLL 402 solution (2 mM) at $30\text{ }^\circ\text{C}$ (a) and at $60\text{ }^\circ\text{C}$ (b). Top: differential heating power vs. time. Bottom: integrated heats of reaction normalized to amount of injected DPPG vs. molar ratio R_c . Scales in (a) and (b) are chosen identical for better comparison.

However, the binding to a gel phase membrane (Figure 3.13a) is much more exothermic than the binding to a fluid state membrane (Figure 3.13b). The total heat that is released during the titration up to a mixing ratio of $R_c = 1$ is -2.79 kcal/mol in case of gel phase binding as

opposed to $-0,58$ kcal/mol in the case of fluid state binding. This difference between the binding enthalpies of gel and fluid phase binding should be reflected in the phase transition enthalpy of the DPPG/PLL complex. If binding lowers the total enthalpy of the system in gel phase and does only marginally affect the enthalpy of the liquid crystalline phase, the phase transition enthalpy of the complexes should be consequently higher than that of a pure membrane⁷. This finding correlates well with the stabilisation of the gel phase, which was detected by DSC.

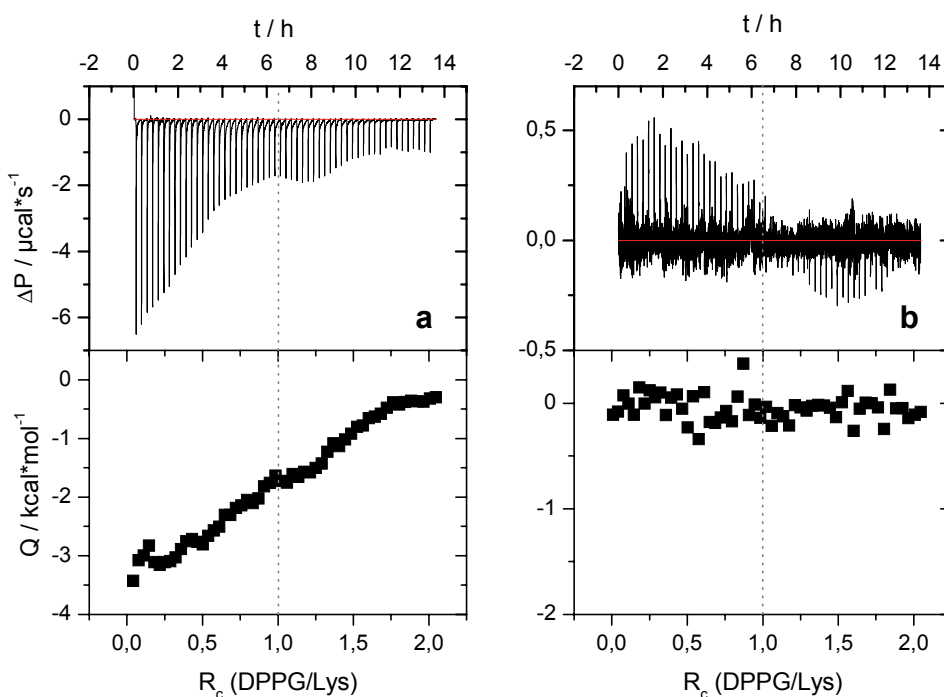


Figure 3.14: Titration of DPPG vesicles (20 mM) in into PLL 14 solution (2 mM) at 30 °C (a) and at 60 °C (b). top: differential heating power vs. time. Bottom: integrated heats of reaction normalized to amount of injected DPPG vs. molar ratio R_c . Note the different scales in a and b.

An interesting feature of the differential binding isotherms is the deviation of the normal sigmoidal shape just before the saturation ratio is reached. Before the binding saturates the released heat increases noticeably, producing a pronounced minimum in the differential binding isotherm. Thermodynamically this behaviour can be described by a sudden onset of a high cooperativity (Heimburg and Biltonen 1994; Mosior and McLaughlin 1992b). The mechanistic origin, though, is not very clear. There are some possible explanations: 1.) The proximity of the minimum to the isoelectric point ($R_c = 1$) suggests that the additional enthalpy arises from vesicle aggregation. However, aggregation is observed also at R_c values higher and lower than unity. 2.) It is possible that the vesicles rupture or form pores as the R_c value gets

⁷ This correlation will be more intensively discussed in section 4.3.

closer to one. This gives excess PLL, that is still present in the calorimeter cell, access to the lipids of the inner monolayer. The sudden rise in potential binding sites might produce the highly negative enthalpies. The assumption that pores form preferentially at R_c close to charge neutralization ratio has been proven by dye release measurements (see chapter 4.6 and Reuter et al., unpublished results) Furthermore the saturation ratio of $R_c = 1$ suggests that every lipid molecule binds one lysine residue, i.e. the inner monolayer of the vesicles must be accessible at some point during the titration. 3.) Structural transitions of either the lipid or the peptide might be triggered by the binding. Apart from having an own enthalpic contribution this transitions might increase the binding constant. Only this case can be regarded as a true cooperative event (Heimburg and Biltonen 1994). Structural transitions of the peptide have been shown by FT-IR spectroscopy (see chapter 3.3). It has also been shown that the binding constant (estimated from the influence on T_m) correlates with the helical content of the peptide. Especially the short peptide PLL 14, which does not adopt α -helical structures, has been shown to behave differently than longer PLLs.

This difference can also be shown by ITC experiments (Figure 3.14). PLL 14 binds with a much lower binding constant to DPPG gel state membranes than PLL 402, as can be estimated from the lower slope of the differential binding isotherm in the saturation range. In the case of PLL 14 binding to fluid state DPPG nearly no binding enthalpy could be detected. Nevertheless, IR experiments showed that also PLL 14 has an influence on fluid DPPG membranes. This indicates that the association of PLL 14 with fluid DPPG membranes has mainly entropic contributions.

It has to be noted that the comparability of ITC and IR experiments is limited, as the applied concentrations are different. The higher absolute concentrations used in IR spectroscopy would lead to noticeable amounts of complex formation even if the binding constant is low. PLL 14 binding does not produce the minimum in the differential binding isotherm that has been detected for all longer PLL. This can be regarded as an indication that helix formation is involved in the cooperative event described above. Furthermore, it is noticeable that binding of PLL 14 does not saturate at $R_c = 1$, as it is the case for all longer PLL. Rather, binding events are detected up to $R_c = 2$. At this ratio every second lipid binds one lysine residue. This suggests that PLL 14 binds only to the outer monolayer of the vesicles and that the lipids of the inner monolayer are not accessible. That implies that PLL 14 binding does not affect the integrity of the vesicles. This observation supports the thesis that a rupture of the vesicles is responsible for the minimum in the differential binding isotherms that is observed for the binding of longer PLL.

3.4.2 Chain length dependent binding

DSC and IR experiments showed that the influence on the membrane phase behaviour and structure is dependent on the PLL chain length. To directly prove that the binding behaviour is chain length dependent, we undertook ITC experiments with different PLL. Figure 3.15 shows the titration curves of POPG titrated to PLL of different chain length at 20 °C. It is clearly visible that the titration profiles exhibit a chain length dependent trend. Every single titration step is followed by a well dissolved biphasic equilibration. This means that two distinct binding (or transition) processes take place, one being endothermic and the other exothermic in nature. The endothermic process decays faster than the exothermic one. The enthalpic balance between the two processes is dependent on the PLL chain length.

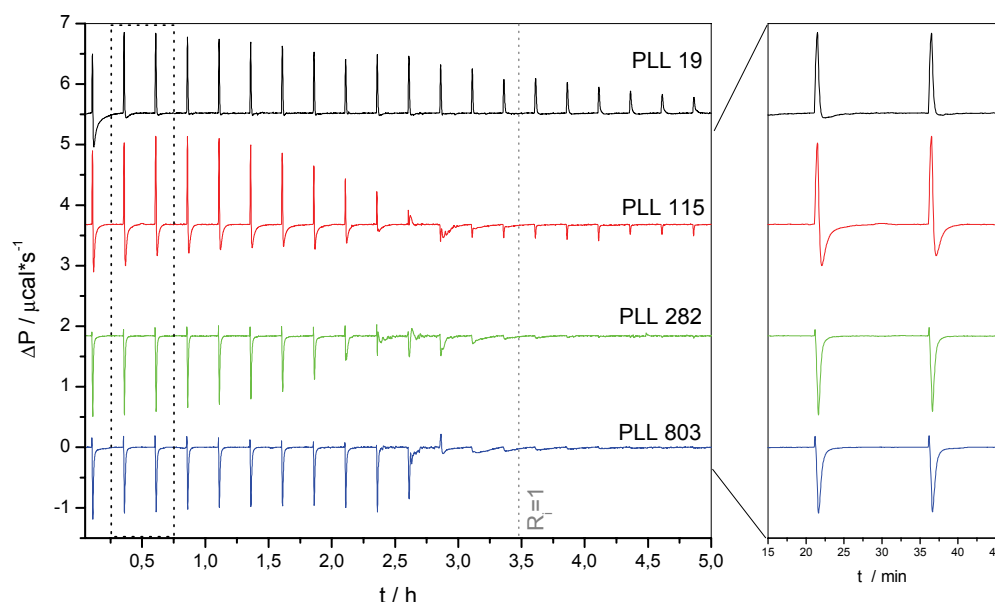


Figure 3.15: Titration of POPG (20 mM) into solutions containing PLL of different chain length at 20 °C. Differential power vs. time plots. For clarity curves are shifted along the y-axis. The right sketch is a close up of titration steps 2 and 3.

As the chain length of PLL increases the exothermic process increasingly dominates the endothermic one. The total enthalpy at saturation is positive for the binding of PLL 19 and negative for the longer PLLs. Especially well dissolved are the two components in the case of PLL 115 binding to POPG membranes.

The occurrence of both, exo- and endothermic binding processes during one titration has also been reported by Ramsay et al. (1986) for the case of myeline basic protein binding to PS membranes and by Heimburg et al. (1994) for the binding of cytochrom c to PG membranes. Both proteins have regions of high lysine accumulation and bind electrostatically to negatively

charged membranes. The authors claim the existence of two different binding events. Whereas Heimburg et al. explain their results with the binding to two different states of the lipid, Ramsay et al. postulate that the exothermic component originates from a “strong association” of the protein with the lipids and the endothermic component from superficial binding and vesicle aggregation. Both explanations may be adopted for the here presented case.

In addition we have to consider the enthalpy of the secondary structure transition of PLL upon binding. The random coil to α -helix transition that has been shown by FT-IR is an exothermic process and may contribute to the over all enthalpy with as much as -1,1 kcal/mol of residues (Chou and Scheraga 1971; Wieprecht et al. 2002). The exothermic contribution of the helix formation explains also the observed chain length dependence because the IR experiments showed that the helical content of the polypeptide increases with the peptide chain length. Wieprecht et al. (2000a; 2000b; 1999) showed for several examples that the helix formation is an important driving force for membrane association and accounts for up to 70% of the total binding enthalpy. Furthermore it has been shown that also the insertion of peptide side chains in the hydrophobic part of the membrane can produce an exothermic reaction enthalpy (Gazzara et al. 1997; Wieprecht et al. 1999). Such interactions are referred to as the “non-classical hydrophobic effect” (Seelig 1997). Monolayer experiments (see below) suggest that such interaction take place and contribute to the over all reaction enthalpy.

The endothermic component of the titration peaks decays fast and always precedes the slower exothermic one. It might originate from the first superficial electrostatic association that is driven by the entropy gain of released counterions and water molecules.

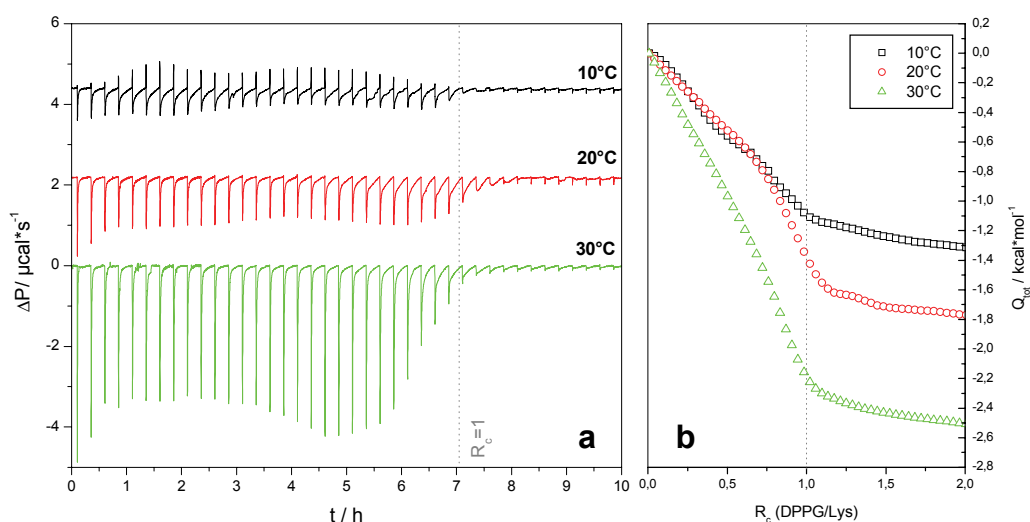


Figure 3.16: Titration of DPPG (20 mM) into a PLL 47 solution (2 mM) at different temperatures below T_m . **a:** differential heating power vs. time. For clarity curves are shifted along the y axis. **b:** total heats of reaction per mol of lysine residue.

3.4.3 Temperature dependent binding

Different binding processes show different temperature dependence. Thus, temperature dependent determination of the binding enthalpy is a tool to elucidate the nature of the binding processes. We undertook temperature dependent binding studies with gel phase membranes (Figure 3.16) as well as with fluid state membranes (Figure 3.17). In both cases the endothermic component that is present at low temperature vanishes as the temperature increases. In contrast, the exothermic component increases, i.e. gets more negative, with increasing temperature.

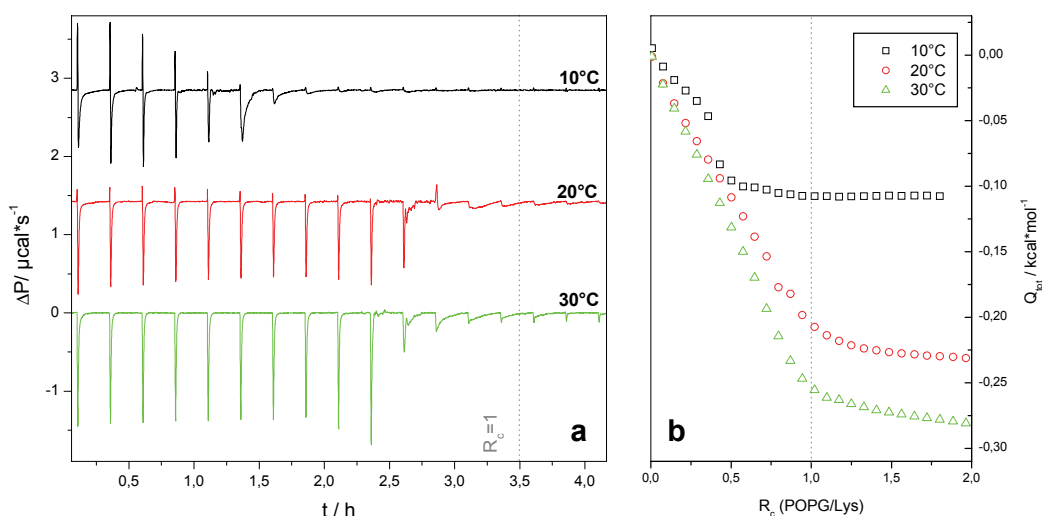


Figure 3.17: Titration of POPG (20 mM) into a PLL 803 solution (2 mM) at different temperatures above T_m . **a:** differential heating power vs. time. For clarity curves are shifted along the y axis. **b:** total heats of reaction per mol lysine monomer.

In the case of titrating fluid POPG vesicles into PLL solution the equilibration kinetic seems to be monophasic after the endothermic vanished at higher temperatures and low lipid contents. But in the vicinity of the saturation another slow exothermic process is showing up. In the case of titrating PLL with gel state DPPG vesicles this third process is already detected at lower temperatures and lower lipid to peptide ratios R_c . But also in this case the contribution of this process is increasing towards the saturation ratio. Probably it can be assigned to vesicle aggregation and/or pore formation.

The overall enthalpy gets more negative with rising temperature for both gel state and fluid state binding. After an estimation of the binding enthalpies from the total heats recorded till saturation the heat capacity change ($\Delta_R C_p$) can be determined according to:

$$\frac{\partial \Delta_R H}{\partial T} = \Delta_R C_p \quad (8)$$

For gel phase binding $\Delta_R C_p$ is $-59.7 \text{ cal mol}^{-1} \text{K}^{-1}$ ($-250 \text{ J mol}^{-1} \text{K}^{-1}$) and for fluid vesicle binding $-8.3 \text{ cal mol}^{-1} \text{K}^{-1}$ ($-31 \text{ J mol}^{-1} \text{K}^{-1}$) (Figure 3.18). The negative values indicate that hydrophobic interactions take place. In case of the gel phase binding an additional effect might arise from a hydrophilic hydration in the headgroup region, which would also produce a negative $\Delta_R C_p$. Hints for a better hydration of the carbonyl groups are given by IR spectroscopy (see Figure 3.8). Enthalpies that originate from helix formation should be reduced with increasing temperature because the helicity of the peptide is reduced as the temperature rises (Figure 3.11). Thus the helix formation on the membrane surface should contribute with a positive $\Delta_R C_p$. This effect is more pronounced in the fluid phase than in the gel phase, as the helicity is much more affected by temperatures above the phase transition (see Figure 3.11). Therefore, this effect lowers the absolute values of $\Delta_R C_p$ for fluid phase binding more than in the case of gel phase binding.

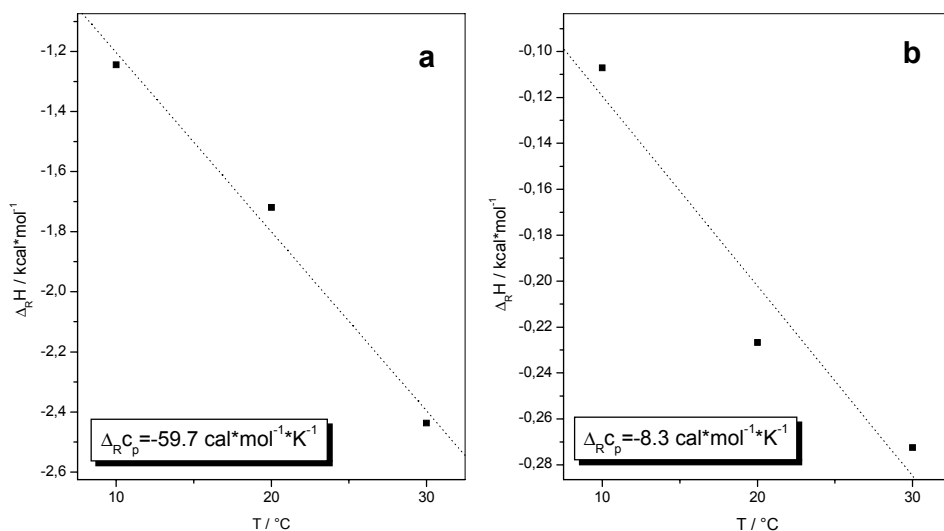


Figure 3.18: Temperature dependences of estimated reaction enthalpies of the titration of gel state DPPG vesicles into PLL 47 (a) and fluid state POPG vesicles into PLL 803 (b).

To reveal the contribution of helix formation to the total binding enthalpy and to its temperature dependence we performed additional experiments with poly(D,L-lysine) (PDLL). PDLL is a statistic copolymer of D-lysine and L-lysine. The inserted D-enantiomers prevent the formation of chiral superstructures as α -helices. Thus, titration experiments with PDLL can be used to measure binding enthalpies of polylysine without the contribution of helix formation. The helix formation enthalpy can then be calculated as:

$$\Delta H^{helix} = \Delta H^{PLL} - \Delta H^{PDLL} \quad (9)$$

The result of titrating a PDLL solution with POPG vesicles is shown in Figure 3.19. The enthalpy of PDLL binding is even positive under the same conditions where the enthalpy of

PLL binding is negative. The difference between the respective enthalpies is exothermic and can be assigned to helix formation. The determined value of $-288 \text{ cal mol}^{-1}$ is low compared to values given in literature for the random coil to α -helix transition in bulk solution ($-1100 \text{ cal mol}^{-1}$) (Chou and Scheraga 1971). This can be explained by the fact that helix formation on the surface of liquid crystalline DPPG membranes is not complete (see IR section). However, the result proves that helix formation contributes with an exothermic enthalpy to the process of PLL binding to DPPG membranes.

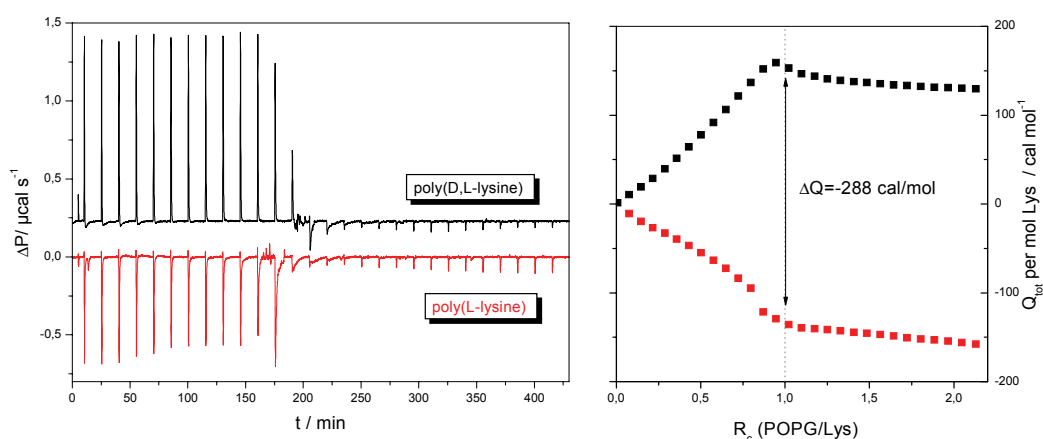


Figure 3.19: **a:** titration of POPG vesicle into solutions of poly(D,L-lysine) (—) and poly(L-lysine) (—) at 20 °C. **b:** total heats of reaction per mol of lysine monomer of the titrations shown in (a). Colours are chosen identical.

To test the notion that helix formation contributes with a positive $\Delta_R C_p$ to the total heat capacity difference between bound and unbound state, PDLL was titrated with POPG vesicles at different temperatures (Figure 3.20). It can be seen that $\Delta_R C_p$ is more negative in the case of PDLL binding to fluid membranes ($-15 \text{ cal mol}^{-1} \text{ K}^{-1}$) than in the case of PLL binding to fluid membranes ($-8.3 \text{ cal mol}^{-1} \text{ K}^{-1}$; Figure 3.18). The difference is, as predicted, positive and can be explained with thermal unfolding of PLL helices on the membrane surface. Furthermore, it is seen that binding of PDLL is endothermic at all examined temperatures. This shows that the binding of polylysine is entropy driven if the helix formation enthalpy is disregarded.

This interpretation is based on the assumption that the binding of PLL and PDLL is the same except for the helix formation. However, the lack of secondary structure formation influences also other binding parameter. Thus, the experiments can only be regarded as a proof of principle and the exact values should not be over-interpreted.

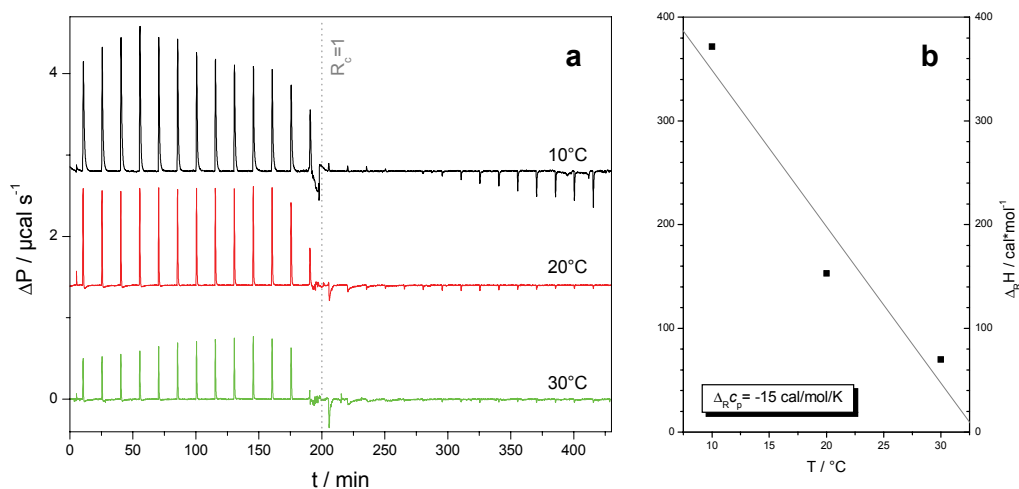


Figure 3.20: **a:** Titration of POPG vesicles to solutions of poly(D,L-lysine) ($n = 215$) at different temperatures. **b:** temperature dependence of total heats of binding, determined from the curves shown in (a) at $R_c = 1$.

3.5 Monolayer experiments

In addition to bilayer experiment, we also performed experiments with monolayers at the air/water interface. A monolayer can be regarded as half of a lipid bilayer and all effects that are mainly due to headgroup interaction can be studied with this model system. The advantage of such experiments is that processes as vesicle aggregation and fusion or pore formation are excluded by the experimental setup. Furthermore, the monolayer is a very well defined and easily controllable system. The monolayer is ideally flat and bending energies and vesicle size effects don't play a role. The number of accessible lipids is precisely known and the phase state can be controlled by the number of spread lipids and the available area.

Here the results of PLL interaction with DPPG Monolayer are only shortly described. More thorough discussions and interpretations are given in chapter 4.4, where the results of PLA interaction with DPPG monolayers are presented and comparatively discussed with the here presented data.

Figure 3.21 shows the kinetic of PLL binding to DPPG monolayers of different initial surface pressure π_0 . The subphase contains, as in all other experiments, 100 mM NaCl. It is obvious that the initial surface pressure strongly influences the adsorption behaviour of PLL. At low π_0 the surface pressure decreases after PLL insertion. The initial decrease is followed by an increase, suggesting that two consecutive processes take place during PLL adsorption. At higher π_0 the surface pressure of the monolayer increases after a certain lag period, without an initial decrease. A decrease of π can be interpreted with a condensation of the lipids, which

is well explainable with the electrostatic screening of the headgroup charges upon PLL adsorption. The consecutive increase is probably due to an insertion of the peptide side chains in interfacial region of the condensed domains.

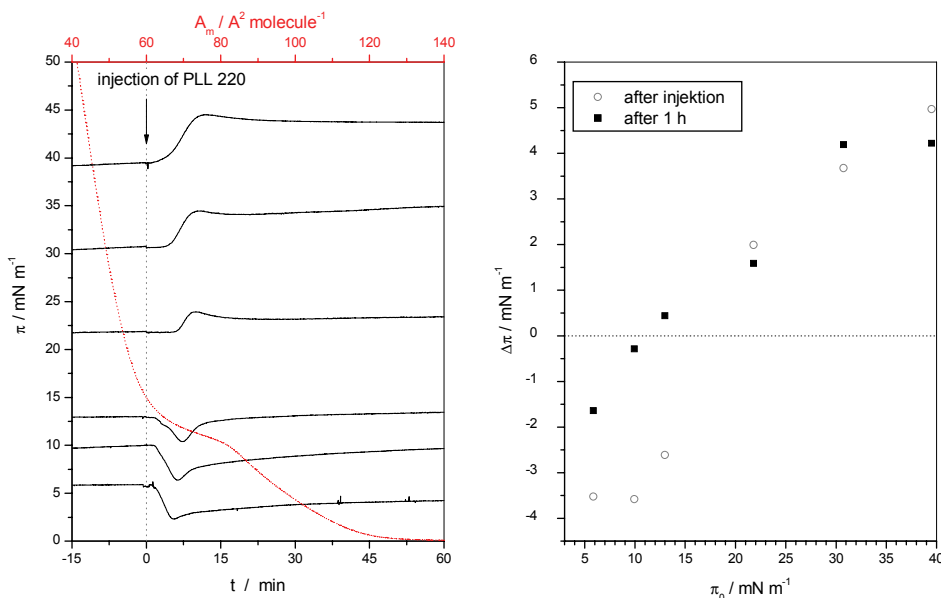


Figure 3.21: Left: Adsorption kinetics of PLL 220 at DPPG monolayers at different starting surface pressures on a subphase of 100 mM NaCl solution in H₂O. PLL (10 μl , 15 mM) was injected underneath the monolayer at $t = 0$. The red curve (top scale) is the surface pressure/Area isotherm of DPPG at 20 °C, which is given to identify the monolayer phase state. **Right:** Changes in surface pressure after injection of PLL vs. initial surface pressure.

At higher π_0 the monolayer is already in the condensed state (LC). Thus, the interacting peptide is not able to further condense the monolayer. Nevertheless, the peptide adsorbs to the lipid headgroups and after a while apparently inserts into the monolayer. The adsorption is driven by electrostatic interactions of the positively charged polypeptide and the negatively charged membrane. The insertion might have a contribution of hydrophobic interactions between the hydrocarbon spacer, which separates the lysine ammonium group from the peptide backbone, and the hydrophobic part of the membrane. That this is indeed the case has been shown by adsorption experiments with oligolysines derivatives bearing shortened side chains (penta(α,ω -diaminoacids)). As the hydrophobic spacer gets shorter, the pressure increase that follows the injection underneath a condensed DPPG monolayer gets smaller and the condensing effect gets higher. If the hydrophobic spacer is shorter than three CH_2 units no insertion can be observed any more (Hörnke et al., unpublished results). An additional driving force could be the avoidance of unfavourable electrostatic interaction between the adsorbed polypeptides, leading to a burying of the charged side chains into the monolayer's headgroup region, were their charges are screened by the lipid charges. A similar model for amphipatic

peptides has been proposed by Zuckermann and Heimburg (2001). Finally, it shall be noted that apart from the absolute value of π_0 the phase state of the monolayer influences the adsorption behaviour. All examined liquid expanded (LE) monolayers ($\pi_0 < 10$ mN/m) get condensed upon PLL interaction, which inserts consecutively into the condensed domains. In contrast, liquid condensed (LC) monolayers get penetrated without being condensed before.

Schafer (1974) did adsorption experiments of PLL to negatively charged PS-monolayers in the LE phase and observed a very similar binding behaviour as we describe here. He also reported that an initial decrease of pressure is followed by a consecutive increase and reasoned that the first process is due to a condensation of the lipids and the second to an insertion of the peptide in the lipid monolayer. However, he did not vary the initial surface pressure π_0 and thus no adsorption isotherms at higher initial pressures were reported.

3.6 X-ray diffraction

More insight in the structural organisation of DPPG/PLL complexes could be obtained by X-ray investigations. This was done in a wide temperature range from -30 to 70 °C. As has been shown by several authors the DPPG shows a very peculiar thermotropic polymorphism at temperatures lower than T_m (Degovics et al. 2000; Kodama et al. 1999; Takahashi et al. 1992; Tenchov et al. 2001; Zhang et al. 1997). Several metastable gel and subgel phases have been reported, whose existence is depended on heating rates and incubation temperatures and times. Thus we chose a constant thermal treatment for all measurements which included the exertion of lyotropic stress by freezing out of excess water (Förster and Brezesinski 1989). To be able to assess the influence of added PLL we first investigated the powder patterns of pure DPPG suspended in water and a phosphate buffer containing 100 mM NaCl. Subsequently we examined the complexes of DPPG with short and long PLL, of which PLL 14 and PLL 402 are chosen as the here presented representatives.

3.6.1 Polymorphism and structure of DPPG in pure water

The bilayer polymorphism of aqueous DPPG dispersions without additives is similar to that of the well-documented DPPC. A detailed analysis, however, shows that some peculiarities exist due to the existence of the charged headgroup. In addition to the sub-, pre- and main-transition temperatures (T_{sub} , T_{pre} , T_m), metastable and recrystallized phases were observed (Table 1). The scattering of DPPG in pure water is characterized by broad reflections in the WAXS and SAXS region, a few higher orders of the layer repeat distance, and a pronounced temperature dependence of the scattering intensities (Figure 3.22).

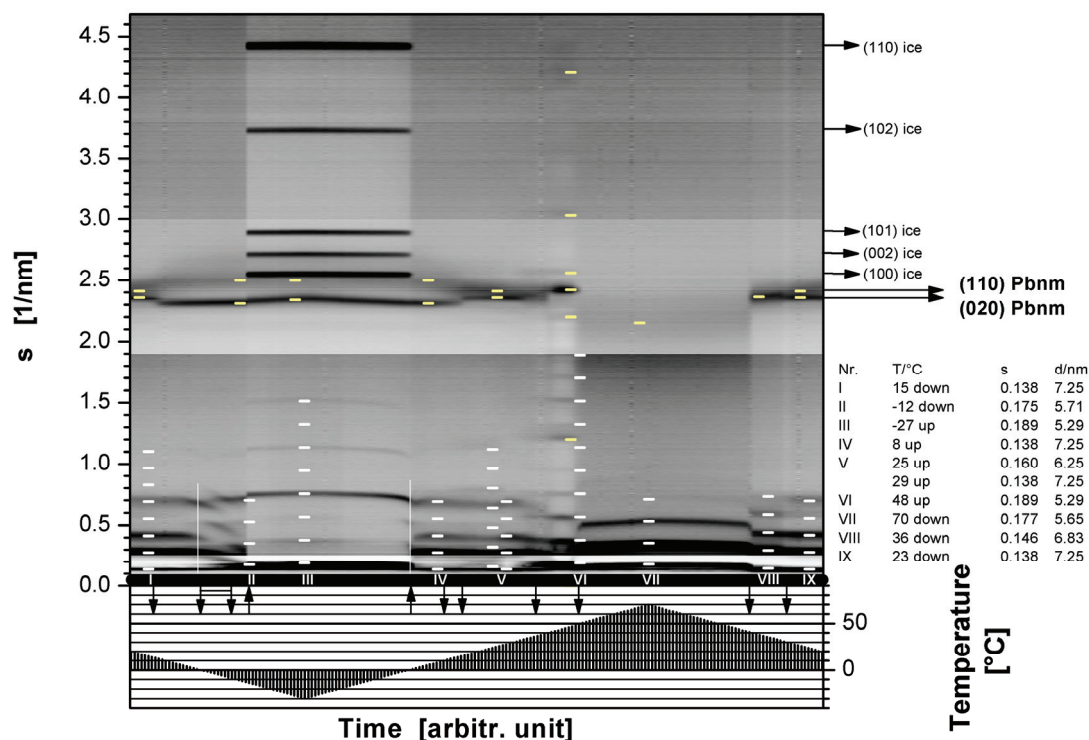


Figure 3.22: X-ray contour diagram of an aqueous suspension of DPPG (Na⁺-salt) prepared with pure water (pH 7). The scattering intensities (gray values) are shown in the upper part as a function of reciprocal lattice spacing (ordinate) and temperature (abscissa). In the lower part the temperature course during the experiment is shown as a ramp. The *arrows pointing downwards* indicate the transition temperatures of the lipid. Interconnected arrows indicate the on and offset of a phase transition range. The two *arrows pointing upward* indicate the onset of freezing and melting of water. In the temperature range between the upward pointing arrows additional intense ice reflections are seen. Reflections that originate from the same lattice are indicated by *horizontal short dashes* in white (layer repeat distances) or in yellow (acyl chain lattice). The layer repeat distances at some selected temperatures (I – IX) are given on the right hand side. Two light *vertical lines* are drawn at 0 °C to illustrate the super cooling and eventually the freezing point depression of water.

On cooling, a change in the short spacings (WAXS) without large change in the long spacings (SAXS) is observed at 14 °C (T_{sub}) indicating a transition affecting only the chain packing mode. At 5 °C (T_{ss}) a further transition is indicated by changes in the long spacings. In this case, however, the short spacings are unchanged. In a temperature region down to -10 °C a two-phase region is observed. A decrease of the lamellar repeat distance from 7.25 nm to 5.71 nm is observed accompanied by additional packing transformations. In this temperature region probably changes in the headgroup conformation, position of the counter ions, and in hydration occur. The subgel phase L_{c_m} appearing at 14 °C is metastable with respect to a stable L_c phase with a long-range lateral molecular order, which would produce additional short spacings in the range of 1.0 – 2.0 nm⁻¹ (Blaurock and McIntosh 1986; Raghunathan and Katsaras 1996; Wilkinson and McIntosh 1986). In the metastable phase the WAXS region is mainly affected by a spreading out of the fingerprint reflections (Figure 3.22).

Table 1: Layer repeat distances and phase transition temperatures of pure DPPG systems and DPPG/PLL mixtures evaluated from the analysis of X-ray powder patterns.

repeat distances in phases (d_L / nm)	DPPG + PLL			DPPG + NaCl	DPPG+ pure water
	$n = 1181$	$n = 402$	$n = 14$		
$Lc_m + \text{ice}$	6.41	6.41	5.40	5.29	5.29
Lc_m	6.29	6.29	6.29	5.88	5.71
$L\beta_A$	6.37	6.37	6.37	7.25	7.25/6.25
Cr	–	–	–	5.29	5.29
$L\alpha$	5.88	5.88	5.88	5.13	5.65
transition temp. / °C					
T_{melt}	–	–	–	50	50
T_{recryst}	–	–	–	22	36
T_m	50	49	45	43	40
T_{pre}	–	–	–	33	31
T_{sub}	19	20	18	16	15
T_{ss}	–	–	–	7	1
ΔT_{ice}	–7	–8	–8	0	0

Phases: Lc_m metastable subgel phase, $L\beta_A$ gel phase, Cr recrystallized phase, $L\alpha$ liquid-crystalline phase. **Temperatures:** *melt* melting of Cr phase, *recryst* recrystallization, *m* main-transition, *pre* pre-transition, *sub* sub-transition, *ss* solid-solid transition, ΔT_{ice} freezing point depression.

The appearance of ice reflections due to the freezing of trapped water gives rise to a further decrease of the layer repeat distance down to 5.29 nm and also influences the chain packing of the lipid molecules (Förster and Brezesinski 1989). Up to 8 sharp orders of the layer reflections are observed and indicate a stack of well ordered bilayers. The changed structure factors reflect the modification of the electron density profile.

The observed temperature dependence of the layer reflections on heating is caused by a successive pre-melting of ice and a small rehydration of the headgroups (Kodama and Aoki 2001). At 0 °C all ice is melting and water is entering the interbilayer space. The bilayer repeat distance reaches a value of 7.25 nm as initially observed. However, the initial chain packing mode was different. At T_{sub} the typical fingerprint scattering of the gel phase $L\beta_A$ appears. On further heating the gel phase does not directly transform into the fluid $L\alpha$ phase. Rather a recrystallization into a crystalline structure Cr takes place ($T_{\text{recryst}} = 37$ °C) which then transforms at $T_{\text{melt}} = 50$ °C into an $L\alpha$ phase. In the phase Cr the headgroups are probably dehydrated as concluded by the coincidence of the layer repeat distances in the Cr phase with those observed at temperature where the water has been frozen out (–30 °C). However, the different structure factors indicate different electron densities within the same repeat distances. The recrystallized structure has an oblique subcell indicated by three fingerprint reflections.

The additional spacing at $s = 1.20 \text{ nm}^{-1}$ is taken as hint for a long range order within a molecular lattice (Takahashi et al. 1992; Wilkinson and McIntosh 1986). Because the melting temperature (Table 1) of the Cr phase is 9.2 K higher than the reported $T_m = 40.8 \text{ }^\circ\text{C}$ of the ripple phase ($P\beta$) of DPPG (Durvasula and Huang 1999), it is evident that the phase Cr must be a stable crystalline phase. Upon heating above $50 \text{ }^\circ\text{C}$ the liquid-crystalline phase $L\alpha$ is observed. On immediate cooling from the liquid-crystalline $L\alpha$ phase, the common polymorphism $L\alpha - P\beta' - L\beta_A$ appears.

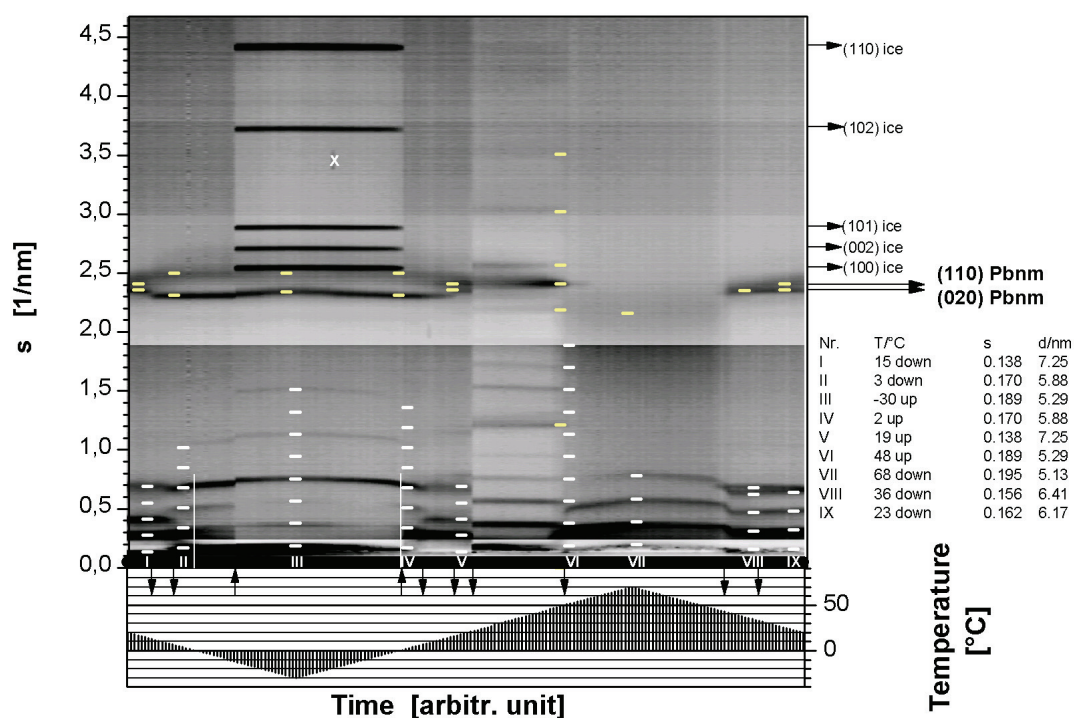


Figure 3.23: X-Ray contour diagram of DPPG in an aqueous buffer/salt suspension (100 mM NaCl, 20 mM phosphate buffer). For explanations see Figure 3.22.

3.6.2 Polymorphism and structure of DPPG in NaCl solution

We then investigated the behaviour of DPPG in the presence of additional NaCl and phosphate buffer (Figure 3.23). The temperature behaviour of the short spacing (WAXS) is the same as in the sample without additional salt. But the SAXS reflections become sharper indicating a better bilayer stacking order. On cooling from room temperature again changes in the WAXS ($13 \text{ }^\circ\text{C}$) and SAXS ($8 \text{ }^\circ\text{C}$) are observed at the transition into the Lc_m phase. After supercooling and the freezing of the trapped water, the orders of the layer repeat distance appear with their typical structure factor. On heating, the transitions appear to be fully reversible at the respective temperatures. The presence of additional salt does not lead to a melting point depression of the excess water. This indicates that the added ions are located at the membrane surface and not in the free bulk water. The most striking difference to the

sample prepared in pure water is that the recrystallization temperature for the phase Cr is decreased by about 15 K. The transition temperature (T_{melt}) into the $L\alpha$ phase is unchanged as well as the repeat distances which were measured for the different phases (Table 1). On cooling from the $L\alpha$ phase, again the usual ripple phase $P\beta'$ appears before the gel phase $L\beta_A$ is formed.

The increase in temperature results not only in the melting of the chains and formation of liquid-crystalline phases, but also leads to changes in hydration and in the condensation of the counterions at the interface of the bilayer. Hydration water can be released by the ions and the observed recrystallization is then induced. This was found before in DMPG alkaline earth cation systems (Garidel et al. 2000a). It is therefore plausible that one effect of the salt containing buffer is to make the recrystallization easier.

3.6.3 Influence of poly(L-lysine) on the bilayer structure

After having investigated thoroughly the reference systems we examined the influence PLL has on the membranes structure and polymorphism. At the first glance it is visible that the addition of PLL to DPPG strongly increases the stacking order of the bilayer. Up to nine higher orders of the repeat distance are detectable. The repeat distance is only slightly temperature dependent. It remains almost constant even for the different gel phase polymorphs (Figure 3.24 and Figure 3.25). For longer PLL the repeat distance is only changed in the $L\alpha$ phase. In case of PLL 14 addition, also the freezing of the water alters the repeat distance. In contrast to the strong influence of PLL on the layer stacking, the chain packing modes are not altered to a measurable extent.

In all DPPG/PLL mixtures a freezing point depression of water was observed. It proves that the counterions are liberated by PLL binding and reduce the chemical potential of excess water. This effect is independent of the chain length of PLL. The sub-transition is not affected by the polypeptides whereas the main-transition temperatures increase with increasing chain length of the PLL (Table 1). This finding parallels the results of the DSC and IR measurements, even if the absolute values of ΔT_m are slightly different. In all PLL containing samples the pre-transition was suppressed, which is also in accordance with the DSC measurements. Furthermore no recrystallization processes occurs in the DPPG/PLL mixtures.

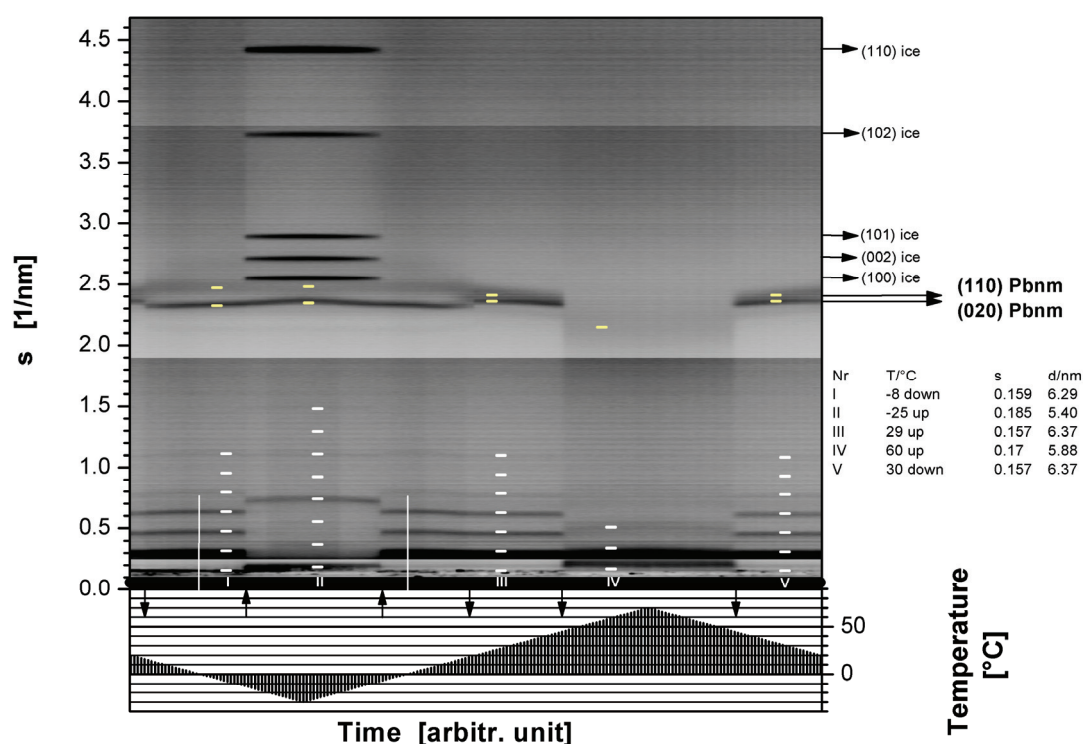


Figure 3.24: X-Ray contour diagram of a DPPG / PLL 14 mixture ($R_c = 1$). For explanations see Figure 3.22.

In the $L\alpha$ phase an increase of the repeat distance by 0.75 nm is measured. However, for the gel phase, the layer repeat distance decreases by ca. 0.90 nm to values of 6.37 nm which is approximately the value for DPPG in pure water without salt. In the Lc_m phase the repeat distance is increased by 0.5 nm and a change in the structure factor clearly indicate that the PLL in the Lc_m phase is inserted in between adjacent headgroup layers. The variation of the repeat distances in uncomplexed DPPG is due to different degrees of hydration and is a function of added salt and water (Wilkinson and McIntosh 1986). In the mixtures with PLL one can imagine that the inserted PLL bridges the adjacent headgroups after liberation of the counterions which leads to nearly constant repeat distances even if the phase state of the lipid changes.

After freezing of the water the phase behaviour is dependent on the chain length of the bound peptide. Again the shortest PLL ($n = 14$) behaves differently than the longer ones. It shows the surprising effect that with the freezing of trapped water a repeat distance is observed which is characteristic for pure DPPG. Also the structure factor of the 8 orders of the layer repeat distance is identical with that of pure DPPG. This indicates that short PLL is squeezed out from the interbilayer space during freezing of excess water and returns with the melting of ice.

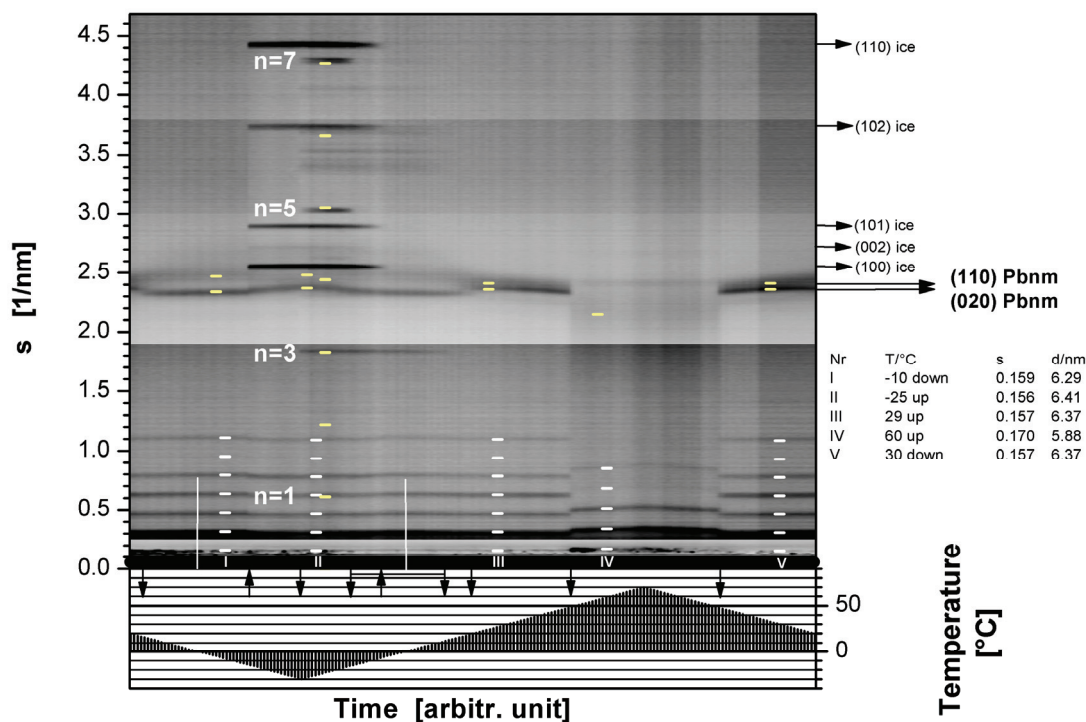


Figure 3.25: X-Ray contour diagram of a DPPG / PLL 402 mixture ($R_c = 1$). For explanations see Figure 3.22. In addition to the chain packing reflections the reflections, originating from the 1 D helix lattice are marked with yellow dashes. The hypothetical positions of the reflections of the orders 1,2,4,6 which are not measured are marked as well.

By contrast longer PLLs stay bound in the interbilayer space. This can be concluded from the increased repeat distance, with respect to the uncomplexed membrane ($\Delta d_L = 1.12$ nm) and the altered SAXS intensities. Moreover additional reflections appear at low temperature (-30 °C) in the WAXS region when DPPG is complexed with longer PLLs (Figure 3.25). Since the freezing out of the water does not have a large influence on the structure factor of the subgel phase and the acyl chain packing remains nearly unaffected these additional reflections must originate from the bound polypeptide. They are interpreted as caused by a 1D lattice of the PLL α -helices embedded between adjacent headgroup layers of opposing bilayers. That longer PLL form helices upon binding to ordered DPPG bilayers has been shown by FT-IR spectroscopy. That these helices are intercalated between the bilayers can be deduced from the altered repeat distances and structure factors. Nevertheless the helices are flexible and unordered in all higher temperature phases (Papadopoulos et al. 2004). At low temperature the helices apparently become stiff and after the freezing out of excess water they can order in a parallel packing mode.

A more detailed evaluation of the additional reflections and the layer repeat distances enabled us to create a model for the DPPG/PLL complex. The strongest additional reflections could be interpreted as the 3rd, 5th and 7th order of a 1.65 nm periodicity (Figure 3.25). Such a

distance is characteristic for a 1D parallel packing of PLL helices, which was tested by modelling and was measured in the bulk (Suwalsky and Llanos 1977). This value is somewhat less than the diameter of a fully extended PLL helix (1.8 nm). Apart from an interdigitation of the side chains of neighbouring helices (Suwalsky and Llanos 1977) this might be due to a small deformation of the helix cross section, probably by bending of the charged side chains towards the oppositely charged bilayer interface.

Further we examined the thicknesses of the different components within one layer repeat distance in more detail. The difference between the layer repeat distance and the helix periodicity yields a distance of 4.76 nm which should be correlated to the thickness of a DPPG bilayer. It is consistent with values from an electron density profile of a DPPG/PLL mixture ($R_c = 0.5$) reported by Takahashi et al. (1992). They measured a distance of 4.46 nm between the phosphate groups across the bilayer. The difference between both values (4.76 vs. 4.46 nm) is physically reasonable if one takes into account that the phosphate groups of DPPG carry glycerol moieties and that also bound water is still present. However, if the helices are deformed, they might be more extended in direction of the bilayer normal than perpendicular to it. If so, side chain moieties should be buried in the headgroup region of the bilayer. Indications for such an interaction are already given by monolayer and ITC experiments. The thickness of the hydrophobic region can be set constant to 3.45 nm assuming all trans configured acyl chains and a tilt angle of 32° for all DPPG phases (Blaurock and McIntosh 1986). With these values we can now present a comprehensive model for the DPPG/PLL complexes (Figure 3.26).

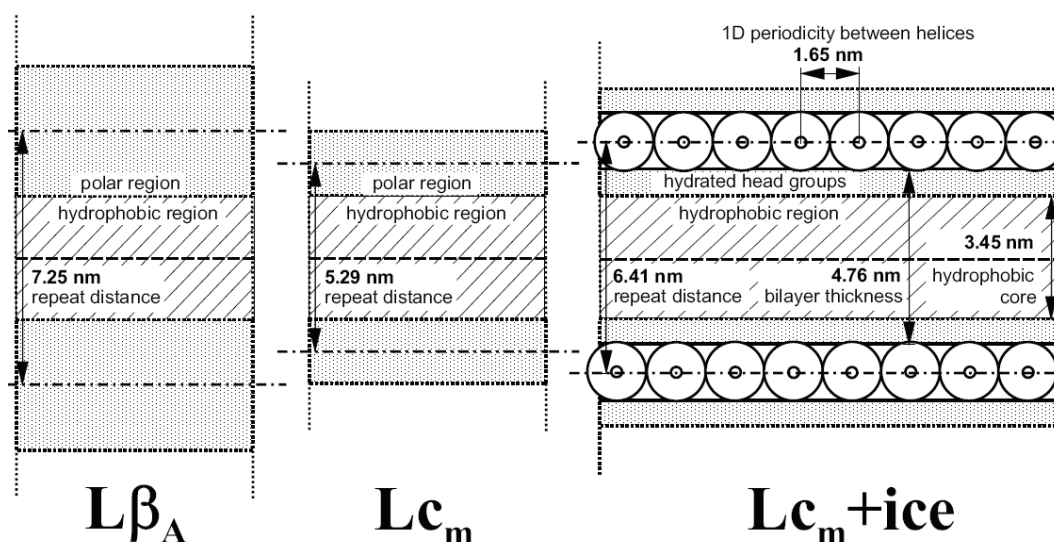


Figure 3.26: Model for a DPPG/PLL complex illustrating the observed 1D helix periodicity in the metastable subgel phase $Lc_m + ice$. For comparison the bilayer structures of the phases $L\beta_A$ and Lc_m for pure DPPG (Na^+ -salt) are also shown. The polar region consists of hydrated headgroups, counterions including buffer ions with their hydration shell, and water.

Complexes with a similar geometry but opposite charge have already been found for the system of cationic lipids and anionic DNA (Radler et al. 1997). Here, the double-stranded DNA is much stiffer so that the regular ordering of the double-helices is already present at room temperature, whereas the polypeptide lattice forms only at very low temperatures and under lyotropic stress.

Short PLLs ($n = 14$) are not able to form α -helices. Nevertheless the layer repeat distances in mixtures with PLL 14 in the phases Lc_m (T above ice melting), $L\beta_A$, and $L\alpha$ are the same as those observed for longer PLLs, which are intercalated between the opposing bilayers as unordered helices. Apparently the side chains are randomly oriented to both sides towards the headgroups of the DPPG layers and thus take up similar space.

The layer repeat distance is essentially constant in the gel phases and changes only when the $L\alpha$ phase is reached. Here, the PLLs increased the repeat distance of the fluid lamellar phase by about 0.75 nm compared to pure DPPG in salt/buffer solution. This increase and a changed intensity profile of the layer reflections prove that PLL stays inserted in the interbilayer space even for fluid lipids. This is additional proof that the helix to coil transition that was detected by IR spectroscopy at temperatures exceeding T_m is not due to desorption of the PLL. Rather PLL undergoes this secondary structure transition in the membrane bound state.

3.7 Summary

The interactions of the positively charged peptide poly(L-lysine) (PLL) with negatively charged PG containing membranes (DPPG, POPG, DPPG/DPPC, DPPG/DMPC) was investigated as a function of temperature, the peptide chain length, membrane composition and peptide content (R_c). The influence of PLL on the thermotropic phase behaviour of the membranes was studied extensively by DSC, FT-IR spectroscopy and X-Ray powder diffraction. The thermodynamics of binding could be assessed by ITC. Furthermore, FT-IR gave information about the hydrophobic order of the membrane, the headgroup hydration, and the secondary structure of the binding peptide. X-Ray diffraction was used to yield information about the structure of the formed complex. Finally, mechanistic information could be deduced from monolayer and ITC experiments.

Stabilization of the gel phase

DSC experiments revealed that PLL binding increases the main phase transition temperature T_m of pure DPPG by about 1–5 °C. The exact value of increase depends on the PLL chain length. In general longer PLLs increase T_m more than shorter ones. However, steric hindrance in the case of longer PLLs and highly charged membranes can counteract this trend.

These results obtained by DSC were supported by FT-IR experiments. X-ray diffraction showed that PLL stabilizes the membrane gel phase and prevents recrystallization. Furthermore, FT-IR experiments showed that the acyl chain order in the hydrophobic part of the membrane is increased upon PLL binding, which is concluded from the downshift of the $\nu_s(\text{CH}_2)$ vibrational band by about 1 to 1.5 cm^{-1} . This was found for both, the gel and liquid crystalline phase.

Membrane hydration

A downshift of the carbonyl stretching vibration ($\nu(\text{CO})$) shows that hydrogen bonds to the hydrating water molecules get stronger or better oriented. Water molecules get immobilized in the restricted volume between the bilayer interface and the bound PLL. ITC experiments show that water is released from the hydrophobic part of the membrane, which could be shown by the negative $\Delta_R C_p$ in both, gel and liquid crystalline phase.

Secondary structure

Analysis of the amide I vibrational band showed that long PLL forms an α -helix when it is bound to a negatively charged DPPG membrane with high surface charge density, whereas it is a random coil in bulk solutions. When the membrane surface charge is diluted by the co-addition of neutral lipids (DPPC, DMPC), the conformation of the bound peptide depends on the phase state of the lipid membrane.

Lipid demixing

In mixed DPPG/DPPC membranes PLL binding induces phase separation in the gel phase of the membrane and PLL is bound in α -helical conformation to the negatively charged DPPG rich domains. Domain formation in the gel phase was proven by DSC and FT-IR experiments. Passing into the lipid crystalline phase the lipids remix and domain formation is reduced. This results in a α -helix to random coil transition of the peptide at the phase transition temperature of the mixed membrane.

X-ray analysis

X-ray diffraction showed that binding of PLL stabilizes the lamellar structure of the membranes. The membranes organized in well ordered bilayer stacks. Intercalated PLL bridges adjacent bilayers. The bilayer repeat distance implies that longer PLLs are bound as α -helix and short PLL as unordered strands. When DPPG/PLL complexes are cooled below the freezing of water two different effects were observed. Short chain PLLs, which do not form helices, were reversible squeezed out from the interbilayer space when the freezing of water occurred. In the system with long chain PLLs, however, a 1D ordering of the α -helices with a

specific distance was observed. Complexes with a similar geometry have already been found for the system of cationic lipids and anionic DNA (Rädler et al. 1997). Here, the double-stranded DNA is much stiffer so that the regular ordering of the double-helices is already present at room temperature. For the polypeptide system, the observation of ordered α -helices is new and can apparently only occur when the α -helices become stiff at low temperature concomitant with the freezing of water. Furthermore, X-ray diffraction gave direct evidence for the counterion release that occurs upon binding of the peptides. This could be shown by the pronounced freezing point depression of the bulk water.

Binding enthalpies

ITC experiments showed that the positive entropy change of counter-ion release is complemented by a negative binding enthalpy. Thus both, entropy and enthalpy favour the complex formation, which results in high binding constants. The enthalpy of binding gets the more negative, the longer the PLL is. This correlates well with the propensity for helix formation. Thus it is concluded that helix formation is an additional driving force of binding. This is also shown by the fact that short PLL ($n = 14$) as well as poly(D,L-lysine), which do not form helices, bind with a positive enthalpic contribution, i.e. binding is solely entropy driven. The binding to fluid membranes is much less exothermic than binding to gel phase membranes. Also this effect can be correlated to the lower helicity of PLL on the surface of fluid membranes. The negative $\Delta_R C_p$ values that have been deduced from temperature dependent ITC experiments imply that hydrophobic interactions are involved in the binding process.

Monolayer adsorption

The contribution of hydrophobic interactions could be confirmed by monolayer adsorption experiments, which show that the peptide inserts into the lipid headgroup region of condensed monolayers. The decreased insertion of peptides with shortened side chains shows that the insertion is indeed driven by hydrophobic interaction. However, PLL adsorbs to liquid expanded membranes (LE) and condenses the monolayer. This shows that the PLL-DPPG interaction consist of both, electrostatic and hydrophobic contributions.

4 Interaction of polyarginine with PG containing membranes

4.1 Introduction

Despite the large interest in the so called “arginine magic” (see chapter 2.2) only few articles are available dealing with well defined model systems to elucidate the detailed binding mechanism of arginine polypeptides to lipid membranes.

Tsogas et al. (2005a; 2006; 2005b) examined the interaction of arginine monomers, polyarginine and guanidylated dendrimers with di-hexadecyl-phosphate (DHP) containing vesicles. They reported that arginine monomers influence the lipid phase behaviour, as the main transition temperature T_m is decreased and the transition enthalpy ΔH is increased. ITC experiments showed that arginine monomers binds stronger to gel phase DHP-membranes than to fluid DHP-membranes. The authors further argued that some monomers penetrate the membrane and are transported into the vesicles' interior (Tsogas et al. 2005b). From ζ -potential and fluorescence experiments they concluded that polyarginine is located at the vesicles interface as long as the membrane is in the gel state, but that it penetrates the membrane in the liquid crystalline state (Tsogas et al. 2005a). Guanidylated dendrimers induced fusion of the vesicles and a reduction of T_m . Under certain conditions the dendrimers might also be translocated into the vesicles interior (Tsogas et al. 2006).

In contrast to these findings Goncalves et al. (2005) reported that nonaarginine (R_9) neither inserts nor translocates through a POPG/POPC (3:7) bilayer, but binds within some distance to the headgroup region. They determined high binding constants ($8.2 \cdot 10^4 \text{ M}^{-1}$) and binding enthalpies (-2.5 kcal/mol) from ITC experiments and evaluated the electrostatic contribution of binding to be 33 % of the total free energy.

Similar calculations, yielding similar values, were performed by Hitz et al. (2006) on the basis of fluorescence experiments. They reported that PLA binding to POPG/POPC (7:3) membranes leads to bilayer rigidifications followed by the release of the aqueous content of the vesicle. Furthermore, they showed that PLA binding to the vesicles follows a two step kinetic, with a first step being probably electrostatically driven and a second one non-electrostatically.

This work shall contribute to the understanding of the binding mechanism of PLA to negatively charged membranes. It is not the objective of the work to examine the translocation through the lipid bilayer. Rather, we want to reveal the mechanism of binding, which always has to precede a possible translocation. A focus point is the influence the peptide binding has on membrane properties. Our model system comprises PLA of different chain length and PG vesicles and monolayers. The influence of PLA binding on the membranes phase behaviour

was determined in a series of DSC experiments. ITC studies revealed the binding characteristics in both, the gel and the fluid membrane state. Mechanistic information was deduced from monolayer experiments. FT-IR spectroscopic experiments revealed the influence of PLA binding on the membrane organization and hydration as well as the secondary structure of the peptide. Finally, dye release experiments were performed to examine the possibility of pore formation in the vesicles, induced by polypeptide binding.

These different experiments were used to deconvolute electrostatic and non-electrostatic contributions to the binding process. The existence of these two contributions will be evident from all the presented data.

After insight into the PLA binding process is achieved, it will be compared to PLL binding, which was discussed in the foregoing chapter.

4.2 Differential scanning calorimetry

4.2.1 Influence of PLA on the phase behaviour of DPPG membranes

As in the case of PLL interaction a series of DSC experiments was performed under variation of i) the peptides chain length ii) the lipid-to peptide mixing ratio R_c and iii) the membrane composition.

DSC curves of pure DPPG and its complexes with PLA of different chain lengths at a mixing ratio of $R_c = 1$ are presented in Figure 4.1. The PLA chain length was varied in 4 steps from 69 to 1183 monomer units. The phase transition temperature of pure DPPG (40.8 °C) and the transition enthalpy (10,7 kcal/mol) agree well with the values reported in literature (Durvasula and Huang 1999; Huang and Li 1999; Zhang et al. 1997). By addition of PLA this transition is only marginally affected. Nevertheless, a small effect is seen. The two shorter peptides, PLA 69 and PLA 184 decrease T_m slightly, by $\Delta T_m = -0.8$ °C and -0.2 °C, respectively. The two longer PLAs ($n = 649$ and $n = 1183$) increase T_m by as little as $\Delta T_m = 0.2$ °C and 0.1 °C, respectively. These shifts are unexpectedly small. In general one would expect a much higher positive shift upon binding of a positively charged polyelectrolyte to the negatively charged DPPG bilayer. Shielding the electrostatic repulsion between neighbouring lipid molecules reduces their lateral distance and results in an increased hydrophobic contact of the acyl chains. This and the connected gain in Van-der-Waals energy stabilizes the gel phase and shifts the transition to higher temperatures. The shift that can be attributed to such electrostatic shielding of the PG headgroup charges (ΔT^{el}) amounts to 5.5 °C (Cevc et al. 1980). This behaviour was detected for PLL binding to DPPG membranes (Schwieger and Blume 2007). All effects that exceed ΔT^{el} or produce a negative ΔT originate from - or have a contribution of - non-electrostatic interactions, such as specific binding

(including hydrogen bridging), structural changes, changes in hydration, or hydrophobic interactions. This is definitely the case for PLA binding to DPPG bilayers. Certainly, PLA binding leads to electrostatic screening of the headgroup charges. But this effect must be counteracted by opposing effects that shift the phase transition to lower temperatures. These different effects are balanced in a way that the overall shift of T_m is close to zero. This thesis is supported by the fact that positive as well as negative shifts are observed for PLA of different chain length. It can be assumed, that the principle effects of binding are the same for all PLA, but that these effects are balanced differently for PLA of different chain length, resulting in a slightly positive ΔT_m in the one case and in a slightly negative ΔT_m in the other. In general, chain length dependencies are expected for polyelectrolytes binding to charged surfaces. This arises from the fact that the main driving force of binding is the entropy win achieved by counterion release (Montich et al. 1993; Wagner et al. 2000). This effect is greater the more counterions are released upon the binding of one polymer chain. Consequently, the binding constant, which has an entropic and an enthalpic contribution, is getting larger for longer polyelectrolyte chains. This increase in binding constant is counteracted by sterical and kinetical effects (Novellani et al. 2000; Ulrich et al. 2006). Thus generally trends reverse at a certain chain length, as has been shown for the DPPG/PLL system (see chapter 3 or Schwieger and Blume 2007).

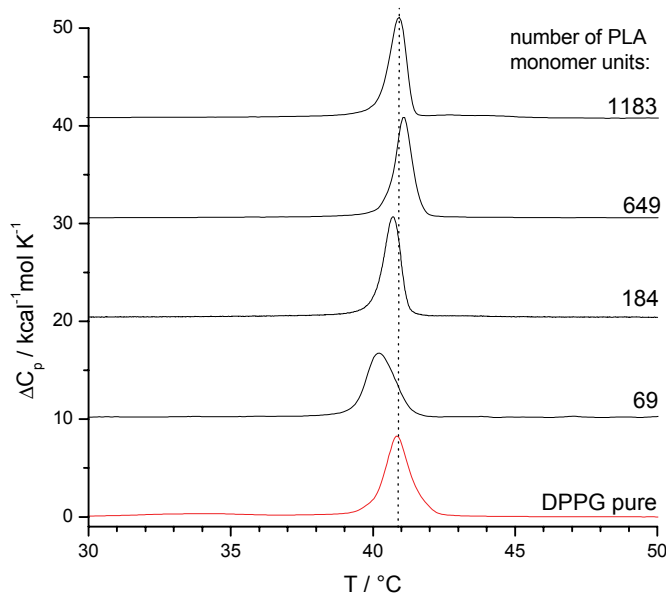


Figure 4.1: DSC-plots of the gel-to-liquid-crystalline phase transition of DPPG/PLA complexes with an equimolar charge ratio ($R_c = 1$) and different PLA chain length. The vertical dotted line is added as an eye guide at the phase transition temperature of the uncomplexed lipid membrane. Measurements are performed in 100 mM NaCl solution at pH = 6.

The pre-transition that is observed for the uncomplexed DPPG bilayer at 34.6 °C is abolished upon addition of PLA. The pre-transition is the transition from the gel phase L_{β} temperature / °C to the ripple phase P_{β} . It is very sensitive to changes in the bilayer environment and structure. A suppression of the pre-transition was reported for different peptides and anaesthetics (Heimburg 2000) as well as for high salt concentrations (Blume and Garidel 1999) or Small Unilamellar Vesicles (SUV). In the present case screening of the surface charges, changes in hydration structure (see IR section), and a pronounced stabilisation of the lamellar bilayer geometry might be responsible for the disappearance of this transition.

The enthalpy of the main transitions (ΔH^{main}) is affected as well and shifted to slightly lower values. $\Delta\Delta H^{\text{main}}$ is about -1.5 kcal/mol for all PLA/DPPG complexes with respect to the main transition enthalpy of the pure DPPG membrane. With respect to the overall gel to fluid transitional enthalpy, which includes the pre-transition enthalpy ($\Delta H^{\text{gel} \rightarrow \text{fluid}} = \Delta H^{\text{pre}} + \Delta H^{\text{main}}$), the decrease is even higher and results in values of about -2.5 kcal/mol. Since the transition enthalpy is given by

$$\Delta H^{\text{trans}} = T \cdot \Delta S^{\text{trans}} \quad , \quad (10)$$

a decrease in the transition entropy is expected if the transition temperature stays more or less constant and the transition enthalpy decreases. A reduced ΔS^{trans} indicates that the fluidization of the membrane is hindered by PLA binding.

Finally attention shall be focused on changes in half width of the transition peaks. The half width is inversely correlated with the cooperativity of the melting process. The cooperative unit (*c.u.*), being a measure for the number of molecules that change their phase stat at the same time (Garidel et al. 2000b), can be calculated on basis of a simple two state model ($\text{Gel} \rightleftharpoons \text{fluid}$) (Trauble 1971), yielding:

$$c.u. = \frac{\Delta H_{\text{vH}}}{\Delta H_{\text{calor.}}} = \frac{4RT^2 C_{\text{max}}}{\Delta H_{\text{calor.}}^2} \quad (11)$$

with ΔH_{vH} being the van t'Hoff Enthalpy of melting, evaluated from the temperature dependence of the equilibrium constant and ΔH_{calor} being the integral of the Δc_p curve.

From Figure 4.1 it is obvious, that the cooperativity is decreased upon binding of the shortest PLA and increased upon binding of the longer ones. In the latter case the *c.u.* is increased from 108 to about 180 molecules. An increased cooperativity is however, an astonishing result. There are many examples for decreased cooperativities upon peptide binding, whereas no example for an increased cooperativity of the lipid main transition is reported. An increased cooperativity must be due to a better lateral coupling of the lipids in the bilayer, which might be facilitated if the headgroup charges are screened by the binding peptide. Hitz et al. (2006) report that fluid POPC/POPG bilayers are rigidified upon PLA interaction. It might be possible that the cooperativity in such rigidified domains is increased, resulting in a sharper transition peak. Interestingly Tsogas et al. (2005b) reported that the sub-

transition of a DHP membrane showed an increased cooperativity after addition of arginine monomers. Nevertheless, also in their experiments the main transition is broadened, i.e. the cooperativity is decreased. They further report a reduction of T_m upon interaction of DHP containing bilayers with arginine monomers. This supports our thesis, that there must be an arginine specific process that is destabilizing the gel phase of the membranes. Nevertheless they find, contrary to our results, an increase in ΔH^{trans} .

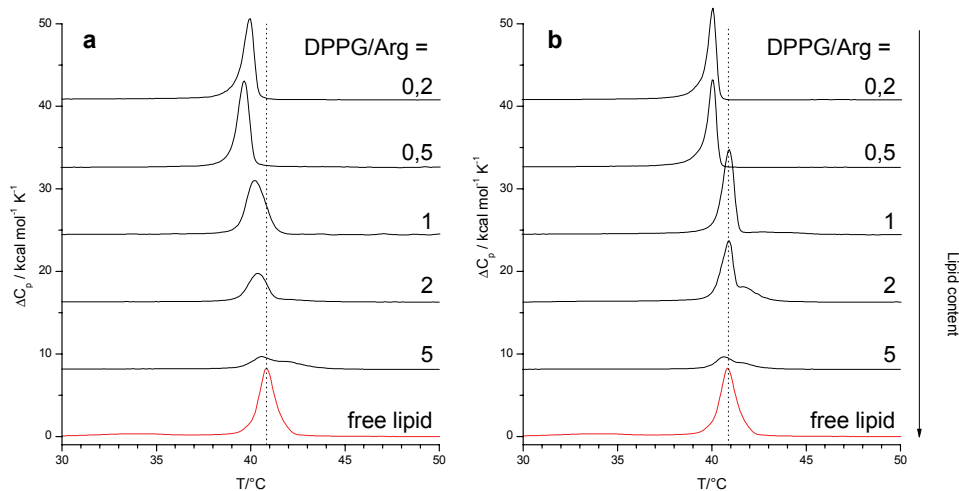


Figure 4.2: DSC plots of the gel-to-liquid crystalline phase transition of DPPG vesicles complexed with **a)** PLA 69 and **b)** PLL 1181 as a function of the lipid/Arg mixing ratio (R_c). The vertical dotted line is added as an eye guide at the phase transition temperature of the uncomplexed lipid membrane. Measurements are performed in 100 mM NaCl solution at pH = 6.

In Figure 4.2 the DSC curves of DPPG/PLA complexes at different mixing ratios R_c are presented. R_c is always given with respect to the charges under the assumption, that the DPPG molecules as well as the arginine side chains each carry one negative and one positive charge, respectively. This assumption is reasonable as the experiments were performed at a pH of 6 - 7, which is far from the two pK_{app} values which are 2.9 and 12.5 for DPPG and PLA, respectively. This means that the DPPG is completely deprotonated and PLA is completely protonated.

Obviously two situations can be distinguished, which are the lipid excess and peptide excess complexes. The transition temperatures T_m of the peptide excess complexes ($R_c < 1$) are always decreased with respect to T_m of a uncomplexed DPPG membrane. The ΔC_p curves change neither position nor size and shape below a R_c of 0.5, indicating that excess peptide doesn't influence the membrane organisation any more but remains unbound in the solution. Nevertheless, a change is still visible between the curves at $R_c = 1$ (which is charge compensating ratio) and $R_c = 0.5$. This allows us to conclude that complexes formed under peptide excess are overcharged, leading to a surface charge reversal. This is a common effect

for polyelectrolyte binding (May et al. 2000; Netz and Joanny 1999) and is used extensively to build polyelectrolyte capsules by layer-by-layer deposition (Decher 1997; Sukhorukov et al. 1998). The extent of overcharging depends on the PLA chain length, as can be deduced from the fact that the curves measured at $R_c = 1$ are more resemblant to the lipid excess behaviour for longer PLA chains and to the peptide excess behaviour for shorter PLA chains. This means that the saturation limit shifts to lower R_c values, when the PLA chain gets longer, i.e. the overcharging is more pronounced for longer PLA chains. This can be easily understood, because unbound loops and ends of the polymer that extend in the solution are responsible for the overcharging effect and these loops and ends are getting more frequent with increasing polymer chain length (Chodanowski and Stoll 2001). In the lipid excess regime ($R_c > 1$) T_m is unaffected (longer PLA) or decreases slightly (shorter PLA). It is obvious that here the Δc_p peaks change continuously in position, shape, peak heights and integral area dependent on the peptide content. Peaks get smaller, i.e. transitions get more cooperative with increasing peptide content, with the highest cooperativity being achieved at the saturation ratio. This can be explained by all of the lipid molecules being in one and the same, namely the bound, state.

The transition enthalpy ΔH^{trans} increases with the increasing peptide content but is always lower than the transition enthalpy of the unbound membrane (ΔH^0). Papahadjopoulos (1975) describes two typical situations. Binding of charged peptides to membrane surfaces leads to a ΔH^{trans} that is higher than ΔH^0 and increases with increasing peptide content. Conversely, insertion of the peptide into the membrane leads to a ΔH^{trans} that is lower than ΔH^0 and decreases with increasing peptide content. The measured dependency for PLA binding to PG membranes does not fit in none of these models. The fact that ΔH^{trans} is always lower than ΔH^0 suggests that PLA inserts into the membrane. However, the increase of ΔH^{trans} with increasing peptide content, suggests an electrostatic interaction. This ambiguous behaviour leads once more to the conclusion that PLA binding cannot be explained by one of these simple one step models, but is rather an interplay of different processes.

Also the peak symmetry is different in lipid and peptide excess complexes. Whereas the lipid excess complexes show shoulders and extended wings on the high temperature side of the transition peaks, the peptide excess transitions extend more to the low temperature side. An asymmetric peak is indicative for a better interaction of the added peptide with one of the two phases. If the peak shows an extended wing or shoulders at the low temperature side, the peptide interacts better with the fluid phase than with the gel phase, if the peak extends to the high temperature side, the interaction with the gel state is favoured. The wings arise from an accumulation of the peptide in one or the other phase in the two phase region of the melting process (Ivanova and Heimburg 2001). Following this interpretation, we suggest that in the overcharged complexes PLA binding to the fluid phase is favoured, whereas at lower peptide content PLA binding to the gel state of the membrane is favoured.

4.2.2 Influence of PLA binding on the miscibility of DMPC/DPPG membranes

By adding the zwitterionic DMPC to the membrane the surface charge is reduced, which has effects on binding constants, saturation concentrations and steric constraints during the binding process. Moreover the two kinds of lipids may phase segregate and form differently composed domains. Such a demixing has been shown for PLL binding to mixed membranes (see chapter 3.2.2). It is believed that demixing plays an important role in biological systems to provide specific environments for protein binding and/or activation. Since PC and PG lipids show nearly identical bilayer structure (Watts et al. 1981), transition temperatures and enthalpies (Durvasula et al. 1999), these two molecules are ideally miscible if they have the same acyl chain lengths (Garidel et al. 1997). The difference of two CH_2 units in the acyl chain length of DMPC and DPPG leads to negative nonideality parameters, which point to a tendency for complex formation (Garidel et al. 1999). Nonetheless the coexistence range is small and the DSC curves of the mixtures show one cooperative phase transition. Despite this small nonideality, we chose this system as a means to monitor lipid demixing, because demixing results in two distinguished transition peaks.

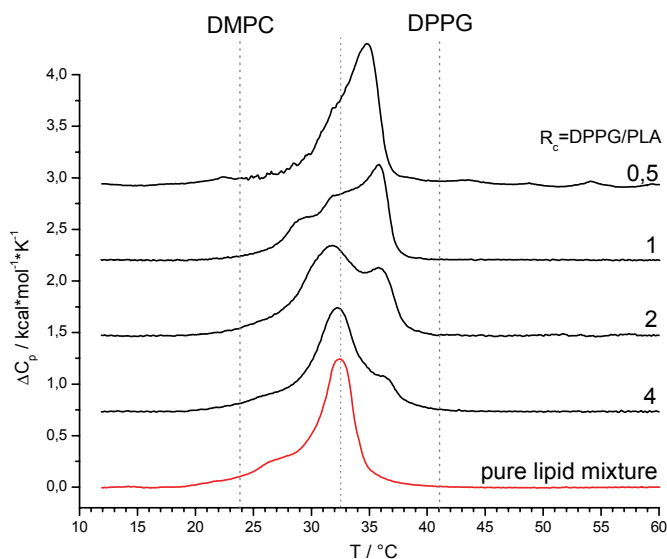


Figure 4.3: DSC plots of the binary lipid mixture DMPC/DPPG complexed with various amounts of PLA 184 resulting in the indicated charge ratios (R_c) of lipid charge / peptide charge. The vertical dotted lines indicate the main phase transition temperature of pure DMPC, the uncomplexed lipid mixture DMPC/DPPG = 1/1 and pure DPPG (from left to right). Measurements are performed in 100 mM NaCl solution at pH = 6.

The influence of PLA addition on the phase transition of an equimolar mixed DMPC/DPPG membrane is shown in Figure 4.3. It is obvious that the transition peak splits in at least two components upon PLA addition. The two components are shifted to lower and higher temperatures, respectively. The higher component, which is centred at around 36 °C, is increasing its intensity with increasing peptide content, whereas its position is rather stable. The lower component decreases in intensity and is shifted to lower temperature, as the peptide content increases. This behaviour can be interpreted with partial demixing of the lipids. PLA induces the formation of a PG rich domain, with a transition shifted to higher temperature. PLA is bound to this domain. The rest of the lipids are gathered in a consequently DMPC rich uncomplexed domain, with a lower transition temperature. That PLA does only interact with the negatively charged DPPG and not with the neutral DMPC was tested in a control experiment (data not shown). The more peptide is added, the more lipids get organised in the domain with bound PLA, depleting more and more DPPG in the other domain. Therefore, the transition temperature of the DMPC rich domain continuously decreases. In contrast, the DPPG rich binding domain seems to be unchanged in composition, which is probably favourable for PLA binding.

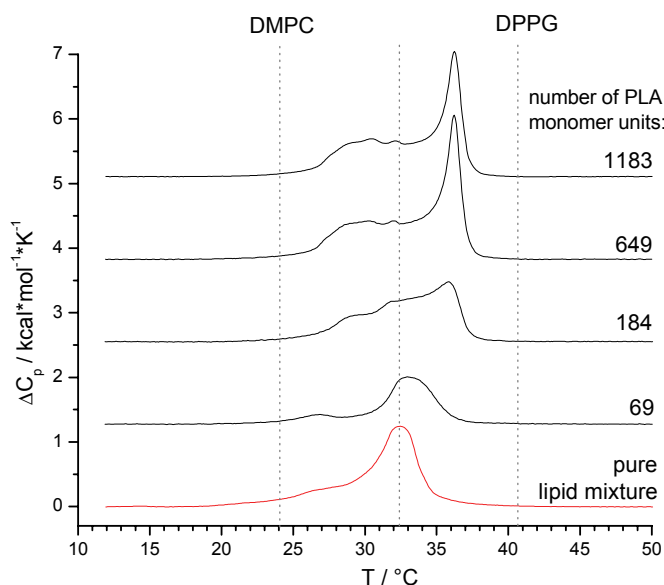


Figure 4.4: Binary lipid mixture of DMPC and DPPG in an 1/1 mixing ratio (mol/mol) (red) and complexed with PLA of different chain lengths in amounts to give a final charge ratio ($R_c = \text{DPPG}/\text{PLA}$ monomer) of 1. The vertical dotted lines indicate the main phase transition temperature of pure DMPC, the uncomplexed lipid mixture DMPC/DPPG = 1/1 and pure DPPG (from left to right). Measurements are performed in 100 mM NaCl solution at pH = 6.

However, in the transition curve of the overcharged complex ($R_c = 0.5$) a separated DMPC component is not well resolved and the ΔC_p maximum is shifted downward with respect to the

complex of $R_c = 1$. This is in agreement with Denisov et al. (1998), who state that domains dissipate if the total polyelectrolyte charge exceeds the total lipid charge.

The data presented in Figure 4.3 are data from the second heating scan. Data from the second cooling scan show in principle the same behaviour, but the component at lower temperature shows a more pronounced supercooling than the one at higher temperature. This supports the explanation that the two peaks originate from separate processes (e.g. the melting of separate domains) and not from a very asymmetric transition.

A further indication for this interpretation arises from the characteristic changes the transition peaks undergo in dependency of the PLA chain length. The corresponding DSC curves are presented in Figure 4.4. The shortest PLA ($n = 69$) affects the transition only marginally, whereas all longer PLAs induce splitting of the transition peak into three components. The high temperature component, which is assigned to the PG rich peptide bound domain, increases in intensity and cooperativity with increasing PLA chain length. The low temperature component, reflecting the transition of PC enriched membrane parts, is considerably broader, indicating a less well-defined structure of these membrane parts.

A third component can be identified which does not change position with respect to the transition midpoint of the uncomplexed membrane. This indicates that a certain fraction of lipids is not accessible for the binding polymer. This might be the inner lamella of multilamellar vesicles or precipitated vesicles that are not in equilibrium with the supernatant, or sterically or electrostatically shielded surfaces. The described trend of changes in transition behaviour is interpreted with a higher domain formation capacity of the longer polypeptides. This is in good agreement with models presented in literature (Franzin and Macdonald 2001) and was also observed for PLL induced domains. According to Macdonald et al. (1998) domain areas are proportional to the square root of the polyelectrolyte mass. Nevertheless, there seems to be an upper limit for this relationship. This is concluded from the fact that the Δc_p curves of membranes complexed with the two longest PLAs ($n = 649$ and $n = 1183$) basically resemble.

The finding of domain formation led us to investigate more thoroughly the effect of PLA binding on the miscibility of mixed DMPC/DPPG membranes. According to Hac et al. (2005) domain formation is not necessarily reflected by macroscopic phase separation. If the domains are too small they are not recognized as independent phases. Therefore, the question arises whether the domain formation results in a miscibility gap in the phase diagram. Hence, we performed more experiments with different DMPC/DPPG mixing ratios. The DSC curves of different mixed membranes without and with PLA in a charge-to-charge mixing ratio of $R_c = 1$ are presented in Figure 4.5a.

The transition curves for the complexes containing PC excess over PG are considerably broadened, gaining intensity at the high temperature side. In addition all the peaks show the above-mentioned structuring in two or three components. The complexes containing more PG than PC show increased phase transition cooperativity upon complexation with PLA. This was

already shown to be a property of pure DPPG/PLA complexes, which consequently turns up again in the DPPG rich complexes.

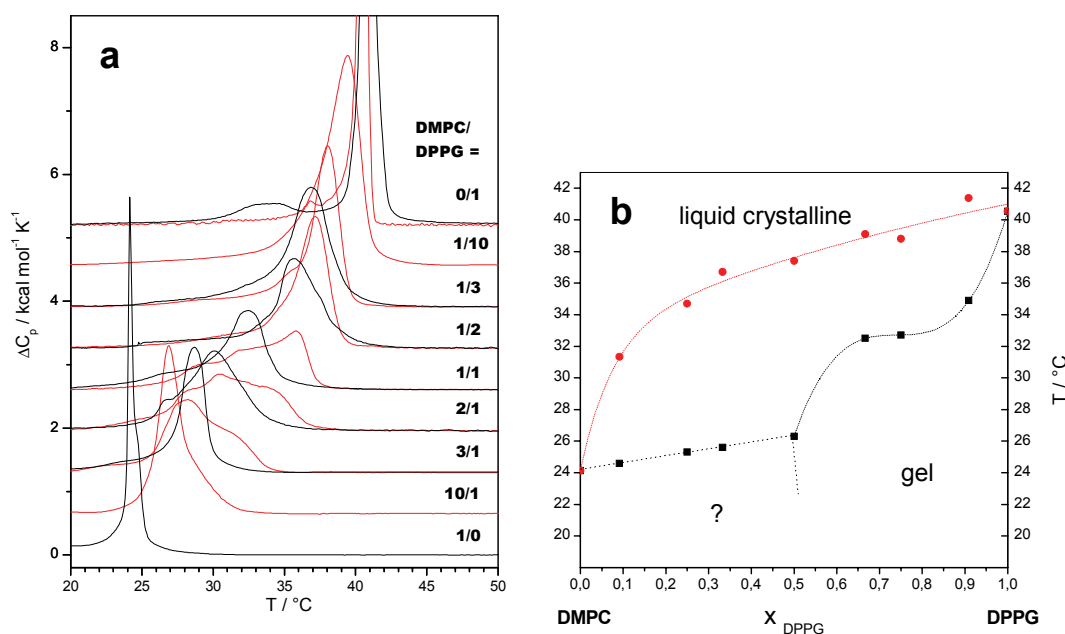


Figure 4.5: **a:** DSC plots of the phase transition range of different binary lipid mixtures DMPC/DPPG (—) and of the respective mixtures complexed with adequate amounts of PLA 184 to yield a lipid-to-peptide charge ratio of one ($R_c = 1$) (—). **b:** possible phase diagram for the mixture DMPC/DPPG being complexed with PLA 184 constructed from T_{on} (●) and T_{off} (■) of the red graphs shown in a.

On- and offset temperatures of the transition curves (T_{on} and T_{off}) were used to construct a phase diagram for DMPC/DPPG mixtures with bound PLA (Figure 4.5b). The liquidus curve, which is given by the mole fraction dependence of T_{off} , increases continuously. Thus there is no indication for lipid demixing in the liquid crystalline phase. However, the liquidus curve is asymmetric showing a steep increase at low PG mole fractions. T_{on} , which determines the solidus curve, is nearly constant for the membranes with low PG content, including the 1/1 PC/PG mixture. This is an indication for a gel phase miscibility gap. Mixtures containing more PG than PC show a continuous increase in T_{on} . Thus for those membranes no demixing is expected.

However, T_{on} and T_{off} can not be determined very precisely and depend strongly on the baseline that is defined during the data analysis. It is especially not clear whether the solidus curve at low PG contents is horizontal or not. The plateau in the solidus curve is not as nicely pronounced as in the case of PLL binding. It might also be that the solidus curve shows a slight increase in this region of the phase diagram. Moreover using T_{on} and T_{off} as delimiter of the phase boundaries is only a very rough estimation, because peak broadening by low cooperativity is not taken into account (Johann et al. 1996). To validate the hypothesis of a gel

phase miscibility gap more proof is necessary. Another attempt to investigate the miscibility will be described in the IR section (section 4.5).

4.3 Isothermal titration calorimetry

After DSC experiments indicated that at least two processes are involved in PLA binding to DPPG membranes that influence the lipid phase transition in a different manner, we performed more experiments to elucidate the character of these processes. Isothermal titration calorimetry (ITC) is capable of monitoring minute changes in binding enthalpy upon stepwise addition of one reactant to the other. Compared to the PLL experiments, the titration was performed in the reversed manner (titrating PLA into PG vesicle suspension). In the case of PLA binding, this gave the better experimental results.

Figure 4.6 shows the titration curves and the integral heats of the reaction of different PLA with DPPG vesicles at 10 °C below T_m . The heat profiles clearly show that the binding of one adequate PLA to DPPG involves two processes, one being endothermic and the other being exothermic. Up to a binding of approximately 0.4 equivalents of PLA ($R_c = 2.5$) the binding is endothermic. Further titration to higher peptide contents leads to an exothermic reaction, which is indicating a change in binding mechanism. The highest amount of heat is released at a peptide content of 0.5 ($R_c = 2$). Further titration results in a decay of the reaction enthalpy to zero. Fitting these decays with a simple one site binding model yields binding constants in the range of 10^3 to 10^4 M⁻¹.

The same experiments performed at a temperature 10 °C above T_m (see Figure 4.7) show that the binding of PLA to fluid membranes is exothermic for all titration steps. Nevertheless, the initial decrease of the reaction enthalpies might be due to an endothermic process that is still underlayed but over-compensated by the exothermic one. But also a cooperative binding would explain the initial decrease. Cooperativity could be due to structural changes either of the membrane or the peptide during the binding process that facilitates subsequent binding. It is possible that a change of the peptides' secondary structure upon binding produces such an effect. Yet, also the reduction of dimensionality during the binding process of polyelectrolytes produces an apparent cooperativity (Mosior and McLaughlin 1992b).

The maximal heat is released at a binding ratio of about one. Exceeding this ratio results in a steep decrease of the reaction enthalpy per titration step, indicating high binding constants (10^5 to 10^7 M⁻¹) and a 1 to 1 binding stoichiometry.

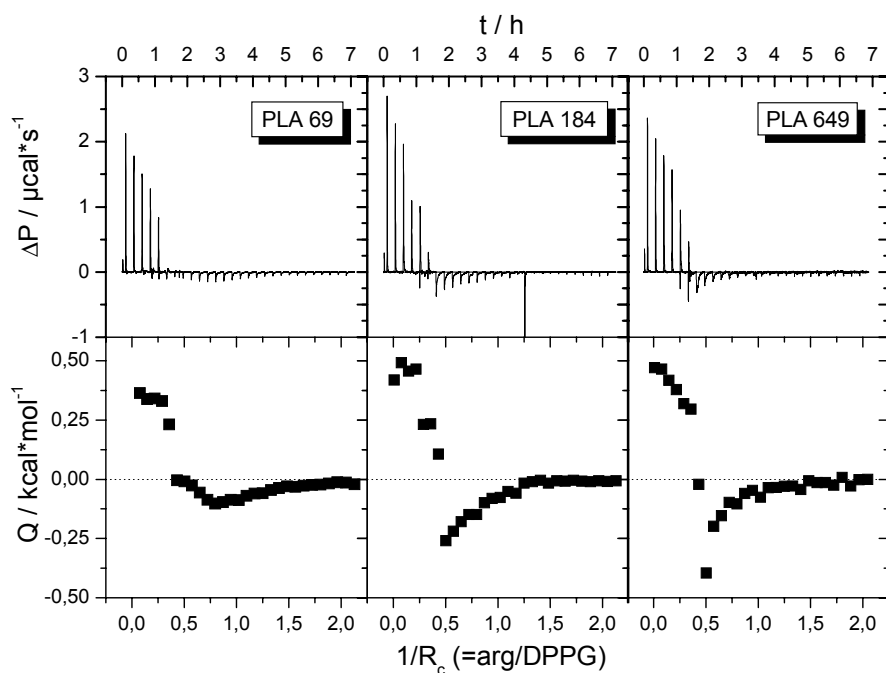


Figure 4.6: Titration curves of gel phase DPPG vesicles (LUV, $r = 50$ nm, 2 mM total lipid) with PLA of different chain length with (20 mM) at 30 °C. **Top:** heating power vs. time. **Bottom:** integral heats of reaction per mole of injectant (PLA) vs. mixing ratio.

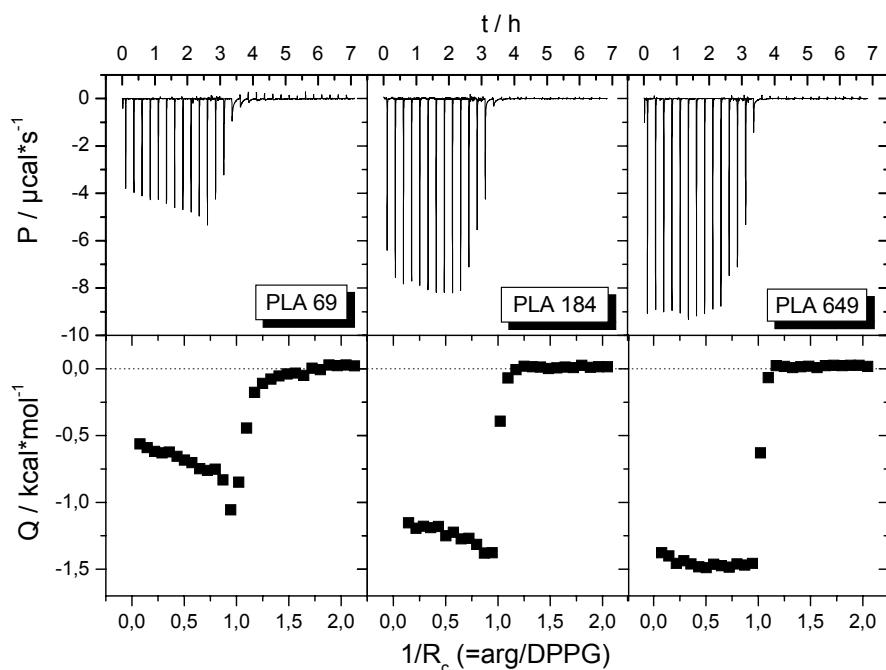


Figure 4.7: Titration curves of fluid phase DPPG vesicles (LUV, $r = 50$ nm, 2 mM total lipid) with PLA of different chain length with (20 mM) at 50 °C. **Top:** heating power vs. time. **Bottom:** integral heats of reaction vs. mixing ratio.

The binding of PLA to fluid state vesicles is clearly chain length dependent, which is more clearly seen, if the total heat of reaction per mol of lipid is plotted against the molar ratio (see Figure 4.8). To calculate these heats, the heats per injection have to be corrected by a volume factor that reflects the displacement of cell content during each injection. Heats are detected only in the cell volume and not in the supernatant solution. For the calculation it is assumed that supernatant and cell content always have the same composition and that the reaction takes place after the injection volume has been displaced from the cell. According to these considerations the following equation was derived to calculate the total heat of reaction per mol of cell content (in this case: lipid):

$$Q_{tot}^{cell} = \sum_i \left[\frac{Q_i^{inj} \left(1 + \left(\sum_i v_i^{inj} / v_{cell} \right) \right)}{c_{cell}^0 \cdot v_{cell}} \right] \quad (12)$$

with i being the number of injection, Q_i^{inj} and v_i^{inj} the heat and the volume of injection, v_{cell} the cell volume and c_{cell}^0 the concentration of the reactant in the cell before the first injection.

With increasing PLA chain length the total heats of reactions as well as the binding constants increase, as can be concluded from their shape of the titration curves. Comparison of the binding of PLA of the same chain length to gel state and fluid vesicles shows that binding to fluid state vesicles is much more exothermic than to gel state vesicles. The differences in reaction enthalpies range between -0.8 kcal/mol (PLA 69) and -1,5 kcal/mol (PLA 649). As binding to the two states of the membrane and the phase transitions of pure and bound membrane can be regarded as a cyclic process these heats are connected according to:

$$\Delta_t H_{L/P}^{g \rightarrow fl} = \Delta_t H_L^{g \rightarrow fl} + \Delta_B H^{fl} - \Delta_B H^g \quad (13)$$

with $\Delta_t H_{L/P}^{g \rightarrow fl}$ being the gel to fluid transition enthalpy of the lipid/peptide complex, $\Delta_t H_L^{g \rightarrow fl}$ the transition enthalpy of the free lipid, and $\Delta_B H^{fl}$ and $\Delta_B H^g$ the binding enthalpies of the peptide to the fluid and the gel phase, respectively. Thus the binding enthalpies should contribute to the phase transition enthalpy measured in the DSC experiments (see Figure 4.1 and Figure 4.2). If, as in the here presented case, the difference between the last two terms in equation (13) is negative (i.e. exothermic), the transition enthalpy of the membrane/PLA complex is reduced with respect to the transition of the free membrane. This explains, at least partly, the unexpected reduction of transition enthalpies which were reported above.

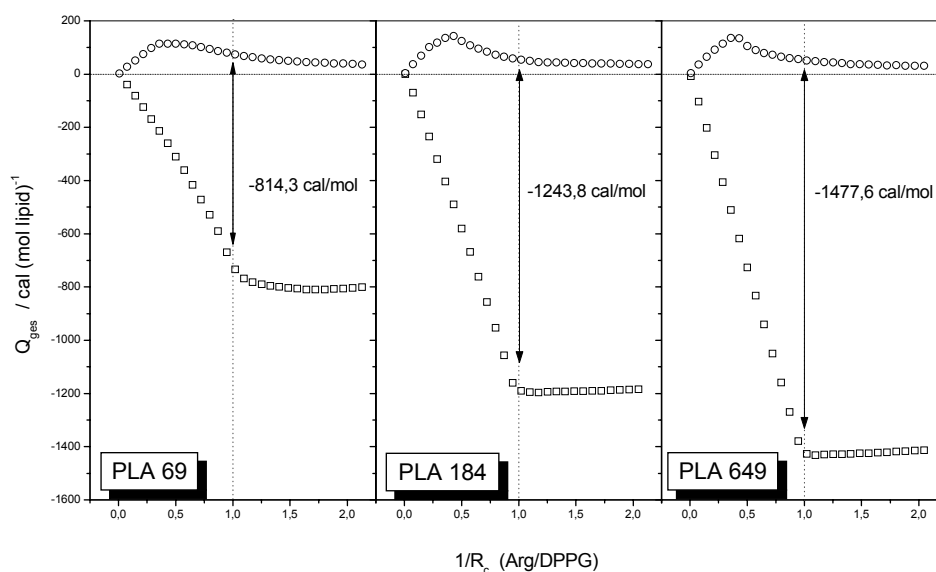


Figure 4.8: Total heat of reaction per mol of lipid released upon PLA binding to DPPG vesicles at 30 °C (circles) and 50 °C (squares). The differences between both curves at a molar ratio $R_c = 1$ are given in the graphs.

The ITC experiments give direct evidence for at least two distinct binding processes, but still mechanistic information is lacking. Nevertheless, besides the different binding constants and enthalpies it was observed that also the binding stoichiometry of PLA binding to gel phase or fluid phase membranes is different. Whereas binding to fluid vesicles shows a 1 to 1 stoichiometry, gel state vesicles seem to be saturated at a peptide content of 0.5 ($R_c = 2$) or even below. A stoichiometry of two lipids per peptide monomer is expected, if one assumes, that binding is electrostatic and that only the lipids of the outer monolayer of the vesicle are accessible. This explains the gel state binding stoichiometry. A stoichiometry of 1, as found for PLA binding to fluid vesicles, would consequently mean that all the lipids of a vesicle are accessible, i.e. the vesicle is ruptured or the peptide is translocated through the membrane.

Indeed, arginine rich macromolecules have been found in the lumen of vesicles and cells after application to the outside (Mitchell et al. 2000; Rothbard et al. 2004; Sakai et al. 2006; Wender et al. 2000). The pathway of translocation is an issue of an ongoing discussion and not yet clear (see introduction).

We showed by cryo-TEM imaging (Figure 4.25), that fluid POPG vesicles are not completely ruptured upon PLA binding. Moreover we performed dye release experiments that showed that the vesicle content does not completely mix with the external volume (see 4.6). Thus, it might be that transient pores (Tang et al. 2007) are formed that allow the peptide to migrate into the vesicle and to bind to the inner monolayer.

The notion that more PLA interacts with membranes in the fluid state than in the gel state, was also reported by Tsogas et al. (2005a), who showed by zeta potential measurements that more PLA was necessary to neutralise anionic DHP containing vesicles in the fluid phase as compared to the gel phase. Moreover they showed by fluorescence quenching that the PLA content in the bulk phase was reduced to a higher extent in the presence of fluid vesicles than in the presence of gel phase vesicles. They argued that PLA is partially incorporated in the lipid bilayer at temperatures above T_m .

Translocation pathways through the hydrophobic core of the membrane are discussed in the published literature (Fuchs and Raines 2006). Indeed it was shown that PLA might be transferred into and transferred through hydrophobic environments (e.g. chloroform, octane) after complexation to amphiphilic anions (Rothbard et al. 2004; Sakai et al. 2006). Also anionic phospholipids have been shown to alter the hydrophilicity of PLA drastically facilitating a transport to hydrophobic media (Sakai and Matile 2003; Tang et al. 2007). Hitz et al. (2006) state that only 25–30 % of the free energy of interaction between PLA and POPG containing vesicles is of electrostatic origin. The rest is attributed to hydrogen bonding and/or hydrophobic interactions.

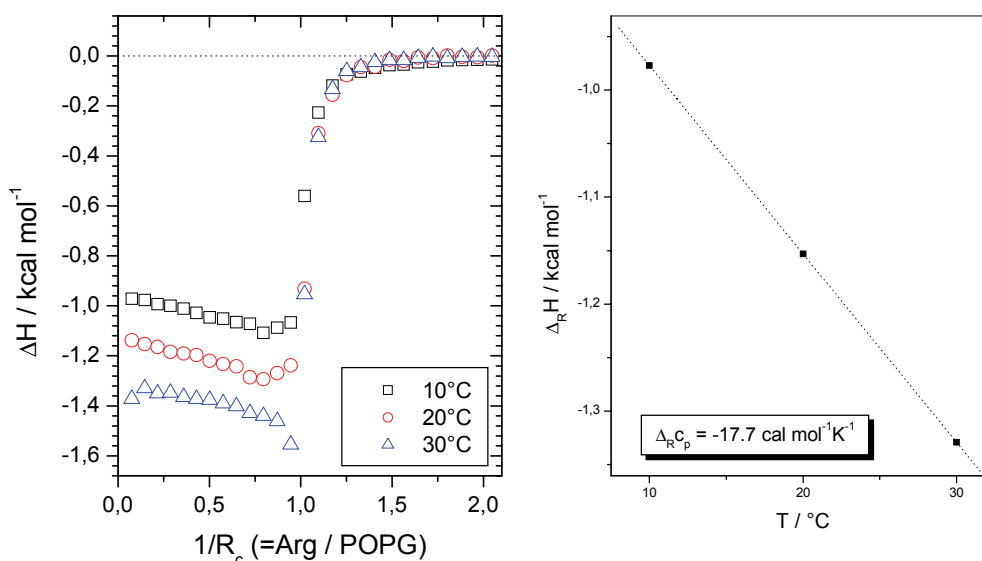


Figure 4.9: Left: Integrated heats of reaction resulting from stepwise titration of PLA 649 ($v_{\text{inj}} = 10 \mu\text{l}$, $c = 20 \text{ mM}$) to POPG vesicles (LUVs, $r = 50 \text{ nm}$, $c = 2 \text{ mM}$) at different temperatures. Right: Temperature dependence of estimated reaction enthalpies.

Temperature dependent ITC experiments showed that hydrophobic interactions indeed play a role in PLA/PG complex formation (see Figure 4.9). It can be seen that the enthalpies of the titration of PLA 649 into a suspension of fluid POPG vesicles decreases with increasing temperature. The temperature dependence of $\Delta_R H$ gives according to equation (8) the change in heat capacity during the reaction. A negative $\Delta_R C_p$ is indicative for a release of water from

hydrophobic surfaces (Blume 1983; Garidel and Blume 1999), thus implying that hydrophobic interaction between PLA and the membrane take place or the hydrophobic contact between the membrane lipids is intensified. $\Delta_R C_p$ is also influenced by ion binding to the membrane surface with subsequent release of hydration water from the interaction zone. However, these effects would produce a positive $\Delta_R C_p$ and thus counterbalance the effect that arises from hydrophobic dehydration. It was shown that the electrostatic binding of oligoarginine (R_9) to heparinsulfate (a polyanion) produces a positive $\Delta_R C_p$ (Goncalves et al. 2005). Thus it is unlikely that the negative value we measured can be attributed to any aspect of headgroup interaction. $\Delta_R C_p$ of PLA binding to POPG vesicles was estimated to be $-17.7 \text{ cal mol}^{-1}\text{K}^{-1}$ ($-74 \text{ J mol}^{-1}\text{K}^{-1}$), which formally corresponds to the removal of two hydrocarbon hydrogen atoms from contact with water (Gill and Wadso 1976). But since the hydrophilic contribution to $\Delta_R C_p$ is not known this value remains uncertain. The same temperature dependence could also be shown using saturated DPPG instead of POPG (data not shown).

4.4 Monolayer experiments

To further elucidate the mechanism of PLA binding to PG membranes, we performed monolayer experiments at the air water interface. A monolayer is a very simplified membrane model, mimicking only one leaflet of a membrane. Thus, not all processes that take place in volume phases can be observed. Possible processes such as aggregation, fusion, pore formation, or translocation that might account for energetic effects, cannot be examined in monolayer experiments. But the reduction in possible responses to PLA binding is also a strength of these experiments. Only the first steps of binding are detected and can be separated from subsequent structural changes that often make volume experiments difficult to interpret.

Monolayers of DPPG were spread on an aqueous subphase containing 100 mM NaCl at different surface pressures π_0 . After injection of PLA into the subphase we recorded the changes of surface pressure as a function of time (Figure 4.10). The shape of the recorded surface pressure curves is strongly dependent on the initial pressure π_0 . Two general situations can be distinguished: If PLA is injected underneath a monolayer at low π_0 , the surface pressure decreases first and increases in a second step, reaching an equilibrium value higher than π_0 . If PLA is injected underneath a monolayer at high π_0 , the surface pressure increases, reaching a plateau ca. 20 min after injection.

Which of the two cases is observed seems to be dependent on the phase state of the monolayer. Monolayers can exist in different phases. At low surface pressures (π) and high areas per molecule (A_m) the monolayer is in the liquid expanded phase (LE), which is, with respect to lipid order and mobility (but not in the headgroup cross sectional area), comparable to the liquid crystalline phase (L_α) of a bilayer. At higher surface pressure and low area per

molecule the monolayer is in the so called liquid condensed phase (LC) which is comparable to the gel phase (L_{β}) formed by bilayers. The transition pressure (π_{tr}) observed under the here chosen conditions is 10 mN/m (see Figure 4.11 or underlayed π - A isotherm in Figure 4.10).

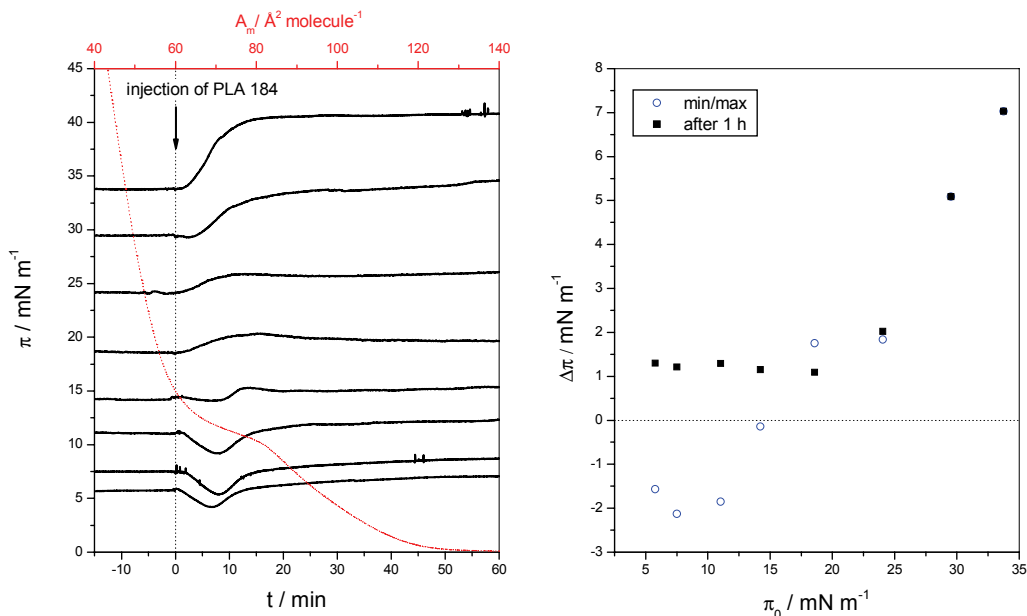


Figure 4.10: **Left:** Adsorption kinetics of PLA 184 at DPPG monolayers at different starting surface pressures on a subphase of 100 mM NaCl solution in H₂O. PLA (10 μ l, 15 mM) was injected underneath the monolayer at $t = 0$. The red curve (top scale) is the surface pressure/Area isotherm of DPPG at 20 °C, which is given to identify the monolayer phase state. **Right:** Changes in surface pressure after injection of PLA vs. initial surface pressure.

The decrease in surface pressure upon PLA binding to LE monolayers indicates that the lipids get condensed and the molecular area and mobility is lowered. This is due to electrostatic adsorption to the interface and shielding of the headgroup charges. The subsequent increase in surface pressure is interpreted as an insertion of the arginine side chains into the headgroup region of the monolayer, thus, decreasing the molecular area per lipid molecule. This binding mechanism is also found in the LE/LC phase transition region.

When all lipids are in the condensed state ($\pi_0 > 15$ mN/m) no decrease of π is detected upon PLA interaction but the injection is now directly followed by an increase of π . This increase is higher the higher the initial surface pressure of the monolayer is. The lack of the initial decrease implies that lipids, which are organised in a liquid condensed monolayer are not further condensed by PLA adsorption. The peptide side chains, though, still insert between the lipid headgroups. At the monolayer-bilayer equivalence pressure, which was found to be ca. 30 mN/m (Blume 1979), PLA addition increases the surface pressure, i.e. the peptide inserts into the monolayer. Because at this pressure the lipid organisation in the monolayer

should be the same as in a bilayer at the same temperature, it can be assumed that also gel state DPPG vesicles are penetrated by PLA.

The differences of pressures reached after 1 h of interaction and the initial values π_0 are given in Figure 4.10b. Interestingly these $\Delta\pi$ values are almost constant in the range of $\pi_0 < 20$ mN/m, which is the range of LE monolayers and the coexistence range LE/LC. When all lipids are in the condensed state $\Delta\pi$ increases with π_0 . This relationship is quite unexpected, because commonly reported relationships are inverse, i.e. $\Delta\pi$ depends inversely proportional on π_0 , which is explainable with the peptide being more readily inserted in a more loosely packed monolayer (Bringezu et al. 2007; Demel et al. 1973; Dyck and Loesche 2006; Kimelberg and Papahadjopoulos 1971; Maget-Dana 1999).

An explanation for the increasing $\Delta\pi$ values with increasing π_0 can be given under inspection of the π - A isotherms, which are presented in Figure 4.11. The isotherm of DPPG on a pure NaCl subphase shows a transition pressure π_t of 10 mN/m, with a corresponding molecular area of 80 \AA^2 and a collapse area of 40 \AA^2 . These values correspond well with DPPG isotherms, reported in the literature (Grigoriev et al. 1999; Sacre and Tocanne 1977). If DPPG is spread on PLA containing subphases the molecular area per lipid is increased in the LE phase as well as in the LC phase, indicating an insertion of PLA into the monolayer. This confirms the interpretation of the pressure increase detected in the adsorption experiments. The $\Delta\pi$ values given above correspond to the pressure difference of the pure DPPG isotherm and the isotherm of DPPG on a PLA containing subphase at a constant molecular area (see up pointing arrows in Figure 4.11). This pressure difference increases when the compressibility of both monolayers decreases under compression (i.e. the isotherms become steeper). The effect of an increasing pressure differences is even more pronounced when the compressibility of the DPPG monolayer with inserted PLA decreases more than that of the pure DPPG monolayer. This can be, indeed, observed for the isotherms of LC phase monolayers (see Figure 4.11). This increasing difference in surface pressure between both isotherms with decreasing A_m is equivalent to the increase in $\Delta\pi$ with increasing initial monolayer pressure π_0 , which was observed in the adsorption experiments.

This correlation exists as long as the inserted polypeptide is not squeezed out from the monolayer at the exclusion pressure π_{ex} . In the case of PLA inserted into DPPG monolayers π_{ex} is higher than 40 mN/m. The high exclusion pressures indicate a strong interaction between the lipids and inserted PLA. The high exclusion pressures are also responsible for the unusual relation between $\Delta\pi$ and π_0 .

The lower compressibility of monolayers with bound PLA as compared to pure DPPG monolayers indicates that the insertion of PLA leads to a better order of the lipids. Probably, the monolayer compensates for the area reduction per lipid molecule, that is caused by PLA insertion, by ordering of lipid molecules that are still in the unordered LE phase. Brewster

angle microscopy showed that such unordered LE domains still exist at surface pressures significantly higher than π_{tr} (Vollhardt et al. 2000).

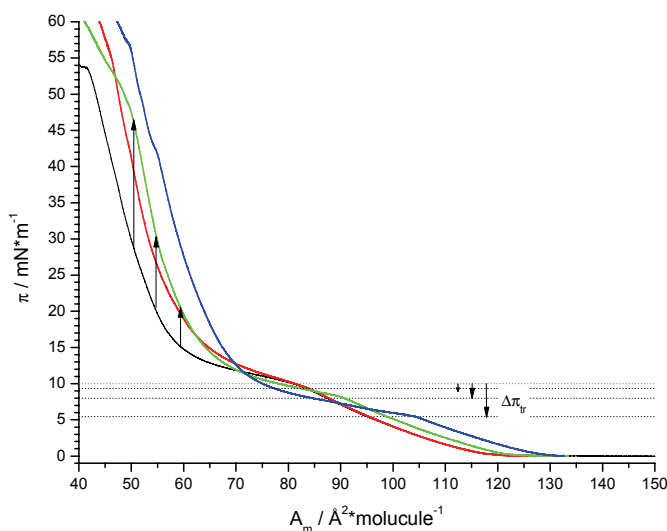


Figure 4.11: Surface pressure vs. Molecular area isotherms of DPPG, spread on different subphases : — 100 mM NaCl, — 100 mM NaCl + 0.5 mM PLA 69, — 100 mM NaCl + 0.5 mM PLA 184, — 100 mM NaCl + 0.5 mM PLA 1183. The dotted lines indicate the transition pressure of the respective monolayers. The upward pointing vertical arrows indicate the expected pressure increase in the adsorption experiments, performed at constant area. The downward pointing arrows indicate the decrease of π_{tr} upon polypeptide adsorption.

Also the reduction of the transition pressure π_{tr} shows that the interaction with PLA favours the formation of the LC phase. The reduction of π_{tr} is similar to the increase in the transition temperature of DPPG bilayers (see DSC section). Figure 4.11 shows that the extent of π_{tr} decrease depends on the PLA chain length. The longer the PLA chain, the lower is π_{tr} . This correlates well with the increase in T_m with increasing PLA chain length that was detected by DSC.

The π - A isotherms further show that also the magnitude of increase in average molecular area per lipid molecule depends on the PLA chain length. In general, the increase is higher the longer the PLA chain is, which implies that longer PLA insert to a higher extent into the monolayer than shorter ones.

The monolayer experiments support the interpretation of the DSC data as well as of the ITC data given before. The increase of π after injection of PLA and the increased molecular areas in the π - A isotherms show that the peptide interacts not only superficially but inserts to a certain extent in the lipid membrane or monolayer respectively. This differs from the interpretations of Goncalves et al. (2005). They stated on basis of ^2H -NMR experiments that the interaction of R_9 with POPG/POPC bilayers is only superficial. However, these differences might be due to the different degrees of polymerisation.

In principle, the same effects have been found for PLL interaction with DPPG monolayers. However, direct comparison of the $\Delta\pi$ values measured in adsorption experiments shows that the pressure decreases (LE phase) are more pronounced in the case of PLL adsorption and the pressure increases (LC phase) are more pronounced in the case of PLA adsorption. This shows that PLL has a higher propensity to condense the monolayer and PLA has a higher propensity to insert into the monolayer. This is in good agreement with the results of the other experiments presented before.

4.5 Infrared spectroscopy

Transmission FT-IR spectroscopy was used to separately monitor the influence of PLA binding on different parts of the bilayer. We evaluated the changes of the methylene and carbonyl stretching vibrational bands to retrieve information on the hydrophobic and interfacial region of the membrane, respectively. In addition we monitored the secondary structure changes the peptide undergoes upon binding to the membrane by analysing the amide I absorption band. Furthermore, the influence of PLA binding on the lateral phase separation in mixed DMPC/DPPG membranes was examined. All IR experiments were performed with a lipid to peptide mixing ratio of $R_c = 1$ and as a function of temperature.

4.5.1 Complexes with pure DPPG

The CH₂ stretching bands

The frequency of the CH₂ stretching vibration ($\nu(\text{CH}_2)$) is sensitive to the order of the hydrocarbon chains in the hydrophobic part of the membrane. In Figure 4.12 the wavenumbers of the $\nu_s(\text{CH}_2)$ vibrational bands of DPPG and its complexes with PLA of different chain length are presented as a function of temperature. The transition temperature T_m of the membrane can be determined from the point of inflection. It is only marginally influenced by PLA binding. In the case of PLA 184 binding it is slightly decreased ($\Delta T_m = -0.9$ °C) and in the case of binding PLA 69 and 649 it is slightly increased ($\Delta T_m = 0.4$ °C). The absolute values are below the resolution of the experiment and should not be over-interpreted. However, they reproduce very well the results of the DSC experiments.

Additional information can be deduced from the absolute values of the vibrational frequencies. In both, the gel and the liquid crystalline phase the wavenumber of $\nu_s(\text{CH}_2)$ is reduced upon interaction of the membrane with PLA. This effect was already seen for the interaction with PLL, which in contrast to PLA, significantly increased the transition temperature of the membrane. This shows that the two effects are independent.

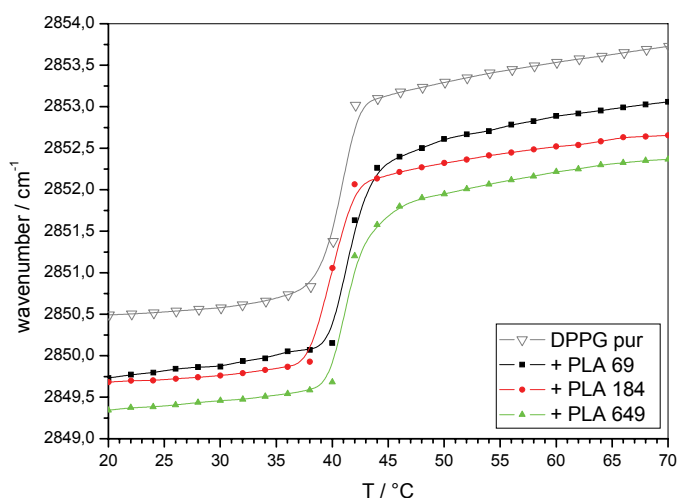


Figure 4.12: Wavenumber of the maximum of the $\nu_s(\text{CH}_2)$ vibrational band of DPPG (∇) and DPPG in the complexes DPPG with PLA 69 (\blacksquare), PLA 184 (\bullet), and PLA 649 (\blacktriangle). The Lipid-to-peptide mixing ratio $R_c = 1$. Measurements are performed in 100 mM NaCl solution in D_2O , at pD = 7.

A lower CH_2 stretching vibrational frequency is normally interpreted with a higher order of the acyl chains (Tamm and Tatulian 1997). One major contribution could be attributed to the ratio of gauche to trans conformers within one acyl chain (Cameron et al. 1981). This interpretation has been confirmed by the analysis of the CH_2 wagging bands which are very sensitive to the number and sequence of gauche and trans conformers within the hydrocarbon chain (Senak et al. 1991; Tuchtenhagen et al. 1994).

But also other effects influence the band positions. Large influence has the nature and the charge of the lipid headgroup. Protonation (and thus neutralization) of the PG headgroup results in a reduction of the CH_2 stretching vibrational frequencies (Tuchtenhagen et al. 1994). The same is the case for PA headgroups. This can be attributed to a reduction in electrostatic repulsion between adjacent headgroups, which allows a closer contact between the acyl chains and increases the van der Waals interaction energies. Stronger interchain interaction is thus reducing the $\nu(\text{CH}_2)$ frequencies. The same explanation can be adopted for the electrostatic screening by PLA binding (as it was already done for PLL binding).

However, in the present case this explanation remains unsatisfactory in one aspect. In the case of PG or PA protonation, as well as in the case of PLL binding, the increased hydrophobic contact results in an increase of T_m . This is not the case for PLA binding. Thus, there must be still another contribution. It was found that the stretching vibrational frequencies are influenced by other factors than acyl chain ordering. Kodati et al. (1994) showed for DPPC and hexadecane that partial deuteration of the hydrocarbon chains increases the frequencies of $\nu_s(\text{CH}_2)$ and $\nu_{as}(\text{CH}_2)$, whereas the order parameters are not influenced. Equally, Kerth (2003) showed that the CH_2 stretching vibrational frequencies of DPPC membranes are increased if

some of the lipids had perdeuterated chains or one of the lipids acyl chains (*sn*-1 or *sn*-2) was deuterated. This effect was explained by a reduction of interchain vibrational coupling. Vice versa, this means that a decrease of the stretching vibrational frequencies, as it is observed in the present case, could be due to an increased interchain vibrational coupling. This could be accomplished by a restriction of the rotational motion of the acyl chains, induced by peptide headgroup interaction. If that is the case, an additional effect should arise from the coupling of the librotorsional modes with the methylene stretching mode (Kodati et al. 1994). If the librotorsional motion is hindered by polypeptide binding, the reduction of the $\nu_s(\text{CH}_2)$ frequency should be even enhanced.

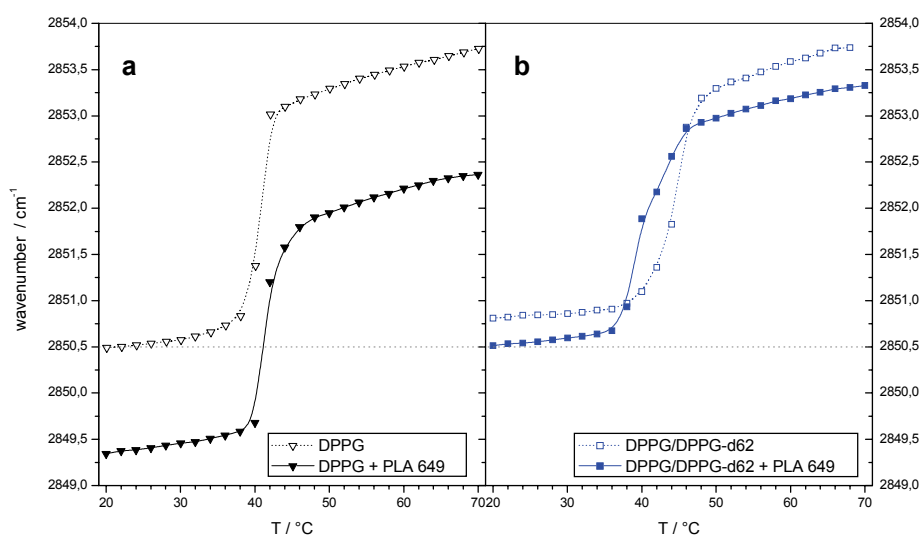


Figure 4.13: Wavenumber of the maximum of the $\nu_s(\text{CH}_2)$ vibrational band of **a**) DPPG (∇) its complex with PLA 649 (\blacktriangledown) and **b**) DPPG in a mixed DPPG/ d_{62} -DPPG membrane (\square) and its complex with PLA 649 (\blacksquare).

To prove the influence of interchain vibrational coupling we examined the complexes of PLA formed with mixed DPPG/DPPG- d_{62} membranes, which are chemically and structurally identical to a DPPG membranes (Figure 4.13). As a result of the isotopic dilution, the interchain vibrational coupling of the CH_2 groups is disturbed. This is reflected by the higher wavenumber of the $\nu_s(\text{CH}_2)$ vibration of the mixed membrane if compared to a completely undeuterated membrane ($\Delta\tilde{\nu} = 0.32 \text{ cm}^{-1}$). When the peptide now interacts with the isotopically diluted membrane, the interchain coupling cannot be increased (even if the geometry is more favourable), because the CH_2 chain cannot couple with the neighbouring CD_2 chain. As a result, the $\nu_s(\text{CH}_2)$ frequency in the DPPG/ d_{62} -DPPG/PLA complex is decreased to a much lesser extent ($\Delta\tilde{\nu} = -0.3 \text{ cm}^{-1}$) than in the DPPG/PLA complex ($\Delta\tilde{\nu} = -1.2 \text{ cm}^{-1}$). This result proves that the frequency decrease is not interpretable solely on the basis of a higher hydrocarbon order. Rather, an important contribution arises from

increased interchain vibrational coupling due to peptide headgroup interaction. The $\nu(\text{CH}_2)$ frequency decrease that is still observed in the isotopically diluted sample is explainable with the fact, that the isotopic dilution is only statistical and the coupling of the two adjacent acyl chains of one lipid molecule is not hindered in any case. Furthermore, reduced intrachain coupling of librotorsional modes with the CH_2 stretching vibrations might still account for some $\nu_s(\text{CH}_2)$ decrease, because this effect, being an intramolecular one, is not affected by isotopic dilution.

With this new finding we also reinvestigated the polylysine complexes of DPPG (Figure 4.14). In principle, the same effects are visible in this system. The decrease of the $\nu_s(\text{CH}_2)$ frequency is about the same in the PLL and the PLA sample as long as completely undeuterated membranes are used (Figure 4.14a). If the membrane is isotopically diluted this decrease is reduced in both cases.

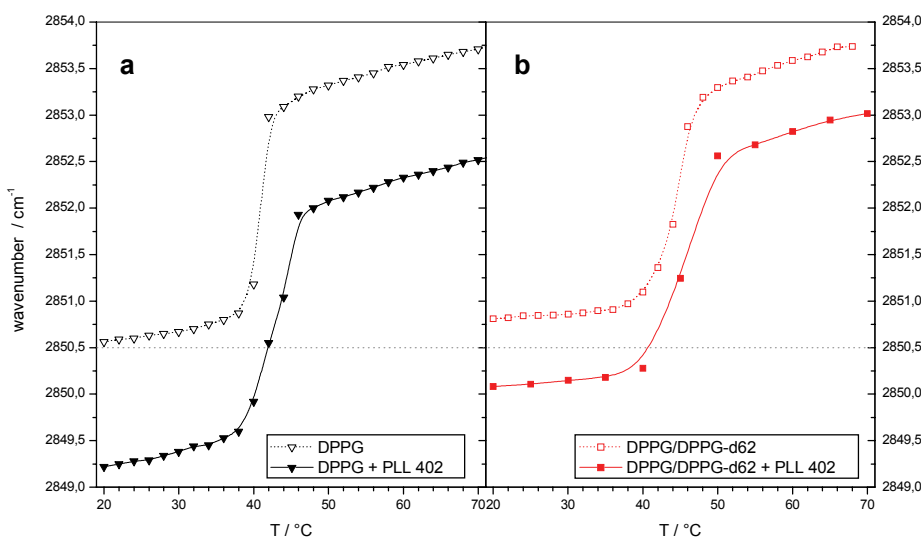


Figure 4.14: Wavenumber of the maximum of the $\nu_s(\text{CH}_2)$ vibrational band of **a)** DPPG (∇) its complex with PLL 402 (\blacktriangledown) and **b)** DPPG in a mixed DPPG/ d_{62} -DPPG membrane (\square) and its complex with PLL 402 (\blacksquare).

However, if the isotopically diluted membrane is complexed with PLL, the wavenumber of $\nu(\text{CH}_2)$ is still more decreased than in the case of complexation with PLA ($\Delta\tilde{\nu} = -0.7 \text{ cm}^{-1}$ as compared to -0.33 cm^{-1}). This means that in the case of PLL binding indeed, part of the wavenumber reduction can be attributed to a conformational ordering of the acyl chains, as it was proposed in section 3.3. This higher influence of the ordering is also reflected by the fact that PLL increases T_m of a DPPG membrane, whereas PLA does not.

The lipid C=O band

As stated above, the C=O stretching vibrations of the lipid ester groups respond to the degree of interfacial hydration (Blume et al. 1988; Lewis et al. 1994). Thus, they provide a good tool to assess the degree of water penetration, which can be influenced by polypeptide binding. The broad band that is observed at about 1740 cm^{-1} is a superposition of at least two underlying components, which can be demonstrated by the second derivative spectra (Figure 4.15b). The two underlying bands arise from non hydrated carbonyl groups (ca. 1741 cm^{-1}) and a carbonyl monohydrate (ca. 1722 cm^{-1}) (Blume et al. 1988). During the phase transition, the molecular area is increased, which allows more water molecules to penetrate into the headgroup region. As a consequence, the contribution of the lower frequency component to the overall CO vibrational band increases. This is demonstrated in Figure 4.15 for a DPPG/PLA complex. It can be seen that the C=O vibrational band is broad in the liquid crystalline phase and does not have a well-defined maximum. This prevents the simple analysis that was applied in section 3.3. Hence, we performed a more detailed analysis by fitting the bands with two underlying components and comparing their intensities and positions.

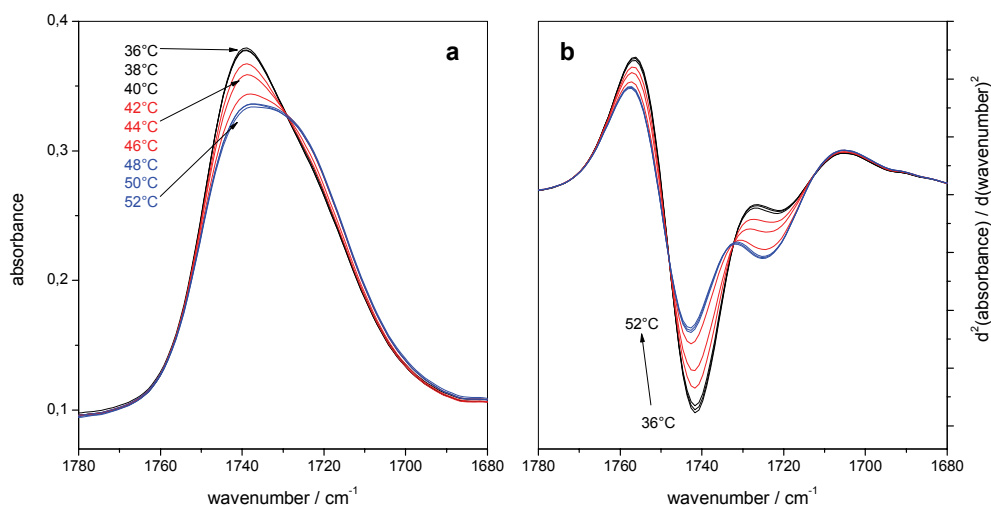


Figure 4.15: Carbonyl stretching vibrational bands ($\nu(\text{CO})$) of the complex DPPG + PLA 1183 at temperatures close to the gel to liquid phase transition region (a) and its second derivatives (b). The lipid-to-peptide mixing ratio $R_c = 1$.

As fitting parameters for the band positions, we used the minima determined from the second derivative spectra and allowed a variance of $\pm 1\text{ cm}^{-1}$. As fitting functions, simple Gaussians were used. A combination of Gaussians and Lorentzians did not give better results. Before fitting, a baseline was subtracted in the spectral region of $1660 - 1800\text{ cm}^{-1}$. The results of the analysis of different DPPG/PLA complexes at temperatures below and above the phase transition are depicted in Figure 4.16.

In general, the band component indicating the presence of hydrated C=O groups, loses intensity as DPPG is complexed with PLA. However, the hydration of gel phase membranes is only marginally influenced by PLA binding. Binding of the shortest PLA ($n = 69$) does not change the integral intensities of the two components, at all. The longer PLAs ($n = 184$ and $n = 1183$) increase the contribution of the non hydrated C=O group by some percent. This effect seems to be chain length dependent. The longer the PLA the higher is the contribution of the non-hydrated C=O group. The lower frequency component not only loses intensity but also shifts to slightly lower wavenumber. This means that the carbonyl groups are less hydrated when PLA is bound to the membrane but the remaining water molecules are bound by stronger hydrogen bonds. This is probably due to the fact that the water molecules, being trapped between membrane and peptide, are restricted in their reorientational motion which results in better oriented hydrogen bonds (Laroche et al. 1991). This coincides also with the conclusions drawn from the $\nu(\text{CH}_2)$ band analysis, namely that also the lipid molecules are hindered in their rotational diffusion.

In the liquid-crystalline phase, more pronounced effects are observed. By complexation of the membrane with PLA, the contribution of the non-hydrated carbonyl species is now increased by about 10%. This means that the fluid phase of the membrane is much less hydrated if PLA is bound. During the $L_{\beta'} \rightarrow L_{\alpha}$ phase transition water does not permeate into the membrane headgroup region to the same amount, because bound PLA reduces the accessibility of the carbonyl groups. Also in the fluid phase, the wavenumber of lower frequency component is shifted to lower values, indicating that hydration water forms more directed hydrogen bonds. In contrast to the gel phase complex, the fluid phase complex shows no chain length dependency with respect to hydration. The short PLA 69 has the same influence as the longer ones.

These findings complement well the results discussed above. Also the ITC experiments showed a dehydration, which could be deduced from the negative $\Delta_R C_p$ values. Furthermore, monolayer experiments showed that LE monolayers get condensed upon PLA binding, which reduces the intermolecular space necessary for hydration. Moreover, inserted PLA side chains reduce the space available for water molecules and compete with the lipid C=O groups for the remaining water of hydration.

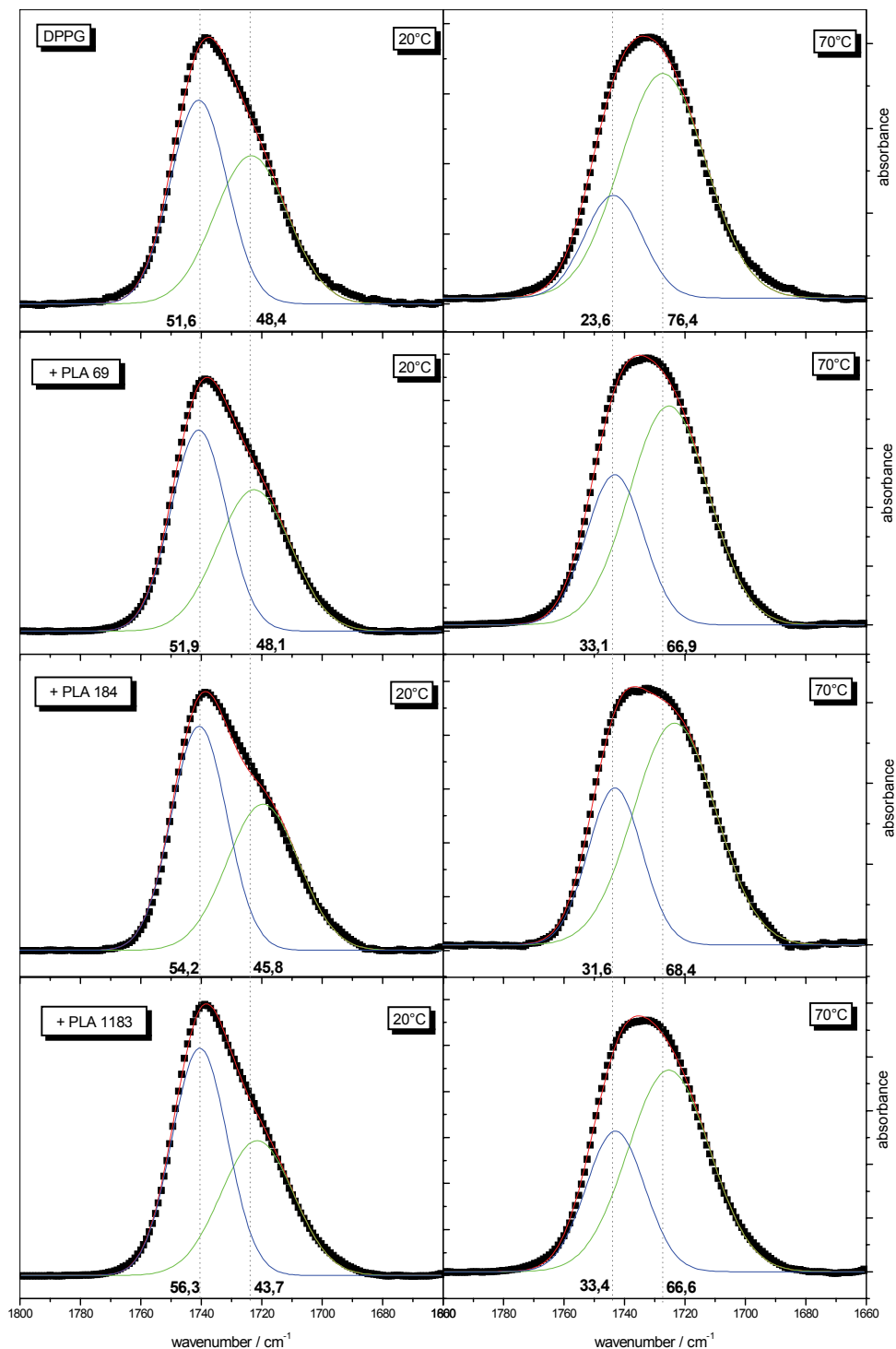


Figure 4.16: Carbonyl stretching vibrational bands of DPPG (top panels) and its complexes with PLA of different chain length (lower panels) at 20 °C (left panels) and 70 °C (right panels). The experimental bands (■) are fitted with 2 Gaussians (—, —), representing two distinct states of hydration. The summation of the fit components is shown in red (—). The relative integral intensities of the single components are given as percentages underneath the respective fitting curve. The vertical dotted lines indicate the positions of the fit components of pure DPPG.

The secondary structure of PLA in solution

The secondary structure of the peptide plays an essential role during the binding process and influences the thermodynamics and the structure of the formed complex, as has been already shown for the DPPG/PLL complexes. A convenient tool to determine the secondary structure of the peptide is the analysis of the amide I absorption band. Unfortunately, the data about the secondary structure of PLA available from literature are not as comprehensive as it is the case for PLL. No IR experiments have been published that can serve as a good reference system for the identification of different secondary structure elements which contribute to the amide I band contour of PLA. The use of the general band assignments that are developed for proteins (Goormaghtigh et al. 1994a, 1994b; Goormaghtigh et al. 1990; Tamm and Tatulian 1997) is questionable because the amide absorption of homopolypeptides often deviates from the general case. Therefore, we undertook a series of measurements to identify the frequencies of the amide I bands of PLA in different secondary structures.

PLA has been thoroughly studied in solutions of different chemical composition by CD spectroscopy. This gave us the opportunity to re-evaluate the same systems via FT-IR spectroscopy. The most comprehensive study was done by Ichimura et al. (1978). They examined the influence of different mono- and multivalent counterions on the secondary structure of PLA and proposed that a specific binding of tetrahedral anions leads to a coil to helix transition. Thereby, the anion should be able to bridge two guanidyl residues via electrostatic interactions and hydrogen bonding. In pure water PLA was found to form a random coil. Anions that induce a α -helix formation are SO_4^{2-} , ClO_4^- , $\text{P}_2\text{O}_7^{4-}$ at neutral pH as well as SO_3^{2-} , CO_3^{2-} and HPO_4^{2-} at higher pH. Increasing the ionic strength using other salts, results in a formation of β -structures and precipitation of the PLA. In context with membrane binding it is worth to mention that H_2PO_4^- is not inducing an α -helical conformation of PLA. Miyazaki et al. (1978) reported that PLA helices formed in ClO_4^- solution, unfold to give a random coil at higher temperature. The melting temperature is dependent on the ClO_4^- concentration. They report as well that PLA helices are more stable than PLL helices, i.e. the free energy of helix formation is more negative. Rifkind (1969) showed that PLA helices were formed in dioxan/water mixtures. X-ray diffraction studies on the secondary structure of PLA were performed by Suwalsky and Traub (1972). They showed that the secondary structure of PLA is dependent on the water content of the sample. Hydrating PLA with 20 water molecules per arginine monomer, results in the formation of β -sheets. On reducing the water content to 5 molecules per monomer or less, α -helices are formed. Whether helix formation can be induced by pH increase, as it was shown for PLL, is controversially discussed in literature (Ichimura et al. 1978; Rifkind 1969). Clear is that the high $\text{p}K_{\text{app}}$ of PLA (12.5) makes this approach difficult (Sakai et al. 2006; Sakai and Matile 2003).

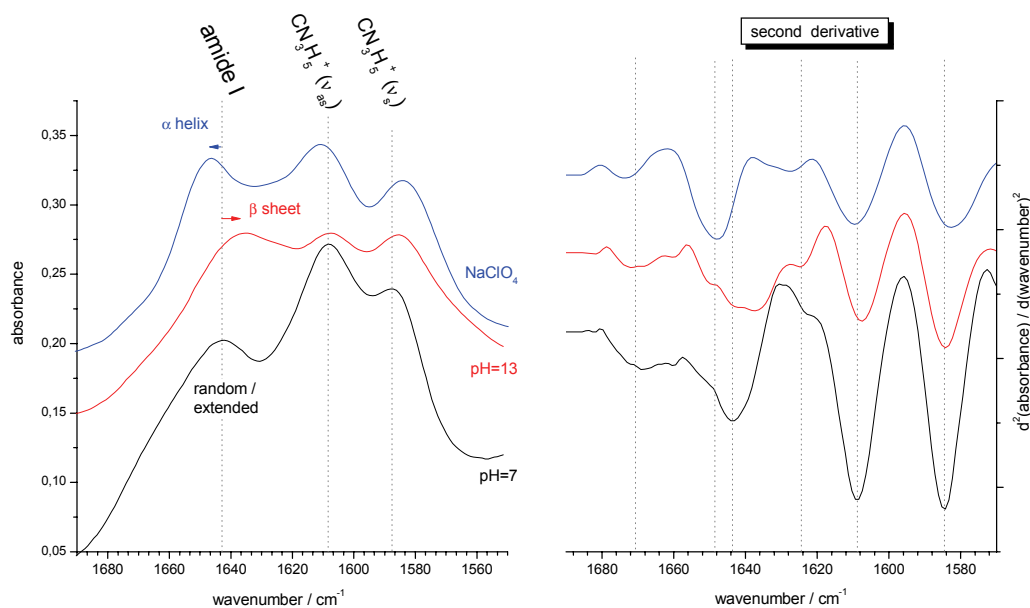


Figure 4.17: Amide I and guanidinium vibrational bands of poly(L-arginine) in — random coil (100 mM NaCl, pH=7), — β -sheet (100 mM, NaCl, pH = 13), and — α -helical (150 mM NaClO₄, pH = 7) conformation (**left**) and its second derivatives (**right**).

With this information we re-investigated the described systems via IR spectroscopy. Figure 4.17 shows amide I bands of PLA in three different secondary structures. A peculiarity that impedes the interpretation of these bands is the superposition of the amide I band with the arginyl side chain vibration. However, single components can be deconvoluted in the second derivative spectra. The symmetric and antisymmetric guanidyl stretching vibrations give rise to absorption bands at 1584 cm^{-1} and 1608 cm^{-1} , respectively (Barth and Zscherp 2002; Chirgadze et al. 1975).

As reference system for the random coil structure, we used PLA dissolved in pure water at pH 7. In this conformation, the amide group absorbs at 1644 cm^{-1} . Spectra of PLA in 100 mM NaCl solution did not differ from those recorded in salt free solution. Thus, it is assured that in all reported experiments PLA is added in a random conformation. The α -helical conformation was induced by a 250 mM NaClO₄ solution (Ichimura et al. 1978; Martinez et al. 2007; Miyazaki et al. 1978). The amide I band of α -helical PLA is shifted to slightly higher wavenumbers (ca. 1648 cm^{-1}). The same component could be identified in dioxane and SO₄²⁻ solution, however, to a lower extent. The existence of a helix was proven by thermal unfolding, following the experiments of Miyazaki et al. (1978) (**Figure 4.18**). As the temperature is raised, the band at 1648 cm^{-1} vanishes and a band at the position that was assigned to random conformers evolves. This process is completely reversible on cooling.

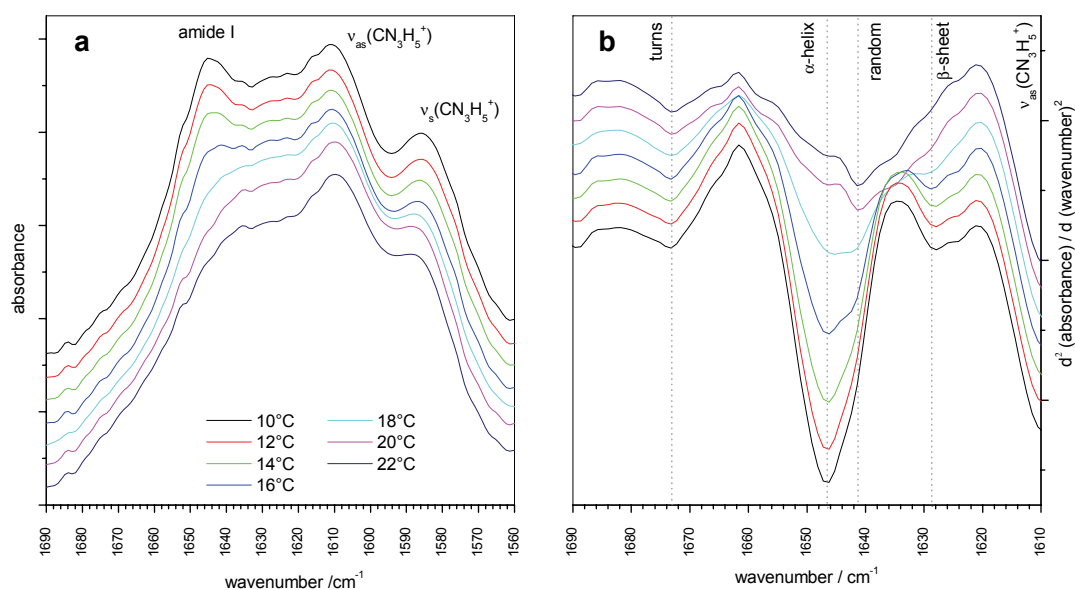


Figure 4.18: Amide I and guanidinium vibrational bands of PLA 649 in 100 mM NaClO₄ at different temperatures **(a)** and their second derivatives in the amide I region **(b)**. Note that the order of the graphs is reversed in **(b)**

More difficult to identify was the typical amide I band position of a β -sheet structure. Raising the pH of a PLA solution above the pK_{app} shifts the band position to lower wavenumber (Figure 4.17). In the second derivative spectra, several components are visible, with the lower frequency components probably being due to β -sheet structures. To unambiguously assign a frequency to the amide I vibration of a β -sheet, we performed experiments at low water content, as suggested by Suwalsky and Traub (1972). A sample with a D₂O content of 20 molecules per side chain was prepared and measured in an open IR cell, allowing the water to evaporate in course of the measurement. To assist the evaporation, we performed heating and cooling cycles. Under these conditions a β -sheet should transform into an α -helix during the measurement. The results are presented in Figure 4.19. All detected spectra consist of two components, of which one is the typical α -helix vibrational band. The other component showing up between 1620 cm⁻¹ and 1625 cm⁻¹ is consequently assigned to a β -sheet vibration. As the temperature increases, the α -helix component decreases and the β -sheet band increases and shifts to slightly lower wavenumbers. At high temperature a small random coil component is visible. On cooling, the whole process is reversible, but due to evaporation of the water the α -helix to β -sheet transition is shifted to higher temperature (Figure 4.19). This is in good agreement with the finding that at low water content PLA α -helices are more stable than β -sheets (Suwalsky and Traub 1972) and is taken as confirmation that the proposed band assignments are reasonable.

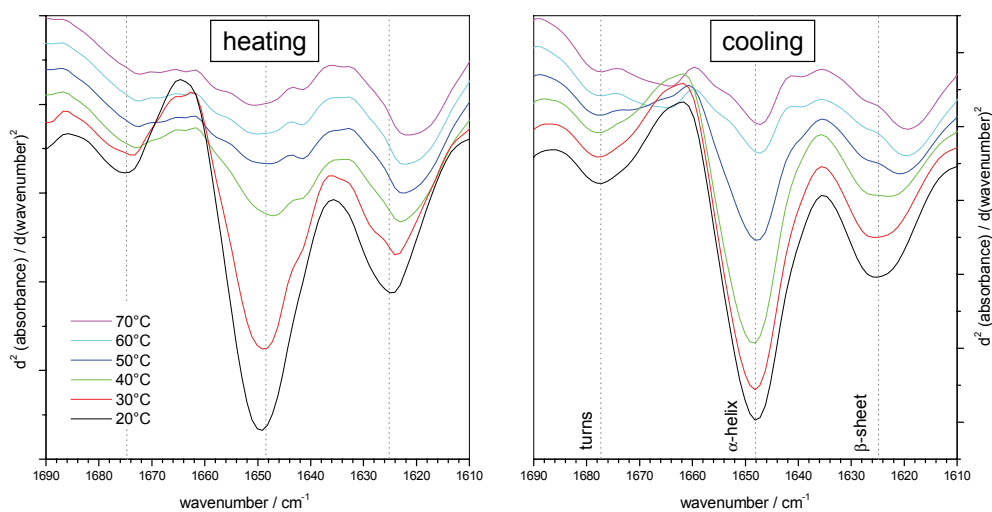


Figure 4.19: Second derivative spectra of PLA 649 prepared in 20 mol D2O per mol of Arg side chain and measured in an open cell, allowing the water to evaporate during the measurement. **Left:** heating cycle; **Right:** cooling cycle.

Combining this information, we are now able to assign typical vibrational frequencies to distinct secondary structures. The results are summarized in Table 2. The high frequency component that is present in all discussed spectra is assigned to turn structures.

Table 2: Left: Wavenumbers of amide I vibrations of poly(L-arginine) in different secondary structures. **Right:** Wavenumber of side chain vibrations of Poly(L-arginine).

Secondary structure	Wavenumber of amide I band / cm^{-1}
β -sheet	1620 – 1630
random coil	1642 – 1644
α -helix	1646 – 1648
turns	1670 - 1680

Side chain vibration	Wavenumber / cm^{-1}
$\nu_{\text{as}}(\text{CN}_3\text{H}_5^+)$	1584
$\nu_{\text{as}}(\text{CN}_3\text{H}_5^+)$	1608

Secondary structure of PLA bound to DPPG membranes

With the knowledge of the band positions in the amide I region, we then examined the secondary structure PLA adopts upon binding to DPPG membranes. Figure 4.20 shows spectra in the amide I and guanidyl stretching vibration region of PLA of different chain length bound to DPPG at 10 °C and 70 °C, respectively. The band shape is as well dependent on the length of the PLA as on temperature. With increasing chain length the band is shifted to lower vibrational frequencies, indicating an increase in β -sheet elements. With increasing

temperature the band position is shifted to higher frequencies, i.e. in the region that was assigned to random coil and α -helical structures. The temperature dependence is most pronounced for the PLA of intermediate chain length ($n = 184$). Interestingly also the guanidyl stretching vibrations are influenced by membrane binding. Independent on PLA chain length and temperature, they are shifted to lower wavenumbers. This must be due to an interaction of the arginine side chain with the phospholipid headgroups. A downshift of the guanidyl stretching vibrations was also shown in SO_4^- solution (Chirgadze et al. 1975), which is known to bridge adjacent arginine side chains via hydrogen bonding (Ichimura et al. 1978). Thus, the measured downshift of the bands is an indication that PLA interacts with DPPG headgroups via hydrogen bonding. However, we measured a downshift of the guanidyl bands also in dioxane/ D_2O solution and in very high concentrated saline (2 M NaCl). Therefore, also dehydration could be responsible for the effect.

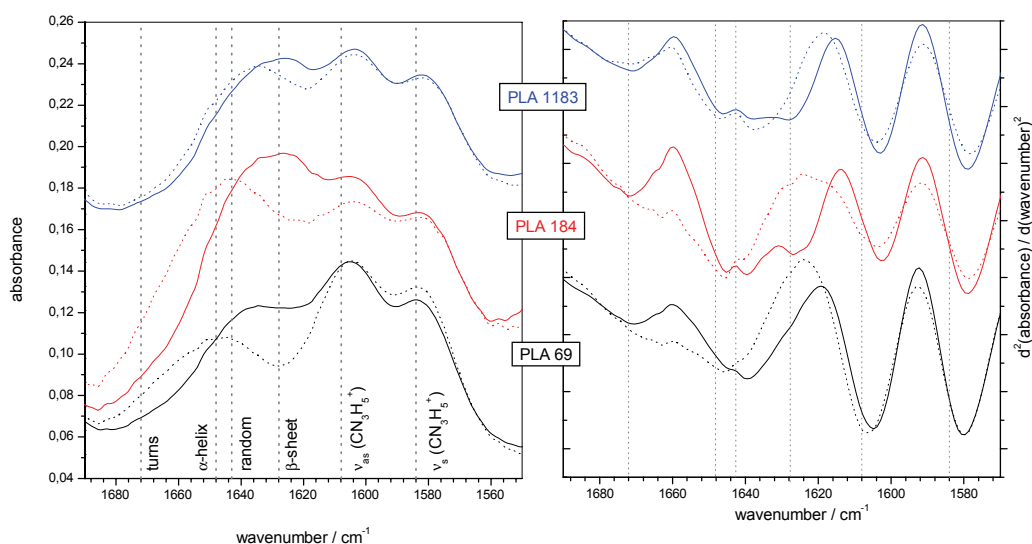


Figure 4.20: Left: Amide I and guanidyl bands of PLA of different chain length bound to DPPG membranes at 10 °C (solid lines) and at 70 °C (dotted lines) and **right:** its respective second derivatives.

The second derivative spectra of the amide I region reveal that a mix of structural elements is present in every sample. This is illustrated in detail in Figure 4.21. The spectra of the two longer PLA ($n = 184$ and $n = 1183$) show 3 distinct components at 1645.5 cm^{-1} , 1639.5 cm^{-1} and 1627 cm^{-1} . In the spectra of PLA 69 only the two higher frequency components are present. Furthermore, in all spectra a high frequency component at 1671 cm^{-1} is resolved, which is due to turn vibrations. The lowest component can be unambiguously assigned to β -sheet structures. The two remaining components at 1639.5 cm^{-1} and 1645.5 cm^{-1} should arise from random coil and α -helix vibrations, respectively. This is suggested by the sequence of the bands in the spectra. However, the frequencies are slightly lower than those determined for PLA in solution. This might be caused by the lower polarity of the membrane

headgroup region as compared to bulk water. This should strengthen the intramolecular H-bonds of the peptide, which shifts the absorption maxima of the amide I vibration to lower frequencies.

Following this interpretation, we can describe the binding behaviour as follows: Longer PLA binds in a mixture of helix, random and β -sheet conformation to DPPG membranes at low temperatures. The β -sheet content increases with increasing PLA chain length. As the temperature is raised, first, the β -sheet unfolds to give more peptide in random conformation. At higher temperature, more α -helix is formed on expense of the random coil conformers. Short PLA does not form a β -sheet upon binding. The short peptides are bound mainly in a random conformation at low temperatures. As the temperature is increased, the peptide transforms increasingly into α -helices. The reason for the presence of different secondary structure motives in one sample might be the existence of differently bound peptide. Peptide that is superficially adsorbed adopts most likely another secondary structure than peptide that is inserted in the headgroup region. That both binding mechanisms exist has been shown by monolayer and ITC experiments (see above). However, the secondary structure of the bound peptide does not directly depend on the lipid phase state, as no distinct change is observed at T_m .

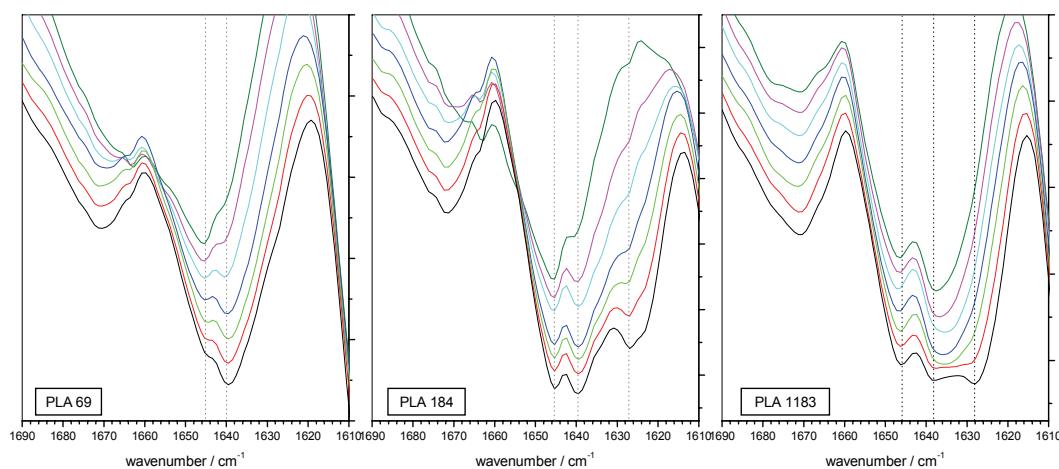


Figure 4.21: Second derivative spectra in the amide I region of different PLA bound to DPPG membranes at — 10 °C, — 20 °C, — 30 °C, — 40 °C, — 50 °C, — 60 °C and — 70 °C. The vertical dotted lines indicate vibrational components due to different structural elements.

Despite all experimental efforts, the band assignments in the spectral region between 1638 cm^{-1} and 1646 cm^{-1} remain somewhat uncertain. Alternatively to the given interpretation the higher frequency band at 1645.5 cm^{-1} could be assigned to random coil vibration. The lower frequency band at 1639.5 cm^{-1} would then arise from a conformation that was not present in bulk solution. For instance it is known that 3_{10} helices (Prestrelski et al. 1991) or bent helices (Jackson et al. 1989) have amide I bands at lower wavenumbers than α -helices.

Also different unordered structures are imaginable, for instance, a more extended conformation in the fully charged state in solution and a more coiled structure that forms upon charge compensation at the membrane surface. The assignment of the band at 1639.5 cm^{-1} to an ordered structure would satisfy the expectation that all ordered secondary structure elements thermally unfold.

Which of the two interpretations is valid can not be decided at the moment. Clear is, however, that longer PLA bind in β -sheet conformation to gel phase DPPG membranes. This is different to the binding behaviour of PLL, which formed solely α -helices and random coils at the membrane surface.

4.5.2 Complexes with mixed DMPC/DPPG membranes

Miscibility of DMPC-d₅₄ and DMPA

To complement the DSC studies about the influence of PLA on the miscibility of PC/PG bilayers, we performed IR experiments on the same system. We used the same experiments as were described above in the PLL section (3.3.2), the only variation being the substitution of the DPPC-d₆₂ component by DMPC-d₅₄. This proved to be the better model system to study domain formation in the case of PLA binding because the transition temperatures of eventually formed domains are better separated. This approach was already used for the DSC experiments.

Figure 4.22 shows the experimental results. In pure DMPC-d₅₄/DPPG mixed membranes, the frequencies of CD₂ and CH₂ stretching vibrations show the same temperature dependence. This indicates that the lipids are completely miscible. The transition temperature of the mixed DMPC-d₅₄/DPPG membrane is $31.3\text{ }^{\circ}\text{C}$. After addition of PLA, the miscibility is reduced. The temperature dependence of the $\nu(\text{CH}_2)$ and $\nu(\text{CD}_2)$ is now different. The DMPC component (deuterated acyl chains) melts in a very wide transition range beginning at $24\text{ }^{\circ}\text{C}$ and ending at the temperature where also the transition of the DPPG component is completed. In contrast, the DPPG component undergoes a ν transition in a small temperature range. The midpoint of the DPPG transition is increased with respect to T_m of the uncomplexed lipid mixture. The increase is the higher, the longer the PLA chain is.

These findings are in excellent agreement with the results of the DSC experiments (see Figure 4.4). They can be interpreted with the presence of a DPPG enriched binding domain with a well defined composition and a less defined DMPC enriched reservoir. The melting begins in the membrane regions that are the most depleted in DPPG molecules somewhat higher than the transition temperature of pure DMPC-d₅₄ (19.7°C) (Fidorra et al. 2007). This indicates the possible presence of a gel-gel miscibility gap, at compositions of $x_{\text{DPPG}} < 0.5$.

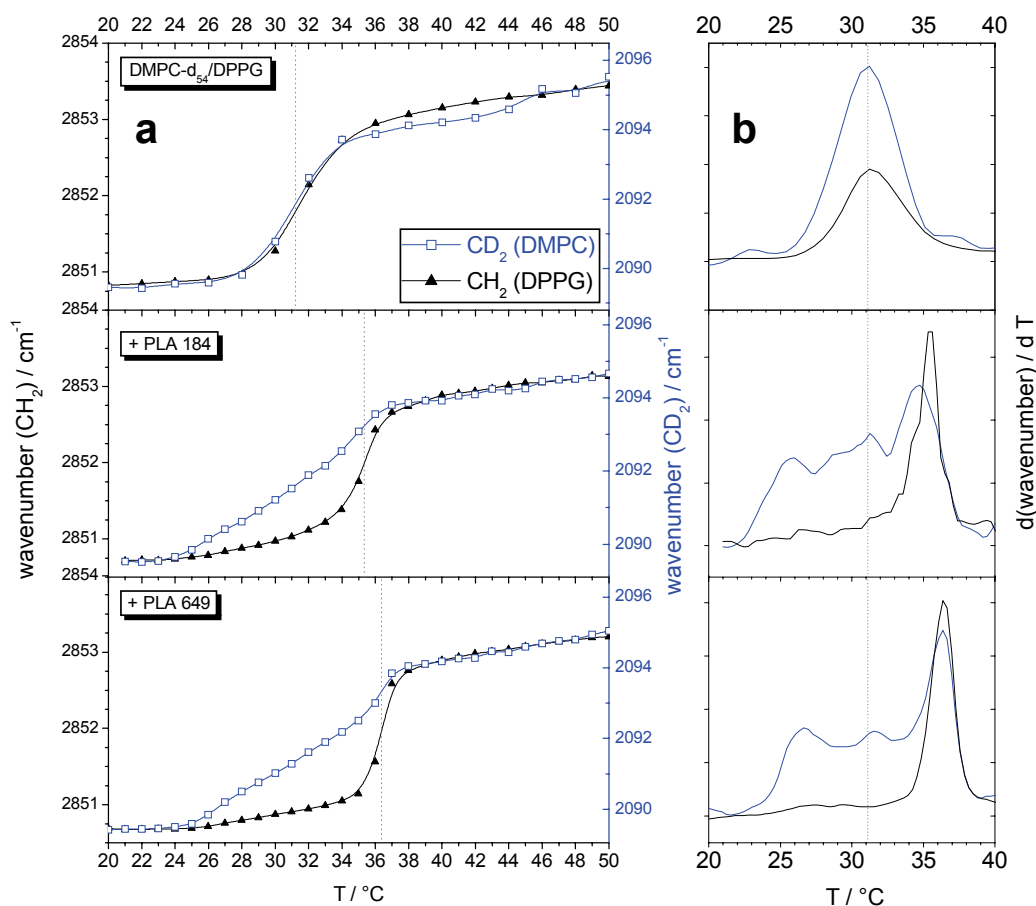


Figure 4.22: a: Maxima of symmetric methylene stretching vibrational bands of either component of a mixed DMPC-d₅₄/DPPG membrane (top panel) and its complexes with PLA 184 (middle panel) and PLA 649 (lowest panel). The CD₂ stretching vibrations (□), originating from the DMPC component, are shown in blue (right scale) and the CH₂ (▲) stretching vibrations, originating from the DPPG component, are shown in black (left scale). For comparability the left and the bottom scale is the same for all three panels. The vertical dotted lines indicate the midpoint of transition of the DPPG component (steepest slope). **b:** The first derivatives of the curves presented on the left hand side in the transition range. The colours are chosen as in the left panels.

The broad transition range of the DMPC component opposed to the rather sharp DPPG transition indicates a very asymmetric gel/liquid crystalline phase transition region. The PLA binding domain is DPPG enriched but is not pure DPPG. This can be deduced from the transition temperature, which is considerable below T_m of a pure DPPG membrane (41 °C). Furthermore, this is indicated by the absolute values of the CH₂ stretching vibrational frequencies, which are not significantly decreased with respect to the $\nu_s(\text{CH}_2)$ frequencies of the uncomplexed lipid mixture. Following the interpretation given above (section 4.5.1), this shows that the interchain coupling of the $\nu_s(\text{CH}_2)$ vibrations is still reduced by intercalated CD₂ chains, which, belong to admixed DMPC-d₅₄ molecules.

The derivatives of the wavenumber-temperature curves (Figure 4.22) reveal well the transition temperature ranges of the single components. From these curves it can be seen that the DMPC component of DMPC-d₅₄/DPPG/PLA complexes melts in three steps. The same behaviour was observed by DSC experiments (Figure 4.3). However, DSC is only able to detect the summation of the effects originating from both membrane constituents. With the help of the IR experiments, the three step melting behaviour can be assigned to the DMPC component.

Secondary structure of PLA bound to mixed PC/PA membranes

As has been shown for the DPPG/DPPC/PLL complexes, domain formation in mixed membranes can trigger secondary structure changes of the bound peptide. Therefore, we examined also the secondary structure of PLA bound to a mixed DPPC/DPPG membrane at different temperatures. Indeed, it can be seen that the secondary structure differs from that PLA adopts upon binding to pure DPPG membranes (Figure 4.23). Second derivative spectra reveal that the positions of the amide I components differ from those that were described above. In principle, two components are found at 1634 cm⁻¹ and 1645 cm⁻¹. At higher temperatures, a further band develops at 1653 cm⁻¹. In addition, turn structures that give rise to a vibrational band at about 1670 cm⁻¹ are present in all the spectra. Contrary to the spectra of PLA bound to pure DPPG, no β -sheet vibrations are found. The bands that are found in the spectra originate from α -helix and coil structures. The difficulties of an exact assignment have been discussed above. Interesting is the temperature dependent shift of the bands. In contrast to the case of PLA binding to pure DPPG, the band intensities do not change continuously over the whole temperature range. Rather, the band that is located at 1635 cm⁻¹ shifts at T_m of the mixed membrane to higher wavenumbers (Figure 4.23c). This shows that the phase transition of the lipid induces a secondary structure change of the bound peptide. The phase transition of the lipid acyl chains and the bound peptide start at the same temperature. However, the temperature range of the transition is broader for the peptide than it is for the acyl chains. Probably, the peptide secondary structure transition follows the phase transition of the membrane.

These findings are very similar to what was found for PLL complexes with mixed DPPC/DPPG membranes and can be explained in the same manner. The charge density of the gel phase domains is higher than that of the remixed liquid crystalline membrane. Only if the charge density is high, the side chain charges of the peptide are electrostatically screened, allowing the peptide to adopt a secondary structure. But probably the charge density is not high enough for the formation of a β -sheet, even in the gel state domain with increased DMPA content.

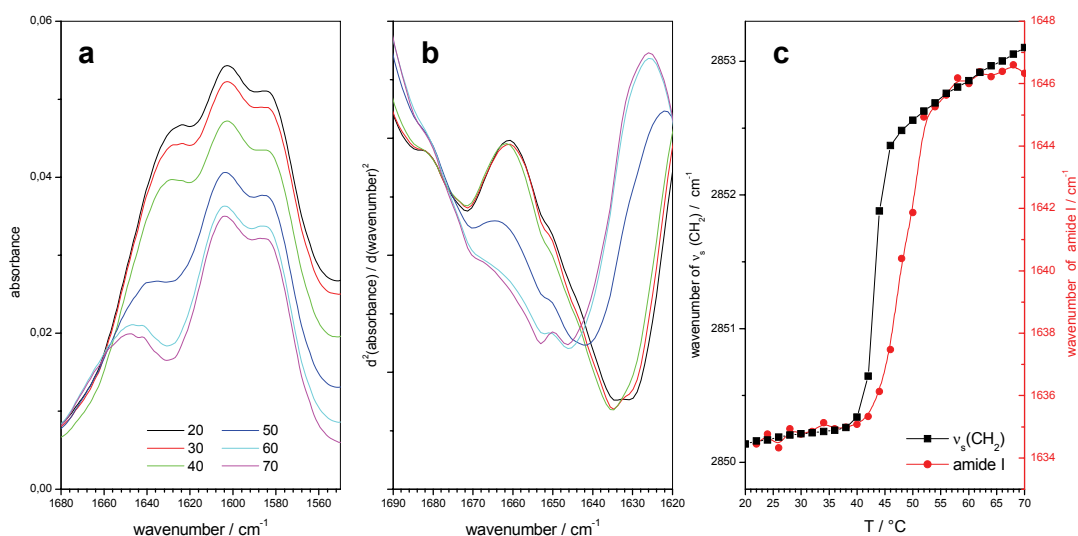


Figure 4.23: **a:** Amide I and guanidyl stretching vibrational bands of PLA 649 bound to DPPC/DPPG mixed membranes at different temperatures. **b:** Second derivatives of curves presented in **a** in the region of the amide I band. **c:** Temperature dependence of the amide I band components as revealed by the second derivatives (●) and the frequencies of $\nu_s(\text{CH}_2)$ (■).

4.6 Fluorescence experiments

The experiments described before show that PLA interacts not only superficially with PG bilayers, but rather inserts to some extent into the headgroup and interfacial region. The question arises how much the bilayer integrity is affected by the interaction with the polypeptide. Therefore, dye release experiments were performed. A fluorescence dye in self quenching concentration (80 mM calcein) was included in the aqueous interior of vesicles. As long as the barrier function of the vesicles membrane is retained, no fluorescence can be detected. If, the membrane integrity is disturbed, dye can be released from the vesicle into the bulk solution, were due to the dilution, it is not any longer self quenching. Thus, the fluorescence intensity rises, as the membrane gets porous or vesicles are ruptured. ITC and DSC experiments showed that PLA binding to fluid PG membranes saturates at concentrations where, assuming a 1:1 stoichiometry, also lipids of the inner lamella have to interact with the peptide. Therefore, PLA might either be translocated through permanent or transient pores that are induced by PLA binding, or the vesicles disrupt. In both cases the membrane structure will be disturbed and enclosed dye can efflux.

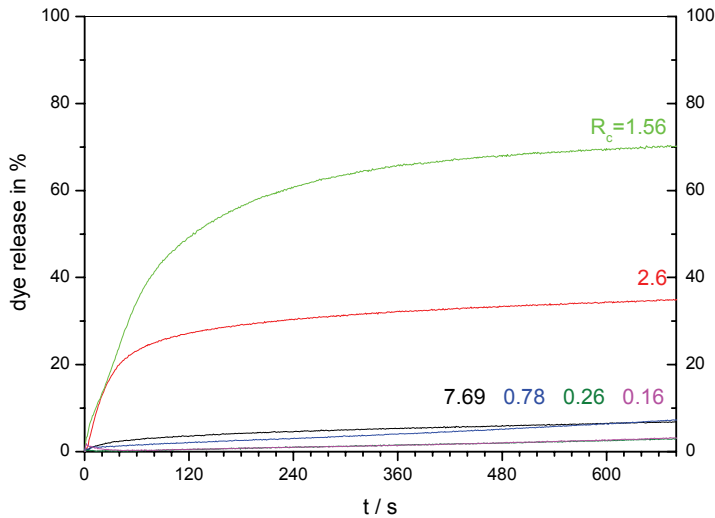


Figure 4.24: Kinetics of dye release from POPG vesicles after interaction with PLA 69. The POPG/Arg mixing ratios (R_c) are (—) 7.69; (—) 2.6; (—) 1.56; (—) 0.78; (—) 0.26; (—) 0.16. The curves are normalized to the dye release from POPG vesicles induced by addition of TRITON X. The dye release is given in percent of this maximal value.

An example of dye release kinetics is shown in Figure 4.24. It can be seen that PLA induces dye release from fluid state POPG vesicles only at certain concentrations. If excess PLA concentrations or excess lipid concentrations are used, the bilayer integrity is not affected. However, PLA induces dye efflux, if added in the concentration that leads to neutralization of the outer vesicle monolayer ($R_c = 2$). This finding was confirmed for all examined systems, independent of the peptide chain length and the membrane composition. This implies that a prerequisite for pore formation is charge neutralization of the outer monolayer by PLA. A neutral PG/PLA complex might then overcome the hydrophobic barrier and form transient pores. These pores might be the pathway for peptide translocation as well as for dye efflux. Such a model was also proposed by Tang et al. (2007), who postulated on the basis of NMR experiments that phospholipid/arginine complexes form toroidal pores in PE/PC membranes.

The fact that the dye is not completely released indicates that the vesicle structure is not destroyed and that pores or defects that allow the dye to escape from the vesicle interior are only transient. This is supported by cryo-TEM images, which show that the vesicle structure is retained even if aggregates are formed (Figure 4.25).

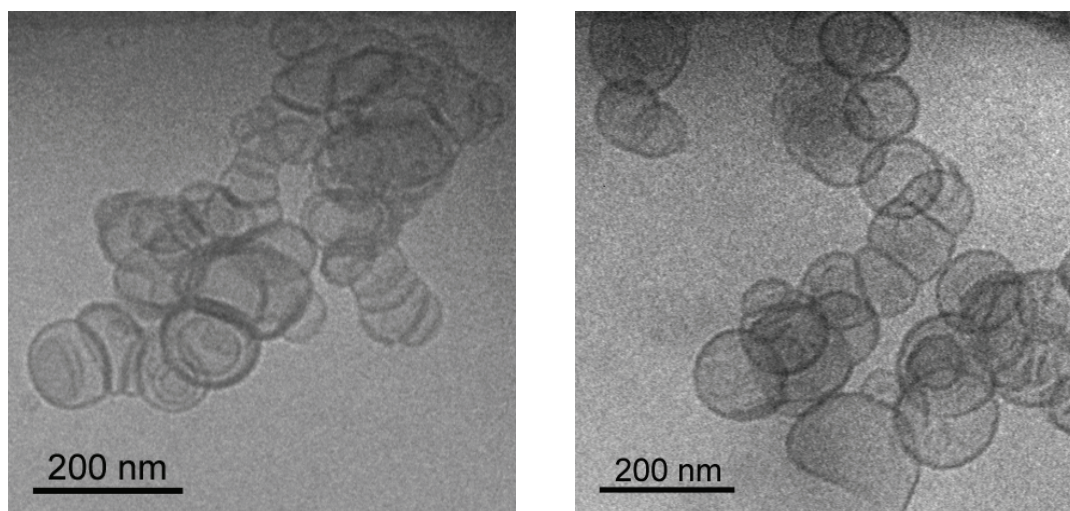


Figure 4.25: Cryo-TEM images of a 20 μM POPG vesicles suspension after addition of 50 μM PLL 649 ($R_c = 0.4$) (left) and 10 μM PLL 14 ($R_c = 2$) (right). Quenching was performed from room temperature, where POPG vesicles are in the fluid state.

If the experiments are performed with DPPG gel state vesicles the maximal dye release is reduced (Figure 4.26). This shows that the bilayer structure in the gel phase is not as strongly perturbed by PLA binding as in the liquid crystalline phase. This indicates that “fluid” lipid molecules are necessary for pore formation. The dye efflux is further reduced when zwitterionic PC is admixed to gel phase or fluid phase membranes. This effect can be attributed to the reduced electrostatic attraction and to the fact that the uncomplexed and mobile PC molecules might compensate membrane defects that are induced by peptide adsorption.

Very similar trends are also observed for PLL binding to PG containing membranes. However, the absolute values of PLL induced dye release are in all cases lower than those detected in comparable PLA experiments (Figure 4.26). This confirms the proposition given in the foregoing chapters. PLL interacts more electrostatically with PG membranes than PLA and hydrophobic as well as hydrogen bonding interactions that lead to peptide insertion are less important for PLL binding than for PLA binding.

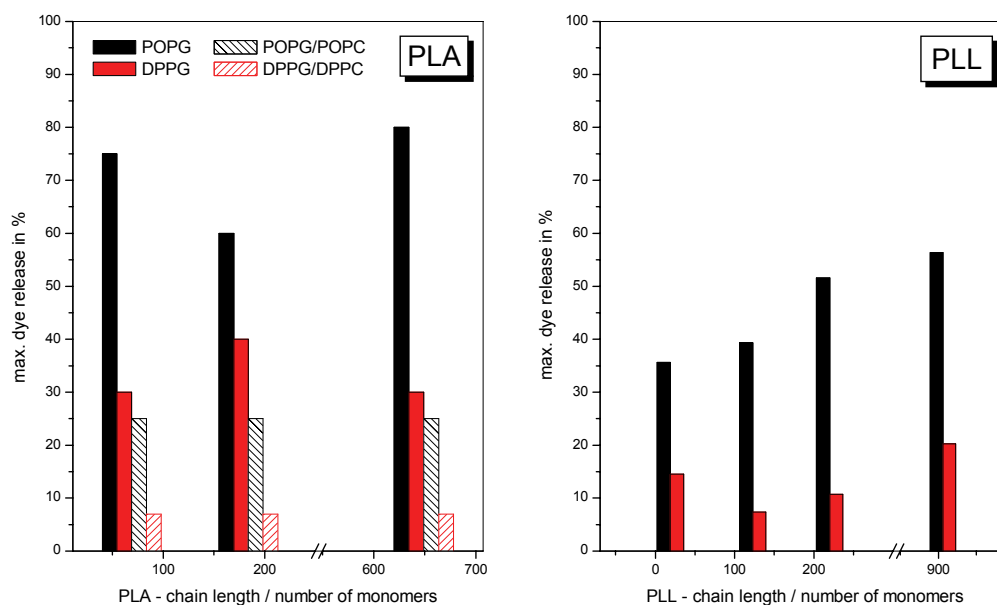


Figure 4.26: Percentages of maximal dye release from vesicles composed of POPG (■), DPPG (■) and its mixtures with POPC (black dashed) or DPPG (red dashed) induced by PLA (left) or PLL (right) of different chain length.

4.7 Summary

In this chapter the binding behaviour of the positively charged polypeptide PLA to negatively charged DPPG membranes was studied as a function of PLA chain length, the lipid to peptide mixing ratio R_c and the phase state of the membrane.

Thermotropic phase behaviour

DSC experiments revealed that the influence of PLA binding on the main phase transition temperature T_m of DPPG membranes is unexpectedly small. T_m is shifted to slightly lower or higher values dependent on the chain length of the binding peptide. This is attributed to the presence of different binding processes that are compensating each other. The cooperativity of the main phase transition is decreased in lipid excess complexes. In contrast, the cooperativity is increased in peptide excess complexes. This indicates that well defined PLA/DPPG complexes are formed.

Binding thermodynamics

To prove the existence and reveal the nature of different binding processes we performed ITC and monolayer experiments. ITC revealed indeed at least two different processes in PLA binding to gel state membranes, one of them being endothermic and the other being

exothermic. Moreover, it was found that the binding to fluid phase membranes is energetically favoured. This could be deduced from the more negative binding enthalpies $\Delta_R H$ and the higher binding constants K in case of PLA binding to fluid membranes as compared to gel state membranes. Longer PLAs bind more exothermic and with higher binding constants than shorter ones.

Hydrophobic interactions

Besides electrostatic also hydrophobic interactions contribute to PLA binding, as shown by temperature dependent ITC measurements on fluid POPG membranes. The determined negative $\Delta_R C_p$ is indicative for the release of water molecules from hydrophobic surfaces. Thus, it can be assumed that hydrophobic parts of the arginyl side chain get buried in the membrane during the binding process. By monolayer adsorption and dye release experiments could be shown, that indeed the binding is not only superficial but that moieties of the polypeptide insert into a DPPG membrane.

Monolayer adsorption

Monolayer experiments provide evidence for at least two consecutive binding processes. The peptide has a condensating effect on monolayers of low initial pressure π_0 (LE phase). This condensation is reflected by a surface pressure decrease ($\Delta\pi < 0$). It is followed by an insertion of the peptide or parts of the peptide into the monolayer, which results in a final surface pressure increase ($\Delta\pi > 0$). Monolayers of high π_0 (LC phase) are not condensed any more but still penetrated by the peptide. A surprising result is that $\Delta\pi$ increases with increasing π_0 . This could be attributed to a difference in compressibility of the free and the bound monolayer and the high peptide exclusion pressures. This shows that the lipid monolayer strongly interacts with the inserted peptide.

Interfacial hydration

Structural information on the organisation of the DPPG/PLA complexes could be derived from FT-IR experiments. The analysis of the C=O stretching vibrational bands showed that PLA binding releases water molecules from the interfacial membrane region. Especially in the fluid crystalline phase, hydration of the carbonyl groups is reduced by PLA binding. This supports the results of ITC and monolayer experiments, which predict water release and side chain insertion. However, the remaining water molecules are bound by stronger hydrogen bonds. The water molecules are better oriented and restricted in their reorientational motion.

Acyl chain order

Lipid molecules are also restricted in their rotational dynamics. This could be deduced from the increased interchain coupling of the methylene dipoles, which reduces the frequencies of the CH₂ stretching vibrations. It could be demonstrated by isotopic dilution experiments that these coupling effects have to be taken into account, if CH₂ stretching vibrational frequencies are interpreted.

Secondary structure

The amide I vibrational frequencies of PLA in different secondary structures were analysed. The results were used to identify the structure PLA adopts upon binding to DPPG membranes. It was shown that longer PLAs bind in a β -sheet conformation to gel phase membranes. This β -sheet unfolds to a random coil when the temperature is raised. Shorter PLAs do not form β -sheets upon binding. The reduction of the membranes charge density by co-addition of zwitterionic DPPC prevents the formation of β -sheets. The existence of α -helical structures at higher temperatures is proposed but cannot be proven on the basis of the performed experiments.

Lipid demixing

DSC and IR experiments with mixed PC/PG membranes showed that PLA induces domain formation in gel phase PC/PG membranes. Upon PLA binding a PG enriched binding domain is formed. The phase diagram shows a very wide and asymmetric gel - liquid crystalline coexistence region.

Binding of PLA to negatively charged PG containing membranes shows typical electrostatic features but has also noticeable non electrostatic contributions. This confirms the results given by Hitz et al. (2006) and Goncalves et al. (2005). The non electrostatic contribution arises from hydrophobic interactions of the arginyl side chain with the interfacial membrane layer. But also hydrogen bonding might be involved which was already reported to play a key role in arginine interaction with membrane lipids (Rothbard et al. 2004; Rothbard et al. 2005; Tang et al. 2007).

4.8 Comparison of PLL and PLA binding to PG membranes

Although PLL and PLA are very similar in structure and charge (see chapter 2.2), their binding behaviour is remarkably different. These differences can only be explained if other than electrostatic interactions are involved. Comparison of the binding behaviour and the complex properties is very instructive to reveal the specificities of the two amino acids lysine and arginine. Differences and similarities in the interaction of PLL and PLA with PG containing membranes will be shortly summarized in the following paragraphs.

Transition temperature

PLL and PLA influence the gel to liquid crystalline phase transition of DPPG membranes differently. Whereas PLL increases T_m by about 4–5 °C, PLA has nearly no effect on T_m . The influence of PLL is well explainable with electrostatic interaction at the membrane surface, which stabilizes the gel phase of the membranes. The transition behaviour of the PLA/DPPG complex can only be explained if non electrostatic interactions compensate for the electrostatic effect.

Domain formation

PLL as well as PLA binding to mixed PC/PG membranes leads to reduced miscibility of the membrane lipids. Domains with increased PG content are formed to provide a high electrostatic surface potential for peptide binding. PLL binding leads to a macroscopic miscibility gap in gel phase membranes if the PG content is lower than 50 %. There are also indications for fluid-fluid demixing for membranes with higher PG content (60–80 %).

PLA binding influences the PC-PG phase diagram in a similar way, but the effects are less pronounced. Possibly, PLA binding also leads to gel phase demixing in membranes with low PG content. In contrast, fluid demixing is not observed for PLA binding.

The reason for domain formation is the favourable electrostatic interaction of the peptides with highly charged domains. The fact that demixing is more obvious for PLL binding shows that electrostatic interactions are more important for PLL binding than for PLA binding.

Binding enthalpies

ITC studies revealed substantial differences in PLL and PLA binding to PG containing membranes. While PLL interacts with an exothermic ΔH with gel phase membranes and nearly no enthalpic contribution for fluid state binding, PLA behaves exactly opposite. PLA binding to fluid membranes is clearly exothermic, whereas the total heat released upon PLA binding to gel phase membranes is nearly zero. However, from the titration curves it can be seen that exo-

and endothermic processes are present, but compensate each other. The negative heat capacity change during the reaction ($\Delta_R C_p < 0$) implies that hydrophobic interactions play a role in both, PLL and PLA binding. However, $\Delta_R C_p$ is more negative in the case of PLA binding, which can be attributed to a higher hydrophobic contribution to the binding process.

Hydration of the membrane interface

The different interaction modes of PLL and PLA with membranes in different phase states are reflected by their different influence on the hydration of the interfacial carbonyl groups. Gel phase membranes are better hydrated if PLL is bound, while PLA binding does not influence gel phase hydration. In contrast, PLA binding dehydrates the carbonyl group of membranes in the liquid crystalline phase, whereas PLL binding has no influence on the carbonyl hydration in this phase state.

Probably, inserted PLA side chains replace water molecules from the interfacial region. Remaining water molecules have to be shared by the guanidyl group and the lipid carbonyl group. Guanidinium competes much more with the carbonyls for hydration water than the lysine groups do, because of its higher polarity and the presence of more hydrogen bonding sites. In bulk solution one arginine side chain binds six water molecules, whereas one lysine side chain binds only two (Collantes and Dunn 1995). PLL probably entraps water molecules in the inter-headgroup space without competing for them. The dehydrating effect of PLA binding is reflected by a tendency of the membrane to form recrystallized phases before acyl chain melting (Förster et al., unpublished results). PLL, by contrast, which increases the hydration of the gel phase and does not affect the hydration of the fluid phase, suppresses any tendency for recrystallization.

Acyl chain order

The methylene stretching vibrational frequencies decrease upon PLL and PLA binding, which is normally interpreted with an increase of the acyl chain order. However, it could be shown that this effect is mainly due to increased interchain vibrational coupling. If vibrations of neighbouring acyl chains are decoupled by isotopic dilution (i.e. partial deuteration), the effect of decreasing $\nu(\text{CH}_2)$ frequencies vanishes nearly completely in the case of PLA binding. In the case of PLL binding the effect gets smaller, but a decrease of the $\nu(\text{CH}_2)$ frequencies is still encountered, even when the vibrations are decoupled. This remaining decrease is attributed to acyl chain ordering. This leads to the conclusion that PLL binding has a higher ordering effect on the lipid acyl chains than PLA binding.

Secondary structure

PLL and PLA adopt different secondary structures upon binding to PG membranes. PLL forms a α -helix on the surface of DPPG gel phase bilayers. At temperatures higher than T_m the helix gradually unfolds. Prerequisite for helix formation upon binding is a sufficiently high surface potential of the membrane. If the surface potential is lowered by admixing of zwitterionic lipids at conditions where no demixing occurs, no helix will be formed.

In contrast, PLA adopts a β -sheet conformation upon binding to gel state DPPG membranes. Temperature increase and admixing of zwitterionic lipids have similar effects on the β -sheet as on the α -helix in the case of PLL binding. However, after unfolding of the β -sheet the structure is not pure random coil. Rather another secondary structure element is preserved. This might be due to a conformation of inserted peptide moieties, which differs from the secondary structure the peptide adopts upon adsorption to the surface.

Monolayer adsorption

In principle PLL and PLA have the same effects on a DPPG monolayer. An expanded monolayer (LE phase) condenses after peptide adsorption. The condensation is followed by insertion of peptide side chains in the condensed domains. Both peptides insert in condensed monolayers (LC phase). This shows that hydrophobic interactions play a role in both, PLL and PLA binding. However, the condensating effect is more pronounced in the case of PLL adsorption, whereas insertion is more evident in the case of PLA adsorption. This shows again that electrostatic interactions are more important for PLL binding, whereas hydrophobic interactions are more prominent in PLA binding.

Dye release

Both, PLA and PLL induce dye release from fluid POPG vesicles when added in an amount that compensates the outer monolayer charges. However, dye release is much higher in the case of PLA binding than in the case of PLL binding. This confirms the conclusions drawn from monolayer adsorption experiments. PLA inserts more deeply into the lipid bilayer and induces defects and/or pore formation. The reason is its higher propensity to form stable charge compensated complexes with the phospholipid headgroup. Higher hydrophobic interactions lead then to insertion into the bilayer. Lower hydrophobicity and remaining charge density prevents PLL from inserting to the same extent.

Chain length dependencies

All described effects are dependent on the chain length of the polypeptide. In general the effects are more pronounced, if the polypeptide is longer. This dependency is valid for both, PLL and PLA. In the case of PLL binding the chain length dependencies were investigated in

more detail. It was shown that the chain length dependency reverses at a certain length. Here steric constraints compete with thermodynamic effects. The shortest PLL ($n = 14$) behaves in many aspects differently than predicted from the chain length dependencies. This distinct behaviour could be attributed to its inability to form a defined secondary structure.

5 Interaction of polylysines and polyarginines with PA containing membranes

To complement the studies on the interaction of basic homopolypeptides with phosphatidylglycerol (PG) bilayers and to reveal the influence of the lipid headgroup structure, experiments were performed using phosphatidic acids (PA) as negatively charged membrane constituent. PA and PG are both singly negatively charged at neutral pH. The charge of PA molecules is, due to its small headgroup, directly exposed at the membrane surface, whereas the charge of PG molecules is sterically and energetically shielded by the glycerol moiety. This might lead to closer and stronger electrostatic interactions of the peptides with PA membranes. Moreover, the tendency of the peptides to insert into the headgroup region of the membrane might be reduced if the charge is presented directly on the surface. Finally, also specific interactions, i.e. hydrogen bonding with the phosphate or carbonyl group should be intensified and interactions with the hydrophobic core might be facilitated. Furthermore, it shall be examined whether the specificities of lysine and arginine binding that have been outlined in the preceding chapters are reproduced if a different membrane system is used.

5.1 Thermotropic phase behaviour

5.1.1 Polylysine / PA complexes

Poly(L-lysine) has a stronger influence on the thermotropic phase behaviour of PA membranes compared to PG membranes. The DSC curves of equimolar PLL/DMPA complexes ($R_c = 1$) are shown in Figure 5.1. With longer PLL ($n = 71 - 803$) bound to DMPA membranes the main component of the phase transition is centered at 75 °C, which is ca. 25 °C higher than T_m of uncomplexed DMPA (51.2 °C). A small peak is detected at 54.7 °C, slightly above T_m of pure DMPA. The cooperativity of both transition steps and the total enthalpy of the transition are strongly decreased with respect to the transition of pure DMPA. These effects indicate that longer PLLs interact very strongly with DMPA membranes and stabilize the gel phase structure markedly. The stabilisation of the gel phase is much more pronounced, than in the case of DPPG complexation.

Binding of shorter PLL ($n = 19$) has a much smaller effect on the phase behaviour of DMPA. The transition temperature is increased by 3.5 °C and coincides with the first transition step of longer PLL/DMPA complexes. Transition enthalpy and cooperativity of the PLL 19/DMPA complex are very similar to those of pure DMPA. Differences in binding

behaviour of the shortest PLL and longer PLL were also detected in the case of binding to DPPG membranes and have been attributed to the inability of short PLL to form α -helical structures upon binding. However, in the present case this difference is much more pronounced. The influence of secondary structure formation will be discussed below.

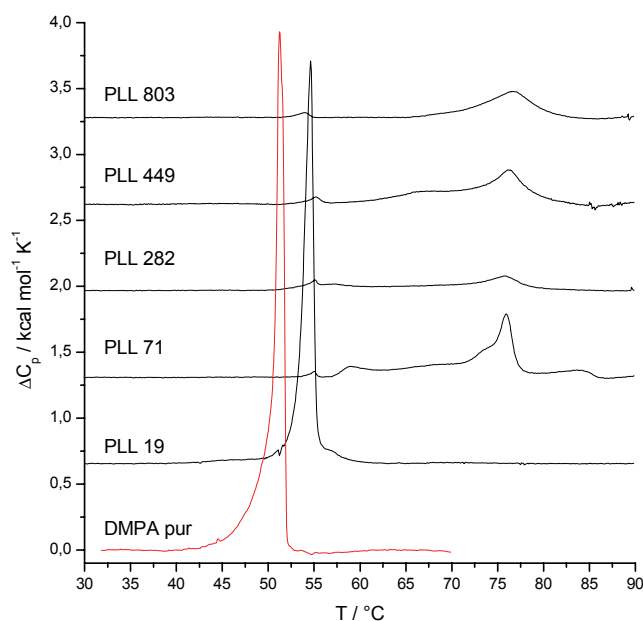


Figure 5.1: DSC-plots of the gel-to-liquid-crystalline phase transition of DMPA/PLL complexes with an equimolar charge ratio ($R_c = 1$) and different PLL chain lengths. Measurements were performed in 100 mM NaCl solution at pH = 6.

Figure 5.2 shows how the phase behaviour of DLPA/PLL complexes is influenced by the lipid to peptide mixing ratio R_c . Interestingly the phase behaviour of pure DLPA is not markedly influenced as long as only minor amounts of PLL are added ($R_c > 1$). The high temperature transition is only detected for complexes formed with equimolar amounts of PLL or with PLL excess. Obviously a complete neutralization of the PA headgroup charges is necessary to stabilize the gel phase structure. Consequently, the transition temperature is maximal, if lipid as well as peptide charges are completely neutralized in the complex of equimolar composition ($R_c = 1$). When the peptide content is further increased ($R_c < 1$) T_m decreases slightly. Furthermore, the lower temperature transition step is shifted below T_m of uncomplexed DLPA membranes. A decrease of T_m could principally be explained with a partial deprotonation of PA headgroups ($PA^- \rightarrow PA^{2-}$). However, the IR spectra of the complexes do not show an increased PO_3^{2-} stretching vibrational intensity. Thus, it can be assumed that the degree of protonation is not markedly affected by PLL binding.

The fact that PLL binding in molar ratios of $R_c > 1$ does not affect the lipid phase transition distinguishes the binding to PA membranes from the binding to PG membranes. In the latter

case also lipid excess complexes ($R_c > 1$) showed an increased phase transition temperature and occasionally a splitting of the transition peaks in two components. However, the composition dependence of T_m at $R_c < 1$ is similar to that determined for DPPG/PLL complexes.

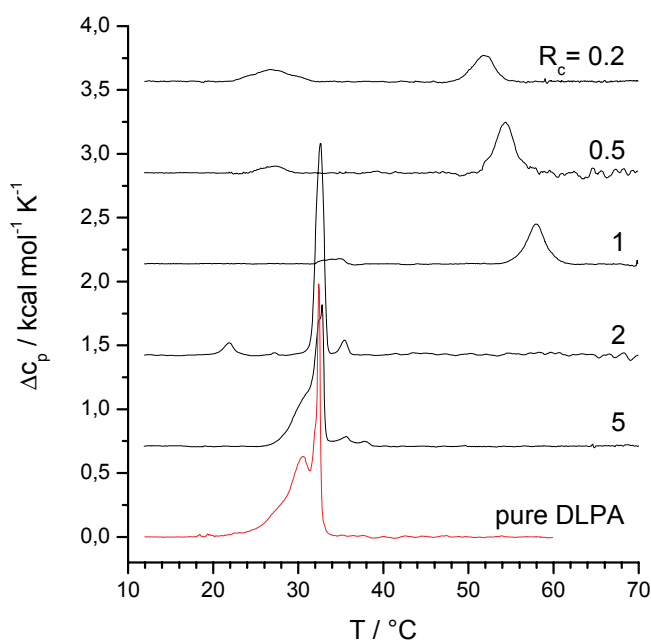


Figure 5.2: DSC-plots of the gel-to-liquid-crystalline phase transition of DLPA/PLL 282 complexes at different mixing ratios R_c . Measurements were performed in 100 mM NaCl solution at pH = 6.

Similar transition behaviour of PLL/PA complexes at neutral pH was also reported by other authors (Laroche et al. 1988; Takahashi et al. 1996). Some studies were also performed at pH = 9, where the second proton of the PA headgroup dissociates under influence of cation binding (see introduction). Also under these conditions T_m increases upon PLL binding with respect to the phase transition temperature of pure PA membranes (Galla and Sackmann 1975b; Hartmann and Galla 1978; Hartmann et al. 1977).

A comparable transition behaviour was also found for Ca^{2+} /PA complexes (Garidel 1997). This similarity implies that PLL binding to PA membranes is mainly electrostatically driven.

5.1.2 Polyarginine / PA complexes

Poly(L-arginine) affects the phase behaviour of PA membranes much less than polylysine. If DMPA membranes are complexed with equimolar amounts of PLA ($R_c = 1$), T_m increases only slightly (2 – 5 °C) (Figure 5.3). The amount of increase is dependent on the PLA chain length. The longer the PLA chain, the larger is the increase in T_m after complexation. The transition of DMPA complexed with the shortest PLA ($n = 69$) clearly shows two components.

The first transition component is found at T_m of uncomplexed DMPA membranes. It is concluded, that this component originates from uncomplexed membrane parts. Small amounts of uncomplexed membrane are also present in the DMPA complexes with longer PLAs.

This phase behaviour is consistent with the already observed specificities of PLL and PLA binding on the one hand and PG and PA membranes on the other hand. As in the case of binding to DPPG membranes, the shift in T_m induced by PLA binding is smaller than the shift induced by PLL binding. Concomitantly, the transition temperature of PA membranes is more influenced than that of PG membranes. If, as outlined in the preceding chapters, an increase of T_m is to be explained with electrostatic shielding of the headgroup charges, it can now be concluded that 1.) electrostatic interactions are more important in the case of PLL binding than in the case of PLA binding and 2.) electrostatic interactions are more significant for binding to PA membranes than for of binding to PG membranes. Consequently, electrostatic contributions to the complex formation are the highest if PLL interacts with PA membranes and the lowest if PLA interacts with PG membranes. This is reflected by an increase of T_m by 25 °C in the former case and 0 °C in the latter case.

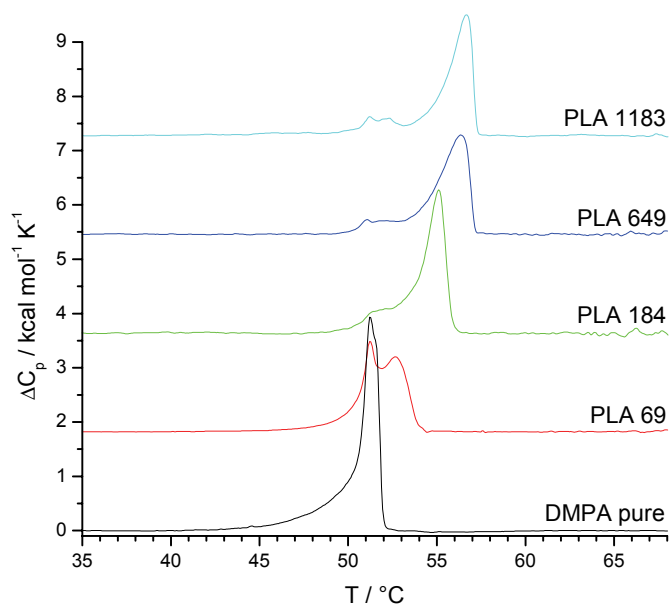


Figure 5.3: DSC-plots of the gel-to-liquid-crystalline phase transition of DMPA/PLA complexes with an equimolar charge ratio ($R_c = 1$) and different PLA chain length. Measurements were performed in 100 mM NaCl solution at pH = 6.

The influence of the composition R_c of PLA/DMPA complexes on T_m is presented in Figure 5.4. Complexes formed with lipid excess ($R_c > 1$) show always a two step melting behaviour. The transition temperatures of the two components are constant at all complex composition $R_c \geq 1$, but the intensity of the higher temperature component increases on expense of the lower temperature component as the peptide content increases. This behaviour indicates the

coexistence of uncomplexed membrane parts and PLA bound domains of well defined composition. This shows that bound PLA is not uniformly distributed over the whole membrane surface but rather clusters in binding domains. This is not explainable on basis of purely electrostatic interaction, which should lead to spreading of the charges over the accessible surface. Consequently, PLA binding must induce structural changes in the lipid organisation that cause an immiscibility of bound and unbound lipid molecules. On the one hand this could be changes in the organisation of the hydrocarbon core of the membrane, e.g. tilt angle variations or the organisation of the acyl chains in incommensurate lattices. On the other hand, PLA binding could influence the hydrogen bond network that interconnects adjacent lipid molecules in PA membranes. However, the fact that the phase transition temperature is increased shows that this network is not totally disrupted.

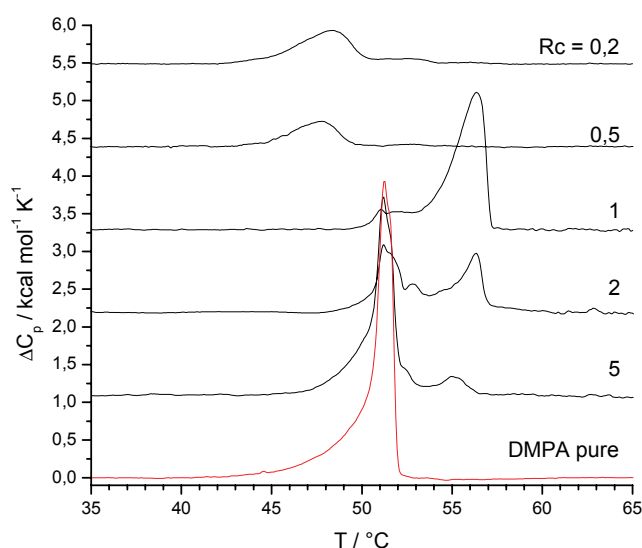


Figure 5.4: DSC-plots of the gel-to-liquid-crystalline phase transition of DMPA/PLA 649 complexes at different mixing ratios R_c . Measurements are performed in 100 mM NaCl solution at pH = 6.

Complexes formed with excess of PLA ($R_c > 1$) show completely different transition behaviour. The transition temperature is now decreased by 3.5 °C with respect to T_m of uncomplexed DMPA membranes. No higher temperature transition is recorded. The transition at decreased temperatures resembles the lower component of the transition of PA membranes being complexed with PLL excess and might be due to similar membrane structures. However, PA/PLL complexes show a second transition component at highly increased temperatures. Similarities also exist with DPPG/PLA complexes, where addition of PLA excess also decreased the phase transition temperature of the lipid membrane.

In all cases, where PLA is involved in the complex formation, as well as in the cases, where PA membranes are involved in complex formation differences in the phase transition

behaviour of lipid excess complexes and peptide excess complexes are encountered. The only case, where T_m changes continuously with R_c is that of PLL binding to PG membranes. Probably PLL adsorbs to PG membranes by means of unspecific electrostatic interactions (eventually followed by unspecific hydrophobic interactions), which does not lead to the formation of stoichiometric complexes. In contrast, PLA and PA membranes favour the formation of stoichiometric complexes by the involvement of specific hydrogen bonds.

5.2 Domain formation in mixed DMPC/DMPA membranes

5.2.1 Influence of PLL binding

Due to the low transition enthalpies of PA/PLL complexes, DSC proved not to be an appropriate technique to monitor the phase behaviour of mixed DMPC/DMPA under influence of PLL binding. However, it is known that PLL binding induces domain formation in PC/PA mixed membranes at neutral pH (Laroche et al. 1988) and also at pH = 9 (Galla and Sackmann 1975a; Hartmann and Galla 1978; Hartmann et al. 1977). We reinvestigated the system using FT-IR spectroscopy at neutral pH.

Figure 5.5 shows the temperature dependence of the symmetric methylene stretching vibrational frequencies of either component of a DMPC- d_{54} /DMPA mixture (1:1, mol/mol), before and after addition of PLL. The uncomplexed mixed membrane shows a nearly ideal mixing behaviour with small tendencies for pair formation (Garidel et al. 1997a). Thus the phase transition region is rather small and the midpoints of the DMPC- d_{54} transition and the DMPA transition are only separated by 0.7 °C.

If PLL is added to the mixed membrane ($R_c = 1$) the phase transition range is broadened and both components undergo separate phase transitions with different temperature dependence. This indicates the formation of DMPC and DMPA enriched domains in the transition range. The midpoints of the transitions of the DMPC- d_{54} and the DMPA component are shifted to 6.4 °C lower and 7.25 °C higher temperatures, respectively, with respect to the transition temperature of the uncomplexed membrane, but are still different from the transition temperatures of the pure components. This shows that the domains, although being enriched in one component, are not pure in composition but contain fraction of both lipid species. The DMPC- d_{54} transition extends over a wide temperature range from 20 – 50 °C. The transition of the DMPA component is sharper. The midpoint of the transition of this domain is close to T_m of an uncomplexed DMPA membrane, which shows that the binding domain contains only small fractions of DMPC at the melting temperature.

A indication for demixing in the gel phase is given by the fact that at low temperatures the $\nu_s(\text{CH}_2)$ frequencies of the complexed membrane are decreased with respect to those of the uncomplexed membrane. The methylene stretching vibrations of adjacent acyl chains of the

uncomplexed mixed DMPC-d₅₄/DMPA membrane are decoupled by isotopic dilution (see section 4.5.1). The decrease of the $\nu_s(\text{CH}_2)$ frequencies of the complexes can be explained by increased coupling of the vibrations, which has to be a consequence of demixing of the lipids. At temperatures above the phase transition the $\nu_s(\text{CH}_2)$ frequencies of the complexed membrane reach the same values, as those of the uncomplexed membrane. Therefore, it can be assumed, that lipids remix in the fluid state of the membrane.

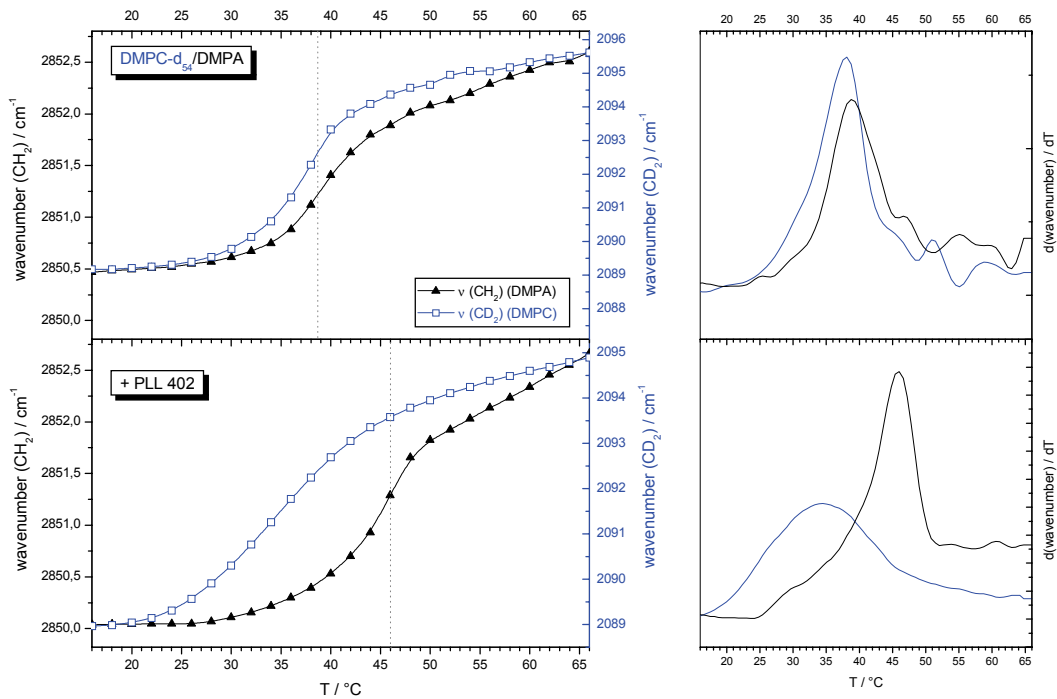


Figure 5.5: Left: Maxima of symmetric methylene stretching vibrational bands of either component of a mixed DMPC-d₅₄/DMPA membrane (upper panel) and its complexes with PLL 402 (lower panel). The CD₂ stretching vibrations (□), originating from the DMPC component, are shown in blue (right scale) and the CH₂ (▲) stretching vibrations, originating from the DMPA component, are shown in black (left scale). For comparability the left and the bottom scale is the same for both panels. The vertical dotted lines indicate the midpoint of transition of the DMPA component (steepest slope). Right: First derivatives of the curves presented on the left hand side normalized to the wavenumber difference in the melting region. The colours are chosen as in the left panels.

5.2.2 Influence of PLA binding

The phase transition of DMPC/DMPA mixed membranes being complexed with PLA could be observed by DSC. Figure 5.6 presents the transition curves of uncomplexed and complexed membranes of different composition. The uncomplexed membranes show nearly ideal mixing behaviour. In contrast, the complexes of DMPC/DMPA mixed membranes with PLA undergo a clear two step phase transition, giving rise to two well dissolved peaks in the DSC thermograms. Membranes with a PC content of more than 50 % clearly show a gel phase

miscibility gap between a pure DMPC phase and a DMPA enriched phase. There are indications for fluid-fluid demixing in membranes containing more than 66% DMPA.

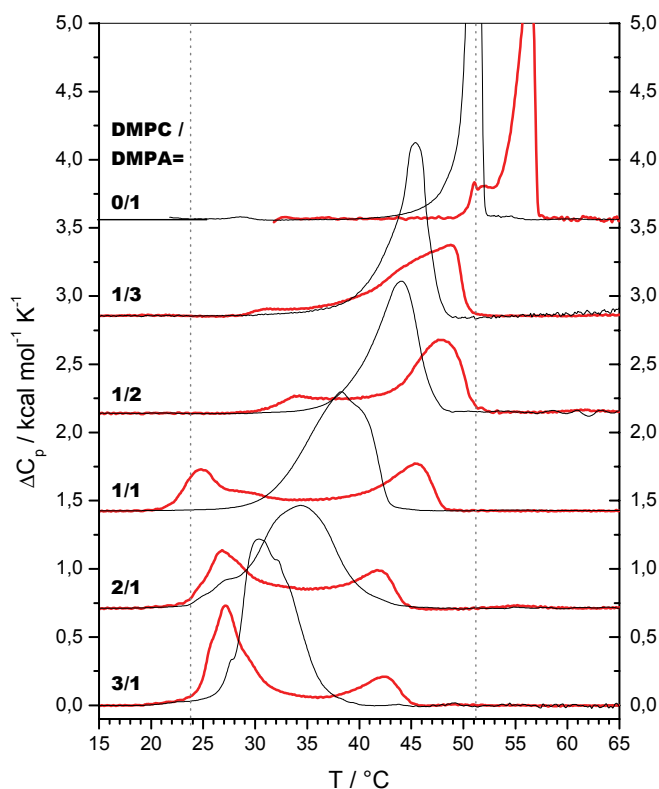


Figure 5.6: DSC plots of the phase transition range of different binary lipid mixtures DMPC/DMPA (—) and of the respective mixtures complexed with adequate amounts of PLA 649 to yield a lipid-to-peptide charge ratio of one ($R_c = 1$) (—). Measurements are performed in 100 mM NaCl solution at pH = 6.

Similar observations have been made for PLL and PLA complexes with PG containing mixed membranes (Figure 3.4 and Figure 4.5). However, in the present case the domain formation is much more obvious because of the well dissolved transition peaks. This is related to the results that even in complexes of pure DMPA and PLA domains with bound PLA coexist with domains of free lipids.

Also IR experiments were performed with the complex of PLA and PC/PA membranes. The result is shown in Figure 5.7. The transition range is broadened and the two lipid species undergo separate phase transitions, as it was observed for the case of PLL binding to mixed PC/PA membranes. However, there are some features that distinguish PLA binding from PLL binding. 1.) The end temperature of the transition is lower in the case of PLA binding than in the case of PLL binding. This reflects the fact that PLA influences the phase transition temperature less than PLL, which has already been shown for the binding to pure DMPA membranes. 2.) The temperature range of PC melting is wider and that of PA melting is

smaller in the case of PLA binding to PC/PA mixed membranes, as compared to PLL binding. This shows that the phase diagram is very asymmetric. Over a long temperature range only the PC component melts, enriching the gel phase domains in PA. The PA component is stabilized in the gel phase by the interaction with PLA. The PA enriched gel phase domains then melt simultaneously in a small temperature range. A sharp phase transition of the negatively charged lipid component has also been shown for the case of PLA binding to mixed PC/PG membranes (see Figure 4.4 and Figure 4.22). Thus, it can be concluded that it is a specific property of PLA to reduce the interaction between neutral and negatively charged lipids in the melting range. 3.) The frequencies of the CH_2 stretching vibrations of fluid phase mixed membranes are increased with respect to the $\nu_s(\text{CH}_2)$ frequencies of the uncomplexed mixed membrane. In this case decoupling can not be the explanation, because already the admixing of DMPC- d_{54} in uncomplexed membranes should decouple the methylene stretching vibrations by isotopic dilution. Thus, the result indicates that PLA binding increases the conformational freedom of the acyl chains in the DMPA enriched binding domain at temperatures higher than T_m . Probably, this can be explained with the propensity of PLA to disturb the bilayer structure by insertion.

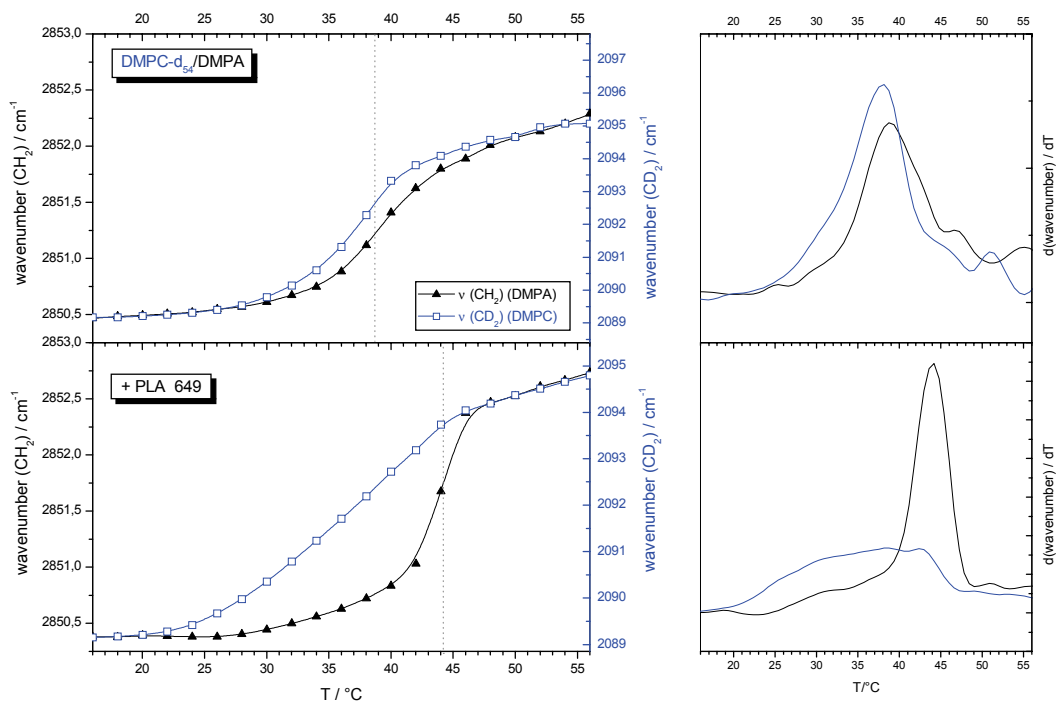


Figure 5.7: Left: Maxima of symmetric methylene stretching vibrational bands of either component of a mixed DMPC- d_{54} /DMPA membrane (upper panel) and its complexes with PLA 649 (lower panel). The CD_2 (\square) stretching vibrations, originating from the DMPC component, are shown in blue (right scale) and the CH_2 (\blacktriangle) stretching vibrations, originating from the DMPA component, are shown in black (left scale). For comparability the left and the bottom scale is the same for both panels. The vertical dotted lines indicate the midpoint of transition of the DMPA component (steepest slope). Right: First derivatives of the curves presented on the left hand side normalized to the wavenumber difference in the melting region. The colours are chosen as in the left panels.

5.3 Binding enthalpies

5.3.1 PLL binding to PA membranes

ITC studies revealed remarkable differences between binding of PLL to PA and PG membranes. Figure 5.8 presents titration traces and the respective binding isotherms of the titration of DLPA vesicles into PLL solution. At 10 °C DLPA membranes as well as DLPA/PLL complexes are in the gel phase. At this temperature the binding is endothermic. At 60 °C, where DLPA and DLPA/PLL complexes are organized in the liquid crystalline phase, the binding is exothermic. At intermediate temperature (35 °C), the vesicles that are titrated to the PLL solution are in the fluid state but the formed complexes are still in the gel state. Therefore, the measured enthalpy has contributions of the fluid to gel phase transition (exothermic) and gel phase binding (endothermic).

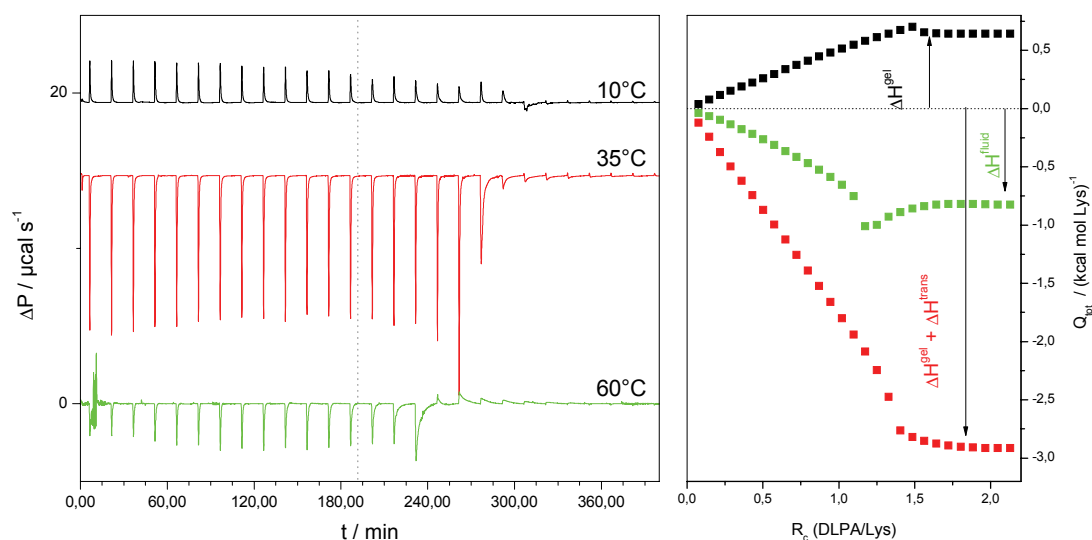


Figure 5.8: Titration of DLPA (20 mM) into PLL 282 solution (2 mM) at (—) 10 °C, (—) 35 °C, (—) 60 °C. **Left:** differential power vs. time plots, **Right:** total heats of reaction normalized to the PLL concentration.

The fact that fluid state binding (60 °C) is more exothermic than gel phase binding (10 °C) is exactly the opposite of what was detected for PLL binding to DPPG membranes. Binding to PG membranes is more exothermic if the membrane is in the gel state rather than in the fluid state (see Figure 3.13). This different binding behaviour must be due to a different balance of various contributions to ΔH . Contributions of secondary structure transition and headgroup hydration will be discussed below. In addition, changes of the acyl chain order induced by PLL binding have to be considered.

It is known from X-ray experiments that the acyl chain packing of gel phase PA membranes is not affected by PLL binding (Takahashi et al. 1991). In contrast, PLL binding to fluid PA bilayers has been reported to increase the acyl chain order. This was shown by ESR (Hartmann and Galla 1978) and NMR spectroscopy (Laroche et al. 1990). Similarly, the low $\nu(\text{CH}_2)$ frequencies of fluid PA/PLL complexes (see Figure 5.11) indicate a bilayer rigification induced by PLL binding to fluid PA membranes. The results show that fluid PA vesicles being titrated into PLL solution undergo a structural change, even at temperatures higher than T_m of the complex. This contributes with an exothermic heat to the enthalpies measured in ITC experiments. For gel phase binding this contribution is absent, which makes gel phase binding less exothermic than fluid phase binding.

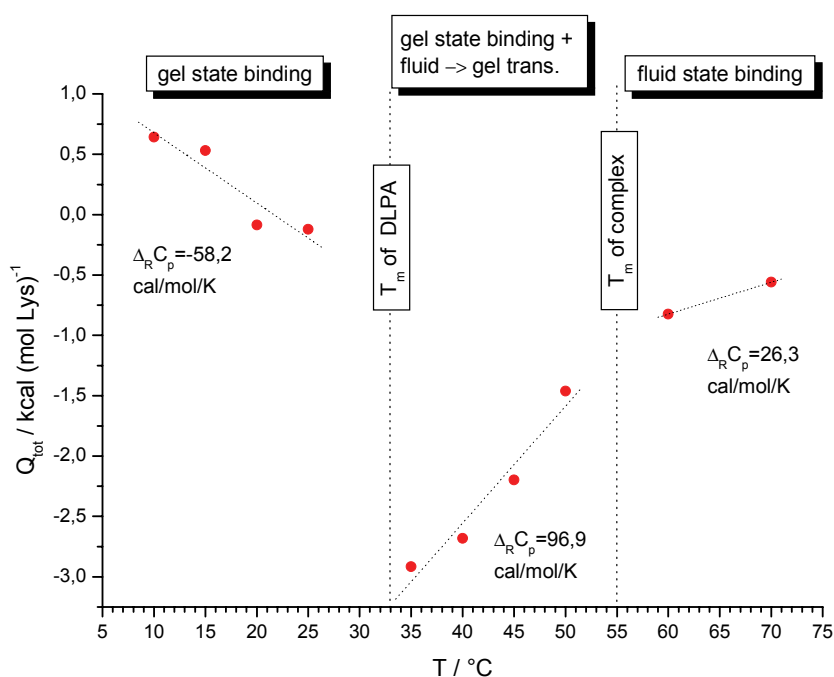


Figure 5.9: Total heats released during the titration of DLPA into PLL 282 in dependence of temperature. The heats are normalized to one mole of cell content (Lys) and determined at $R_c = 2$. The vertical lines indicate the transition temperatures of pure DLPA and a DLPA/PLL complex.

The temperature dependence of the reaction enthalpy is depicted in Figure 5.9. In the temperature range of the DLPA gel phase ($T < 33\text{ °C}$) the binding enthalpy decreases with rising temperature, i.e. $\Delta_R C_p$ is negative. This implies that also in the case of PLL binding to gel phase DLPA membranes hydrophobic interactions are involved. The value of $-58\text{ cal mol}^{-1}\text{K}^{-1}$ compares well with the value detected for PLL binding to DPPG gel phases. However, IR experiments suggest that the contribution of hydrophilic hydration is higher in the case of DLPA membranes (see below). Consequently, the contribution of hydrophobic dehydration to the negative $\Delta_R C_p$ would be lowered, which indicates that PLL inserts less

readily into DLPA bilayers than into DPPG bilayers. It will be shown by monolayer adsorption experiments that this assumption is reasonable (see below).

Between 33 °C and 55 °C the measured enthalpies are a summation of gel phase binding enthalpy and fluid to gel phase transition enthalpy of the titrated vesicles. That explains the sudden decrease of the reaction enthalpy to exothermic values. Also $\Delta_{\text{R}}C_{\text{p}}$ has contributions from binding and phase transition contributions. The measured positive value of $\Delta_{\text{R}}C_{\text{p}}$ is probably due to the fact that the phase transition of the complex is not sharp. Rather, the enthalpy of the complex increases continuously in this temperature range. This is reflected by DSC curves that do not return to the baseline between the first and the second transition step as well as by continuously increasing $\nu(\text{CH}_2)$ frequencies in the same temperature range (see Figure 5.11). The broad gel to fluid phase transition decreases the reaction enthalpy with increasing temperature.

Above T_{m} of the DLPA/PLL complex (55 °C) $\Delta_{\text{R}}C_{\text{p}}$ is slightly positive. A less negative $\Delta_{\text{R}}C_{\text{p}}$ for fluid phase binding than for gel phase binding was also found for PLL binding to PG membranes and was attributed to the compensation of hydrophobic effects by effects of headgroup hydration and polypeptide unfolding. That these effects play also a role in the present case will be shown in the IR section (section 5.5 and 5.6). In the case of PLL binding to fluid DLPA membranes the negative contribution to $\Delta_{\text{R}}C_{\text{p}}$ is apparently over-compensated by positive contributions. This might be due to increased positive contributions or to decreased hydrophobic interactions if compared to PG membrane binding. Indications for the later explanation arise from monolayer adsorption experiments (see section 5.7).

The described phase and temperature dependence of the reaction enthalpies is very similar to what has been measured for Ca^{2+} binding to PA bilayers (Garidel 1997). This similarity was already shown to exist in respect to the thermotropic phase behaviour and suggests once more that PLL binding to PA bilayers is mainly driven by electrostatic interactions.

5.3.2 PLA binding to PA membranes

The binding enthalpies of PLA binding to PA membranes do not differ significantly from those of PLA binding to PG membranes. In both cases, the binding to fluid state vesicles is more exothermic than the binding to gel state vesicles. However, the total heats released are slightly higher in the case of binding to PA membranes (Figure 5.10). The enthalpies of PLA binding to DLPA gel phase membranes are exothermic, while those for binding to DPPG gel phase are slightly endothermic. The more negative ΔH for binding to gel phase DLPA membranes is reflected by the larger increase of T_{m} and the smaller decrease of the transition enthalpy of the PA/PLA complexes as compared to the PG/PLA complexes.

The reaction enthalpies of PLA binding to DLPA membranes do not show any temperature dependence, neither for gel phase binding nor for fluid phase binding. This is different to what was found for PLA binding to PG membranes. The absence of a negative $\Delta_{\text{R}}C_{\text{p}}$ is not due to

the lack of hydrophobic interactions, as will be shown by monolayer adsorption experiments (see Figure 5.18). Probably hydrophilic dehydration (see Figure 5.14) compensates the negative $\Delta_R C_p$ that arises from hydrophobic dehydration.

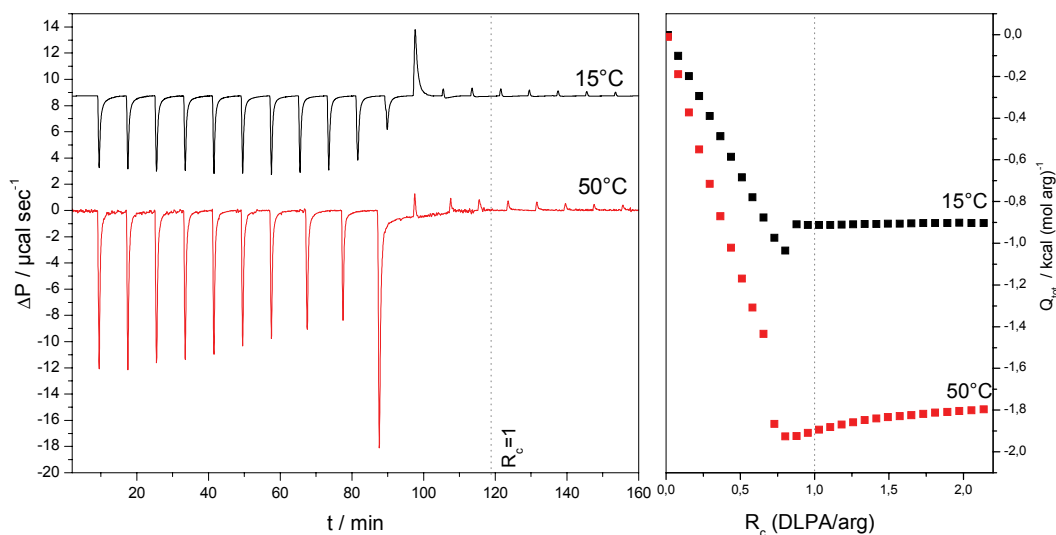


Figure 5.10: Titration of DLPA into PLA 184 at (—) 15 °C and (—) 50 °C. **Left:** differential power vs. time plot. **Right:** total heats of reaction normalized to moles of cell content (PLA).

5.4 The methylene stretching vibrations

5.4.1 Polylysine / PA complexes

Figure 5.11 depicts the temperature dependence of the $\nu_s(\text{CH}_2)$ frequencies of DLPA and its complexes with PLL of different chain length. The complex of DLPA and the shortest PLL ($n = 14$) performs the chain melting transition at slightly higher temperatures than the uncomplexed DLPA membrane. Complexes of DLPA with longer PLL perform a two step phase transition with the first step being found at the same temperature as T_m of DLPA/PLL 14. The second transition step is observed at 20 – 25 °C increased temperatures with respect to T_m of the uncomplexed DLPA membrane. These results are in good agreement with the data of the DSC experiments. However, DSC showed that the second transition step is connected with the higher enthalpy change, whereas IR spectroscopy indicates that a high proportion of chain melting has already occurred at lower temperature. This might be due to the fact that enthalpic contributions to the second transition step arise from conformational reorganisation of the headgroup layer and/or the adsorbed polypeptide.

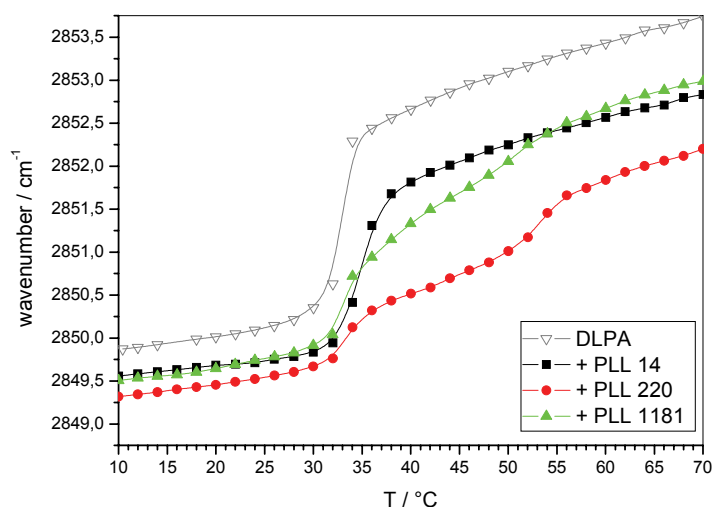


Figure 5.11: Symmetric CH_2 stretching vibrational frequencies of DLPA (∇) and its complexes with PLL 14 (\blacksquare), PLL 220 (\bullet) and PLL 1181 (\blacktriangle) at mixing ratios of $R_c = 1$ as a function of temperature.

The $\nu_s(\text{CH}_2)$ frequencies of the complexes are decreased with respect to those of the uncomplexed membrane. The decrease is higher for complexes in the fluid phase than for complexes in the gel phase. If the proportion of frequency decrease observed for gel phase complexes is attributed to increased interchain vibrational coupling, there is still a remaining component for the fluid complexes. This indicates that the order of the fluid phase membrane is reduced by PLL binding and confirms the results of Hartman and Galla (1978) and Laroche (1990) (see section 5.3).

5.4.2 Polyarginine / PA complexes

The temperature dependence of the $\nu_s(\text{CH}_2)$ frequencies of PLA/DLPA complexes is shown in Figure 5.12. The chain melting transition temperature is only slightly increased by PLA binding. The increase is higher in case of longer PLAs. However, fractions of the complexes of DLPA and longer PLA melt already at the transition temperature of the uncomplexed membrane. These finding reproduces well the results of the DSC experiments.

Interestingly, the $\nu_s(\text{CH}_2)$ frequencies of the complexes are not decreased compared to the $\nu_s(\text{CH}_2)$ frequencies of the uncomplexed membrane. This indicates that PLA binding does not increase the vibrational coupling of and the conformational order of the acyl chains.

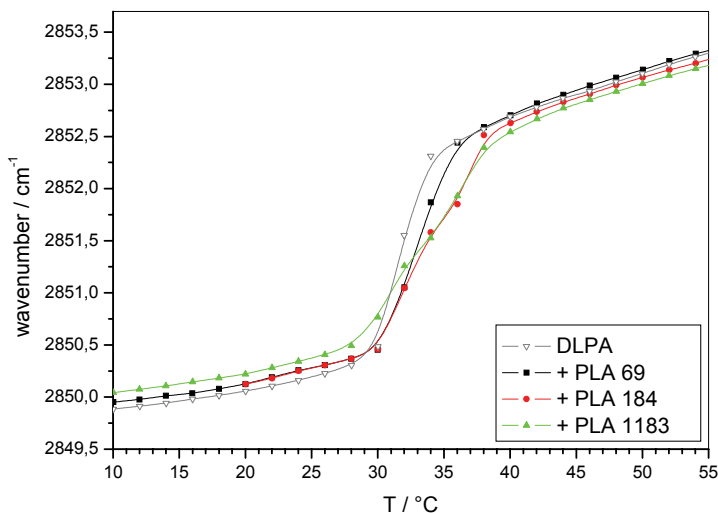


Figure 5.12: Symmetric CH₂ stretching vibrational frequencies of DLPA (∇) and its complexes with PLA 69 (\blacksquare), PLA 184 (\bullet) and PLA 1183 (\blacktriangle) at a mixing ratio of $R_c = 1$ as a function of temperature.

5.5 Influence of polypeptide binding on the interfacial hydration

5.5.1 PLL binding

As shown above, the frequency and the shape of the carbonyl stretching vibration band are indicative for the degree of interfacial hydration. The carbonyl bands of DLPA and the DLPA/PLL complexes were analysed at 10 °C and 60 °C, where DLPA as well as the complexes are in the gel and the fluid state, respectively (Figure 5.13). As mentioned before, the bands consist of two components, which originate from the vibrations of non-hydrated (1740 cm^{-1}) and hydrated (1720 cm^{-1}) carbonyl groups. In the case of the DLPA/PLL complexes a third band that originates from an amide I vibration (1680 cm^{-1}) was included in the fit⁸. The fit results show that PLL binding to gel phase DLPA membranes causes an increase in intensity of the lower frequency band on expense of the higher frequency band. This is indicative for a stronger hydration of the lipid carbonyl groups. The same effect was observed for PLL binding to gel state DPPG membranes. However, in the present case it is much more pronounced. Whereas PLL binding increases the intensity of the lower frequency C=O band by 9 % for the case of binding to DPPG, it increases the intensity 23.5 % for the case of binding to DLPA.

⁸ The carbonyl bands were fitted as described in chapter 4.5.1. The amide band was fitted by 10% Gaussian and 90% Lorentzian. The position was fixed to the value determined from the second derivative bands. Half width and intensity were estimated and fixed before fitting of the C=O bands.

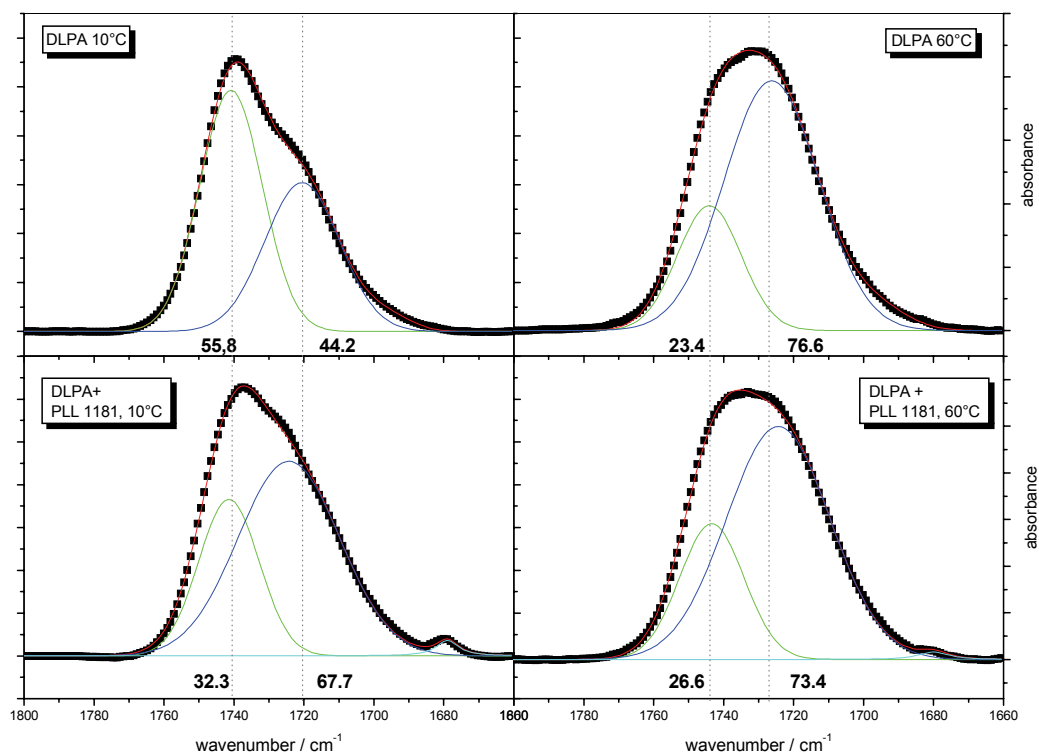


Figure 5.13: Carbonyl stretching vibrational bands of DLPA (upper panels) and its complex with PLL 1181 (lower panels) at 10 °C (left panels) and 60 °C (right panels). The experimental bands (■) are fitted with 2 Gaussians (—, —), representing two distinct states of hydration. In the case of the complexes also one component of the β -sheet amide I band is included in the fit (—). The summation of the fit components is shown in red (—). The relative integral intensities of the carbonyl band components are given as percentages underneath the respective fitting curve. The vertical dotted lines indicate the positions of the fit components of pure DLPA. All analysed bands originate from the cooling scan.

As it has been outlined before (chapter 3.3) this effect can not be explained with the penetration of additional water molecules into the interfacial membrane region. Rather existing water molecules get confined by binding of the polypeptide to the headgroup layer. This lowers their reorientational motion and increases the probability of hydrogen bonding. Similar effects have been observed for Ca^{2+} binding to DMPA membranes. Laroche et al. (1991) found that although water is released from the membrane by Ca^{2+} binding, the C=O band is influenced in a way that implies better hydration. They suggested that water molecules are trapped in the headgroup region and form strong hydrogen bonds with the carbonyl groups.

Comparison of PA/PLL and PG/PLL complexes suggests that more water molecules are trapped in the carbonyl region of PA membranes than of PG membranes. This difference might be due to the different secondary structure the peptide adopts upon binding (see below).

The effect of PLL binding on the interfacial hydration of fluid DLPA membranes is small. However, a tendency for dehydration is observable. This can be easily explained by the fact that the PLL has an ordering effect on the bilayer structure in the liquid crystalline phase

(Hartmann and Galla 1978; Laroche et al. 1990). The lower bilayer expansion allows less water to penetrate into the bilayer interface during the phase transition.

5.5.2 PLA binding

The effect of PLA binding on the hydration of DLPA bilayers is nearly identical to the effect it has on DPPG bilayers. Binding to the gel phase does hardly affect the hydration at all and binding to fluid phase membranes slightly dehydrates the lipid carbonyl groups (Figure 5.14). The interpretation for this effect is the same as given before for PLA binding to DPPG membranes. The dehydration originates from insertion of arginine side chains, which replace water molecules from the interface and compete for the remaining ones. PLA has no ordering effect on fluid DLPA bilayers, which can be concluded from the unaffected methylene stretching vibrational frequencies (Figure 5.12). Therefore, the alternative interpretation that was given for the dehydrating effect of PLL on fluid PA bilayers can be excluded for the case of PLA binding.

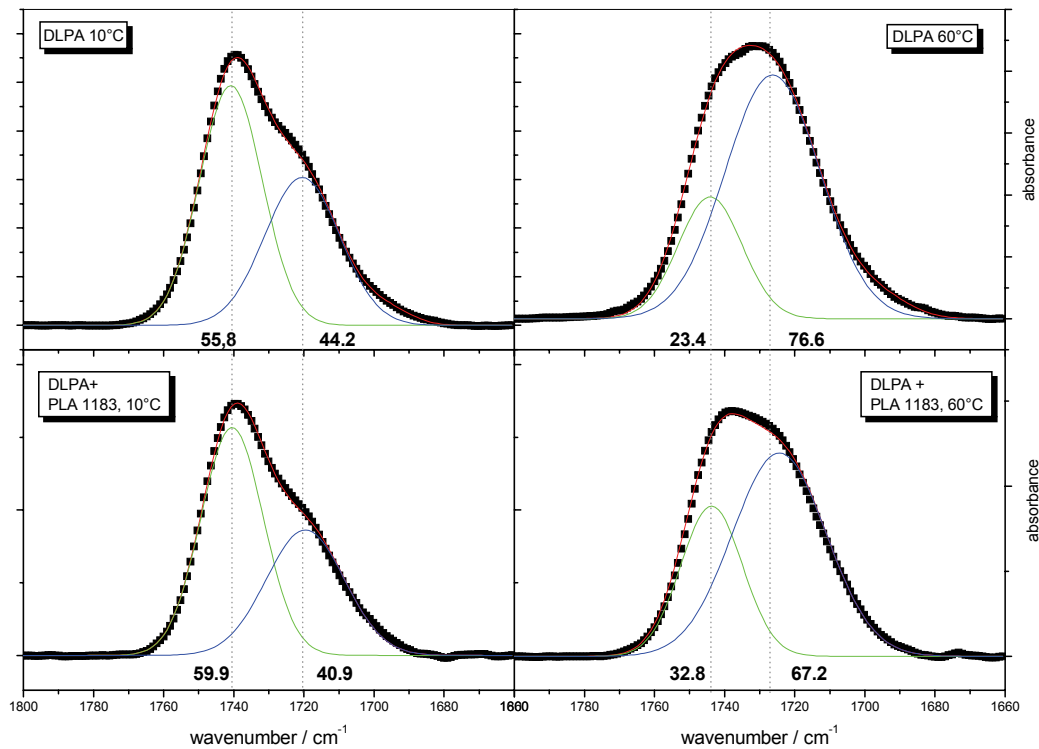


Figure 5.14: Carbonyl stretching vibrational bands of DLPA (upper panels) and its complex with PLA 1183 (lower panels) at 10 °C (left panels) and 60 °C (right panels). The experimental bands (■) are fitted with 2 Gaussians (—, —), representing two distinct states of hydration. The summation of the fit components is shown in red (—). The relative integral intensities of the carbonyl band components are given as percentages underneath the respective fitting curve. The vertical dotted lines indicate the positions of the fit components of pure DLPA.

5.6 Secondary structure of the polypeptides

5.6.1 PLL

Figure 5.15a presents the amide I bands of PLL 1181 being bound to a DLPA membrane at various temperatures. In the temperature range of 10 °C to 50 °C the bands show two maxima at 1611 cm⁻¹ and at 1679 cm⁻¹. This is clearly indicative for the formation of polylysine β -sheets on the surface of DMPA membranes. Upon heating the β -sheets are stable until the phase transition of the DMPA/PLL complex is completed. The first transition step (33 °C) does not affect the secondary structure of the adsorbed polypeptide. The second transition step of the complex at ca. 55 °C is connected with a secondary structure transition of the bound polypeptide from β -sheet to random coil. This can be deduced from the appearance of a broad band at 1642 cm⁻¹ and the concomitant reduction of the typical β -sheet vibrational bands. But even at 70 °C contributions of β -sheet vibrations are present in the spectrum. This shows that the polypeptide does not unfold completely and implies the existence of higher order domains in the fluid state of membrane. The notion of polypeptide unfolding concomitant with the second transition step of the complex suggests that the respective DSC transition peaks contain contributions from peptide unfolding. This explains that this transition step is better distinguished in DSC experiments, which monitor the enthalpy changes of the whole complex than in IR experiments. In IR experiments only the changes in the order of the hydrocarbon core of the membrane were followed. The formation of β -sheets upon binding to gel phase DLPA membranes can be observed for all longer PLLs, but not for PLL 14. PLL 14 binds in random coil conformation independent on the temperature and the phase state of the membrane (Figure 5.15b).

The secondary structure PLL adopts upon binding to negatively charged membrane surfaces is different for DLPA and DPPG binding. It was shown that in the case of binding to DPPG membranes PLL adopts an α -helical structure (see section 3.3). This difference is probably due to the higher electrostatic interaction of PLL with PA, which leads to a better neutralization of the lysine side chain charges. Charge neutralization is a prerequisite for the formation of both secondary structures but probably more important for the formation of a β -sheet, because the side chain to side chain distance is shorter than in the α -helical structure.

Despite the formation of different secondary structures upon binding to PG and PA membranes the temperature and polypeptide chain length dependence of these structures shows some similarities. In both cases the shortest polypeptide, PLL 14, does not form an ordered secondary structure, but binds in the random coil conformation. Longer PLLs form an ordered secondary structure upon binding to both membranes at temperatures lower than T_m of the respective complex. Upon heating above the gel to fluid phase transition temperature the adsorbed polypeptide unfolds in both cases into a random coil. The secondary structure transition seems to be more cooperative and better coupled to the lipid phase transition in the

case of the β -sheet/DLPA complexes than in the case of the α -helix/DPPG complexes. This shows that the β -sheet structure is more sensitive to the reduction of the membrane charge density that arises from the bilayer expansion at the gel to fluid phase transition.

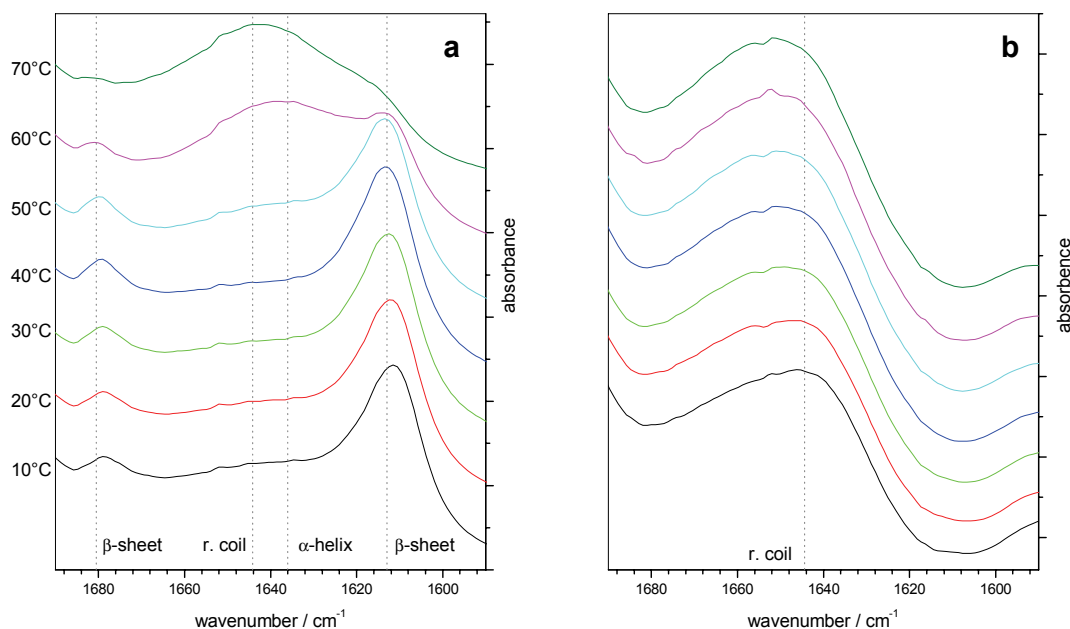


Figure 5.15: Amide I bands of PLL 1181 (a) and PLL 14 (b) bound to a DLPA membrane at — 10 °C, — 20 °C, — 30 °C, — 40 °C, — 50 °C, — 60 °C and — 70 °C.

The formation of PLL β -sheets upon binding to PA membranes was also reported by Takahashi et al. (1996) and Laroche (1988; 1990), who used X-ray diffraction and Raman spectroscopy, respectively to monitor the PLL secondary structure. However, the temperature and chain length dependencies these authors report are somewhat different from the results presented here. Both authors describe that long PLL retains its β -sheet structure while being bound to fluid PA membranes. Further they claim that also short PLL ($M = 4000$, $n = 20$) adopts a β -sheet conformation upon binding to gel state PA membranes.

The latter discrepancy might be due to slightly different PLL chain length. In the present work PLL with a chain length of 14 monomer units was chosen as representative for short polylysine. The above cited authors refer with the term “short” to a PLL chain length of approximately 20 monomer units. It might be that this length is already sufficient to form β -sheet structures, whereas PLL 14 is still too short.

Takahashi et al. (1996) used the presence of a typical reflection in the X-ray powder pattern⁹ as indication for the existence of β -sheets on fluid membrane surfaces. However, that doesn't exclude the existence of random coil conformers, which cannot be observed by X-ray

diffraction. Therefore, no statement can be made about the fraction of peptide being in one or the other conformation. The existence of minor fractions of β -sheet conformers is not contradictory to our results.

Laroche et al. (1988; 1990) analysed the secondary structure of bound PLL by means of Raman spectroscopy. They conclude from experiments performed on DMPA/PLL complexes at 70 °C that the β -sheet of long PLL does not unfold in the fluid state of the complex. However, at 70 °C the gel to fluid phase transition of such complexes is not completed. Measurements at higher temperature would be necessary to proof their suggestion. The high transition temperature of DMPA/PLL complexes is the reason why IR-experiments of this study were performed with DLPA, which decreases the transition temperature by ca 20 °C and allows the examination of fluid state complexes at moderate temperatures.

5.6.2 PLA

The secondary structure PLA adopts upon binding to DLPA and DPPG membranes is similar. Amide I and guanidyl stretching vibrational second derivative spectra of different DLPA/PLA complexes are presented in Figure 5.16. The band assignments have been discussed in section 4.5.1. At temperatures, where the complexes are in the gel state three secondary structure elements can be distinguished. Besides turn and random coil elements a well resolved β -sheet vibration is present in the spectra. With increasing temperature, the β -sheet unfolds into a random coil conformation. The most obvious change of the secondary structure takes place between 30 and 40 °C, which is the gel to fluid transition range of the complexes.

The symmetric and antisymmetric guanidyl stretching vibrational bands are both shifted to lower wavenumbers with respect to the vibrations of unbound PLA. This indicates the existence of hydrogen bonding interactions between the guanidyl group and the lipid headgroup.

This binding behaviour is very similar to what was observed for PLA binding to DPPG membranes. Nevertheless, some small differences exist. The most obvious difference is that in the case of PLA binding to DLPA membranes also the shortest examined PLA ($n = 68$) forms a β -sheet structure, whereas it binds to DPPG membranes as a random coil. This shows that the propensity of DLPA membranes to induce β -sheet formation of bound PLA is higher than that of DPPG membranes. This trend was already shown for the case of PLL binding. Furthermore, the different amide I band components are better resolved in the case of PLA binding to DLPA than in the case of binding to DPPG. This indicates that the different secondary structures are better defined, i.e. the β -sheet PLA adopts on DLPA surfaces is more regular than that formed on DPPG surfaces. Concomitantly, its unfolding is better coupled to

⁹ The 0.47 nm spacing, which reflects the distance between interconnected β -strands.

the phase transition of the membrane than in the case of DPPG binding. Finally, the guanidinium vibrational bands are shifted to lower wavenumbers in the case of DLPA binding than in the case of DPPG binding. This shows that the donated hydrogen bond are stronger, which is probably due to the closer contact to the acceptor groups.

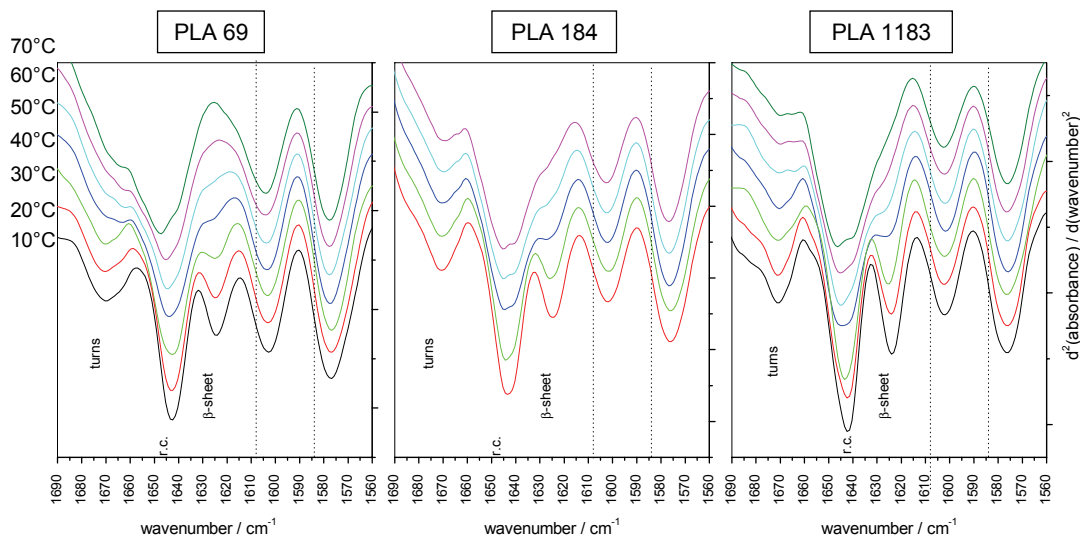


Figure 5.16: Second derivative spectra in the amide I and guanidinium stretching vibrational region of different PLA bound to DLPA membranes at — 10 °C, — 20 °C, — 30 °C, — 40 °C, — 50 °C, — 60 °C and — 70 °C. The vertical dotted lines indicate the frequencies of asymmetric and symmetric guanidyl stretching vibrations of uncomplexed PLA. Spectra are recorded in the cooling scan.

5.7 Polypeptide adsorption to DMPA monolayers

5.7.1 PLL adsorption

It was shown in chapter 3.5 that PLL readily inserts into DPPG monolayers. The insertion was attributed to electrostatically driven adsorption to the membrane surface and consecutive hydrophobically driven incorporation of lysine side chains. Bilayer experiments showed that PA membranes are much more stabilized by PLL binding than DPPG membranes, that the fluidisation of the hydrocarbon core is hindered, and that PLL adopts a different secondary structure. The question then arose whether PLL inserts equally well into DMPA monolayers.

Figure 5.17 shows the kinetics of PLA adsorption to a DMPA monolayer at 25 °C. At this temperature the phase behaviour of PA monolayers is comparable to that of PG monolayers at 20 °C. The recorded π - t curves resemble those of the DPPG/PLL system. The adsorption follows a two step mechanism. At low initial pressures π_0 injection of PLL leads to a condensation of the monolayer which is followed by insertion of lysine moieties into the aggregated domains. This behaviour is reflected by isotherms, whose initial decrease is

followed by a consecutive increase. At higher initial pressures, where the lipid monolayer is in the liquid condensed state (LE), the surface pressure directly increases after PLL injection.

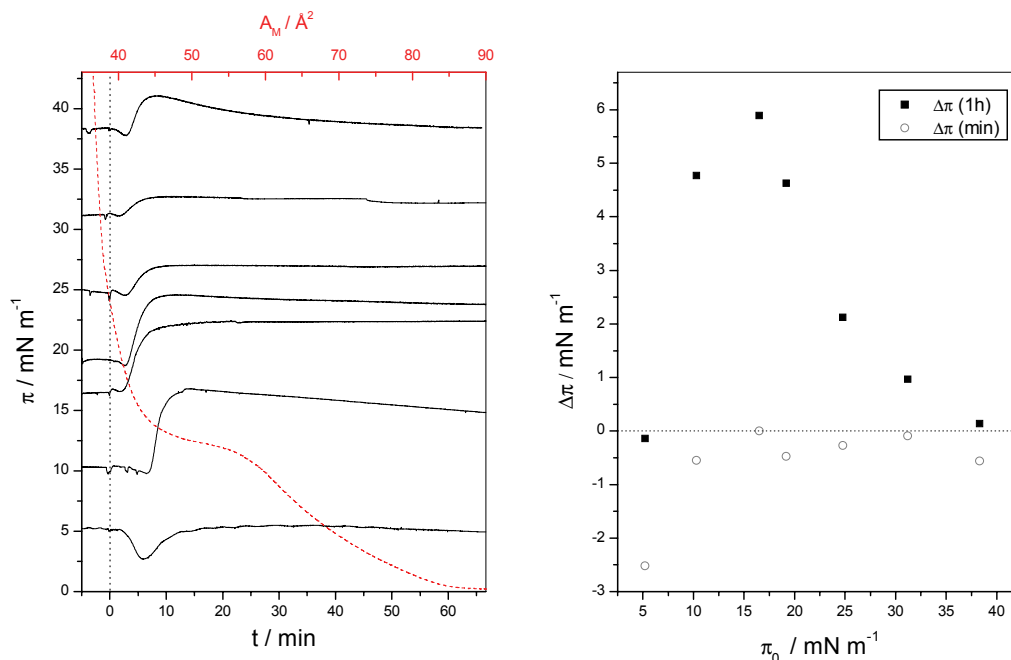


Figure 5.17: **Left:** Adsorption kinetics of PLL 220 at DMPA monolayers at different initial surface pressures on a subphase of 100 mM NaCl solution in H_2O (—). PLA (10 μl , 50 mM) was injected underneath the monolayer at $t = 0$. The π/A isotherm of DMPA at 25 $^\circ\text{C}$ (—) (top scale) is given to identify the monolayer phase state. **Right:** Changes in surface pressure after injection of PLA vs. initial surface pressure determined 60 min after injection (■) and at the minimum of the π/t curves (○)

This finding is similar to what has been observed for DPPG monolayers. However, the extent of pressure increase ($\Delta\pi$) and its dependence on the initial surface pressure of the uncomplexed monolayer (π_0) are different between DPPG and DMPA monolayers. In the case of DMPA monolayers $\Delta\pi$ increases with π_0 till a maximum is reached at a π_0 of approximately 15 mN/m . The maximal $\Delta\pi$ that was detected is 6 mN/m . At higher initial pressures ($\pi_0 > 15$ mN/m) $\Delta\pi$ decreases with increasing π_0 . This shows that PLL inserts less readily into a condensed DMPA monolayer the tighter the lipid molecules are packed. This behaviour is the expected one and was observed for various peptides interacting with lipid monolayers (Dyck and Loesche 2006; Kimelberg and Papahadjopoulos 1971; Maget-Dana 1999). In contrast, for PLL adsorption to DPPG monolayers a continuous increase of $\Delta\pi$ with rising π_0 was observed (see Figure 3.21). However, the maximal $\Delta\pi$ that is caused by PLL insertion into DPPG monolayer at high initial pressures π_0 compares to the maximal values detected for PLL insertion into DMPA monolayers at much lower π_0 . This suggests that the same processes take place on both monolayers at different initial pressures π_0 .

Comparison of the $\pi-A$ isotherms shows that at equal surface pressures DMPA monolayers (at 25 $^\circ\text{C}$) are more condensed, than DPPG monolayers (at 20 $^\circ\text{C}$), i.e. the respective molecular

areas are lower. Furthermore, the compressibility of condensed DMPA monolayers is smaller than that of condensed DPPG monolayers. Moreover, DMPA monolayers perform a second order phase transition ($LC \rightarrow S$) at 27 mN/m, which could not be detected for DPPG monolayers. These findings show that at comparable ambient conditions DMPA monolayers are more ordered than DPPG monolayers. This explains the lower propensity of PLL to insert into condensed DMPA monolayers than into condensed DPPG monolayers.

5.7.2 PLA adsorption

The results obtained from PLA adsorption experiments on DMPA monolayers (Figure 5.18) support well the already outlined trends regarding the specificities of the two polypeptides as well as regarding the lipid headgroup influence. The principle shape of the $\Delta\pi$ over π_0 plot that was determined for PLA adsorption to DMPA monolayers resembles that of the system PLL/DMPA. In both cases $\Delta\pi$ reaches a maximum at intermediate π_0 and then decreases with further increase of π_0 . Hence it can be concluded that this insertion behaviour is due to the specific organisation of the DMPA monolayer. Comparison of the absolute values of $\Delta\pi$ shows that PLA inserts more readily into DMPA monolayers than PLL. The maximal $\Delta\pi$ achieved by PLA insertion is 12 mN/m, which is twice as high as the maximal $\Delta\pi$ achieved by PLL insertion.

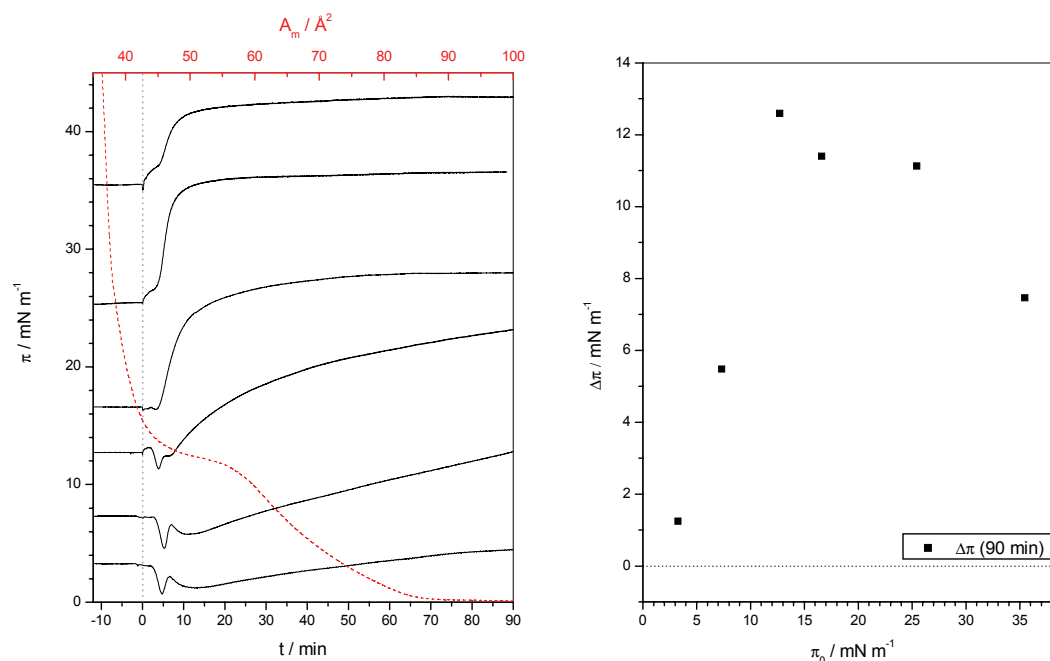


Figure 5.18: Left: Adsorption kinetics of PLA 184 at DMPA monolayers at different initial surface pressures on a subphase of 100 mM NaCl solution in H_2O (—). PLA (10 μl , 50 mM) was injected underneath the monolayer at $t = 0$. The π/A isotherm of DMPA at 25 °C (—) (top scale) is given to identify the monolayer phase state. Right: Changes in surface pressure after injection of PLA vs. initial surface pressure determined 90 min after injection.

This compares qualitatively, as well as quantitatively, very well with the trends that have been deduced from the adsorption of both polypeptides to DPPG monolayers. In the latter case PLA also causes a maximal pressure increase that is twice as high as that caused by PLL (8 mN/m as compared to 4 mN/m). Thus, two conclusions can be drawn: 1) The polypeptides insert more readily into DPPG monolayers than into DMPA monolayers. This is due to the tighter packing of DMPA as compared to DPPG. 2.) PLA has a higher propensity to insert into monolayers than PLL, which is due to the better charge compensation of the guanidyl group and the resulting higher hydrophobicity of the arginine side chain as compared to the lysine side chain. Probably specific hydrogen bonding contributes also to this effect.

The adsorption kinetics of PLA to DMPA further shows some interesting peculiarities. Contrary to the former discussed cases, the adsorption rates apparently depend on the phase state of the monolayer. The insertion of PLA into LE monolayers is much slower than the insertion into LC monolayers. The isotherm recorded in the LE/LC coexisting range shows an intermediate insertion rate. However, the first step of PLA interaction with LE monolayers, namely the condensation, is fast. That shows that the slower insertion is not due to slower diffusion. From IR experiments it is known, that the secondary structure of PLA is clearly affected by the phase state of the bilayer. Thus, it is suggested that the different insertion kinetics are connected with different insertion rates of peptide in different secondary structure or with different rates of secondary structure formation on the lipid surface.

Maget-Dana et al. (1997) reported that peptides in random coil conformation (LKKL_n and KL_n) insert slower into lipid monolayers than in α -helical or β -sheet conformation. However, they refer only to the secondary structure of the peptide in solution. Thus, it might be that the slow process they observe is the secondary structure formation at the membrane/water interface. Indeed Reynaud et al. (1993) showed that the same peptides form ordered secondary structures in contact with lipid vesicles. Indications that PLA also undergoes a structural transition in contact with LE monolayers and that this is the rate limiting step arise from the shape of the π/t curves. Besides condensation and insertion a third process can be distinguished in all isotherms. This process leads to a second dip in the π/t curves recorded at low π_0 and to a small plateau in the π/t curves recorded at higher π_0 . Such discontinuities are often attributed to reorganisations of the adsorbed peptide (Maget-Dana 1999; Shafer 1974) and are believed to originate in the present case from the secondary structure formation. Due to the fact that charge neutralization of the side chains is necessary to allow the peptide to fold, this process will be slowed down at the interface of an expanded monolayer with low surface charge density.

5.8 Summary and comparison of polypeptide binding to PG and PA membranes

In the preceding chapters the interactions of PLL and PLA with PG membranes were comprehensively described. This chapter presents studies of the interaction of the same polypeptides with PA membranes. On the one hand, PLL and PLA specificities that were deduced from the binding to PG membranes were corroborated under investigation of a PA membrane binding. On the other hand, it was an objective to reveal the influence of the lipid headgroup structure on the polypeptide-membrane interaction. Therefore, the obtained results of PLL and PLA binding to PA membranes are summarized and compared to the binding to PG membranes in the following two paragraphs.

PLL binding to PA membranes as compared to PG membranes

The interaction of PLL with PA membranes is remarkably different from the interaction with PG membranes. Two phase transition steps were observed. The main component is shifted to much higher temperatures ($\Delta T_m = 25\text{ }^\circ\text{C}$) as in the case of PG membrane binding ($\Delta T_m = 5\text{ }^\circ\text{C}$). Even at this increased temperature the membrane is not completely fluidized. Interestingly, the phase transition behaviour is only influenced if $R_c \leq 1$. PLL adopts a different secondary structure upon binding to gel phase PA membranes (β -sheet) than to gel phase PG membranes (α -helix). The enthalpy of PLL binding to PA membranes is more negative in the case of fluid phase binding than in the case of gel phase binding. This is opposite to what was shown for PG membranes. Furthermore, the hydration of the lipid carbonyl groups is much more increased by PLL binding to PA membranes (23 %) than to PG membranes (9 %). Monolayer adsorption experiments showed that PLL inserts less readily into PA membranes at high surface pressure as compared to PG membranes. At lower π_0 the insertion into PA monolayers is preferred over the insertion into PG monolayers. However, at the bilayer-monolayer equivalent pressure (30 mN/m) the insertion is only weak.

Most of these differences can be explained with increased electrostatic interaction strength between PLL and PA as compared to PLL and PG. Consequently, both, lipid and peptide charges are better compensated, which results in the high transition temperatures, the denser packing of the acyl chains in the fluid phase, and the formation of a PLL β -sheet upon binding to gel phase PA membranes. The strong complexation of the headgroup region counteracts the tendency of the acyl chains to undergo a melting transition. This leads to two transition steps, of which the first is dominated by chain melting and the second by headgroup and peptide reorganisation. The monolayer experiments reflect both, the strong interaction and the better membrane organisation. The former leads to higher insertion at low surface pressures and the latter to reduced insertion at high π_0 .

With respect to many properties, the influence of PLL on PA membranes is similar to that of Ca^{2+} . This supports the conclusion, that electrostatics dominate the interaction of PLL with PA, with hydrophobic interactions and hydrogen bonding being of minor importance.

PLA binding to PA membranes as compared to PG membranes

In contrast to PLL, PLA interacts similarly with PA and with PG membranes. Binding enthalpies, carbonyl group hydration, and secondary structure of the polypeptide are very similar in both cases. Effects that are due to electrostatic interaction are somewhat enhanced upon interaction with PA membranes. This is reflected in a slightly increased transition temperature ($\Delta T_m = 5^\circ\text{C}$) and the formation of a more regular β -sheet structure by the polypeptide. However, this enhancement is much less pronounced than in the case of PLL binding. This shows again, that electrostatics is less important for PLA binding than for PLL binding.

Remarkable is the pronounced demixing of zwitterionic PC and negatively charged PA molecules upon binding of PLA to mixed membranes. This is attributed to the tendency of PA to form an intermolecular hydrogen bond network in the headgroup layer. Possibly PLA participates in this network by donating hydrogen bonds. The existence of such specific PLA - PA interactions is implied by the fact that also pure PA membranes form well defined binding domains if PLA is added in minor concentrations ($R_c > 1$). Furthermore, decreased guanidinium stretching vibrational frequencies support this conclusion. Monolayer experiments show a high increase of the surface pressure at intermediate π_0 and a somewhat reduced but still noticeable increase at high π_0 . Thus, they reflect the high propensity of PLA to insert into lipid monolayers as well as the better organisation of PA monolayers as compared to PG monolayers.

Conclusions

The presented experiments on polypeptide interaction with PA membranes support well the specificities in PLL and PLA binding that have been deduced from their interaction with PG membranes. Furthermore, they revealed which properties of the lipid membrane modulate the interaction. The order of the hydrophobic core, the ability of the headgroups to participate in hydrogen bonding, and the location of the headgroup charges with respect to the membrane surface are important parameters that influence the interaction.

6 Summary

Electrostatic forces are important in the interaction of proteins with biological membranes. Many proteins contain clusters of positively charged amino acids, whereas biological membranes contain fractions of negatively charged lipids. A model system was chosen to study this electrostatic interaction in detail. It comprises homopolymers of the positively charged amino acids lysine and arginine (PLL and PLA) and membranes composed of the negatively charged lipids phosphatidylglycerol (PG) or phosphatidic acid (PA).

The aim of this study was to determine possible non-electrostatic contributions to the interaction between positively charged polypeptides and negatively charged membranes and to reveal the balance between electrostatic and non-electrostatic effects. Furthermore, the influence of polypeptide binding on membrane as well as peptide properties was investigated. Finally, the influence of the specific chemical structure of the amino acid side chain and the lipid headgroup on the complex formation was examined.

A combination of different methods allowed a comprehensive view on organisation and thermodynamics of the formed complexes. DSC and IR spectroscopy were used to study the thermotropic phase behaviour of the complexes as well as the ability of PLL and PLA to induce domain formation in mixed lipid membranes. IR spectroscopy was further used to study the influence of polypeptide binding on acyl chain order and interfacial hydration as well as the secondary structure of the bound polypeptide. Binding enthalpies and heat capacity changes were determined by ITC. X-ray diffraction experiments revealed the organisation of the complex. Monolayer experiments provided information on peptide insertion into the lipid headgroup layer. Finally, dye release experiments were used to study the propensity of PLL and PLA to induce pore formation in the lipid membrane. The results will be summarized in the following paragraphs.

Thermotropic phase behaviour

Electrostatic shielding of the headgroup charges by PLL and PLA binding stabilizes the gel phase and increases the main transition temperature. This effect is more pronounced for polypeptide binding to PA membranes as compared to PG membranes. Concomitantly, the effect is more pronounced for PLL binding than for PLA binding. Consequently, the increase in T_m is the highest for PLL/PA complexes. Conversely, PLA binding to PG membranes has only a marginal effect on T_m .

The smaller effect of PLA is due to destabilizing non-electrostatic interactions that balance the effect of electrostatic shielding. The adsorption of the polypeptides to PG membranes is due to unspecific electrostatic and hydrophobic interactions, whereas PA membranes favour the formation of stoichiometric complexes, which is thought to be due to the involvements of

hydrogen bonding. This is deduced from the dependency of T_m on the lipid to peptide mixing ratio (R_c).

Domain formation

Mixed membranes, being composed of zwitterionic (PC) and negatively charged lipids (PG or PA) show the clear tendency for gel phase demixing if they are complexed by the polypeptides. The PC component is excluded from a polypeptide binding domain that is enriched in PG or PA, respectively. For compositions of $x_{PC} \geq 0.5$, a gel phase miscibility gap was suggested. The tendency for domain formation is higher in PC/PA membranes than in PC/PG membranes. This is due to the stabilisation of PA enriched domains by hydrogen bonding.

Binding enthalpies

In most of the titration experiments exothermic binding enthalpies were detected. However, PLL/PA as well as PLA/PG binding is slightly endothermic when the membrane is in the gel phase. Endothermic binding enthalpies show that entropic contributions to the complex formation, such as counterion or water release, must exist. $\Delta H^{\text{fluid}} < \Delta H^{\text{gel}}$ for PLA/PG, PLA/PA, and PLL/PA complex formation. In contrast, $\Delta H^{\text{gel}} < \Delta H^{\text{fluid}}$ for the formation of a PLL/PG complex. The interpretation of the heats of reaction is not straight-forward, because they contain contributions of several effects. The exothermic contribution of secondary structure formation could be proven by comparison of PLL binding and poly(D,L-lysine) binding. The latter is a random copolymer of D-lysine and L-lysine, which doesn't form regular secondary structures. An exothermic contribution of polypeptide induced membrane reorganisation is evident for the PLL/PA complexes.

The heat capacity changes ($\Delta_R C_p$) for binding were determined by temperature dependent measurements of the binding enthalpies. For nearly all polypeptide/membrane systems, $\Delta_R C_p$ is negative. This indicates that a change in the hydrophobic interactions occurs, i.e. hydration of apolar groups is reduced. It is concluded that the polypeptides do not only bind superficially, but insert to some extent into the bilayer.

Acyl chain order

PLL and PLA binding increases the order of the hydrocarbon chain of the lipids. This was deduced from a decrease in methylene stretching vibrational frequencies. The ordering effect of PLL binding is higher than that of PLA binding. Concomitantly, the order of PG membranes is more increased than the order of PA membranes. The gel phase and the liquid crystalline phase of PG membranes are influenced to the same extent. In contrast, binding of PLL to PA membranes increases the order of the liquid crystalline phase more than that of the gel phase. PLA binding to PA membranes has no effect on the acyl chain order.

On basis of isotopic dilution experiments it was shown that not only the conformational order of the acyl chains contributes to the decrease in the $\nu(\text{CH}_2)$ frequencies. Also increased interchain vibrational coupling by polypeptide binding has to be considered.

Interfacial hydration

The frequency of the carbonyl stretching vibration was used as an indicator for interfacial hydration. The way the carbonyl hydration is influenced clearly depends on the interacting polypeptide. PLL binding increases the interfacial hydration of both, PG and PA gel phase membranes. This is caused by stronger hydrogen bonding of trapped water molecules in the interfacial membrane region. The effect is more pronounced for PA membranes compared to PG membranes, which reflects the stronger interaction of PLL with PA membranes. The hydration of the liquid crystalline phase is only marginally affected by PLL binding.

In contrast to PLL, PLA reduces the interfacial hydration of both membranes. PG and PA membranes are similarly affected. In both cases fluid phase membranes are more dehydrated than gel phase membranes. The dehydration is caused by release of water molecules due to PLA insertion into the headgroup layer.

Secondary structure of the polypeptides

Both polypeptides are in random coil conformation in bulk solution at neutral pH. The electrostatic repulsion between the charged side chains prevents the formation of defined secondary structures. Upon binding to negatively charged membranes the polypeptides adopt secondary structures. This is possible because the side chain charges are neutralized by the membrane counter charge.

Which type of secondary structure is formed depends on the peptide as well as on the membrane. Longer PLL forms an α -helix upon binding to gel phase PG membranes. Binding to gel phase PA membranes induces the formation of a β -sheet. Both structures unfold when the temperature is raised above T_m of the respective complex. PLL bound to mixed PC/PG membranes undergoes a very cooperative secondary structure transition at the phase transition temperature of the complex. The shortest PLL ($n = 14$) does not form secondary structures. The difference in PLL secondary structure in PG and PA complexes is due to the different electrostatic interaction strength.

Longer PLA forms a β -sheet in both gel phase PG and gel phase PA complexes. The shortest PLA ($n = 69$) forms a β -sheet only in PA complexes, while it binds in random coil conformation to PG membranes. As in the case of PLL binding, the phase transition of the complexes triggers the unfolding of the bound polypeptides. This correlation is most pronounced for the PLA/PA complex.

Monolayer adsorption

Monolayer adsorption experiments show that both, PLL and PLA insert into lipid monolayers. This proves that hydrophobic interactions contribute to the polypeptide-membrane binding. The propensity of insertion is higher for PLA than for PLL. This is due to the higher hydrophobicity of PLA and the better compensation of PLA side chain charges. These results support well the conclusions drawn from ITC and DSC experiments. At the monolayer–bilayer equivalence pressure PG monolayers are more readily penetrated than PA monolayers. This reflects the higher order of PA acyl chains and the lower compressibility of PA monolayers.

Pore formation

Dye release experiments were used to investigate how PLL and PLA binding influences the bilayer integrity. Both polypeptides induce pore formation in lipid vesicles when the outer monolayer is neutralized ($R_c \approx 2$). Pore formation is higher in fluid membranes than in gel phase membranes. PLA binding causes more pore formation than PLL binding. This shows once more that PLA inserts more deeply into the membranes and has higher impact on the membrane order. Because the dye efflux is not complete, it is believed that the pores are transient. By cryo-TEM imaging it was shown that the vesicles are not completely ruptured upon polypeptide binding.

X-ray analysis

PLL stabilizes the lamellar structure of DPPG membranes. In gel and subgel phases PLL α -helices are intercalated between adjacent bilayer lamella. The headgroup to headgroup distance of adjacent lamella is determined by the helix diameter. At temperatures below the freezing point of free water, PLL helices are ordered in a parallel fashion in the interbilayer space and form a one dimensional lattice. A pronounced freezing point depression proves that PG and PLL counterions are released into the bulk solution. The gain in entropy connected with this process is one of the driving forces for polypeptide–lipid membrane interaction.

7 Conclusions

The positively charged polypeptides PLL and PLA strongly interact with membranes, containing the negatively charged lipids PG or PA. Electrostatic attraction between the oppositely charged molecules is one of the driving forces for this interaction - but not the only one. Various experiments revealed further contributions to the polypeptide-membrane interaction:

- The gain in entropy connected with the counterion release and the release of water from hydrophobic groups is an important driving force for the polypeptide-membrane interaction.
- Hydrogen bonding between the amino acid side chains and the membrane headgroup contributes to the polypeptide-membrane interaction.
- A further important contribution is the hydrophobic interaction of the amino acid side chains with the membrane. Due to this interaction, the polypeptides do not only bind superficially to the membrane surface, but insert to a certain extent into the headgroup region.
- In addition, the enthalpy of secondary structure formation of the polypeptide decreases the free energy of complex formation.

The different balance between these effects leads to specificities in PLL and PLA interaction with the membranes as well as to specificities in the interaction of the polypeptides with differently composed membranes.

- Electrostatic contributions are more important for PLL binding than for PLA binding. Vice versa PLA binding is more influenced by hydrophobic interactions and hydrogen bonding.
- Electrostatic and hydrogen bonding interactions are more important for PA membranes as compared to PG membranes. Vice versa, hydrophobic interactions are more important in the polypeptide interaction with the more loosely packed PG membranes as compared to PA membranes.

This study contributes to the understanding of the interaction of charged peptides with biological membranes. Interactions that were thought to be predominantly electrostatic are revealed to have noticeable non-electrostatic contributions. The gained knowledge about lysine and arginine specificities might contribute to the understanding of their function in biological systems.

8 Zusammenfassung

Elektrostatische Wechselwirkungen spielen eine wichtige Rolle in der Protein- oder Peptidbindung mit biologischen Membranen. Viele Proteine und Peptide besitzen Bereiche, in denen positiv geladene Aminosäuren (Arginin, Lysin, Histidin) akkumulieren. Dagegen besitzen biologische Membranen meist eine negative Überschussladung.

Im Rahmen dieser Arbeit sollte die Wechselwirkung zwischen geladenen Peptiden und geladenen Membranen genauer untersucht werden. Dazu wurde ein Modellsystem gewählt, das aus den zwei positiv geladenen Homopolypeptiden Poly(L-Lysine) (PLL) und Poly(L-Arginin) (PLA) besteht sowie aus negativ geladenen Membranen, die Phosphatidylglycerole (PG) oder Phosphatidsäuren (PA) enthalten.

Ziel war es, herauszufinden, in welcher Weise und zu welchem Anteil elektrostatische und nicht-elektrostatische Wechselwirkungen zu der Bindung beitragen. Es wurde untersucht, wie die Bindung typische Membraneigenschaften (Umwandlungstemperatur, Packung der Fettsäureketten, Hydratisierung, Domänenbildung) sowie typische Peptideigenschaften (Sekundärstruktur) beeinflusst. Weiterhin wurde untersucht, welchen Einfluss die spezifische chemische Struktur der Aminosäuren und der Kopfgruppe des Lipids auf die Bindung und die Eigenschaften des entstehenden Komplexes hat.

Es wurden folgende Ergebnisse erzielt:

- PLL und PLA bilden feste Komplexe mit PG- und PA-haltigen Membranen. Die elektrostatische Anziehung der entgegengesetzt geladenen Moleküle spielt eine große Rolle bei der Wechselwirkung. Darüber hinaus wurden auch nicht-elektrostatische Bindungsbeiträge nachgewiesen.
- Der Entropiegewinn der Gegenionenfreisetzung sowie der Freisetzung von Wassermolekülen aus dem hydrophoben Bereich der Membran ist eine Triebkraft der Wechselwirkung zwischen geladenen Polypeptiden und geladenen Membranen. Außerdem tragen Wasserstoffbrückenbindungen sowie die Enthalpie der Sekundärstrukturbildung des bindenden Peptides zur Erniedrigung der freien Komplexbildungsenthalpie bei.
- Hydrophobe Wechselwirkungen zwischen den Aminosäure-Seitenketten und den Membranlipiden begünstigen die Bindung. Dadurch binden die Polypeptide nicht nur an die Membranoberfläche, sondern insertieren auch die Kopfgruppenregion der Membranen.
- Diese Wechselwirkungen tragen in unterschiedlichen Anteilen zu der PLL- und PLA-Bindung an negativ geladene Membranen bei. Die Bindung von PLL ist im Wesentlichen elektrostatisch getrieben, während bei der PLA-Bindung hydrophobe Wechselwirkungen und Wasserstoffbrückenbindungen eine wichtige Rolle spielen.

- Die unterschiedlichen Eigenschaften von PG- und PA-Membranen beeinflussen die Wechselwirkung mit den Polypeptiden. Die Zugänglichkeit der geladenen Phosphatgruppe, die Fähigkeit zur Wasserstoffbrückenbindung mit den Polypeptiden und die unterschiedliche Ordnung der Kohlenwasserstoffketten der Lipidmoleküle beeinflussen die Eigenschaften der gebildeten Komplexe. Elektrostatische Wechselwirkungen und Wasserstoffbrücken Bindungen spielen eine größere Rolle bei der Polypeptid-Bindung an PA Membranen. Dagegen sind hydrophobe Effekte wichtiger in der Polypeptid-Wechselwirkung mit PG Membranen als mit PA Membranen.

Diese Arbeit leistet einen Beitrag zum Verständnis der Wechselwirkung zwischen geladenen Peptiden und biologischen Membranen. Es wurde gezeigt, dass die Wechselwirkungen nicht ausschließlich elektrostatischer Natur sind, sondern auch wichtige nicht-elektrostatische Anteile haben. Diese nicht-elektrostatischen Anteile bewirken Unterschiede zwischen der Bindung von Lysin und Arginin und zwischen der Bindung an verschiedene Membranen.

9 Appendix

9.1 Materials

9.1.1 Polylysines

The poly(L-lysines) (PLLs) with degrees of polymerisation ranging from 14 to 1181 (determined by viscosity) as well as the poly(D,L-lysine) (PDLL) with a degree of polymerisation of 215 were purchased from Sigma-Aldrich (Steinheim, Germany) and used without further purification. Bromide was used as counter ion. PLL concentrations are given in mol lysine monomer/l.

9.1.2 Polyarginines

The poly(L-arginines) (PLAs) with degrees of polymerisation of 19, 184, 906 and 1184 (determined by viscosity) were purchased from Sigma-Aldrich (Steinheim, Germany) and used without further purification. Chloride was used as counter ion. PLA concentrations are given in mol arginine monomer/l.

9.1.3 Lipids

1,2-Dipalmitoyl-*sn*-glycero-3-phosphocholine (DPPC) and 1,2-dipalmitoyl-*sn*-glycero-3-phosphoglycerol (DPPG) were a gift from Nattermann Phospholipid GmbH (Cologne, Germany). DMPC, POPC, and the deuterated lipids DPPC-d₆₂, DMPC-d₅₄, and DPPG-d₆₂ were purchased from Avanti Polar Lipids (Alabaster, Alabama, USA). POPG, DMPA, and DLPA were purchased from Genzyme Pharmaceuticals (Liestal, Switzerland). The lipids were used without further purification. Lipid mixtures were prepared by mixing solutions of the lipids in CHCl₃/MeOH (2:1) and evaporating the solvent under a slight stream of nitrogen at a temperature of 50 °C. Remaining traces of solvent were removed at 50 °C under vacuum overnight.

9.1.4 Others

- NaCl, CHCl₃, and CH₃OH were bought from Roth GmbH (Karlsruhe, Germany).
- Na₂HPO₄ and NaH₂PO₄ were bought from Merck KGaA (Darmstadt, Germany).
- D₂O, NaOD, DCl, and Triton X-100 were bought from Sigma-Aldrich, Chemie GmbH (Steinheim, Germany).
- Calcein and Dextran G50 were bought from Fluka Chemie GmbH (Buchs, Switzerland).

All chemicals were used without further purification.

9.2 Experimental

9.2.1 Vesicle preparation

Pure or mixed lipids were dispersed in aqueous solution containing 100 mM NaCl by cyclic heating over the phase transition temperature and repeated vortexing. LUVs were prepared by extrusion through a 100 nm polycarbonate membrane using a Liposofast-Extruder (Avestin). Vesicle size was determined by dynamic light scattering using an ALV-NIBS / HPPS spectrometer (ALV-Laser Vertriebsgesellschaft m.b.H., Langen, Germany). MLVs were prepared by sonication at temperatures above phase transition temperatures in an ultrasonic water bath. Vesicle preparations were stored in the refrigerator at ca. 4 °C.

9.2.2 Differential scanning calorimetry

Differential Scanning Calorimetry was performed with a Microcal VP-DSC (MicroCal Inc., Northhampton, USA). In all experiments a heating rate was 1 °C/min and a time resolution 4s. Lipid and peptide samples were prepared separately and mixed directly before measurement. The lipid concentration in the calorimetric cell was ranged from 0.25–2.5 mM. Peptide concentration varied according to the desired R_c . Reference was always 100 mM NaCl solution. At least three up- and down scans were performed for each sample to prove the reproducibility. All presented curves originate from the second heating scan.

9.2.3 Infrared spectroscopy

Spectra were recorded using Bruker Vector 22 spectrometer (Bruker GmbH, Germany) equipped with a DTGS detector. PLL-lipid samples were placed between two CaF₂ or BaF₂ windows, which were separated by a Teflon spacer 56 μm or 25 μm in thickness. The hollow sample mount was thermostated by an external circulating water bath (Haake F3 C, Gebr. Haake GmbH, Karlsruhe, Germany). The temperature was controlled with a Pt 100 sensor directly in the cell. Temperature was incremented in steps of 1 or 2 °C and equilibrated 8 min after each step. 64 scans with a spectral resolution of 2 cm⁻¹ were collected and Fourier transformed after 1 level of zero filling. Lipid and peptide samples were prepared separately and mixed directly on the window before measurement. The lipid preparations were used in a concentration of 60 mM. The concentration of the peptide solution was adjusted to yield the desired R_c . For experiments in D₂O solution both, the lipid and the peptide preparations were lyophilized twice and resuspended in D₂O. For data processing the Bruker OPUS FT-IR software was used. Spectra of a 100 mM NaCl solution in H₂O or D₂O, respectively, were used as reference and subtracted from the sample spectra. The presented curves are, if not otherwise stated, recorded on cooling.

9.2.4 Isothermal titration calorimetry

ITC measurements were performed with a MicroCal VP-ITC (Microcal, Inc., Southhampton, MA, USA). The sample cell (1,447 ml) was loaded with the 2 mM vesicle suspension or 2 mM polypeptide solution. The injection syringe (300 μ l) was filled with 20 mM Polypeptide solution or 20 mM vesicle suspension. Both samples were degassed 10 min in vacuum before the experiment. The titrant was injected in steps of 10 μ l into the sample cell which was stirred by the rotating injection syringe with 320 rpm. The equilibration time after each injection was set to 900 s, to allow the cell feedback signal to return to the baseline. The reference power offset was 20 μ cal/s. Heats of dilution were evaluated by injecting polypeptide solutions or vesicle suspensions into NaCl solution. Data were evaluated with the ITC module for ORIGIN software, which is supplied by MicroCal, Inc.

9.2.5 Monolayer adsorption experiments

The monolayer adsorption experiments were performed in a self made PTFE trough, which holds a volume of 11.15 ml and has a surface area of 7.1 cm². The trough was thermostated at 20 °C (in case of DPPG measurements) or at 25 °C (in case of DMPA measurements) with a circulating water bath. The same water bath thermostated as well a plastic hood which covered the whole experimental setup. The surface pressure was recorded using a microbalance (Riegler and Kirstein GmbH, Wiesbaden, Germany) furnished with a Wilhelmy plate. Data were recorded with a self written program. Prior to each experiment the trough was carefully rinsed and the pressure was calibrated. Using the surface pressure of pure water (72 mN/m) and that of air (0 mN/m) as reference points. As subphase a 100 mM NaCl solution was used. The subphase was stirred during the experiment using a small stirring magnet to accelerate diffusion of the added solutes. DPPG was dissolved in a mixture of CHCl₃ and methanol. Appropriate amounts of this solution to reach the desired initial surface pressure were spread on the water surface. The solvent was allowed to evaporate and the lipid film to equilibrate. After a constant surface pressure was recorded for at least 30 min, 10 μ l of a 15 mM (PLL) or 50 mM (PLA) polypeptide solution were injected in the subphase, yielding a bulk concentration of 13.45 μ M or 44.8 μ M, respectively. For injection a feedthrough from the edge of the trough to the subphase interior was used. Therefore, the film was not disturbed by the injection.

9.2.6 Monolayer pressure/area isotherms

Surface pressure vs. molecular area isotherms were recorded using a film balance, equipped with moveable barriers and Wilhelmy plate (Riegler and Kirstein GmbH, Wiesbaden, Germany). Trough area and surface pressure were calibrated using the well known pressure/area isotherms of arachidic acid as reference data. As subphase either a 100 mN NaCl

solution or 100 mM NaCl containing 0.5 mM PLA of different chain length was used. DPPG was spread from a $\text{CHCl}_3/\text{CH}_3\text{OH}$ (2:1, vol:vol) solution using a microsyringe with a precision of 0.33 μl . After evaporation of the solvent the film was compressed with a rate of $2 \text{ \AA}^2 \cdot \text{molecule}^{-1} \cdot \text{min}^{-1}$. The trough was thermostated at 20 °C using an external circulating water bath.

9.2.7 X-ray diffraction

Powder patterns were measured in transmission with a stationary linear position sensitive detector ($2\theta = 0 - 40^\circ$) at room temperature on a stage including a curved primary Ge(111) monochromator and high temperature attachment (STOE & CIE GmbH Darmstadt). The samples were sealed in glass capillaries. Cu $K\alpha_1$ ($\lambda = 0.154051 \text{ nm}$) radiation was used, and the scattering was corrected with respect to an empty capillary. The X-ray patterns were combined in a single contour diagram to continuously present the scattered intensity from the SAXS to the WAXS region ($2\theta = 0 - 40^\circ$, $s = 0 - 4.7 \text{ nm}^{-1}$) between $-30 \text{ }^\circ\text{C}$ and $70 \text{ }^\circ\text{C}$. The heating rate was 4 K h^{-1} (5 min equilibration, 10 min exposition each pattern) for the applied temperature protocol.

The samples for X-Ray diffraction were prepared according the following procedure: From 10 mg lipid a 20 mM lipid/polypeptide ($R_c = 1$) suspension was prepared by addition of an equimolar amount of polypeptide solution, NaCl solution and phosphate buffer, pH 7. The amounts of NaCl and phosphate buffer were chosen in a way to give the desired concentration at the end of the protocol. The mixture was homogenized by sonication and then lyophilized. The powder was resuspended in pure water. The amount of added water was adjusted to obtain a sample with a concentration of 50% (w/w) water and 50 % polypeptide (mol/mol) with respect to the lipid, and concentrations of 100 mM NaCl and 20 mM phosphate buffer with respect to the aqueous component. This preparation was chosen to obtain a homogeneous sample. For comparison, the same preparation procedure was used for the pure lipid suspensions. In addition, a suspension of DPPG in freshly distilled water (pH 7) was investigated to clarify the influence of ionic strength.

9.2.8 Fluorescence experiments

Dye release experiments were performed in a FlouoroMax-2 fluorescence spectrometer (Instruments S.A. GmbH, Grasbrunn, Germany). Measurements were carried out with an excitation wavelength of 490 nm and a emission wavelength of 520 nm. The spectrometer was calibrated prior to every measurement series with the reference values of water and lamp Raman spectra. During the kinetic experiments data were recorded with the time resolution of 1 s. Measurements were performed at room temperature without thermostating (ca. 22 °C). The measurement procedure was as follows: Peptide solution was filled in a stirred PS cuvette (Sarstedt AG & Co., Nürnberg, Germany) in appropriate concentration to yield the final R_c

after addition of a calcein loaded vesicle suspension. The concentration of the lipid suspension was chosen in a way to give a final concentration of 100 μM lipid in the cuvette. The vesicle suspension was added after 30 s of data recording. After 720 s the vesicles were destroyed by addition of Triton X-100 solution.

Preparation of calcein loaded vesicles:

4 mM lipid was suspended in 80 mM calcein solution. Vesicles were prepared by extrusion as described above. External dye was removed by gel exclusion chromatography on a Sephadex G-75 filled column. Sephadex was allowed to swell in 100 mM NaCl solution. The vesicle/calcein suspension was centrifuged two times through freshly prepared columns. The eluent was diluted with the same volume of 200 mM NaCl solution to compensate for the osmotic gradient (80 mM calcein inside, salt free water outside) and prevent the vesicles from rupture. This procedure yields vesicles that are filled with a self quenching concentration of calcein. The exterior solution contains only small amounts of remaining calcein, which do not disturb the fluorescence measurements.

9.3 Summarizing Tables

Table A.1: Some properties of PLL and PLA complexes with PG containing membranes or monolayers. Changes are given with respect to an uncomplexed DPPG membrane or monolayer. \uparrow denotes an increase; \downarrow denotes a decrease.

property	condition	PLL	PLA
T_m	$R_c = 1$	$\uparrow +5\text{ }^\circ\text{C}$	minor changes
	$= f(n)$	\uparrow with n	\uparrow with n
	$= f(R_c)$	\downarrow with $1/R_c$	\downarrow with $1/R_c$
lipid demixing (PC/PG)	gel phase	yes for $x_{PG} < 0.5$	yes for $x_{PG} < 0.5$
	fluid phase	possibly for $x_{PG} > 0.6$	no
$\Delta_R H$	gel	< 0 (-3000 cal/mol)	> 0 (50 cal/mol)
	fluid	< 0 (-600 cal/mol)	< 0 (-1400 cal/mol)
		$\Delta_R H^{\text{gel}} < \Delta_R H^{\text{fluid}}$	$\Delta_R H^{\text{gel}} > \Delta_R H^{\text{fluid}}$
$\Delta_R C_p$		$\Delta_R C_p^{\text{gel}} < \Delta_R C_p^{\text{fluid}} < 0$	$\Delta_R C_p^{\text{fluid}} < 0$
C=O hydration	gel	hydration (+9%)	dehydration. (-4%)
	fluid	no effect	dehydration (-10%)
secondary structure on the membrane surface	PLL 14, PLA 69	random	random
	longer peptides	α -helix	β -sheet fractions
	$= f(T)$	unfolding with $\uparrow T$	unfolding with $\uparrow T$
	$= f(n)$	\uparrow stability with n	\uparrow stability with n
$v(\text{CH}_2)$	gel	\downarrow ca. 1.5 cm^{-1}	\downarrow ca. 1 cm^{-1}
	fluid	\downarrow ca. 1.5 cm^{-1}	\downarrow ca. 1 cm^{-1}
dye release	gel (DPPG)	ca. 10%	ca. 40%
	fluid (POPG)	ca. 50%	ca. 80%
		max for $R_c \approx 2$	max for $R_c \approx 2$
Monolayer adsorption	LE	condensation	condensation
	LC	insertion	insertion
	$\Delta\pi^{\text{max}}$	ca. 4.5 mN/m (at $\pi_0 = 30\text{ mN/m}$)	ca. 8 mN/m (at $\pi_0 = 30\text{ mN/m}$)
	$d(\Delta\pi)/d(\pi_0)$	> 0	> 0

Table A.2: Some properties of PLL and PLA complexes with PA containing membranes or monolayers. Changes are given with respect to an uncomplexed PA membrane or monolayer. \uparrow denotes an increase; \downarrow denotes a decrease.

property	condition	PLL	PLA
T_m	$R_c = 1$	$\uparrow +20\text{ }^\circ\text{C}$ 2 steps for longer PLL	$\uparrow +5\text{ }^\circ\text{C}$
	$= f(n)$	PLL 19: only 1 st step longer PLLs: no change with n	\uparrow with n
	$= f(R_c)$	no effect for $R_c > 1$	$\downarrow -3\text{ }^\circ\text{C}$ for $R_c < 1$
lipid demixing (PC/PG)	gel phase	possibly for $x_{PA} < 0.5$	yes for $x_{PA} < 0.5$
	fluid phase	no	possibly for $x_{PA} > 0.6$
$\Delta_R H$	gel	> 0 (600 cal/mol)	< 0 (-900 cal/mol)
	fluid	< 0 (-800 cal/mol)	< 0 (-1800 cal/mol)
		$\Delta_R H^{\text{gel}} > \Delta_R H^{\text{fluid}}$	$\Delta_R H^{\text{gel}} > \Delta_R H^{\text{fluid}}$
$\Delta_R C_p$	gel	$\Delta_R C_p^{\text{gel}} < 0$	$\Delta_R C_p^{\text{gel}} = 0$
	fluid	$\Delta_R C_p^{\text{fluid}} \geq 0$	$\Delta_R C_p^{\text{fluid}} = 0$
C=O hydration	gel	hydration (+ 23 %)	dehydration. (-3 %)
	fluid	dehydration (- 3 %)	dehydration (-10 %)
secondary structure on the membrane surface	PLL 14, PLA 69	random	β -sheet fractions
	longer peptides	β -sheet	β -sheet fractions
	$= f(T)$	unfolding at $T > T_m$	unfolding at $T > T_m$
$\nu(\text{CH}_2)$	gel	\downarrow ca. 0.5 cm^{-1}	unaffected
	fluid	\downarrow ca. $0.8 - 1.5\text{ cm}^{-1}$	unaffected
Monolayer adsorption	LE	condensation	condensation
	LC	insertion	insertion
	$\Delta\pi^{\text{max}}$	ca. 6 mN/m (at $\pi_0 = 18\text{ mN/m}$)	ca. 12 mN/m (at $\pi_0 = 15\text{ mN/m}$)
	$\Delta\pi$ at 30 mN/m	1 mN/m	8 mN/m
	$d(\Delta\pi)/d(\pi_0)$	> 0 for $\pi_0 < 18\text{ mN/m}$ < 0 for $\pi_0 > 18\text{ mN/m}$	> 0 for $\pi_0 < 15\text{ mN/m}$ < 0 for $\pi_0 > 15\text{ mN/m}$

10 References

- Alakoskela J-MI, Kinnunen PKJ (2007) Thermal Phase Behavior of DMPG: The Exclusion of Continuous Network and Dense Aggregates. *Langmuir* 23:4203-13
- Barth A, Zscherp C (2002) What vibrations tell us about proteins. *Q Rev Biophys* 35:369-430
- Ben-Tal N, Ben-Shaul A, Nicholls A, Honig B (1996a) Free-energy determinants of alpha-helix insertion into lipid bilayers. *Biophys J* 70:1803-12
- Ben-Tal N, Honig B, Bagdassarian CK, Ben-Shaul A (2000) Association entropy in adsorption processes. *Biophys J* 79:1180-7
- Ben-Tal N, Honig B, Peitzsch RM, Denisov G, McLaughlin S (1996b) Binding of small basic peptides to membranes containing acidic lipids: theoretical models and experimental results. *Biophys J* 71:561-75
- Blaurock AE, McIntosh TJ (1986) Structure of the crystalline bilayer in the subgel phase of dipalmitoylphosphatidylglycerol. *Biochemistry* 25:299-305
- Blondelle SE, Lohner K, Aguilar MI (1999) Lipid-induced conformation and lipid-binding properties of cytolytic and antimicrobial peptides: determination and biological specificity. *Biochem Biophys Acta* 1462:89-108
- Blume A (1979) A comparative study of the phase transitions of phospholipid bilayers and monolayers. *Biochem Biophys Acta* 557:32-44
- Blume A (1983) Apparent molar heat capacities of phospholipids in aqueous dispersion. Effects of chain length and head group structure. *Biochemistry* 22:5436-42
- Blume A, Eibl H (1979) The influence of charge on bilayer membranes. Calorimetric investigations of phosphatidic acid bilayers. *Biochem Biophys Acta* 558:13-21
- Blume A, Garidel P (1999) Lipid model membranes and biomembranes. *Handb. Therm. Anal. Calorim.* 4:109-73
- Blume A, Huebner W, Messner G (1988) Fourier transform infrared spectroscopy of ¹³C:O labeled phospholipids hydrogen bonding to carbonyl groups. *Biochemistry* 27:8239-49
- Boggs JM (1987) Lipid intermolecular hydrogen bonding: influence on structural organization and membrane function. *Biochem Biophys Acta* 906:353-404
- Bringezu F, Majerowicz M, Maltseva E, Wen S, Brezesinski G, Waring AJ (2007) Penetration of the antimicrobial peptide dicynthaurin into phospholipid monolayers at the liquid-air interface. *ChemBioChem* 8:1038-47
- Calnan BJ, Tidor B, Biancalana S, Hudson D, Frankel AD (1991) Arginine-mediated RNA recognition: the arginine fork. *Science* 252:1167-71
- Cameron DG, Casal HL, Mantsch HH, Boulanger Y, Smith ICP (1981) The thermotropic behavior of dipalmitoyl phosphatidylcholine bilayers. A Fourier transform infrared study of specifically labeled lipids. *Biophys J* 35:1-16
- Carrier D, Dufourcq J, Faucon JF, Pezolet M (1985) A fluorescence investigation of the effects of polylysine on dipalmitoylphosphatidylglycerol bilayers. *Biochem Biophys Acta* 820:131-9

- Carrier D, Mantsch HH, Wong PTT (1990) Protective effect of lipidic surfaces against pressure-induced conformational changes of poly(L-lysine). *Biochemistry* 29:254-8
- Carrier D, Pezolet M (1984) Raman spectroscopic study of the interaction of poly-L-lysine with dipalmitoylphosphatidylglycerol bilayers. *Biophys J* 46:497-506
- Carrier D, Pezolet M (1986) Investigation of polylysine-dipalmitoylphosphatidylglycerol interactions in model membranes. *Biochemistry* 25:4167-74
- Cevc G (1990) Membrane electrostatics. *Biochem Biophys Acta* 1031:311-82
- Cevc G (1991) Polymorphism of the bilayer membranes in the ordered phase and the molecular origin of the lipid pretransition and rippled lamellae. *Biochem Biophys Acta* 1062:59-69
- Cevc G, Watts A, Marsh D (1980) Non-electrostatic contribution to the titration of the ordered-fluid phase transition of phosphatidylglycerol bilayers. *FEBS Lett* 120:267-70
- Chirgadze YN, Fedorov OV, Trushina NP (1975) Estimation of amino acid residue side-chain absorption in the infrared spectra of protein solutions in heavy water. *Biopolymers* 14:679-94
- Chodanowski P, Stoll S (2001) Polyelectrolyte Adsorption on Charged Particles in the Debye-Hueckel Approximation. A Monte Carlo Approach. *Macromolecules* 34:2320-8
- Chou PY, Scheraga HA (1971) Calorimetric measurement of enthalpy change in the isothermal helix-coil transition of poly-L-lysine in aqueous solution. *Biopolymers* 10:657-80
- Collantes ER, Dunn WJ, 3rd (1995) Amino acid side chain descriptors for quantitative structure-activity relationship studies of peptide analogues. *J Med Chem* 38:2705-13
- De Kruijff B, Cullis PR (1980) The influence of poly(L-lysine) on phospholipid polymorphism. Evidence that electrostatic polypeptide-phospholipid interactions can modulate bilayer/non-bilayer transitions. *Biochem Biophys Acta* 601:235-40
- de Vries AH, Yefimov S, Mark AE, Marrink SJ (2005) Molecular structure of the lecithin ripple phase. *Proc. Natl. Acad. Sci. U. S. A.* 102:5392-6
- Decher G (1997) Fuzzy Nanoassemblies: Toward Layered Polymeric Multicomposites. *Science* 277:1232-7
- Degovics G, Latal A, Lohner K (2000) X-ray studies on aqueous dispersions of dipalmitoyl phosphatidylglycerol in the presence of salt. *J. Appl. Crystallogr.* 33:544-7
- Demel RA, London Y, Van Kessel WSMG, Vossenbergh FGA, Van Deenen LLM (1973) Specific interaction of myelin basic protein with lipids at the air-water interface. *Biochem Biophys Acta* 311:507-19
- Denisov G, Wanaski S, Luan P, Glaser M, McLaughlin S (1998) Binding of basic peptides to membranes produces lateral domains enriched in the acidic lipids phosphatidylserine and phosphatidylinositol 4,5-bisphosphate: an electrostatic model and experimental results. *Biophys J* 74:731-44
- Diederich A, Baehr G, Winterhalter M (1998) Influence of Polylysine on the Rupture of Negatively Charged Membranes. *Langmuir* 14:4597-605
- Dolowy K (1979) Effect of interfacial tension and curvature of charged lipid bilayer-polylysine complexes. *Bioelectrochem. Bioenerg.* 6:305-7

- Durvasula RV, Huang C-H (1999) Thermotropic phase behavior of mixed-chain phosphatidylglycerols: implications for acyl chain packing in fully hydrated bilayers. *Biochem Biophys Acta* 1417:111-21
- Dyck M, Loesche M (2006) Interaction of the Neurotransmitter, Neuropeptide Y, with Phospholipid Membranes: Film Balance and Fluorescence Microscopy Studies. *J. Phys. Chem. B* 110:22143-51
- Eibl H, Blume A (1979) The influence of charge on phosphatidic acid bilayer membranes. *Biochem Biophys Acta* 553:476-88
- Eisenberg M, Gresalfi T, Riccio T, McLaughlin S (1979) Adsorption of monovalent cations to bilayer membranes containing negative phospholipids. *Biochemistry* 18:5213-23
- Engelman DM, Steitz TA, Goldman A (1986) Identifying nonpolar transbilayer helices in amino acid sequences of membrane proteins. *Annu. Rev. Biophys. Biophys. Chem.* 15:321-53
- Epand RM, Gabel B, Epand RF, Sen A, Hui SW, Muga A, Surewicz WK (1992) Formation of a new stable phase of phosphatidylglycerols. *Biophys J* 63:327-32
- Farauo J, Travasset A (2007) Phosphatidic acid domains in membranes: effect of divalent counterions. *Biophys J* 92:2806-18
- Fidorra M, Heimburg T, Seeger HM (2007) Melting of single lipid components in binary lipid mixtures: a comparison between FTIR spectroscopy, DSC and Monte Carlo Simulations. *Los Alamos Natl. Lab., Prepr. Arch., Phys.:*1-12, arXiv:0712.064v1 [physics bio-ph]
- Förster G, Brezesinski G (1989) Lyotropic stress in lipid-water model systems. Structural changes induced by freezing of the solvent. *Liquid Crystals* 5:1659 - 68
- Franzin CM, Macdonald PM (2001) Polylysine-induced 2H NMR-observable domains in phosphatidylserine/phosphatidylcholine lipid bilayers. *Biophys J* 81:3346-62
- Fuchs SM, Raines RT (2006) Internalization of cationic peptides: the road less (or more?) traveled. *Cell. Mol. Life Sci.* 63:1819-22
- Fukushima K, Muraoka Y, Inoue T, Shimozawa R (1988) Conformational change of poly(L-lysine) induced by lipid vesicles of dilauroylphosphatidic acid. *Biophys Chem* 30:237-44
- Fukushima K, Muraoka Y, Inoue T, Shimozawa R (1989) Conformational study of poly(L-lysine) interacting with acidic phospholipid vesicles. *Biophys Chem* 34:83-90
- Futaki S (2005) Membrane-permeable arginine-rich peptides and the translocation mechanisms. *Adv. Drug Delivery Rev.* 57:547-58
- Futaki S, Suzuki T, Ohashi W, Yagami T, Tanaka S, Ueda K, Sugiura Y (2001) Arginine-rich peptides: an abundant source of membrane-permeable peptides having potential as carriers for intracellular protein delivery. *J. Biol. Chem.* 276:5836-40
- Gad AE, Bental M, Elyashiv G, Weinberg H, Nir S (1985) Promotion and inhibition of vesicle fusion by polylysine. *Biochemistry* 24:6277-82
- Galla HJ, Sackmann E (1975a) Chemically induced lipid phase separation in model membranes containing charged lipids. Spin label study. *Biochem Biophys Acta* 401:509-29

- Galla HJ, Sackmann E (1975b) Chemically induced phase separation in mixed vesicles containing phosphatidic acid. Optical study. *J. Am. Chem. Soc.* 97:4114-20
- Garidel P (1997) PHD thesis: the negatively charged Phospholipids phosphatidic acid and phosphatidylglycerol. A: The interaction with alkali earth cations, B: the mixing behaviour with zwitterionic phospholipids department of chemistry. university, Kaiserslautern
- Garidel P, Blume A (1999) Interaction of Alkaline Earth Cations with the Negatively Charged Phospholipid 1,2-Dimyristoyl-sn-glycero-3-phosphoglycerol: A Differential Scanning and Isothermal Titration Calorimetric Study. *Langmuir* 15:5526-34
- Garidel P, Forster G, Richter W, Kunst BH, Rapp G, Blume A (2000a) 1,2-Dimyristoyl-sn-glycero-3-phosphoglycerol (DMPG) divalent cation complexes: an X-ray scattering and freeze-fracture electron microscopy study. *Phys. Chem. Chem. Phys.* 2:4537-44
- Garidel P, Johann C, Blume A (1997a) Nonideal mixing and phase separation in phosphatidylcholine-phosphatidic acid mixtures as a function of acyl chain length and pH. *Biophys J* 72:2196-210
- Garidel P, Johann C, Blume A (2000b) Thermodynamics of lipid organization and domain formation in phospholipid bilayers. *J. Liposome Res.* 10:131-58
- Garidel P, Johann C, Mennicke L, Blume A (1997b) The mixing behavior of pseudobinary phosphatidylcholine-phosphatidylglycerol mixtures as a function of pH and chain length. *Eur Biophys J* 26:447-59
- Gazzara JA, Phillips MC, Lund-Katz S, Palgunachari MN, Segrest JP, Anantharamaiah GM, Snow JW (1997) Interaction of class A amphipathic helical peptides with phospholipid unilamellar vesicles. *J. Lipid Res.* 38:2134-46
- Gill SJ, Wadso I (1976) An equation of state describing hydrophobic interactions. *Proc. Natl. Acad. Sci. U. S. A.* 73:2955-8
- Goncalves E, Kitas E, Seelig J (2005) Binding of oligoarginine to membrane lipids and heparan sulfate: structural and thermodynamic characterization of a cell-penetrating peptide. *Biochemistry* 44:2692-702
- Goormaghtigh E, Cabiaux V, Ruyschaert J-M (1994a) Determination of soluble and membrane protein structure by Fourier transform infrared spectroscopy. I. Assignments and model compounds. *Subcell. Biochem.* 23:329-62
- Goormaghtigh E, Cabiaux V, Ruyschaert J-M (1994b) Determination of soluble and membrane protein structure by Fourier transform infrared spectroscopy. III. Secondary structures. *Subcell. Biochem.* 23:405-50
- Goormaghtigh E, Cabiaux V, Ruyschaert JM (1990) Secondary structure and dosage of soluble and membrane proteins by attenuated total reflection Fourier-transform infrared spectroscopy on hydrated films. *Eur. J. Biochem.* 193:409-20
- Greenfield NJ, Davidson B, Fasman GD (1967) Use of computed optical rotatory dispersion curves for the evaluation of protein conformation. *Biochemistry* 6:1630-7
- Grigoriev D, Krustev R, Miller R, Pison U (1999) Effect of Monovalent Ions on the Monolayers Phase Behavior of the Charged Lipid DPPG. *J. Phys. Chem. B* 103:1013-8

- Hac AE, Seeger HM, Fidorra M, Heimburg T (2005) Diffusion in two-component lipid membranes—a fluorescence correlation spectroscopy and Monte Carlo simulation study. *Biophys J* 88:317-33
- Hammes GG, Schullery SE (1970) Structure of macromolecular aggregates. II. Construction of model membranes from phospholipids and polypeptides. *Biochemistry* 9:2555-63
- Hartmann W, Galla HJ (1978) Binding of polylysine to charged bilayer membranes. Molecular organization of a lipid-peptide complex. *Biochem Biophys Acta* 509:474-90
- Hartmann W, Galla HJ, Sackmann E (1977) Direct evidence of charge-induced lipid domain structure in model membranes. *FEBS Lett.* 78:169-72
- Heimburg T (2000) A model for the lipid pretransition: coupling of ripple formation with the chain-melting transition. *Biophys J* 78:1154-65
- Heimburg T, Angerstein B, Marsh D (1999) Binding of peripheral proteins to mixed lipid membranes: effect of lipid demixing upon binding. *Biophys J* 76:2575-86
- Heimburg T, Biltonen RL (1994) Thermotropic behavior of dimyristoylphosphatidylglycerol and its interaction with cytochrome c. *Biochemistry* 33:9477-88
- Heimburg T, Marsh D (1995) Protein surface-distribution and protein-protein interactions in the binding of peripheral proteins to charged lipid membranes. *Biophys J* 68:536-46
- Hitz T, Iten R, Gardiner J, Namoto K, Walde P, Seebach D (2006) Interaction of alpha -and beta -Oligoarginine-Acids and Amides with Anionic Lipid Vesicles: A Mechanistic and Thermodynamic Study. *Biochemistry* 45:5817-29
- Hörnke M, Schwieger C, Blume A unpublished results
- Huang Ch, Li S (1999) Calorimetric and molecular mechanics studies of the thermotropic phase behavior of membrane phospholipids. *Biochem Biophys Acta* 1422:273-307
- Ichimura S, Mita K, Zama M (1978) Conformation of poly(L-arginine). I. Effects of anions. *Biopolymers* 17:2769-82
- Israelachvili JN (1985) *Intermolecular and Surface Forces: With Applications to Colloidal and Biological Systems*
- Ivanova VP, Heimburg T (2001) Histogram method to obtain heat capacities in lipid monolayers, curved bilayers, and membranes containing peptides. *Phys. Rev. E: Stat., Nonlinear, Soft Matter Phys.* 63:041914/1-12
- Jackson M, Haris PI, Chapman D (1989) Conformational transitions in poly(L-lysine): studies using Fourier transform infrared spectroscopy. *Biochem Biophys Acta* 998:75-9
- Johann C, Garidel P, Mennicke L, Blume A (1996) New approaches to the simulation of heat-capacity curves and phase diagrams of pseudobinary phospholipid mixtures. *Biophys J* 71:3215-28
- Kerth A (2003) *Infrarot-Reflexions-Absorptions-Spektroskopie an Lipid-, Peptid- und Flüssigkristallinen Filmen an der Wasser/Luft Grenzfläche*
- Kim J, Mosior M, Chung LA, Wu H, McLaughlin S (1991) Binding of peptides with basic residues to membranes containing acidic phospholipids. *Biophys J* 60:135-48
- Kimelberg HK, Papahadjopoulos D (1971) Phospholipid-protein interactions. Membrane permeability correlated with monolayer "penetration". *Biochem Biophys Acta* 233:805-9

- Kodama M, Aoki H (2001) Water behavior in phospholipid bilayer systems. *Surfactant Sci. Ser.* 93:247-93
- Kodama M, Aoki H, Miyata T (1999) Effect of Na⁺ concentration on the subgel phases of negatively charged phosphatidylglycerol. *Biophys Chem* 79:205-17
- Kodati VR, El-Jastimi R, Lafleur M (1994) Contribution of the Intermolecular Coupling and Librotorsional Mobility in the Methylene Stretching Modes in the Infrared Spectra of Acyl Chains. *J. Phys. Chem.* 98:12191-7
- Lamy-Freund MT, Riske KA (2003) The peculiar thermo-structural behavior of the anionic lipid DMPG. *Chem. Phys. Lipids* 122:19-32
- Langner M, Kubica K (1999) The electrostatics of lipid surfaces. *Chemistry and Physics of Lipids* 101:3
- Laroche G, Carrier D, Pezolet M (1988) Study of the effect of poly(L-lysine) on phosphatidic acid and phosphatidylcholine/phosphatidic acid bilayers by Raman spectroscopy. *Biochemistry* 27:6220-8
- Laroche G, Dufourc EJ, Dufourcq J, Pezolet M (1991) Structure and dynamics of dimyristoylphosphatidic acid/calcium complexes by deuterium NMR, infrared, and Raman spectroscopies and small-angle x-ray diffraction. *Biochemistry* 30:3105-14
- Laroche G, Dufourc EJ, Pezolet M, Dufourcq J (1990) Coupled changes between lipid order and polypeptide conformation at the membrane surface. A deuterium-NMR and Raman study of polylysine-phosphatidic acid systems. *Biochemistry* 29:6460-5
- Lasch P, Schultz CP, Naumann D (1998) The influence of poly-(L-lysine) and porin on the domain structure of mixed vesicles composed of lipopolysaccharide and phospholipid: an infrared spectroscopic study. *Biophys J* 75:840-52
- Lee B (1991) Solvent reorganization contribution to the transfer thermodynamics of small nonpolar molecules. *Biopolymers* 31:993-1008
- Lehrmann R, Seelig J (1994) Adsorption of Ca²⁺ and La³⁺ to bilayer membranes: measurement of the adsorption enthalpy and binding constant with titration calorimetry. *Biochem Biophys Acta* 1189:89-95
- Lenz O, Schmid F (2007) Structure of Symmetric and Asymmetric "Ripple" Phases in Lipid Bilayers. *Phys. Rev. Lett.* 98:058104/1-4
- Lewis RN, McElhaney RN, Pohle W, Mantsch HH (1994) Components of the carbonyl stretching band in the infrared spectra of hydrated 1,2-diacylglycerolipid bilayers: a reevaluation. *Biophys J* 67:2367-75
- Loura LMS, Coutinho A, Silva A, Fedorov A, Prieto M (2006) Structural Effects of a Basic Peptide on the Organization of Dipalmitoylphosphatidylcholine/Dipalmitoylphosphatidylserine Membranes: A Fluorescent Resonance Energy Transfer Study. *J. Phys. Chem. B* 110:8130-41
- Macdonald PM, Crowell KJ, Franzin CM, Mitrakos P, Semchyschyn D (2000) 2H NMR and polyelectrolyte-induced domains in lipid bilayers. *Solid State Nucl. Magn. Reson.* 16:21-36
- Macdonald PM, Crowell KJ, Franzin CM, Mitrakos P, Semchyschyn DJ (1998) Polyelectrolyte-induced domains in lipid bilayer membranes: the deuterium NMR perspective. *Biochem. Cell Biol.* 76:452-64

- Maget-Dana R (1999) The monolayer technique: a potent tool for studying the interfacial properties of antimicrobial and membrane-lytic peptides and their interactions with lipid membranes. *Biochem Biophys Acta* 1462:109-40
- Maget-Dana R, Brack A, Lelievre D (1997) Amphiphilic peptides as models for protein-membrane interactions: interfacial behavior of sequential Lys- and Leu-based peptides and their penetration into lipid monolayers. *Supramol. Sci.* 4:365-8
- Magzoub M, Graeslund A (2004) Cell-penetrating peptides: small from inception to application. *Q. Rev. Biophys.* 37:147-95
- Martinez J, Talroze R, Watkins E, Majewski JP, Stroeve P (2007) Templating Polypeptides on Self-Assembled Hemicylindrical Surface Micelles. *J. Phys. Chem. C* 111:9211-20
- May S, Harries D, Ben-Shaul A (2000) Lipid demixing and protein-protein interactions in the adsorption of charged proteins on mixed membranes. *Biophys J* 79:1747-60
- McLaughlin S (1989) The electrostatic properties of membranes. *Annual Review of Biophysics and Biophysical Chemistry* 18:113-36
- McLaughlin S, Aderem A (1995) The myristoyl-electrostatic switch: a modulator of reversible protein-membrane interactions. *Trends Biochem. Sci.* 20:272-6
- Menger FM, Seredyuk VA, Kitaeva MV, Yaroslavov AA, Melik-Nubarov NS (2003) Migration of Poly-L-lysine through a Lipid Bilayer. *J. Am. Chem. Soc.* 125:2846-7
- Mitchell DJ, Kim DT, Steinman L, Fathman CG, Rothbard JB (2000) Polyarginine enters cells more efficiently than other polycationic homopolymers. *J. Pept. Res.* 56:318-25
- Miyazaki M, Yoneyama M, Sugai S (1978) Anion-induced conformational transition of poly(L-arginine) and its two homologs. *Polymer* 19:995-1000
- Monera OD, Sereda TJ, Zhou NE, Kay CM, Hodges RS (1995) Relationship of sidechain hydrophobicity and alpha-helical propensity on the stability of the single-stranded amphipathic alpha-helix. *J. Pept. Sci.* 1:319-29
- Montal M (1999) Electrostatic attraction at the core of membrane fusion. *FEBS Lett.* 447:129-30
- Montich G, Scarlata S, McLaughlin S, Lehrmann R, Seelig J (1993) Thermodynamic characterization of the association of small basic peptides with membranes containing acidic lipids. *Biochem Biophys Acta* 1146:17-24
- Mosior M, McLaughlin S (1992a) Binding of basic peptides to acidic lipids in membranes: effects of inserting alanine(s) between the basic residues. *Biochemistry* 31:1767-73
- Mosior M, McLaughlin S (1992b) Electrostatics and reduction of dimensionality produce apparent cooperativity when basic peptides bind to acidic lipids in membranes. *Biochem Biophys Acta* 1105:185-7
- Murray D, Arbuzova A, Hangyas-Mihalyne G, Gambhir A, Ben-Tal N, Honig B, McLaughlin S (1999) Electrostatic properties of membranes containing acidic lipids and adsorbed basic peptides: theory and experiment. *Biophys J* 77:3176-88
- Netz RR, Joanny JF (1999) Adsorption of Semiflexible Polyelectrolytes on Charged Planar Surfaces: Charge Compensation, Charge Reversal, and Multilayer Formation. *Macromolecules* 32:9013-25

- Novellani M, Santini R, Tadrist L (2000) Experimental study of the porosity of loose stacks of stiff cylindrical fibres: influence of the aspect ratio of fibres. *Eur. Phys. J. B* 13:571-8
- Onda M, Yoshihara K, Koyano H, Ariga K, Kunitake T (1996) Molecular Recognition of Nucleotides by the Guanidinium Unit at the Surface of Aqueous Micelles and Bilayers. A Comparison of Microscopic and Macroscopic Interfaces. *J. Am. Chem. Soc.* 118:8524-30
- Papadopoulos P, Floudas G, Klok HA, Schnell I, Pakula T (2004) Self-Assembly and Dynamics of Poly(L-glutamate) Peptides. *Biomacromolecules* 5:81-91
- Papahadjopoulos D, Moscarello M, Eylar EH, Isac T (1975) Effects of proteins on thermotropic phase transitions of phospholipid membranes. *Biochem Biophys Acta* 401:317-35
- Pascher I, Sundell S, Harlos K, Eibl H (1987) Conformation and packing properties of membrane lipids: the crystal structure of sodium dimyristoylphosphatidylglycerol. *Biochem Biophys Acta* 896:77-88
- Prestrelski SJ, Byler DM, Thompson MP (1991) Infrared spectroscopic discrimination between alpha - and 310-helices in globular proteins. Reexamination of Amide I infrared bands of alpha -lactalbumin and their assignment to secondary structures. *Int. J. Pept. Protein Res.* 37:508-12
- Radler JO, Koltover I, Salditt T, Safinya CR (1997) Structure of DNA-cationic liposome complexes: DNA intercalation in multilamellar membranes in distinct interhelical packing regimes. *Science* 275:810-4
- Radzicka A, Wolfenden R (1988) Comparing the polarities of the amino acids: side-chain distribution coefficients between the vapor phase, cyclohexane, 1-octanol, and neutral aqueous solution. *Biochemistry* 27:1664-70
- Raghunathan VA, Katsaras J (1996) Lbeta '->L3c' phase transition in phosphatidylcholine lipid bilayers: a disorder-order transition in two dimensions. *Phys. Rev. E: Stat. Phys., Plasmas, Fluids, Relat. Interdiscip. Top.* 54:4446-9
- Ramsay G, Prabhu R, Freire E (1986) Direct measurement of the energetics of association between myelin basic protein and phosphatidylserine vesicles. *Biochemistry* 25:2265-70
- Reuter M, Schwieger C, Blume A manuscript in preparation
- Reynaud JA, Grivet JP, Sy D, Trudelle Y (1993) Interactions of basic amphiphilic peptides with dimyristoylphosphatidylcholine small unilamellar vesicles: Optical, NMR, and electron microscopy studies and conformational calculations. *Biochemistry* 32:4997-5008
- Rifkind JM (1969) Helix-coil transition of poly-L-arginine: a comparison with other basic polypeptides. *Biopolymers* 8:685-8
- Rothbard JB, Jessop TC, Lewis RS, Murray BA, Wender PA (2004) Role of Membrane Potential and Hydrogen Bonding in the Mechanism of Translocation of Guanidinium-Rich Peptides into Cells. *J. Am. Chem. Soc.* 126:9506-7
- Rothbard JB, Jessop TC, Wender PA (2005) Adaptive translocation: the role of hydrogen bonding and membrane potential in the uptake of guanidinium-rich transporters into cells. *Adv. Drug Delivery Rev.* 57:495-504

- Roux M, Neumann JM, Bloom M, Devaux PF (1988) Deuterium and phosphorus-31 NMR study of pentyllysine interaction with headgroup deuterated phosphatidylcholine and phosphatidylserine. *Eur Biophys J* 16:267-73
- Russ C, Heimburg T, von Grunberg HH (2003) The effect of lipid demixing on the electrostatic interaction of planar membranes across a salt solution. *Biophys J* 84:3730-42
- Sacre MM, Tocanne JF (1977) Importance of glycerol and fatty acid residues on the ionic properties of phosphatidylglycerols at the air-water interface. *Chem. Phys. Lipids* 18:334-54
- Sakai N, Futaki S, Matile S (2006) Anion hopping of (and on) functional oligoarginines: from chloroform to cells. *Soft Matter* 2:636-41
- Sakai N, Matile S (2003) Anion-mediated transfer of polyarginine across liquid and bilayer membranes. *J Am Chem Soc* 125:14348-56
- Sakai N, Takeuchi T, Futaki S, Matile S (2005) Direct observation of anion-mediated translocation of fluorescent oligoarginine carriers into and across bulk liquid and anionic bilayer membranes. *ChemBioChem* 6:114-22
- Schneider MF, Marsh D, Jahn W, Kloesgen B, Heimburg T (1999) Network formation of lipid membranes: triggering structural transitions by chain melting. *Proc. Natl. Acad. Sci. U. S. A.* 96:14312-7
- Schwieger C, Blume A (2007) Interaction of poly(L-lysines) with negatively charged membranes: an FT-IR and DSC study. *Eur Biophys J* 36:437-50
- Seelig J (1997) Titration calorimetry of lipid-peptide interactions. *Biochem Biophys Acta* 1331:103-16
- Senak L, Davies MA, Mendelsohn R (1991) A quantitative IR study of hydrocarbon chain conformation in alkanes and phospholipids: CH₂ wagging modes in disordered bilayer and HII phases. *J. Phys. Chem.* 95:2565-71
- Shafer PT (1974) The interaction of polyamino acids with lipid monolayers. *Biochem Biophys Acta* 373:425-35
- Shai Y (1999) Mechanism of the binding, insertion and destabilization of phospholipid bilayer membranes by alpha-helical antimicrobial and cell non-selective membrane-lytic peptides. *Biochem Biophys Acta* 1462:55-70
- Shibata A, Murata S, Ueno S, Liu S, Futaki S, Baba Y (2003) Synthetic copoly(Lys/Phe) and poly(Lys) translocate through lipid bilayer membranes. *Biochem Biophys Acta* 1616:147-55
- Stern O (1924) The theory of the electrolytic double-layer. *Z. Elektrochem. Angew. Phys. Chem.* 30:508-16
- Sukhorukov GB, Donath E, Lichtenfeld H, Knippel E, Knippel M, Budde A, Mohwald H (1998) Layer-by-layer self assembly of polyelectrolytes on colloidal particles. *Colloids and Surfaces A: Physicochemical and Engineering Aspects* 137:253
- Suwalsky M, Llanos A (1977) An x-ray diffraction study of poly(L-lysine hydrobromide). *Biopolymers* 16:403-13
- Suwalsky M, Traub W (1972) X-ray diffraction study of poly-L-arginine hydrochloride. *Biopolymers* 11:623-32

- Takahashi H, Matuoka S, Kato S, Ohki K, Hatta I (1991) Electrostatic interaction of poly(L-lysine) with dipalmitoylphosphatidic acid studied by X-ray diffraction. *Biochem Biophys Acta* 1069:229-34
- Takahashi H, Matuoka S, Kato S, Ohki K, Hatta I (1992) Effects of poly(L-lysine) on the structural and thermotropic properties of dipalmitoylphosphatidylglycerol bilayers. *Biochem Biophys Acta* 1110:29-36
- Takahashi H, Yasue T, Ohki K, Hatta I (1996) Structure and phase behavior of dimyristoylphosphatidic acid/poly(L-lysine) systems. *Mol. Membr. Biol.* 13:233-40
- Tamm LK, Tatulian SA (1997) Infrared spectroscopy of proteins and peptides in lipid bilayers. *Q. Rev. Biophys.* 30:365-429
- Tanford C (1980) *The Hydrophobic Effect: Formation of Micelles and Biological Membranes*. 2nd Ed
- Tang M, Waring AJ, Hong M (2007) Phosphate-Mediated Arginine Insertion into Lipid Membranes and Pore Formation by a Cationic Membrane Peptide from Solid-State NMR. *J. Am. Chem. Soc.* 129:11438-46
- Tatulian SA (1999) Surface electrostatics of biological membranes and ion binding. *Surfactant Sci. Ser.* 79:871-922
- Tenchov B, Koynova R, Rapp G (2001) New Ordered Metastable Phases between the Gel and Subgel Phases in Hydrated Phospholipids. *Biophys J* 80:1873-90
- Thoren PEG, Persson D, Esbjornner EK, Goksoer M, Lincoln P, Norden B (2004) Membrane Binding and Translocation of Cell-Penetrating Peptides. *Biochemistry* 43:3471-89
- Trauble H (1971) Phase transitions in lipids. Possible switch processes in biological membranes. *Naturwissenschaften* 58:277-84
- Tsogas I, Tsiourvas D, Nounesis G, Paleos CM (2005a) Interaction of Poly-L-arginine with Dihexadecyl Phosphate/Phosphatidylcholine Liposomes. *Langmuir* 21:5997-6001
- Tsogas I, Tsiourvas D, Nounesis G, Paleos CM (2006) Modeling Cell Membrane Transport: Interaction of Guanidinylated Poly(propylene imine) Dendrimers with a Liposomal Membrane Consisting of Phosphate-Based Lipids. *Langmuir* 22:11322-8
- Tsogas I, Tsiourvas D, Paleos CM, Giatrellis S, Nounesis G (2005b) Interaction of L-arginine with dihexadecylphosphate unilamellar liposomes: the effect of the lipid phase organization. *Chem. Phys. Lipids* 134:59-68
- Tuchtenhagen J, Ziegler W, Blume A (1994) Acyl chain conformational ordering in liquid-crystalline bilayers: comparative FT-IR and 2H-NMR studies of phospholipids differing in headgroup structure and chain length. *Eur Biophys J* 23:323-35
- Ulrich S, Seijo M, Stoll S (2006) The many facets of polyelectrolytes and oppositely charged macroions complex formation. *Curr. Opin. Colloid Interface Sci.* 11:268-72
- Umezawa N, Gelman MA, Haigis MC, Raines RT, Gellman SH (2002) Translocation of a beta-peptide Across Cell Membranes. *J. Am. Chem. Soc.* 124:368-9
- Vives E, Brodin P, Lebleu B (1997) A truncated HIV-1 Tat protein basic domain rapidly translocates through the plasma membrane and accumulates in the cell nucleus. *J. Biol. Chem.* 272:16010-7

- Vollhardt D, Fainerman VB, Siegel S (2000) Thermodynamic and Textural Characterization of DPPG Phospholipid Monolayers. *J. Phys. Chem. B* 104:4115-21
- Wagner K, Harries D, May S, Kahl V, Raedler JO, Ben-Shaul A (2000) Direct Evidence for Counterion Release upon Cationic Lipid-DNA Condensation. *Langmuir* 16:303-6
- Wang J, Gambhir A, McLaughlin S, Murray D (2004) A computational model for the electrostatic sequestration of PI(4,5)P2 by membrane-adsorbed basic peptides. *Biophys J* 86:1969-86
- Watts A, Harlos K, Marsh D (1981) Charge-induced tilt in ordered-phase phosphatidylglycerol bilayers evidence from X-ray diffraction. *Biochem Biophys Acta* 645:91-6
- Watts A, Harlos K, Maschke W, Marsh D (1978) Control of the structure and fluidity of phosphatidylglycerol bilayers by pH titration. *Biochem Biophys Acta* 510:63-74
- Wender PA, Mitchell DJ, Pattabiraman K, Pelkey ET, Steinman L, Rothbard JB (2000) The design, synthesis, and evaluation of molecules that enable or enhance cellular uptake: peptoid molecular transporters. *Proc Natl Acad Sci U S A* 97:13003-8
- Wender PA, Rothbard JB, Jessop TC, Kreider EL, Wylie BL (2002) Oligocarbamate Molecular Transporters: Design, Synthesis, and Biological Evaluation of a New Class of Transporters for Drug Delivery. *J. Am. Chem. Soc.* 124:13382-3
- White SH, Wimley WC (1998) Hydrophobic interactions of peptides with membrane interfaces. *Biochem Biophys Acta* 1376:339
- Wieprecht T, Apostolov O, Beyermann M, Seelig J (2000a) Interaction of a mitochondrial presequence with lipid membranes: role of helix formation for membrane binding and perturbation. *Biochemistry* 39:15297-305
- Wieprecht T, Apostolov O, Beyermann M, Seelig J (2000b) Membrane Binding and Pore Formation of the Antibacterial Peptide PGLa: Thermodynamic and Mechanistic Aspects. *Biochemistry* 39:442-52
- Wieprecht T, Beyermann M, Seelig J (1999) Binding of Antibacterial Magainin Peptides to Electrically Neutral Membranes: Thermodynamics and Structure. *Biochemistry* 38:10377-87
- Wieprecht T, Beyermann M, Seelig J (2002) Thermodynamics of the coil-alpha-helix transition of amphipathic peptides in a membrane environment: the role of vesicle curvature. *Biophys Chem* 96:191-201
- Wilkinson DA, McIntosh TJ (1986) A subtransition in a phospholipid with a net charge, dipalmitoylphosphatidylglycerol. *Biochemistry* 25:295-8
- Wilkinson DA, Tirrell DA, Turek AB, McIntosh TJ (1987) Tris buffer causes acyl chain interdigitation in phosphatidylglycerol. *Biochem Biophys Acta* 905:447-53
- Yaroslavov AA, Kuchenkova OE, Okuneva IB, Melik-Nubarov NS, Kozlova NO, Lobyshev VI, Menger FM, Kabanov VA (2003) Effect of polylysine on transformations and permeability of negative vesicular membranes. *Biochem Biophys Acta* 1611:44-54
- Zhang Y-P, Lewis RNAH, McElhaney RN (1997) Calorimetric and spectroscopic studies of the thermotropic phase behavior of the n-saturated 1,2-diacylphosphatidylglycerols. *Biophys J* 72:779-93
- Zuckermann MJ, Heimburg T (2001) Insertion and pore formation driven by adsorption of proteins onto lipid bilayer membrane-water interfaces. *Biophys J* 81:2458-72

11 Acknowledgments

This work could not have been accomplished without the help and support of many people. Therefore I would like to address thanks to:

Prof. Dr. A. Blume for receiving me in his group and supervising this work. I am grateful for stimulating scientific discussions, his confidence, and the support he gave me also in times, where the work did not proceed with ease.

Dr. G. Förster for the X-ray measurements and many long, instructive, and enthusiastic discussions on this topic.

Sandro Keller and Heike Nikolenko (FMP Berlin) for teaching me the fluorescence methods.

Marcell Reuter for taking over the freshly gained knowledge and performing the most part of the dye release measurements during his diploma thesis.

Dr. Annette Meister for performing the cryo-TEM measurements.

Ingrid Schaller and Bettina Fölting for their technical assistance in performing many IR, DSC, and ITC measurements.

All the trainees and diploma students, with whom I had the chance to work together. Many thanks for the experimental help and the opportunity to explain my objectives, the chance to answer questions, and for the concerted efforts we made to find solutions. I very much profited from the manner of working together! These thanks go to Anja Huster, Sebastian Finger, Maria Hörnke, Marcell Reuter, Franziska Faber, Tina Weber, Ahmad Arouri, and Martin Stuthe.

My co-workers for the convenient atmosphere in the group, many discussions, and help to solve big and small problems of the daily scientific life. Thanks are directed to: Dag Leine, Elkin Amado, Martin Schiewek, Katja Beyer, Annette Meister and Andreas Lonitz.

Dr. Andreas Kerth in especially in the former aspect and for his willing, patient, and competent help in any situation.

My family and all my friends, who supported me during the last years and especially during the last months.

12 Publications

Schwieger C, Blume A (2007) Interaction of poly(L-lysines) with negatively charged membranes: an FT-IR and DSC study. *Eur Biophys J* 36:437-50

Förster G, Schwieger C, Faber F, Weber T, Blume A (2007) Influence of poly(L-lysine) on the structure of dipalmitoylphosphatidylglycerol/water dispersions studied by X-ray scattering. *Eur Biophys J* 36:425-35

Oral contributions

Schwieger C, Förster G, Reuter M, Blume A (2006) Interaction of Cationic Polyelectrolytes with Negatively Charged Lipid Bilayers. *2nd Augsburg Winterschool on Complex Materials at Interfaces. March 13 – 16, 2006, Tegernsee, Bad Wiessee*

Schwieger C, Förster G, Reuter M, Blume A (2006) Interaction of Cationic Polypeptides with Negatively Charged Lipid Bilayers. *Workshop of the German Biophysical Society: Dynamics of artificial and biological membranes, March 20 – 22, 2006, Gomadingen*

Schwieger C, Blume A (2006) Comparison of Poly(L-lysine) and Poly(L-arginine) in its Interaction with Negatively Charged Membranes. *Klausurtagung ZIK HaloMEM, August 20 – 28, 2007, Freyburg*

Poster contributions

Schwieger C, Blume, A (2003) Interaction of Poly(L-lysines) with negatively charged membranes, *Arbeitstagung Flüssigkristalle der Deutschen flüssigkristallinen Gesellschaft, 2003, Mainz*

Schwieger C, Arouri A, Blume A (2004) Interaction of negatively charged Membranes with Polyamines, *Annual Meeting of the German Biophysical Society, 2004, Freiburg*

Förster G, Schwieger C, Faber F, Weber T, Blume A (2005) Influence of Poly(L-lysine) on the Structure of Dipalmitoylglycerophosphoglycerol (DPPG) / Water Dispersions, *Arbeitstagung Flüssigkristalle der Deutschen Flüssigkristallinen Gesellschaft, March 16 – 18, 2005, Padderborn*

Schwieger C, Förster G, Blume A (2005) Comparison of two Cationic Peptides Regarding their Interaction with negatively Charged Membranes, *International Biophysics Congress, Aug 27 – Sep 1, 2005, Montpellier*

Förster G, Schwieger C, Blume A (2006) Influence of Poly(L-arginine) on the Structure of Dilauroylphosphatidic Acid (DLPA)/Water Dispersions, *Arbeitstagung Flüssigkristalle der Deutschen Flüssigkristallinen Gesellschaft, March 2006, Freiburg*

Schwieger C, Förster G, Blume A (2006) Interaction of Poly(L-arginine) with negatively charged Bilayers, *Annual Meeting of the German Biophysical Society, Sep 24 – 27 2006, Mainz*

Förster G, Schwieger C, Blume A (2007) Influence of Poly(L-lysine) on the Structure of (DPPC:DPPG = 1:1) / Water Dispersions Studied by X-Ray Diffraction, *International Bunsen Discussion Meeting: Membrane Interaction Peptides and Proteins, March 28 – 31, 2007, Halle*

13 Curriculum vitae

Personal Data:

Family name:	Schwieger
First name:	Christian
Date of Birth:	April 09, 1976
Place of birth:	Halle (Saale), Germany
Nationality:	German
Personal status:	single

Education and working experiences

2002 – 2007	Doctorate and scientific co-worker in the group of Prof. Dr. A. Blume, institute of physical chemistry, Martin-Luther-University, Halle (Saale)
2002	Diploma in Chemistry from the Martin-Luther-University Halle
2001 – 2002	Diploma Thesis on “Interactions of poly(L-lysine) with DPPG containing membranes” in the group of Prof. Dr. A. Blume, institute of physical chemistry, Martin-Luther-University, Halle (Saale)
2000	Erasmus student Montpellier, France at the “Ecole Nationale and Supérieur de Chimie de Montpellier” in the group of Prof. Dr. H.-J. Cristau on the topic of “Aza-Wittig-reactions”
1996 – 2002	Study of Chemistry at the Martin-Luther-University, Halle (Saale) Scholarship from “Cusanuswerk – Bischöfliche Studienstiftung”
1995 – 1996	Civil service at the “Katholische Studentengemeinde Halle” social work, care keeper works, organisation
1995	Abitur (A-levels, school leaving examination)

- 1993 – 1994 Stay in Vancouver, Canada. Visit of the “University Hill High School”
- 1990 – 1995 Grammar school: “Georg Cantor Gymnasium” Halle (Saale), specialized in mathematics and natural sciences.
- 1982 – 1990 Primary school “Otto Schlag” Halle (Saale)

Eidesstattliche Erklärung

Hiermit erkläre in an Eides statt, dass ich die vorliegende Arbeit selbständig verfasst und keine anderen Hilfsmittel als die angegebenen verwendet habe. Ich habe die Arbeit an keiner anderen Hochschule vorgelegt und mich zu keinem früheren Zeitpunkt um den Doktorgrad beworben.

Christian Schwieger